Université de Montréal

Exploring Rac GTPase regulation: The molecular mechanisms governing the DOCK180 and ELMO interaction and the role of this complex in Rac-mediated cell migration

par

Manishha PATEL

Programmes de Biologie Moléculaire

Faculté de Médicine

Thèse présentée à la Faculté des études supérieures

en vue de l'obtention du grade de PhD

en Programmes de Biologie Moléculaire

Février 2011

Université de Montréal
Faculté de Médicine

Cette thèse intitulée:

Exploring Rac GTPase regulation: The molecular mechanisms governing the DOCK180 and ELMO interaction and the role of this complex in Rac-mediated cell migration

Présentée par :
Manishha PATEL

a été évaluée par un jury composé des personnes suivantes :

David HIPFNER, PhD, président-rapporteur
Jean-François CÔTÉ, PhD, directeur de recherche
Morag PARK, PhD, membre du jury
Andrew CRAIG, PhD, examinateur externe
Stephane LEFRANÇOIS, PhD, représentant du doyen

Résumé

Les protéines DOCK180 et ELMO coopèrent ensemble biochimiquement et génétiquement afin d'activer la GTPase Rac1 lors de plusieurs évènements biologiques. Toutefois, le rôle que jouent ces protéines dans la signalisation par Rac est encore mal compris. Nous émettons l'hypothèse que Dock180 agit comme activateur de Rac, alors que ELMO est requis pour l'intégration de la signalisation de Rac plutôt que son activation *per se*. Nous postulons que ELMO agit comme signal de localisation intracellulaire afin de restreindre de façon spatio-temporelle la signalisation de Rac en aval de Dock180, et/ou que ELMO agit comme protéine d'échafaudage entre Rac et ses effecteurs pour amplifier la migration cellulaire.

Dans l'**objectif nº 1**, nous démontrons que le domaine PH atypique de ELMO1 est le site d'interaction principal entre cette protéine et DOCK180. De plus, nous démontrons que la liaison entre ELMO et DOCK180 n'est pas nécessaire pour l'activation de Rac, mais est plutôt essentielle pour faciliter la réorganisation du cytosquelette induite par l'activation de Rac en aval de Dock180. Ces résultats impliquent que ELMO pourrait jouer des rôles additionnels dans la signalisation par Rac. Dans l'**objectif nº 2**, nous avons découvert l'existence d'une homologie structurelle entre ELMO et un module d'autorégulation de la formine Dia1, et avons identifié trois nouveaux domaines dans la protéine ELMO : les domaines RBD, EID et EAD. De façon analogue à Dia1, nous avons découvert que ELMO à l'état basal est autoinhibé grâce à des intéractions intramoléculaires. Nous proposons que l'état d'activation des protéines ELMO est régulé de façon similaire aux formines de la famille Dia, c'est-à-dire grâce à des interactions avec d'autres protéines. Dans l'**objectif nº 3**, nous identifions un domaine RBD polyvalent chez ELMO. Ce domaine possède une double spécificité pour les GTPases de la famille Rho et Arf. Nous avons découvert que Arl4A agit comme signal de recrutement membranaire pour le module ELMO/DOCK180/Rac. Nos résultats nous permettent de supposer que d'autres

GTPases pourraient être impliquées dans l'activation et la localisation de cette voie de signalisation.

Nous concluons qu'à l'état basal, ELMO et DOCK180 forment un complexe dans lequel ELMO est dans sa conformation autoinhibée. Bien que le mécanisme d'activation de ELMO ne soit pas encore bien compris, nous avons découvert que, lorsqu'il y a stimulation cellulaire, certaines GTPases liées au GTP peuvent intéragir avec le domaine RBD de ELMO pour relâcher les contacts intramoléculaires et/ou localiser le complexe à la membrane. Ainsi, les GTPases peuvent servir d'ancrage au complexe ELMO/DOCK180 pour assurer une regulation spatiotemporelle adequate de l'activation et de la signalisation de Rac.

Mots-clés : *Migration cellulaire, DOCK180, ELMO, Rac GTPase, Arl4 GTPase, RBD*

Abstract

DOCK180 and ELMO cooperate biochemically and genetically to activate Rac in several biological events. However, the role of these proteins in Rac signaling is still poorly understood. We hypothesize that DOCK180 functions as a RacGEF, with ELMO binding to DOCK180 being required for integration of proper Rac signaling rather than Rac activation *per se*. We postulate that ELMO acts as a subcellular targeting signal for spatio-temporal restriction of DOCK180-mediated Rac signaling and/or as a scaffold for Rac effectors to enforce cell migration.

In **Aim #1**, we elucidate that the atypical ELMO1 PH is the major DOCK180 binding site. We demonstrate that the binding of ELMO1 to DOCK180 is not necessary for Rac GTP-loading, but is instead required to facilitate Rac-GTP induced cytoskeletal changes following DOCK180 activation. These results imply additional roles for ELMO in mediating Rac signaling. In **Aim #2**, we reveal structural homology between ELMO and an autoregulatory module in the formin, Dia1, and identify three novel domains in ELMOs: the RBD, EID and EAD. Analogous to Dia1, we uncovered that ELMO is autoinhibited via intramolecular interactions at basal state. We propose that the activation state of ELMO proteins is regulated, much like in Dia-family formins, via interaction with other proteins. **Aim #3** identifies a polyvalent RBD in ELMO with dual specificity for Rho and Arf family GTPases. We found Arl4A as a novel membrane recruitment signal for the ELMO/DOCK180/Rac module. Our results may have broad implications in the activation and localization of this pathway by additional GTPases.

We conclude that, at basal levels, ELMO/DOCK180 is complexed, with ELMO in an autoinhibited state in the cytosol. Through cell stimulation, certain GTPases will be activated that now bind the ELMO RBD and alleviate the intramolecular contacts. In this way, the GTPase anchors the activated ELMO/DOCK180 module in place for proper spatio-temporal regulation of Rac activation and signaling.

Keywords : *Cell migration, DOCK180, ELMO, Rac GTPase, Arl4 GTPase, RBD*

Table of contents

List of tables

CHAPTER 2

List of figures

CHAPTER 1

CHAPTER 2

CHAPTER 3

CHAPTER 4

DISCUSSION

List of abbreviations

Abi-1: Abscisic acid insensitive 1
ABP : Actin-binding protein
ADF: Actin depolymerizing factor
Arf: ADP-ribosylation factor
Arl: Arf-like
ARNO: Arf nucleotide-binding site opener
Arp2/3: Actin-Related Proteins 2/3
BAI: Brain-specific Angionesis Inhibitor
Cdc42: Cell division cycle 42
Ced: Cell death
CRIB: Cdc42/Rac1-interactive domain
CrkII: CT10 Regulator of kinase
DAAM: Disheveled-associated activator of morphogenesis
DAD: Diaphanous Autoregulatory Domain
Dbl: Diffuse B-cell lymphoma
DH: Dbl-homology domain
DHR: Dock-Homology Region
Dia: Diaphanous
DID: Diaphanous Inhibitory Domain
DOCK: Dedicator of cytokinesis
DRF: Dia-Related Formin
DTC: Distal tip cell
EAD: ELMO Autoregulatory Domain
ECM: Extracellular matrix
EID: ELMO Inhibitory Domain
ELMO: Engulfment and cell motility
ERK: Extracellular signal-regulated kinase
ERM: Ezrin Radixin Moesin
FAK: Focal Adhesion Kinase
FH: Formin Homology
FHOD: Formin homology domain
FRET: Fluorescence Resonance Energy Transfer
GAPs: GTPase Activating Proteins
GBD: GTPase binding domain
GDIs: Guanine Nucleotide Dissociation Inhibitors
GDP: Guanosine diphosphate
GEFs: Guanine Nucleotide Exchange Factors
GTP: Guanosine triphosphate
HSPC300:hematopoeitic stem/progenitor cell protein 300
IRSp53: Insulin Receptor Substrate p53
IQGAP: IQ motif-containing GTPase activating protein
JNK: c-Jun N-terminal kinase
MBC: Myoblast City

MLC : Myosin Light Chain
MLCK: Myosin Light Chain Kinase
Nap1: Nucleosome Assembly protein
NEDD9: neural precursor cell expressed, developmentally down-regulated 9
NPF: Nucleation Promoting Factor
PA: Phosphatidic acid
Pak: P21/Cdc42/Rac1-associated kinase
PDGF: Platelet-derived growth factor
PH: Pleckstrin Homology
PI3K: Phosphatidylinositol 3-kinase
PIP_2: Phosphatidylinositol 4,5-biphosphates
PIP_3: Phosphatidylinositol 3,4,5-triphosphates
PIP_5-kinase: Phosphoinositide 5-kinase
PLC: Phospholipase C
PLD: Phospholipase D
PtdSer: Phosphatidylserine
PTEN: Phosphatase and tensin homolog
PxxP: proline-rich motif
PVR: PDGF and VEGF-related receptor
Rab: Ras genes from rat brain
Rac: Ras-related C3 botulinum toxin substrate 1
Ran: Ras-related Nuclear Protein
Ras: Rat sarcoma
RBD: Ras-binding domain
Rho: Ras homology
RhoG: Ras homology Growth-related
Rif: Rap-interacting protein
ROCK: Rho-associated coiled-coil containing protein kinase
SH3: Src-homology domain 3
Sra-1: Steroid receptor RNA activator 1
Src : Sarcoma
TC10: Teratocarcinoma clone 10
TCL: TC10-like
uPar: Urokinase plasminogen activator receptor
VEGF: Vascular endothelial growth factor
WASP: Wiskott-Aldrich Syndrome protein
WAVE: Wasp family Verprolin-homologous protein
WH2: WASP-homogy domain 2
Wrch: Wnt-1 responsive Cdc42 homology

Research is what I'm doing when I don't know what I'm doing.

~Wernher Von Braun

If you're not part of the solution, you're part of the precipitate. ~Henry J. Tillman

The most exciting phrase to hear in science, the one that heralds the most discoveries, is not "Eureka!" (I found it!) but "That's funny..." ~Isaac Asimov

For Mom and Dad

Acknowledgements

First and foremost, I would like to thank my supervisor, Dr. Jean-François Côté, for being such an excellent and exceptional mentor to me. From day one, he has instilled his enthusiasm for science into me (I tried to resist, but it was too powerful), and in the process, made me a better scientist. I thank you JF, for having faith in me (because, man, those first few months with molecular biology….I was sure I was going to get fired). Your patience and guidance are always acknowledged and I can't thank you enough for the patience part. Although it has been said that you are the epiphany of a slave driver, I've always found that statement a bit harsh…a bit. In all seriousness, I absolutely loved my experience in your lab. And if I ever graduate, I will miss very much working with you and the Côté lab members. And I KNOW without a doubt, you'll ALL miss benching to my classic rap/hiphop CDs (Don't worry, I'll make you copies). Finally, as difficult as it may be to believe, he did not have to bribe or threaten me to write any of the above.

I would like to take this opportunity to thank my PhD thesis committee members: Dr. Morag Park, Dr. Jean-Philippe Gratton, Dr. David Hipfner, Dr. Andrew Craig and Dr. Jean Vacher. They all helped me improve my critical thinking skills over the course of my PhD. I am grateful for their critiques and recommendations that allowed me to improve both my research and my growth as a scientist.

I thank our collaborators Dr. David Barford and Dr. David Komander for their invaluable insight and excellent work that led to the MBC publication in 2008. I am immensely proud of this paper and all the hard work we put into it. David, you and your crystals rock! ☺

I thank our collaborators Drs Kay Hofmann, Brian Wilkes and Michel Bouvier for the support, effort, and efficiency with which we put out our ELMO autoinhibition work in Current Biology last year.

I also thank our collaborators Dr. Fang-Jen Lee and Tsai-Chen Chiang for the support and effort that was put into our ELMO/Arl4A work.

Thank you to Dominic Filion and Odile Neyret for all their help in anything microscopy related (Dom) and BioMol (Odile), and their patience for all my inane questions. As well, thanks to the lab of Dr. Jacques Archambault, especially to Geneviève Morin, for all their help in the yeast two-hybrid work.

Like JF, Nadine was there from jump and helped me evolve into someone you can actually call a molecular biologist. Thank you Nad, for all your help in training me, and for your advice, professional and non-professional (did you ever think of being a guidance counselor/psychiatrist?). Thanks also for your patience, because I know I wore it thin sometimes (mammalian vectors, bacterial vectors, what's the difference? How does math work?).

Mel is one of the best friends a girl could have. Thank you for all the help and support throughout my PhD and the good times in and outside the lab (especially the mental support…PS. Sex and the City, where have you been all my life? ☺). I thank her also for her infinite sarcasm that almost matches mine. Thanks for your Shakira choreography and for always being in the wrong place at the wrong time so you can share your hilarious stories with us afterwards. If we were the tagteam of Batman and Robin, I don't know which would be which. All I know is, I wouldn't be Robin.

The tandem of Ariane and Rose cannot be forgotten. As part of your trio residing on the dominant side of the lab, I immensely enjoyed working late hours with you and sharing dinners and laughs after work or in between western transfers and antibody incubations. Benching with you two was a pleasure. Thanks to Ariane for her baking and to Rose for being my chocolate supplier (by the way, everyone really misses you guys for that). I will especially remember one night when Rose turned into a benching robot and Ari almost died from laughter (you both know what I'm talking about ☺).

JEN!!! You are the coolest girl I know. I love you for your relaxed attitude and your refined selection of music. I thank you for ALWAYS making sure that we ALWAYS have the essentials in the lab without which we cannot function or work (ie: cookies).

Thanks to Yoran for his microscopy genius. Thank you for being such a good friend; your good-nature and your Zen-like demeanour is always appreciated.

Special shoutout to my fellow scientists and friends Amel and Cass, Amélie, Alex and Michael ☺ (After a grueling day of lab work, what's on the menu ;)), Dominic and Shuo-Fei, Frank, Mark, Martina, Mika (Big Bro) and Caro. Thanks for all the fun times in and out of the lab.

Thanks to my master's lab of Dr. Christian Casanova, with special emphasis on Annie-Hélène, Brian, Éliane, Fred and Martin into tricking me and making me think science was cool. Thanks a lot. Really.

Special thanks to my little brother, Roshan, the only one in my family who has any idea what I'm doing in grad school. And also to my sister, Dipa (otherwise, she'll feel left out), and my cute niece Zen, who made coming to the lab on sunny warm weekends a bit more enjoyable ☺.

Thanks to Manny for making me a stronger person. Thanks to my close and dear friends Christianne, Hugues, Naren, Nicole, Princess, and Sawudat. Although they may not always understand what I'm doing (seriously, how many people really do?), they've always loved and supported me through it.

Special thanks to Ariane, Cass, Jen, Dorothée, Claudia and Nicole who helped me immensely with the formatting and printing of this thesis.

And last, but not least, I want to thank my parents (mummy and deddy) who've raised me to persistent and passionate with anything I do. I love you both very much and thank you for letting me be a kid for so long.

CHAPTER 1

INTRODUCTION

1. The renegade cancer cell

Cancer is a leading cause of death worldwide, accounting for 13% of all deaths [1]. Closer to home, almost 45% of Canadians will develop cancer during their lifetimes, causing death in approximately 25% of the population each year [2]. Rather than the primary tumour, it is cancer metastasis, the colonizing of cancer cells from a primary tumor to secondary sites in the body, which underlies the vast majority of cancer-related deaths.

Lying at the heart of this unwelcome disease is a founder cell, the renegade cancer cell, which deviates from its original internal program and wreaks havoc on an otherwise pristine biological system. The evolution of a metastatic tumour requires tumour cells to overcome a series of hurdles in its path. Triumph of a tumour over these obstacles allows dispatched malignant cells to infiltrate the circulation and burrow into surrounding tissue to found new settlements of destruction.

Presently, patients with metastatic disease have few treatment alternatives besides chemotherapy, hormonal therapy and radiation [3]. Insight into the molecular basis of cellular motility will expand development of novel alternative therapies for cancer patients in the future.

2. The multi-step process of cell migration

Cell migration is an essential feature of all living cells. This highly complex and intricate process is an underlying characteristic of a multitude of biological events, such as embryonic morphogenesis, immune response, tissue repair and regeneration, and angiogenesis. It is equally prominent during pathophysiological processes including cancer cell invasion and metastasis. The modes of cell migration can be divided into two categories: (i) individual (amoeboid or mesenchymal) or (ii) collective (migration of cohesive multicellular units) [4] (**Figure 1.1, pg. 4**). Cell type, constituents of the extracellular matrix, as well as gene expression profiles are key factors that will determine which type of migration a cell will undergo.

Amoeboid migration can be observed during brain development, in hematopoietic stem cells, leukocytes, and even in some cancer cells [5,6]. During this type of motility, cells will appear rounded or ellipsoid in shape and lack mature focal adhesions and stress fibers, leading to low polarity and poor adhesiveness[7,8]. These cells can constantly change their shape and depend on swift forming protrusions and retractions that propel cell movement (**Figure 1.2, pg. 5**).

Mesenchymal migration is a signature of specific cell types, such as, fibroblasts and certain tumour cells [4]. This form of migration can be segmented into five well-defined steps that will lead to directed-cell movement towards a migratory attractant or other gradient (external or internal signals) of some kind: (i) cell polarization,

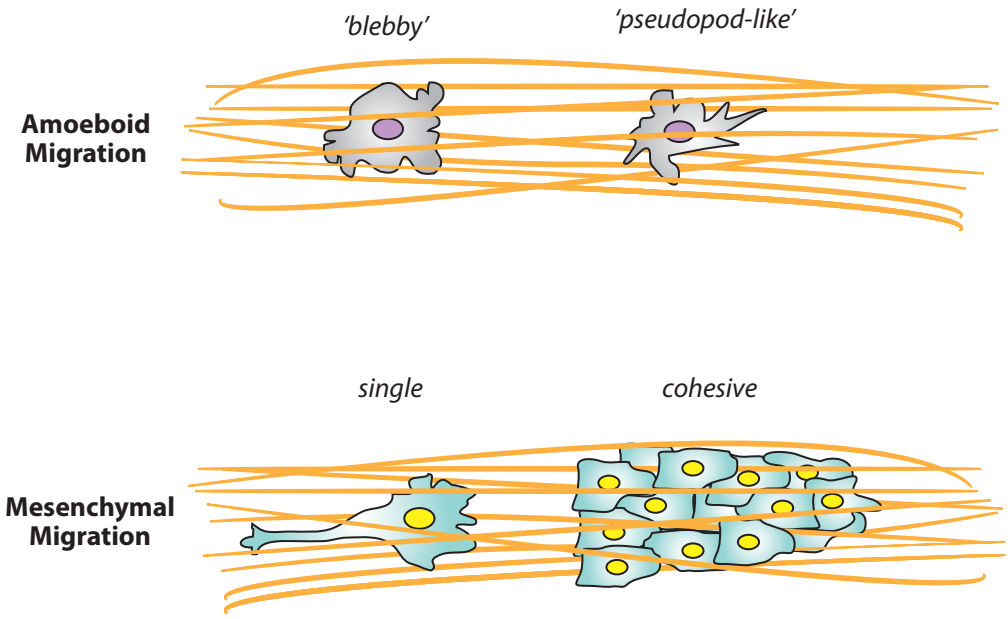

Figure 1.1. Modes of Cell Migration and their Morphologies.
The types of cell motility can be divided into two groups: amoeboid and mesenchymal. Amoeboid migration is characterized by 'blebby'cells that can extend pseudopod-like extensions to infiltrate its three dimensional surroundings. These cells are constant shape-shifters, with poor adhesiveness and low polarity, and use propulsive force to move themselves forward. Mesenchymal migration is characterized by elongated, polarized cells with high adhesive properties. These cells can form cell-cell contacts, and can also migrate as a group of cells commonly referred to as cohesive or collective cell motility. Cells are also in tune with their surroundings and can transition from amoeboid-to-mesenchymal migration and vice-versa as an environmental adaptive response.

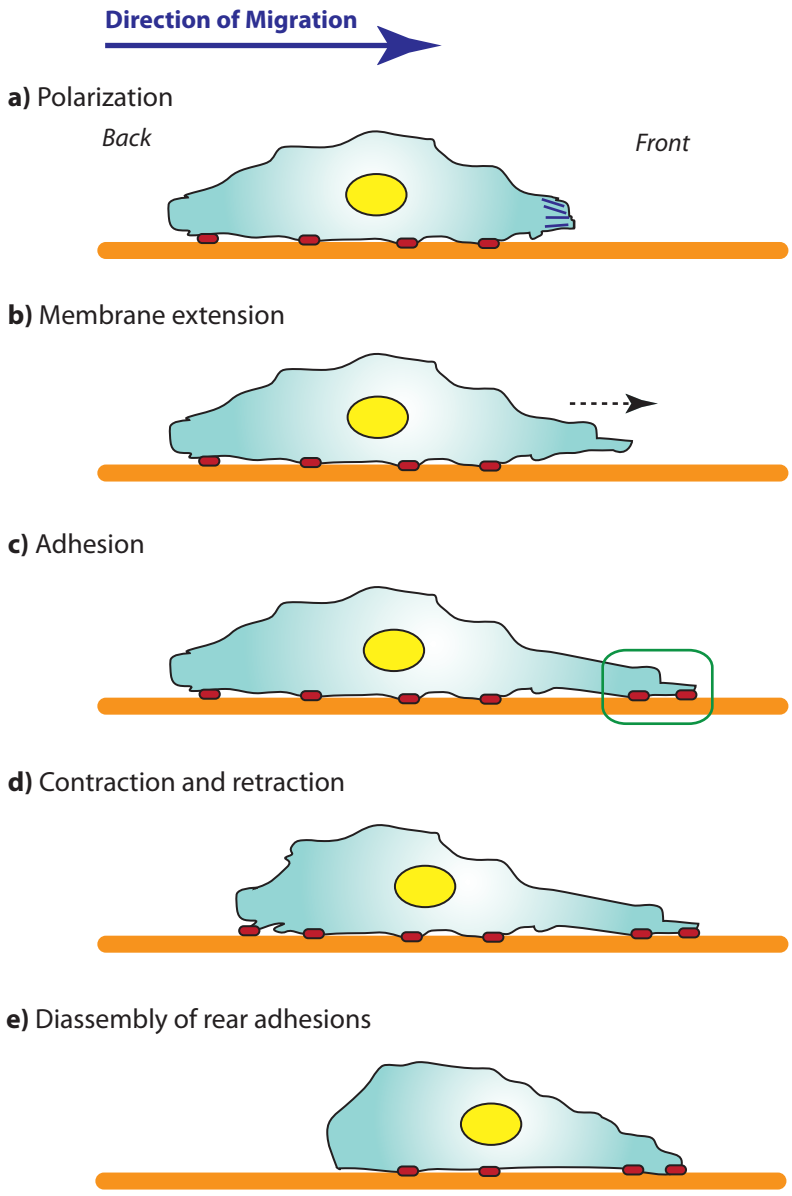

Figure 1.2. Steps of mesenchymal migration.
Mesenchymal migration occurs in distinct steps in response to a stimulus gradient. **a)** Polarization: The cell will react first by spatio-temporally reorganizing its cellular components and growing an extensive actin network in the direction of migration. **b)** Membrane extension: This is followed by protrusion formation (examples include lamellipodia and filopodia). **c)** Adhesion: Cellular extensions then require sites of attachment (green box) to stabilize the protrusive structures. **d)** Contraction and retraction: The cell will use these adhesion sites, as well as the force generated from contraction and retraction of the cell body at the rear of the cell, as a support system to push itself forward. **e)** Disassembly of rear adhesions: Finally, rear adhesion sites will be disbanded to allow for translocation of the cell body.

(ii) membrane protrusion formation at the leading edge, (iii) adhesion, (iv) contraction and retraction of the lagging end, and (v) disassembly of rear adhesion sites [9,10] (**Figure 1.2, pg. 5**). As mesenchymal migration is the focus of this thesis, below, I discuss in more detail the five steps.

2.1 Polarization

A cell must acquire spatial asymmetry of molecular signals to generate the force required for net cell movement. A clear distinction in cell front and rear is observed in a migrating cell (**Figure 1.2a, pg. 5**). A few characteristic molecular changes can be noted at the leading edge, where cells can display accumulation of filamentous actin (F-actin) [11], forward redistribution of chemosensory signaling receptors [12] and/or integrin adhesion receptors [13], and receptor/cytoskeletal crosslinking [14]. Ras family GTPases are key in initiating this polarity (see section 4. The Ras superfamily of GTPases). As well, mounting evidence indicates that specific lipid accumulation also reinforces leading edge formation and maintenance of cell polarity [15]. Restriction of PtdIns(3,4,5)P_3 to the cell front is encouraged by the degradation of lipids at the sides and the back of the cell. PTEN is a phosphoinositide 3'-specific phosphatase that dephosphorylates PtdIns(3,4,5)P_3 to PtdIns(4,5)P_2, and in migratory cells, is found to be excluded from the migratory front [16-18]. In this way, a steep gradient of the lipid signaling molecule, PtdIns(3,4,5)P_3, can be maintained. Additionally, a positive feedback loop consisting of PtdIns(3,4,5)P_3 and the Rho GTPases is proposed to preserve cell polarity by perpetuating GTPase activity, through recruitment of

RhoGEFs to sites of lipid accumulation [19,20]. As well, the Rho GTPase, Rac, has also been shown to directly bind and recruit PI3K at the leading edge, promoting the cycle of PtdIns(3,4,5)P_3 generation and Rac localization [21].

2.2 Membrane extension

At the polarized front, a cell will extend its membrane and form distinct protrusions. The most well-defined of these protrusions are lamellipods (broad, flat, sheet-like structures) and filopods (thin, cylindrical, needle-like projections) [9]. These structures are rich in actin and actin-associated proteins [9,22]. Several actin-binding proteins are key players at this stage, regulating the rate and organization of actin polymerization in protrusions by contributing to the pool of available actin molecules and filaments [23,24].

2.3 Adhesion

Once a cell generates membrane protrusions at the leading edge, adhesion site formations are favoured in order to offer an anchorage point for the moving cell. Through various interactions with the ECM, the cell will form adhesion sites which allows the cell to migrate over them effectively, and they will persist and remain fixed to the substrate until they reach the rear or edge of a cell [9] (**Figure 1.2b, pg. 5**). Rapid turnover ensues for the majority of nascent adhesions, while a few mature behind the leading edge in response to tensile stress [25]. Mature adhesions either go through a round of disassembly or are diminished to form fibrillar adhesions [26,27].

While many molecules can contribute to cell-substratum anchorage, the integrins are major pro-migratory factors and key players in this event. These receptors act as the "feet" of a migrating cell by supporting adhesion to the ECM and by connecting via adaptors with actin filaments on the inside of the cell [28]. Integrin stimulation can induce the activation or phosphorylation of a plethora of migration-related signaling molecules, such as FAK, paxillin, and tensin, that are integral for focal adhesion complex formation [29-31] (**Figure 1.2c, pg. 5**).

2.4 Contraction and retraction

Following the protrusive force that is generated to extend membrane processes, a second contractile force is needed to propel the cell body forward (**Figure 1.2d, pg. 5**). Cell contraction is dependent on the interaction between myosin II and actin filaments attached to adhesion sites [28,32]. Myosin II is activated via myosin light chain (MLC) phosphorylation, resulting in increased contractility and tensile strength to adhesion sites. MLC kinase (MLCK) and Rho kinase (ROCK) are positive modulators of MLC, while MLC phosphatase, which is itself phosphorylated and inhibited by ROCK, is a negative regulator in this instance [33].

2.5 Disassembly of rear adherences

Migration of a cell requires adherences at the rear of the cell to be released. Often, the tension generated by rearmost adhesion sites anchoring the cell to the substratum, is sufficient to physically sever the integrin/actin cytoskeleton link. This

step of migration shows membrane 'ripping', as a major fraction of integrins is left on the substratum as the cell releases and moves forward [9,34] (**Figure 1.2e, pg. 5**). Other contributing factors of rear release are low membrane support by the cytoskeleton in this region, as well as diminished integrin-cytoskeletal connections, and cytoskeletal contraction [9,14]. A combination of these and several, unrelated mechanisms are probably responsible for disassembly of rear adhesions.

It becomes evident that the actin cytoskeleton is an integral component of mesenchymal cell migration; this incredibly dynamic and versatile structure is discussed below.

3. The dynamic actin cytoskeleton

The actin cytoskeleton constitutes the cell's backbone, and supplies the mechanical force required to propel the cell forward in a desired direction. Actin is one of the most abundant proteins in all eukaryotes and is highly conserved between species [35]. Globular actin (G-actin) is a monomer that can readily polymerize into filamentous actin (F-actin). Essentially, monomeric G-actin binds ATP and, soon after assembly into filaments, hydrolyzes ATP, creating helical filaments [36,37] (**Figure 1.3, pg. 10**). These filaments are arranged in a polarized fashion with the 'barbed' or polymerizing end facing the cell membrane and the 'pointed' or depolymerizing end extending into the cytosol (**Figure 1.3, pg. 10**). The process of *de novo* actin filament polymerization can be simplified into three steps: (i) nucleation, (ii) elongation, and

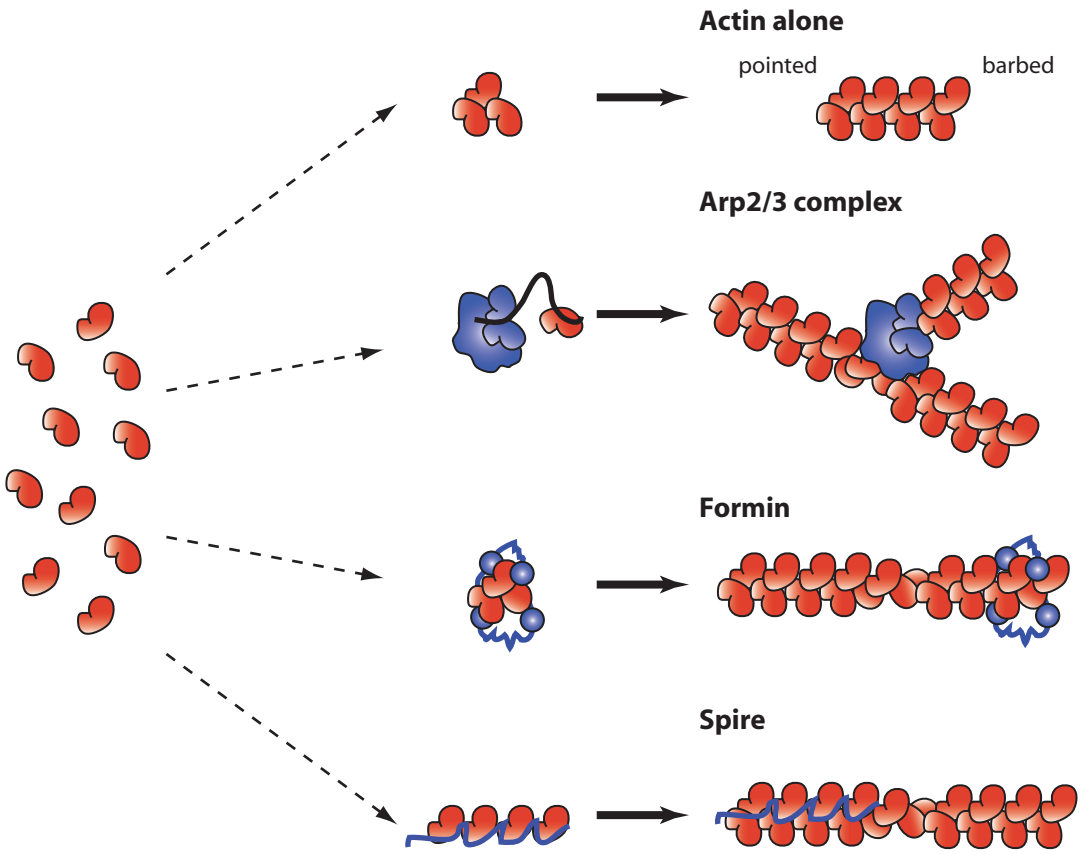

Figure 1.3. Actin filament genesis.
During actin polymerization, actin monomers (G-actin) act as the building blocks of growing actin filaments (F-actin). Spontaneous actin polymerization is an unstable process, where small oligomers of actin filaments are quickly disassembled back to actin monomers. Nucleation promoting factors (NPFs) will bind actin monomers and allow for stable extension of actin filaments. The Arp2/3 complex binds the side of an actin filament and promotes branching of filaments. Formins and Spire bind actin monomers and allow for the growth of linear actin filaments. Formins move along with the filament at the barbed end, while Spire remains stationary at the pointed end of filaments. Adapted from [43].

(iii) termination. During the nucleation phase, initiation of actin polymerization is a slow event, because small oligomers are very unstable, but once overcome, filament elongation is much more rapid [37,38]. This initial step is kinetically unfavourable and exploits nucleation factors to favour assembly of actin-based structures [39]. The 3 known classes of nucleation factors are: the Arp2/3 complex, formin proteins and Spire (discussed below) [40,41,42]. These proteins will aid in the initial nucleation of an actin filament, and then the elongation of an actin filament until the pool of available actin monomers is exhausted to a point where actin polymerization and filament growth has reached a steady-state. During this steady-state, the filament array has a constant length where steady barbed-end growth balances steady pointed-end depolymerization [35].

3.1 Regulators of the actin cytoskeleton

3.1.1 Nucleation factors

Of the aforementioned nucleation factors, the Arp2/3 complex was the first to be identified. This complex consists of seven polypeptides (ARPC1-5, Arp2 and Arp3) and plays a critical role in the generation of arborized filament networks. At the outset, this complex needs to be activated via nucleation promoting factors (NPFs), such as WASP and Scar/WAVE, allowing for the Arp2/3 complex to act as an initiation template for a new filament on an existing filament in a y-branch arrangement with a 70° branch angle [43] (**Figure 1.3, pg. 10**). Coalescing of nucleation and branching

activity via Arp2/3 promotes the formation of a lattice meshwork of actin filaments fundamental for lamellipodia formation and functionality.

The second class of nucleation factors are the multidomain formins. Through their signature Formin Homology 1 (FH1) and FH2 domains, these proteins exercise their actin nucleation and polymerization activity [37,44]. These proteins nucleate linear, unbranched actin filaments and stay bound to the barbed-end of actin polymers preventing the access of capping proteins [44,45,46]. Formin-mediated elongation is further enhanced through its ability to directly bind profilin, an actin-binding protein, allowing for the progressive addition of actin subunits to a growing filament [47]. In this way, formins remain associated with growing barbed-ends, and essentially, 'walk' along the polymerizing filament [43,44]. Interestingly, some formins have the capacity to bundle, sever, or depolymerize actin filaments, indicating the multi-faceted role of these proteins in cytoskeletal processing (**Figure 1.3, pg. 10**) [48-51]. Formins are potent cytoskeletal regulators, as some members also have the ability to bind and influence microtubule dynamics [52-55]. Formins are discussed in more detail in section 5.2 Liberating formins.

The third nucleation factor is Spire, a multidomain protein comprising 4 WH2 domains each capable of binding one actin monomer. Similar to formins, Spire nucleates linear, unbranched actin filaments, although through an entirely different mechanism. Spire recruits and organizes actin monomers to form a pre-nucleation

complex acting as the building block for filament formation from the side [56] (**Figure 1.3, pg. 10**).

The nucleation factors can generate new actin filaments via *de novo* nucleation, pre-existing free barbed ends, or newly exposed free barbed ends due to severing of filaments. In addition to these nucleators, a myriad of actin-binding proteins (ABPs) will sculpt actin structure and dynamics by: capping, stabilizing, severing, depolymerizing, crosslinking, bundling, sequestering or delivering monomers, or by promoting monomer nucleotide exchange [43]. Once nucleated, actin filaments can then be assembled into a wide variety of higher-order cellular structures.

3.1.2 Nucleation Promoting Factors (NPFs)

Alone, the Arp2/3 complex is not a potent actin nucleator. This action requires filament binding by the complex and phosphorylation events to boost nucleation activity [57]. Apart from these two events, NPFs are critical collaborators of actin filament growth. Class I NPFs are categorized into five subfamilies: (i) Wiskott-Alrich Syndrome Protein (WASP) and Neural WASP (N-WASP); (ii) WASP-family verprolin homologue (WAVE, also known as SCAR) 1-3; (iii) WASH; (iv) WHAMM; and (v) JMY [42,58]. All family members contain diverse N-terminal regulatory regions and share at least one VCA (*v*erprolin, *c*entral, *a*cidic) domain, a key structural element, at the C-terminus vital for actin regulation. The VCA domain is responsible for binding simultaneously to G-actin monomers, via the V region, and Arp2/3, via the CA region, priming Arp2/3 for nucleation [58-60]. For these proteins, most research has focused on the WASP and WAVE

members where two models are proposed for the regulation of these proteins. In the past, it was generally accepted that WASP proteins at basal state were regulated via intramolecular inhibitory interactions between its N-terminal GTPase-binding domain (GBD) and C-terminal VCA domain [42,58]. Binding partners for the GBD or surrounding regions (ex. Cdc42 or PIP_2), as well as phosphorylation events affecting the GBD, relieve autoinhibition and activate WASP proteins to serve out many of its functional roles, such as, phagocytic and endocytic structure, stress fiber, and membrane ruffle and lamellipodia formation [61]. However, other findings support the notion that, rather than a monomeric autoinhibited conformation, N-WASP is predominantly found in complex with WASP-interacting protein (WIP) which is thought to stabilize the autoinhibited N-WASP conformation [62,63]. These models are equally attractive and can co-exist, increasing the complexity arising from this regulation.

Unlike WASP, constituents of the WAVE family are not regulated via autoinhibition. Rather, these proteins form a pentameric heterocomplex with ABI, NAP1, SRA1, HSPC300 where the SRA1/NAP1 dimer binds the WAVE/ABI/HSPC300 trimer and inhibits the action through this complex [64,65]. Release comes in the form of specific protein binding to one or more of the complex components, such as Rac-binding via SRA1. Similar to WASP proteins, the WAVE family is suggested to be regulated by additional factors, such as PIP_3 binding and phosphorylation events [65]. Still, there are questions concerning the role of the WAVE complex during Arp2/3 activation; this, and the exact mechanism regulating WAVE activation has stirred up

many conflicts and remains an area of intense research. WASP and WAVE will be discussed further in section 5. Modes of GTPase regulation.

The vast interest in molecules that modulate the actin cytoskeleton has greatlyly expanded our knowledge of signaling cascades manipulating cell movement. Entrenched as critical components of cell migration are the Ras superfamily of small GTPases, and our attention now turns to this limb of the expansive tree of actin regulators.

4. The Ras superfamily of GTPases

The Ras G proteins, also known as Ras GTPases, are key units of central control systems coordinating signaling pathways immersed in numerous aspects of cell biology, such as, cytoskeletal reorganization, cell cycle progression, and gene transcription. Under the umbrella of the Ras superfamily of small GTPases, there are over 150 members in mammals, with evolutionarily conserved orthologs found in *Drosophila*, *C. elegans*, *S. cerevisiae*, *S. pombe*, *Dictyostelium* and plants [66]. Based on sequence and functional similarities, the superfamily is divided into 5 subfamilies: Ras, Rho, Ran, Rab, and Arf [67] (**Figure 1.4, pg. 16**). These enzymes act as molecular switches that are turned on by GTP-binding and turned off by hydrolyzing GTP to GDP, a cycle that is tightly managed by various regulatory proteins [68] (discussed in section 4.2 Rho GTPase regulators) (**Figure 1.5, pg. 17**). Most Ras GTPases display

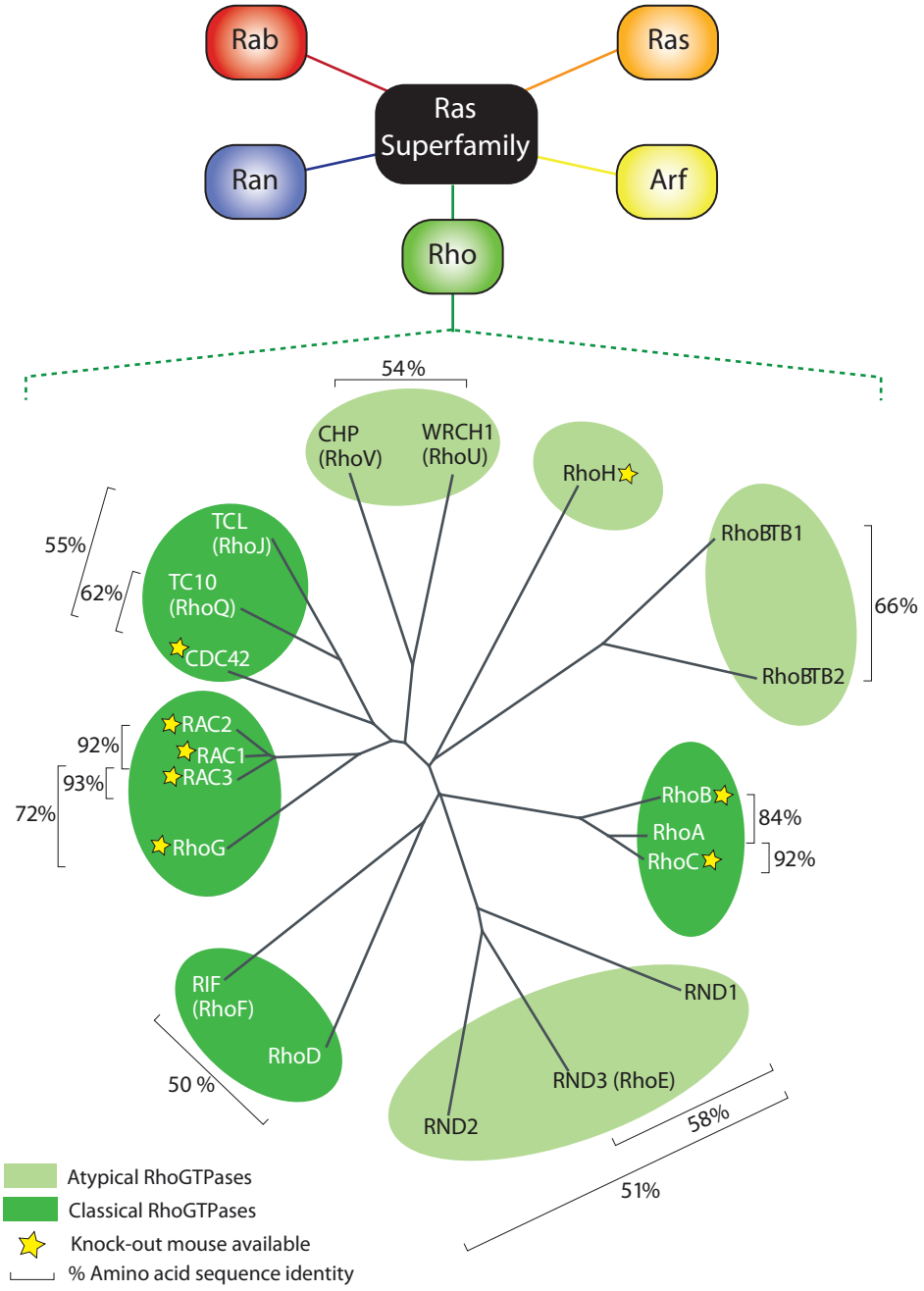

Figure 1.4. The Ras Superfamily of GTPases.
The Ras superfamily consists of over 150 GTPases divided into five subfamilies: Ras, Arf, Rho, Ra, and Rab. Of the five subfamilies, the Rho family is heavily implicated in actin cytoskeletal rearrangement. Rho members are further sub-classified based on primary sequence similarities. Of these, Rac, RhoA, and Cdc42 are the extensively studied and best characterized. These proteins are implicated in a diverse assortment of cellular functions, such as, cytoskeletal rearrangment, gene expression regulation and cell cycle progression. Adapted from [67].

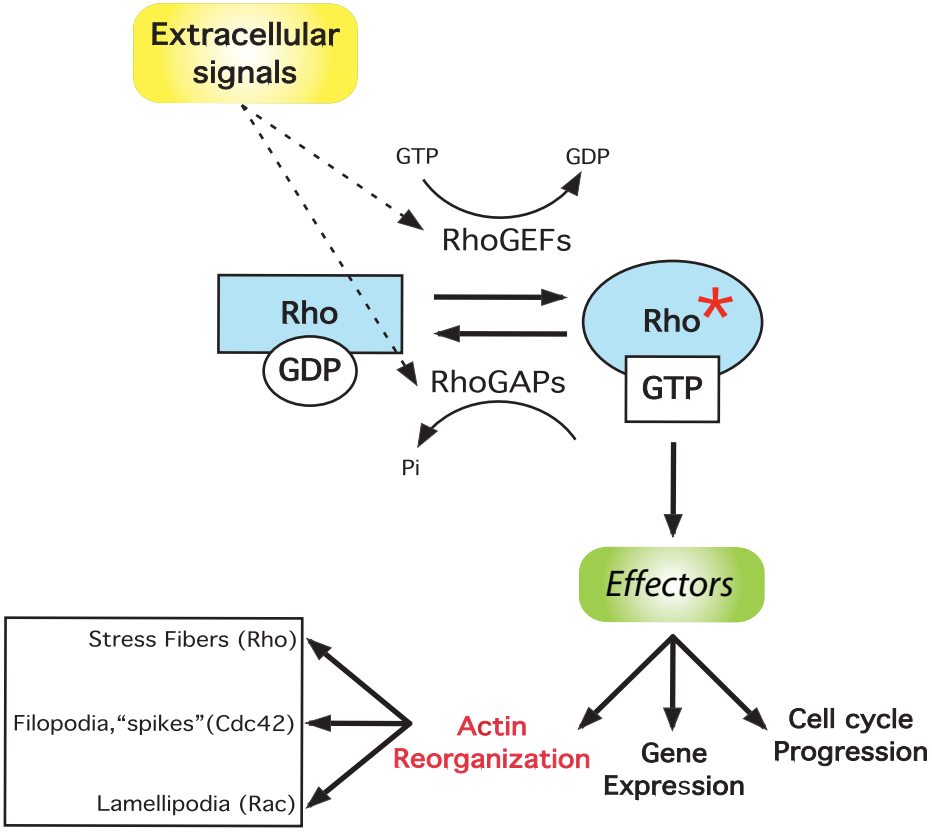

Figure 1.5. The Rho family GTPase cycle
Rho proteins are enzymes that cycle between inactive (GDP-bound) and active (GTP-bound) conformations. This cycling process is promoted by the guanine nucleotide exchange factors (GEFs) which GTP-load and activate the GTPase, while the GTPase activating proteins (GAPs) hydrolyze and downregulate GTPases. Activated Rho proteins couple to specific effectors which mediate diverse biological processes, such as remodeling of the actin cytoskeleton. A few of the active forms of RhoGTPases are associated with distinct actin structures (indicated in figure above). Adapted from [68].

high-affinity binding for GDP and GTP, and have low intrinsic GTP hydrolysis and GDP/GTP exchange activities. Positive regulators are known as guanine nucleotide exchange factors (GEFs) and negative regulators as GTPase-activating proteins (GAPs). As well, members of the Rho and Rab subfamilies are also subject to negative regulation by virtue of guanine nucleotide dissociation inhibitors (GDIs).

Characteristic of all small G proteins are the 'switch regions'. Mechanistically, these regions, termed switch I and switch II, connect to the gamma phosphate of GTP and form the 'loaded spring' conformation. GTP hydrolysis results in the release of the gamma phosphate, unloading the 'spring' and relaxing the structure for a GDP-loaded conformation [69]. Conformational changes in the GTPase switch regions between the two nucleotide-bound structures are sensed by regulatory proteins and effectors to discern nucleotide status of the GTPase. Another important feature of small G proteins is their ability to be lipid modified at their extreme C-termini (ex. Rho GTPases), and in some cases, at their N-termini (ex. Arf GTPases). These modifications allow for the stable anchorage of these relay switches to a lipid bilayer permitting them to fulfill actin regulation at specific sites [70,71].

4.1 The Rho GTPases: versatile actin regulators

The Rho family is a major branch of the Ras family of small GTPases. Members of the Rho family direct a plethora of biological processes, such as, cell cycle progression, gene expression, and most notably, actin cytoskeleton reorganization. This protein

family encompasses over 20 members in the human genome and sequence alignment analysis divides it into 8 subgroups (as depicted in **Figure 1.4, pg. 16**). The Rho GTPases can be described as classical or atypical Rho GTPases. The atypical members diverge in the sense that they are predominately GTP-bound owing either to amino acid substitutions at residues critical for GTPase activity (ie. Rnd proteins and RhoH) or to increased nucleotide exchange activity (ie. RhoU) [72,73]. Rather than being under the influence of GEFs and GAPs, these proteins are thought to be managed via gene expression, protein stability and phosphorylation [73].

Despite the fact that the Ras superfamily is highly conserved in structural detail, each subfamily is associated with a structurally distinct and highly specific family of regulatory elements. Our interests lie at the heart of Rho family GTPases and given the intricate signaling networks powered by these proteins, it becomes obvious the necessity of tight spatio-temporal regulation of their GTP-binding and hydrolysis cycle.

4.2 Rho GTPase regulators

Regulatory factors of Rho GTPases are instrumental for cycling of these proteins from active to inactive states. The sheer volume of GTPase regulators in mammals outnumbers the quantity of known Rho GTPases. A reasonable explanation for this fact is that the specialized function of individual regulators is dependent on spatial-temporal positioning and catalytic selectivity, making it discriminatory for a specific Rho GTPase or more promiscuous towards several Rho proteins. The concerted action of regulatory molecules is said to be required for efficient GTPase signaling to

downstream components [74]. Below, we discuss 3 groups of well-known Rho family GTPase regulators, with special emphasis on guanine nucleotide exchange factors as they are a central topic of this thesis.

4.2.1 Guanine nucleotide exchange factors (GEFs)

GEFs are important positive regulators for the cycling of GTPases from GDP- to GTP-bound. In response to extracellular signaling, these enzymes interact with the switch I and II regions of a GTPase. Structurally, these enzymes promote release of GDP due to the expulsion of the Mg2+ ion from the GTPase, and bind and stabilize the transient nucleotide-free form [69]. The normal function of magnesium is to neutralize the negative charge offered by the phosphate groups and increase nucleotide affinity. Magnesium exclusion promotes nucleotide 'depletion' of the GTPase, readying it for GTP-loading. The nucleotide-free transition state is now free to be loaded with GTP, which is found at higher intracellular levels than GDP, and allows for a Mg^{2+} ion to come in and strengthen the GTPase-GTP bond [48,75]. Dbl was isolated from human B-lymphoma cells and demonstrated to be the first mammalian RhoGEF [76,77]. Now, over 70 members comprise the Dbl family of GEFs, all sharing the Dbl-Homology (DH) catalytic unit responsible for its enzymatic action. Almost all Rho GEFs possess a Pleckstrin Homology (PH) domain adjacent and C-terminal to the DH domain. PH domains can interact with phosphoinositides and proteins [78,79]. This domain is suggested to function as a membrane targeting signal and/or as a key component modulating the catalytic function of the DH domain [75,80-82]. In most cases, this DH-PH

module constitutes the minimal structural unit that can promote nucleotide exchange *in vivo*. Aside from the DH-PH module, RhoGEFs contain a large and diverse array of motifs suggesting an equally diverse mode of RhoGEF regulation reflecting the many biological activities in which these motifs are known to participate.

In the last decade or so, a new family of atypical RhoGEFs has been discovered called the DOCK family (or CZH family) [83]. This family diverges from the classical Dbl family by lacking the ever present DH domain and instead possesses a novel form of the catalytic domain, termed the DOCK Homology Region-2 (DHR-2). The DHR-2 is a distinguishing feature of the DOCK family and is found in all members (mammalian DOCK1-11) [83]. While crystallization of classical DH-PH modules (alone or in complex with their favoured GTPase) allowed us to understand structurally how a GEF activated and selected a Rho GTPase, the mechanism of activation by the DOCK family for their respective GTPases, was unknown [84]. Most recently, the solving of the crystal structure of the DHR-2 of DOCK9 in complex with the Rho GTPase, Cdc42, has revealed a nucleotide sensing element within the α10 helix of the DHR-2. This sensor has the unique ability to 'sense' the nucleotide-bound state of Cdc42 and allows for transient binding of nucleotide-free Cdc42 to the DHR-2. The α10 helix interacts with the GTPase switch I region and clamps open the nucleotide-binding site. In the same instance, a highly conserved Valine at the tip of the α10 helix contributes towards nucleotide release by occlusion of Mg^{2+}. The nucleotide-free GTPase is now stably, but transiently, bound to the DHR-2 and free to be loaded with GTP. Once activated, Cdc42-GTP will be

detected by the α10 helix due to the accompanying presence of Mg^{2+}, leading to α-helix- assisted opening of the switch I region of the GTPase, and finally expulsion of Cdc42-GTP [85]. This study documents for the first time the complete structural mechanism of GTPase exchange by a GEF.

It is becoming increasingly evident that these positive regulators of the Rho GTPase cycle are themselves tightly monitored. Some general mechanisms of regulation include: (i) relief of intramolecular inhibition (ii) stimulation via protein-protein interactions, (iii) intracellular re-localization, and (iv) downregulation of GEF activity [86]. For example, it has been demonstrated that intramolecular contacts between the DH and PH domains constrain Vav2 GEF activity [87]. In response to PI 3-kinase activation and production of the lipid PIP_3, the PH domain binds the lipid and exposes the DH domain to tyrosine phosphorylation, relieving autoinhibitory interactions [88]. Thus, Vav2 exemplifies how two forms of regulation cooperate to reveal GEF activity.

4.2.2 GTPase activating proteins (GAPs)

Although small G proteins are interchangeably termed as GTPases, these proteins have low inherent GTPase activity [89,90]. GAPs are enhancers of this low intrinsic enzymatic activity, leading to accelerated GTPase inactivation by several orders of magnitude [91]. The signature of Rho family GAPs is the evolutionarily conserved RhoGAP domain, sharing at least 20% sequence identity with family members [92]. It is this domain that is responsible for the catalytic function of RhoGAPs.

Biochemically, these enzymes catalyze the stability of a GTPase's intrinsic mobile catalytic machinery, and offer a catalytic residue *in trans* that allows for G protein hydrolysis and release of the gamma phosphate, resulting in a form switch from active GTP- to inactive GDP-bound [93]. Moreover, the multi-domain nature of RhoGAPs has lead to the intriguing hypothesis that multiple signaling pathways may use RhoGAPs as a convergence point, directing tight regulation of GAP activity [90].

Finally, similar to regulatory events presiding over RhoGEFs, data indicates that RhoGAPs can be tightly managed by post-translational modifications, protein-protein interactions, lipid-protein interactions, and/or binding of second messengers [90,91]. These events re-sculpt RhoGAPs and pave the path for translocation of these enzymes to distinct areas requiring GTPase regulation.

4.2.3 Guanine nucleotide dissociation inhibitors (GDIs)

In addition to GEFs and GAPs, another level of regulation is seen with GDIs for the Rab and Rho GTPase subfamilies. These proteins can inhibit the dissociation of bound GDP from the partner GTPase, thus most likely sequestering the GTPase in an inactive form unable to interact with GEFs or GAPs [94,95]. Specifically, GDIs are capable of extracting the membrane-associated, post-translationally modified GDP-bound GTPase from the lipid bilayer via binding of the prenylated C-terminus, thus shielding the lipid-binding moiety from the lipid cell membrane [96-98]. In this fashion, GDIs serve as cytosolic pools of inactive Rab and Rho GTPases. Acting as controllers steering the reversible membrane versus cytosolic pools of GTPases, GDIs need to be disassociated

from GTPases at the opportune time and location. The mechanism of dissociation can come in the form of phosphorylation, protein displacement factors, or even localized increase of specific phospholipids, resulting in GDI/GTPase complex abrogation [99-104].

Interestingly, Hancock and Hall demonstrated *in vitro* that GDIs can complex the active form of a Rho GTPase and prevent GAP activity, possibly allowing for shuttling of Rac-GTP between physically separated activators and effectors in the cell [105]. While initially seen as having a negative regulatory role, GDIs are fast becoming acknowledged as positive regulators that can correctly target and regulate GTPase activities.

4.2.4 Regulation-defective Rho GTPases

The creation of constitutively active and dominant negative versions of Rho GTPases offers powerful tools in studying cellular processes. A constitutively active form of a GTPase carries a mutation that renders it immune to hydrolysis, and therefore locked in the GTP-bound form, forming a GTPase-dead or perpetually active mutant [106-108]. These mutants are de-sensitized to intrinsic GAPs and are activated in a ligand-independent fashion. A second type of activated mutant is personified by a guanine nucleotide-binding deficient variant termed a 'fast'-cycling' protein. These proteins have an accelerated rate of GTPase hydrolysis, with excess intracellular levels of GTP favouring GTP-loading of these mutants [109,110]. Conversely, dominant negative mutants have a single point mutation that confers a nucleotide-free state, competing with wild-type GTPases for GEF binding; these mutants have low affinity for GTP and

are incapable of binding downstream target proteins, forming 'dead-end' complexes via inhibition of GEF function [111]. Another form of GTPases is represented by mutants of the CAAX-box. These mutants are unable to be lipid-modified, thus they cannot be attached to cell membranes and/or are mistargeted resulting in aberrant function of the GTPase [112,113]. The final class of mutants are those that contain select missense mutations in the core effector domain, resulting in differential effector binding. These mutants allow for the study of the contribution of a particular effector for specific GTPase signaling and/or function [114,115]. However, the advent of these powerful tools comes with a negative side. These mutants can have unwanted non-specific effects. Constitutively active mutants can horde effector molecules shared by other GTPases, and effectively inhibit signaling by these other GTPases [116]. Also, dominant-negative GTPases can sequester a GEF that acts on more than one GTPase [117,118]. Therefore, nowadays, more studies are turning to knockdown approaches or knockout animals of GTPases to dissect their functions in cells and *in vivo* [119].

4.3 Specific Rho GTPases

The Rho GTPases RhoA, Rac, and Cdc42 constitute the most highly conserved members and are the most heavily studied and best characterized. All exert intense but notably unique effects on the actin cytoskeleton. RhoA is associated with stress fiber assembly, while Rac induces membrane ruffling and lamellipodia formation, and Cdc42 usually promotes filopodial structures [120] (**Figure 1.6, pg. 26**). As we are

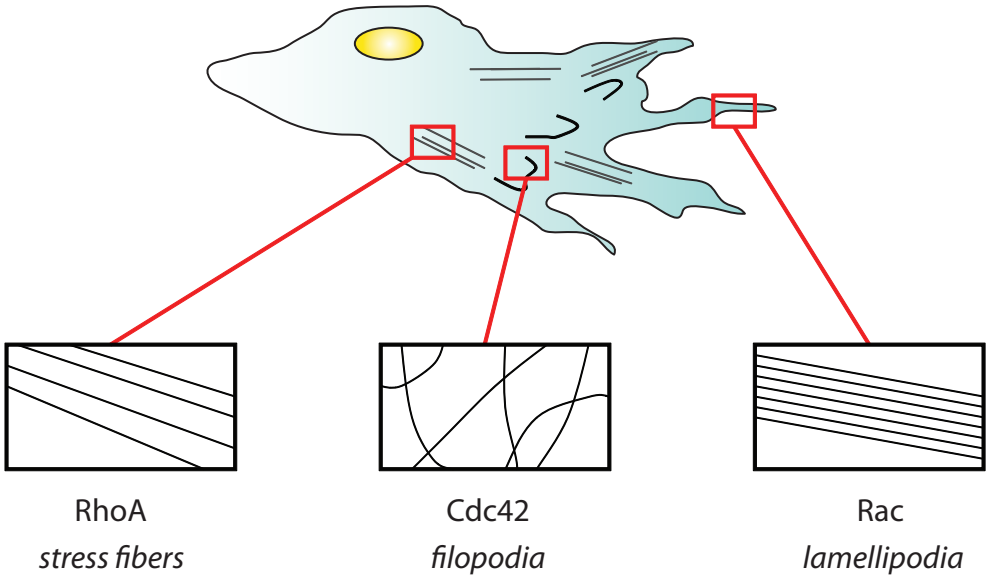

Figure 1.6 . Distinct structures of the actin cytoskeleton
The Rac, Cdc42, and RhoA GTPases, in their active conformation, are commonly associated with distinct features of the actin cytoskeleton. RhoA is responsible for stress fibers. Rac is associated with creating a meshwork of actin filaments that organize into lamellipodia structures and membrane ruffling. And finally, Cdc42 activation leads to formation of tight parellel bundles that create finger-like filopodia structures. Adapted form [120].

interested in studying the elaborate nature of lamellipodia formation, our interest is peaked by the Rac subgroup (Rac1, Rac2, Rac3, and RhoG).

4.3.1 Rac

There are three isoforms of Rac (Rac1-3) in mammals, with over 90% sequence similarity between them [121,122]. Of the three, Rac1 is the most extensively studied and the best characterized. Although involved in a diverse array of biological functions, the Rac proteins are reputed for their action on the cytoskeletal infrastructure of the cell. Specifically, these proteins are famous for creating membrane ruffling and lamellopodia at the cell leading edge [123]. Interestingly, fluorescence resonance energy transfer (FRET)-based assays have revealed Rac-GTP is also found at the non-protrusive rear of fast-moving neutrophils, suggesting active Rac has a hand in both leading edge formation and tail retraction [124]. Protrusive activity is carried out by numerous downstream cytoskeletal remodeling effectors. The serine/threonine kinase Pak was first uncovered as a Rac binding partner in 1995 and years of research have established this duo as a potent actin regulator [125]. At basal levels, a subset of Pak kinases (Pak 1-3) are repressed via intramolecular interactions, and Rac binding is able to unhinge the inhibitory contacts and stimulate kinase activity [126,127]. Myosin, LIM kinase, and cortactin are among the cohort of Pak substrates that influence cell shape and movement [128]. Besides Pak, it is demonstrated that Rac-induced actin remodeling can also occur indirectly through its interaction with the WAVE complex, activating it, and in turn activating the Arp2/3 complex [64]. This occurs in one of two ways: either

through (i) Rac-IRSp53 or (ii) Rac-WAVE complex subunits. Another group actually argues that the Rac-WAVE interaction is a localization signal rather than an activation signal for the WAVE complex at the cell periphery [129].

Intriguingly, Rac1, Rac2 and Rac3 share identical effectors loops and, at least *in vitro*, can bind and activate the same set of effectors [130,131]. However, expression of each of these proteins in cells leads to different phenotypes [122]. There is now ample evidence suggesting that subcellular targeting of these proteins, via the hypervariable C-termini of Rac GTPases, is responsible for this differential pattern [132-134]. Moreover, dissection of expression patterns has found Rac2 to be exclusively expressed in the hematopoietic system, while Rac3 is found predominantly in the adult brain, and Rac1 is distributed ubiquitously in mammals[135-138]. The generation of knock-out and conditional knock-out mice has immensely expanded our knowledge of Rac proteins *in vivo*. In 1998, the group of Katsuki demonstrated that Rac1-null mice are embryonic lethal [139]. These animals die *in utero* by E9.5 and uncover Rac1 involvement in lamellipodium formation, cell adhesion, and cell migration *in vivo*, suggesting that Rac1-mediated cell adhesion is essential for the formation of three germ layers during gastrulation [139]. Conditional knockout mice demonstrate that Rac1 is vital for polarization of neuronal cells through WAVE-induced actin cytoskeleton remodeling [140]. Another Rac1 conditional knockout model mirrors results obtained in *Drosophila*, where Rac1 is deemed necessary for myoblast fusion by remodeling the actin infrastructure at contact sites of fusing myoblasts [141-143].

Neutrophils isolated from Rac2 knockout mice demonstrate faults in cytoskeletal remodeling [144]. Aside from these hematopoietic deficiencies, Rac2-null mice develop normally and are fertile, most likely due to the restrictive expression profile for Rac2. Studies where both Rac1 and Rac2 have been knocked out in the hematopoietic system have offered intriguing insight into the roles of these two GTPases. While both Rac1 and Rac2 are required for B cell development and maintenance, another study has shown that these GTPases manifest distinct functions during actin remodeling, survival, and proliferation in hematopoietic stem cells [145,146]. Therefore, Rac1 and Rac2 display both redundant and unique tasks at different levels of hematopoietic system development and functioning.

In situ hybridization analysis indicates that Rac3 is specifically expressed in several populations of neural cells of the developing mouse [138]. Corbetta and colleagues reveal that Rac3-deficient mice survive embryogenesis in contrast to Rac1 knockout mice, and thus, Rac3 is not strictly required for normal development [147]. Surprisingly, deletion of Rac3 does not create any gross anatomical irregularities and no major effects on brain morphogenesis are detected; it is hypothesized that Rac1 may play a compensatory role here, although no upregulation of Rac1 or Rac2 was noted in the Rac3 knockout mice [147]. However, these mice do display discrete behavioural differences as Rac3 knockout animals present superior motor skills that may be accredited to subtler defects due to Rac3 deletion. In support of complementary roles of Rac1 and Rac3 in neural development, conditional and complete knockout mice of

Rac1 and Rac3, respectively, display motor defects, epilepsy, perturbed brain development, and premature death [148]. In contrast to the balancing act portrayed for Rac1 and Rac3 in brain development, another study found opposing functions for Rac1 and Rac3 during neuronal cell spreading and differentiation. Here, while Rac1 promotes cell spreading and neuritogenesis, Rac3 evokes cell rounding and hampers differentiation [149]. Both Rac1 and Rac3 interact with GIT1, and their divergent effects are correlated with differential modulation of GIT1 signaling, as well as differential subcellular localization of the proteins [150].

4.3.2 RhoG

RhoG is part of the Rho family of GTPases and shares high primary sequence similarity to Rac1 (72%) and Cdc42 (62%). Irrespective of this sequence similarity, RhoG does not bind any known Rac1 and Cdc42 effectors [151]. An eminent RhoG binding partner is ELMO (For further discussion see section 7.2 ELMO). Early studies showed that only active GTP-loaded RhoG can interact with ELMO, and this interaction can activate Rac through the ELMO/DOCK180 complex [152]. It was also concluded that RhoG is critical for integrin-stimulated Rac activation and cell spreading [152]. A more recent study by Meller and colleagues clearly demonstrates that RhoG is not required for integrin-mediated Rac activation and cell shaping. In fact, endogenous RhoG is not detected to be activated via integrin stimulation at all. Rather, RhoG is found to be a component of Rac-independent cell migration [153]. Mice knock-outs of critical Rho GTPases important for integrin-mediated cell spreading and migration, such as, Rac1

and Cdc42, are embryonic lethal [139,154]. A further proof that RhoG is not part of the machinery critical for integrin-mediated cell migration is the fact that RhoG-null mice are viable with subtle defects in the blood system [155]. Clearly, further studies exploring cell type specificities and spatio-temporal location are required to understand the debated involvement of RhoG during mammalian cell migration.

In the following section we will discuss another family of small GTPases, the Arf family, which themselves are integral components of the machinery controling cell shape. We are particularly interested in this family, since, in Aim #3 (Chapter 4) of my thesis, we uncover the Arf family member, Arl4A, as a novel ELMO binding protein.

4.4 The Arf family

The complete human Arf family consists of 29 members, divided into three subfamilies: Arf, Arf-like (Arl) and Sar1 [156]. The biological role(s) of this protein family is not well understood, although some members are well-known to be critical elements regulating membrane trafficking and cytoskeletal re-structuring [157] . Similar to other Ras family members, these proteins are tightly regulated by GEFs and GAPs, and are subject to lipid modifications leading to membrane anchorage [157]. However, the Arf family is divergent from other small G proteins in two distinct ways and these features are universal amongst all members. For one, unlike GTPases that have lipid tail modifications at the C-terminus, the Arf family members are lipid-modified at the N-terminal amphipathic helix via myristoylation [157,158]. This helix is retracted into the protein core in the inactive state, so that inactive Arfs are primarily cytosolic [159]. The

second feature is the interswitch region located between the two switch regions [160,161]. In the inactive form, the interswitch is fastened to the N-terminal helix and blocks the GTP binding site [161]. Once in the GTP-bound form, the interswitch will displace the N-terminal helix and promote its insertion into a lipid membrane. These uncommon features of the Arf family define its members and have many functional consequences. Firstly, the nucleotide state is tightly coupled to membrane binding. Secondly, the link between the amphipathic helix and the rest of the molecule is short, leaving effectors bound to the effector core region very close to the lipid bilayer.

4.5 Arf regulators

4.5.1 Arf GEFs

In a manner reminiscent to Rho GEFs, Arf GEFs positively regulate members of the Arf family. This action is matched with interswitch displacement leading to tight tethering of the N-terminal amphipathic helix to the membrane [160,162]. Studies from yeast to mammals have unveiled a patent trademark for Arf GEFs with regard to domain architecture. These proteins may differ highly in terms of overall structure, but one universal consistency is the ~200-residue Sec7 domain responsible for catalytic function of the GEFs [163,164]. The exception to the rule is mSec12, an Arf GEF for Sar1, which contains no such obvious enzymatic domain [165,166]. Using the Sec7 as a signature, research has exposed 15 Arf GEFs grouped into six evolutionarily conserved families: GBF1, BIG, PSD, IQSEC, cytohesins, and FBXO8 [157].

4.5.2 Arf GAPs

Similar to most Ras GTPases, most Arf members have a slow intrinsic hydrolysis rate. To shut off these proteins, there exists a wide array of ArfGAPs. These GAPs are defined by the unique ~130-residue Arf-GAP domain responsible for promoting GTP hydrolysis, and thus far, have only been shown to act on the Arf subfamily (Arf1-6). To date, 31 human ArfGAPs have been identified and classed into 10 families [167]. Akin to the Arf GEFs, the ArfGAPs families share a signature domain but otherwise can be highly divergent in structure [157,167,168]. Of note is the recently uncovered ELMOD family of ArfGAPs that lack the signature Arf-GAP domain, but displays GAP activity for certain Arf and Arl GTPases [169]. This is the first demonstration of a GAP for an Arl member, which proposes that a whole new realm of regulators is waiting to be discovered for the Arl family.

4.6 Arf6

There are six mammalian Arfs divided into three classes based on their sequence similarity: Class I (Arf1-3), Class II (Arf 4-5) and Class III (Arf6) [170]. The six members of this GTPase family are outnumbered by their regulators, indicating tight management of signaling events is at play here.

Arf1 and Arf6 are the most well studied of the family [157,171-173]. Arf1 is implicated in endoplasmic reticulum-to-Golgi transport, Golgi function, transport from the *trans*-Golgi network, transport in the endocytic pathway and recruitment of

paxillin to focal adhesions [174-178]. Arf6 is attributed with many cytoskeleton remodeling roles and has been found to affect endocytosis, phagocytosis, receptor recycling and the formation of actin rich protrusions and actin-rich membrane ruffles [173,179]. Arf6 can traffic the notorious cytoskeletal remodeller, Rac1, to distinct areas of the cell periphery (see section 5.3.2 Arf6-Rac) and overexpression studies place Arf6 upstream of Rac1 [180-183]. Indeed, it has been demonstrated that Arf6 and Rac1 are able to form a complex, albeit transient, at the cell membrane [184]. Arf6 can also influence actin through other mechanisms. For example, Arf6 has been found to activate phosphatidylinositol 4-phosphate 5-kinase, resulting in the accumulation of PtdIns(4,5)P_2, a lipid that binds to actin regulators [185-188].

In vivo, Arf6 and its GEF, *loner*, play a role during myoblast fusion in *Drosophila*. The *loner*-Arf6 partnership is deemed a controller of dRac1 targeting since *loner* mutants reveal a diffuse pattern of dRac1 localization [189]. In mammals, i*n vivo* knockout studies demonstrate that Arf6 mice die at birth, with principle defects in liver development attributed to inefficient alignment of hepatocytes. However, the molecular mechanisms involved in this deficiency remain a mystery [190].

4.7 Arl4

In the pursuit of identifying additional Arf family members, a whole subfamily of Arf-related proteins was unearthed and termed the Arf-like (Arl) GTPases [191] [192]. In mammals there are 22 identified Arl forms [156]. Although generally similar in structure to traditional Arf GTPases, the Arls GTPases can differ considerably in terms of

mechanisms of intracellular targeting and activation [193]. Arls display a large range of function as they have been implicated as regulators of microtubule-dependent processes (Arl2 and Arl3 [194-198]), lysosome mobility and microtubule binding (Arl8 [199,200]), ciliogenesis (Arl3 and Arl6 [201-206]), and tumorigenesis (Arl11 [207,208]). To date, the roles of most Arl GTPases remain unsolved.

Notable among Arls are the Arl4 proteins (Arl4A, Arl4C, and Arl4D) which have recently emerged as important cytoskeletal regulators [209,210]. In terms of structure, these three proteins are similar to other Arf family members, yet are unique by virtue of a short basic extension at the C-terminus [161] (**Figure 1.7, pg. 36**). Interestingly, the N-terminal amphipathic helices of the Arl4 proteins are shorter and less hydrophobic than those of other Arf family members. Deletion of the C-terminal basic extension in cells results in displacement of Arl4A from the plasma membrane, advocating that this basic extension may function as a support system rather than the major localization factor of Arl4 proteins to membranes [209]. Although this basic extension has also been noted to bear a striking similarity to nuclear localization signals [211,218], none of the full-length proteins of this family are restricted to nuclear compartments [212].

Alignment of primary sequences reveals a close-knit Arl4 family [212]. However, analysis of expression patterns in human tissues paints a different localization picture, with Arl4A predominant in the testis, Arl4C chiefly in brain tissue, but also in spleen, thymus, esophagus, stomach, intestine, and uterus, and Arl4D principally located in kidney, testis, esophagus and uterus [212]. It is noteworthy to mention that

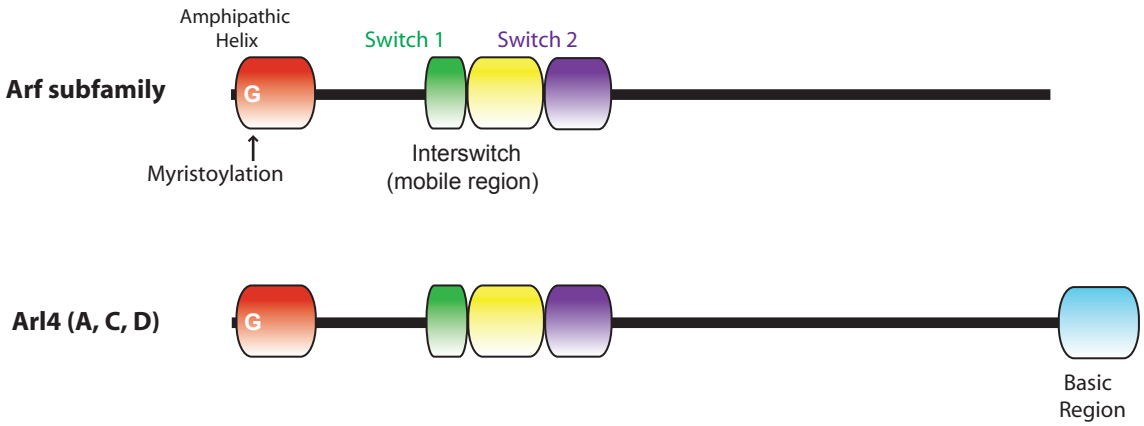

Figure 1.7. The Structure of Arf Family GTPases.
Schematic representation depicting the difference in structure of a typical Arf subfamily member (top) and Arl4 (bottom). Myristoylation occurs at the N-terminus on a conserved Glycine at position 2. Since the N-terminal helix in Arl4 is less hydrophobic than those of other Arf family members, it is hypothesized that its unique C-terminal basic region aids the helix-lipid interaction by offering a stabilizing effect.

these proteins exhibit unusually high guanine nucleotide exchange rates *in vitro* [212], suggesting that they are in constitutively active forms in cells.

In situ hybridization studies of mammalian Arl4A demonstrate developmental regulation of Arl4A mRNA and implicates this protein in spermatogenesis, somitogenesis, and embryogenesis of the central nervous system [213]. A knock-out mouse model of Arl4A supports its role during spermatogenesis [214]. Moreover, these mice are viable and display only a reduced sperm count with fertility being normal in males [214]. Reduced sperm count is often associated with a defect in apoptotic cell removal, where non-clearance of lingering cells marked for death leads to poor sperm quality [215]. In depth *in vivo* analysis of all Arl4 forms with classical and conditional knock-out animals are alluring. These mice would help to decipher differences between the three proteins, and if compensation is an important factor at play.

In 2007, two independent studies demonstrated that the Arl4 family members are capable of binding cytohesins [209,210]. Cytohesins are multidomain proteins that include a Sec7 and PH domain, and are branded ArfGEFs, well-known to contribute to the remodeling of the actin network of cells [173, 159]. As previously mentioned, Arf6 can control several processes such as endocytosis and actin dynamics, and cytohesin-2 (or ARNO) is a major activator of this GTPase [216 173]. To do so, ARNO needs to be recruited from the cytosol to the membrane where Arf6 is located; it has been suggested that this recruitment was occurring through the dual binding capability of the PH domain for phosphoinositides and Arf6 [159,217, 218]. The groups of Munro and Lee discovered that

active Arl4D binds the PH domain of ARNO and recruits the molecule to the membrane and the lipid-binding affinity of the ARNO PH domain is not required for this action [209,210]. Together, these data argue that Arl4D is a novel upstream component controling ARNO and promoting Arf6 activation and cytoskeletal rearrangement [209,210]. However, how the active Arl4 protein is itself targeted to specific locations at the right instances remains an open question.

5. Modes of GTPase regulation

Ras G proteins control numerous protein functions, and are themselves managed by a variety of protein-protein interactions. Many proteins have been cited to positively or negatively influence GTPase signaling. In Chapter 3 of my thesis, we introduce a novel mechanistic hypothesis for Rac GTPase regulation via the DOCK180/ELMO complex that is reminiscent of GTPase regulation via the formins. Highlighted below are some modes of GTPase regulation by formin proteins.

5.1 Liberating formins

Not only are formins actin nucleators, but they also act as Rho family effectors, increasing signaling intricacies downstream of these proteins [219]. In mammals, the DRF family includes Dia1-3, DAAM1-2, FMNL1-3, FHOD1 and FHOD3 [220]. Structurally, this protein family is distinct by virtue of a GTPase Binding Domain (GBD), Diaphanous Inhibitory Domain (DID), Diaphanous Autoregulatory Domain (DAD), and a short basic region at the C-terminus (**Figure 1.8, pg. 39**) [221-225]. Essentially, at basal

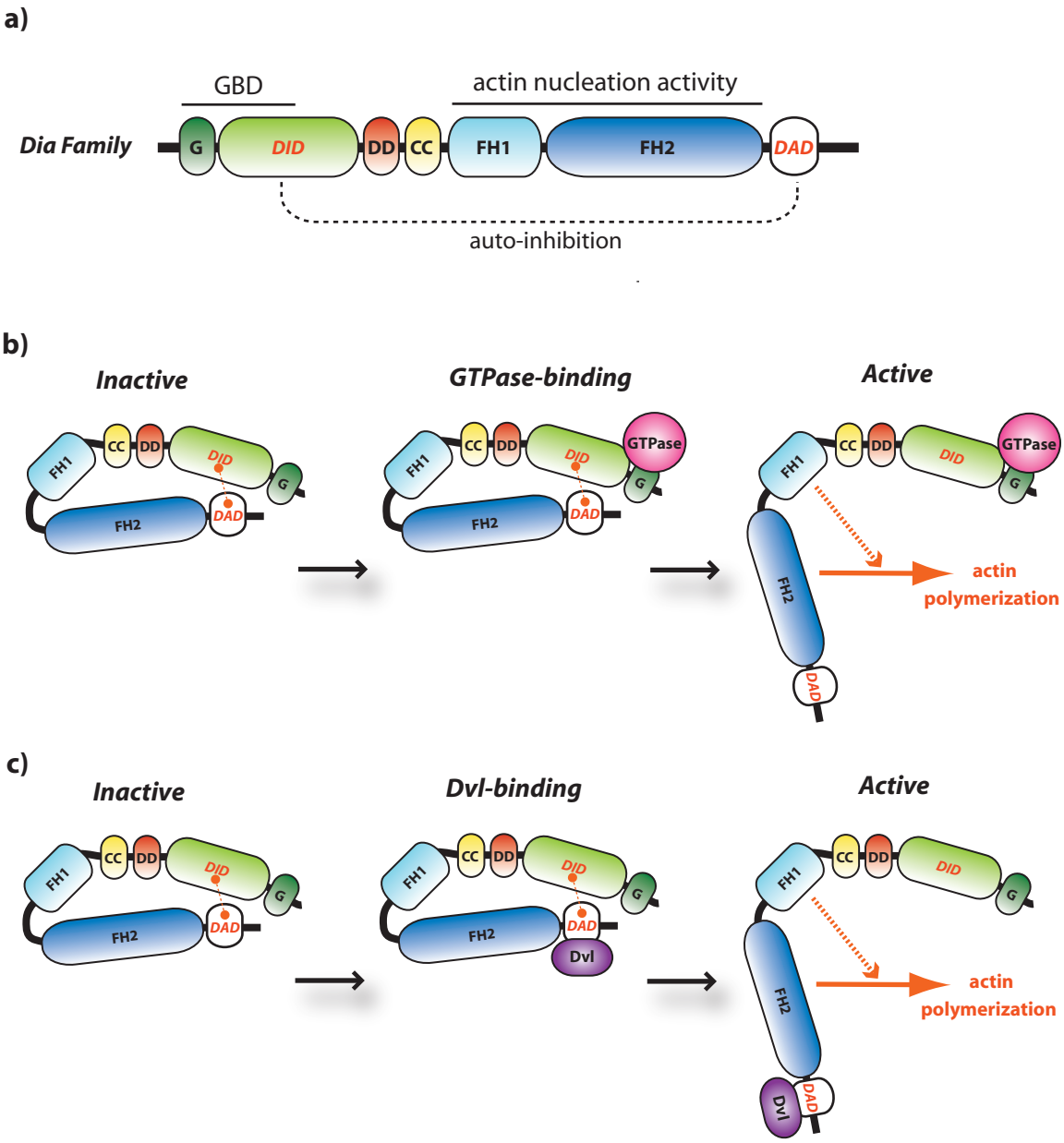

Figure 1.8. Dia family domain architecture and modes of regulation.
a) Schematic representation of the domain structure of Dia-related formins (DRFs). At the N-terminus, the GTPase-binding domain is followed by the inhibitory DID, dimerization domain (DD), coiled-coil region (CC), and the actin nucleation module of FH1 and FH2 regions. Finally, at the C-terminus is the autoregulatory DAD. These formins are repressed via intramolecular contacts between the DID and the DAD at basal levels, masking its actin nucleation activity. Relief of autoinhibition of DRFs can occur through **b)** GTPase binding (ex. RhoA binding to Dia1 GBD) or **c)** C-terminal binding (ex. Dvl binding to DAAM1 DAD).

unstimulated levels, DRFs form a repressed autoinhibited state through intramolecular contacts between the N-terminal DID and the C-terminal DAD. Structurally, the DID is made up of tandem armadillo repeats, known protein-protein interfaces [221], that create a stunning helical arrangement with a hydrophobic groove. The MDxLL consensus motif of the DAD forms a core α helix that collapses into the concave site of the DID hydrophobic groove [224,225]. This repression is released via protein binding to different modules of the DRF, unleashing formin nucleation activity and actin polymerization through the newly exposed dimeric catalytic FH2 domain [226,227, 228, 229, 230, 221] (**Figure 1.8, pg. 39**).

5.2.1 Dia Family

Dia1 is the best structurally and functionally characterized formin to date [231]. Dia1 was first described as an effector for RhoA, with active RhoA binding to the GBD disrupting the intramolecular DID/DAD dormant conformation and inducing formation of thin actin stress fibers [226,227,229,232] (**Figure 1.8, pg. 39**). The importance of the GBD regulatory feature is amplified by the finding that deletion of this domain results in a constitutively active variant of Dia1 that epitomizes strong cytoskeletal remodeling even in the absence of GTPase-binding.

Most recently, Rif, another Rho family GTPase, was found to form complexes with both Dia1 and Dia2 [233, 234]. As is the case for Rho-Dia interactions, the Rif-Dia coupling occurs through the Dia GBD, releasing Dia from its inhibition. Intriguingly, Rif binding to Dia1 and Dia2 induces completely different cytoskeletal forms. While Rif

triggers stress-fiber formation through Dia1, the Rif-Dia2 complex sparks filopodia formation in epithelial cells[233, 234]. Previously, the traditional cytoskeletal structures of stress fibers and filopodia were considered under the control of RhoA and Cdc42, respectively. The influence of Rif on these structures reveals how non-classical Rho GTPases are quickly budding into interception points for creating new signaling avenues for cytoskeletal regulation.

The opening up of autoinhibited DRFs leads to some exciting possibilities. Not only is the actin polymerization activity of these proteins unmasked, but other regions may also only become accessible once the proteins are awakened. Case in point, the Dia1 DID has recently been found to couple with IQGAP1, and this interaction is permitted only once Dia1 is activated through RhoA-binding to its GBD, making the hidden DID region available to IQGAP1 [235]. IQGAP1 is a cytoskeletal scaffold protein that is necessary for subcellular localization of Dia1 in human cells [235]. This interaction also appears to be critical for phagocytic cup formation in macrophages, displaying how a variety of molecules can converge to control the many facets of actin rearrangement.

5.2.2 DAAM1

Restricted in a similar fashion as Dia proteins, DAAM1 needs to be freed from its locked conformation in order to carry out its biological functions. Reports indicate that DAAM1 plays a vital role during *Xenopus* embryogenesis through control of planar cell polarity [236,237]. Similar to Dia1, DAAM1 can bind RhoA through its N-terminal GBD [236].

Interestingly, rather than a Rho GTPase binding-dependent release of autoinhibition, DAAM1 is found to bind Dvl through its C-terminally positioned DAD, leading to downstream RhoA activation possibly through DAAM1 interaction with a RhoGEF and/or RhoGAP. Therefore, in this instance, instead of being turned on via GTPase binding, DAAM1 is an upstream component for Rho activation and modulator of the actin cytoskeleton for noncanonical Wnt signaling and cell motility during vertebrate gastrulation [236] (**Figure 1.8, pg. 39**).

Interestingly, biochemical studies show that Rho does not fully activate the formin Dia1 *in vitro* [44,228,238,239], implying that other mechanisms are at play to render formins to a fully active state. Whether other carboxyl-terminal binding proteins are responsible for their full activation, as is the case for DAAM1, remains to be uncovered [44,228,238].

5.2.3 FHOD1

Crystallization of the N-terminal region of the DRF FHOD1 quickly acknowledged FHOD1 as an outlier of this family in terms of GBD structure. The FHOD1 GBD reveals an ubiquitin superfold very similar to that of the Ras-binding domains (RBDs) of c-Raf1 and PI3 kinase, and has the characteristic of binding Rac and not Rho or Cdc42 [240,241]. As demonstrated for other formin members, the GBD is viewed as a key GTPase docking site that, when engaged, releases and activates the protein. The unusual nature of the FHOD1 GBD (herein referred to as the FHOD1 RBD) is illustrated by deletion experiments that demonstrate that removal of the RBD does

not activate the formin as in Dia. Rather, the interaction with Rac seems to be a recruitment signal and is insufficient in activating the protein [241]. Notably, phosphorylation events by ROCK at three specific sites within the DAD unlock the compressed autoinhibited state and induce F-actin stress fiber assembly [242]. This data points to potential alternative roles of the formin GBD that have yet to be defined [231,243].

5.3 GTPase cascades

An interesting concept that has arisen in recent years is the regulation of Ras GTPases by other Ras GTPases. Nature has evolved a spectacular web of liaisons between members of the Ras family of G proteins, leading to elaborate manipulation of cell shape and motility. Discussed below are the following GTPase cascades: (i) Arf6-Rac, (ii) RhoG-ELMO-DOCK180-Rac1, (iii) Arl4-ARNO-Arf6-Rac1.

5.3.1 Arf6-Rac

Cross-talk between the Arf6 and Rac pathways is present during many biological processes. One of the earliest studies found Arf6 to be required for Rac-mediated membrane ruffling in macrophages, and subsequent research has endorsed this partnership during neurite outgrowth, cell spreading, cell migration, and phagocytosis [180,244-246]. The question of how Arf6 regulates Rac activity is quite complex. One early model suggests Arf6-mediated endosomal trafficking of Rac positions this GTPase at the migrating front of cells. Another model hypothesizes that Arf6 activation will recruit the DOCK180/ELMO complex, a bipartite Rac GEF, to the

leading edge of a cell [180]. The exact mechanism by which Arf6 positions this bipartite GEF to the cell periphery remains obscure. A recent study proposes a direct interaction between Arf6 and DOCK180; essentially, multi-complex formation between ARNO and DOCK180, an Arf6 and Rac GEF, respectively, promotes cell migration. This Arf6-to-Rac signaling entails the interaction of scaffold proteins GRASP and IPCEF with ARNO to direct Arf6 towards Rac [182].

An interesting finding in polarized Madin-Darby canine kidney (MDCK) cells induced to scatter demonstrates that the Arf6 effect on Rac activity is biphasic [247]. Initially, as the cells scatter, the levels of Rac-GTP undergo a transient drop. This decrease in Rac activity may partially be explained by Arf6 recruitment of NM23-H1, an inhibitor of the Rac GEF, Tiam1 [248]. Gradually, Rac-GTP levels are restored as cells take on a migratory phenotype with extensive lamellipods at the leading edge of cells. This latter phase coincides with an increase in Arf6 activity, leading to an interesting idea where Arf6 may act as an attractant for specific Rac GEFs. Therefore, in this cell type, Arf6 acts as both a negative and positive regulator of Rac activation.

Balasubramanian and colleagues suggest that rather than being a delivery system for Rac to the cell periphery, Arf6 can traffic lipid rafts to the membrane to which Rac can then anchor onto [249]. Lipid rafts are known to be transported to the membrane in an integrin-dependent manner, and therefore, this theory offers an attractive mode of Arf6-mediated regulation of Rac that is cell adhesion-dependent.

5.3.2 RhoG-ELMO-DOCK180-Rac1

A genetic cascade starting with RhoG and ending with Rac1 has been demonstrated in both mammalian cells and in *C. elegans*. ELMO is at the heart of this signaling cascade, bringing together the two Rho family GTPases. In mammalian cells, active RhoG binding to ELMO is coupled to localization of the ELMO/DOCK180 and/or ELMO/DOCK4 complexes to the cell periphery for spatially restricted Rac activation and subsequent cell spreading and migration [250,251]. *In vivo* in *C. elegans*, a well-defined signaling network of *ced-2/ced-5/ced-12* (worm orthologs of mammalian CrkII/DOCK180/ELMO, respectively) is positioned upstream of the Rho GTPase *ced-10* (worm ortholog of mammalian Rac1) during phagocytosis of apoptotic cells and cell migration processes [252-254]. *MIG-2* (worm ortholog of mammalian RhoG) is proposed to be an upstream component of this pathway [255]. Here, ELMO is postulated to serve as a scaffold where *MIG-2* binding to the ELMO N-terminus and DOCK180 binding to the ELMO C-terminus, bridge RhoG and Rac, both critical for proper clearance of apoptotic cells.

5.3.3 Arl4-ARNO-Arf6-Rac1

An interesting case of GTPase signaling cascades is offered by the connection between Arl4-Arf6 and Arf6-Rac. Two independent studies revealed that Arl4 is able to bind the Arf6 GEF, ARNO, localize it to the plasma membrane and induce Arf6 activation and cytoskeletal changes [209,210]. Many other studies document that Arf6 activity is required for proper spatial restriction of Rac activation in the cell

[180,181,183,184,256]. It is possible that signaling through Arl4 can assemble Arf6, and in turn, Rac, to the leading edge of a migrating cell where Rac GEFs can locally activate the GTPase.

5.3.4 Rab5-Rac1

Rac-induced cell motility requires a restricted pattern of Rac localization at the leading edge. Although many avenues to constrained localization are possible, a recent study proposes an interesting notion where Rab5 controls endosomal trafficking of Rac to the plasma membrane [257]. Also, it is proposed that Rac is activated on the endosome through simultaneous recruitment of the Rac GEF, Tiam1. In this way, rather than having arbitrary Rac activation at the cell periphery, the Rab5 endosomal pathway will target active Rac to discrete areas of the cell. Intriguingly, this process is dependent on Arf6, as Arf6-knockdown blocked shuttling of Rac from endosomes to the plasma membrane [257]. However, whether the role of Arf6 in this process is dependent on its well documented function in endocytosis or its involvement in targeting lipid rafts to the membrane (sites of Rac attachment) remains to be demonstrated.

6. The DOCK family of atypical GEFs

6.1 History of DOCK discovery

The discovery of DOCK180 (also known as DOCK1) unlocked a gateway to novel regulators of Rho GTPases. First discovered as a Crk-binding protein with unknown function, Hasegawa *et al.*'s initial study revealed that this protein was able to induce

morphological cell changes when artificially targeted to the plasma membrane *in cellulo* [258]. This same group later found DOCK180 to work downstream of integrins and upstream of Rac, and demonstrated that DOCK180 can directly interact with Rac1 [259]. However, the mechanism by which DOCK180 was acting as an activator for Rac was still unknown. Studies in the model organisms *C. elegans* and *Drosophila* identified *ced-5* and Myoblast City (MBC), respectively, as orthologs of mammalian DOCK180 [260,261]. In *C. elegans, ced-5* is required for phagocytosis of cell corpses by engulfing cells and for coordinated migration of gonadal distal tip cells (DTCs), two processes that require active and dynamic restructuring of the actin cytoskeleton [261]. The DOCK180 link to both CrkII and Rac was also made in the worm, as mutants of *ced-2* (worm ortholog of CrkII) and *ced-10* (worm ortholog of Rac1) display the same defects as *ced-5* mutants [261,262]. These three proteins were found to act in the same genetic pathway during phagocytosis of apoptotic cells and DTC migration [262] (**Figure 1.9, pg. 48**). The alliance of *ced-2/ced-5/ced-10* in *C. elegans* was also found to act in mammalian cells during phagocytosis. It was demonstrated that the integrin $\alpha_v\beta_5$ recruits the CrkII/DOCK180/Rac complex for efficient recognition and internalization of apoptotic cells [263].

In *Drosophila*, mutants of MBC are defective in myoblast fusion, dorsal closure and cytoskeletal remodeling [260]. These defects mimic those of mutant dRac1 (fly ortholog of Rac1) leading to the hypothesis that similar to mammalian DOCK180 and

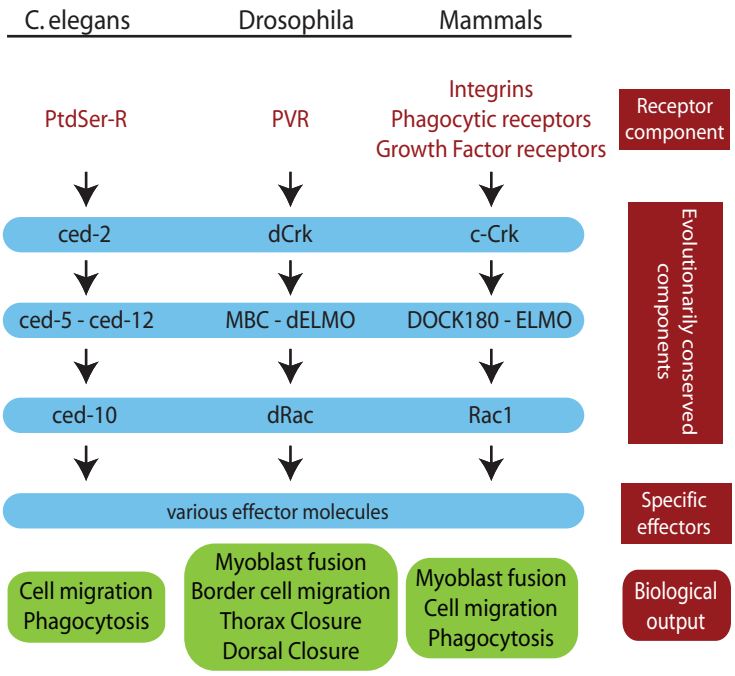

Figure 1.9. Overview of DOCK180 and its orthologs in *Drosophila* and *C. elegans* in various biological processes.
DOCK180, ELMO, and Crk (and their orthologs in the worm and fly) are part of an evolutionarily conserved signaling pathway upstream of the Rho GTPase, Rac. Through various effector molecules, this signaling module has been shown to perform in a plethora of biological processes requiring dynamic cytoskeletal reorganization. Some of these events include cell migration, phagocytosis of apoptotic cells, and myoblast fusion. Adapted from [68].

Rac, and worm *ced-5* and *ced-2*, MBC and dRac1 are part of the same pathway in *Drosophila* [142,264]. Although it seems obvious that these proteins are involved in the same genetic cascade, important questions remained unanswered: How is DOCK180 connected to Rac? Is it a direct activator of Rac or does it act as a scaffold for the true Rac activator?

In comparison to the classical DH-PH Rho GEFs, the DOCK proteins were initially viewed as non-conforming activators of GTPases. Below, we discuss in detail DOCK family members, their evolution as *bona fide* Rho GTPase activators, and their roles in various biological settings.

6.2 Structure and function

The original discovery of the DOCK superfamily was made with primary sequence analysis using human DOCK180. The mammalian DOCK family of GEFs consists of 11 members and is classed into 4 subfamilies based on sequence similarity, structural homology and GTPase-selectivity: DOCK-A (DOCK180, DOCK2, DOCK5), DOCK-B (DOCK3, DOCK4), DOCK-C (DOCK6, DOCK7, DOCK8), and DOCK-D (DOCK9, DOCK10, DOCK11) [265-267] (**Figure 1.10, pg. 50**). The pertinent *Drosophila* and *C. elegans* orthologs, MBC and *ced-5*, respectively, are grouped in the DOCK-A subfamily. Orthologs have also been identified in *D. discoideum* (amoeba), *A. thaliana* (plant) and *S. cerevisae* (fungi), showing conservation of these proteins through evolution [265,266]. Structurally, these unconventional GEFs deviate from classical GEFs due to two defining modules that are exclusive to this protein family: the DOCK Homology

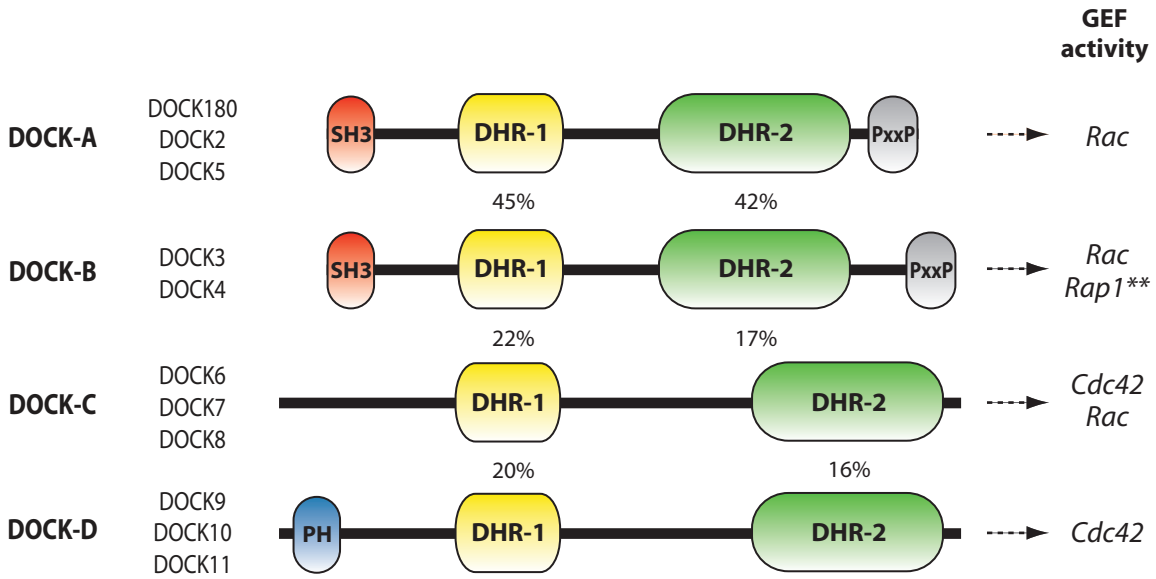

Figure 1.10. The DOCK Family of Atypical GEFs.
There are eleven DOCK180-related proteins in mammals: DOCK1 (DOCK180) - DOCK11. The DOCK members are grouped into four subfamilies (DOCK-A to DOCK-D) depending on sequence similarities and domain architecture. All members contain the signature evolutionarily conserved domains DOCK Homology Region (DHR)-1and DHR-2. The DHR-1 displays lipid-binding and membrane-targeting properties, while the DHR-2 is responsible for GEF activity towards their respective Rho family GTPase(s). The four subfamilies are also grouped via substrate specificity, with DOCK-A and DOCK-B displaying Rac GEF activity, DOCK-C demonstrates dual GEF activity on Cdc42 and Rac, and DOCK-D is specific for Cdc42. One exception is DOCK4, which also demonstrates GEF activity for Rap1 (indicated above by **). Percentages indicate the sequence similarity (identity) between the DHR-1 and DHR-2 between DOCK subfamilies. Adapted from [68].

Region-1 (DHR-1) and DHR-2, with the percentage of identity for these domains decreasing from subfamily DOCK-A to DOCK-D [68,265,266] (**Figure 1.10, pg. 50**). The DHR-2 is responsible for the catalytic function of DOCKs, serving as the counterpart to the enzymatic activity of the DH/PH module of classical GEFs. Studies by many different groups demonstrate that DOCK180, DOCK2-DOCK7, DOCK9 and DOCK10 all display catalytic function towards various GTPases [85,250,268-273].

The DOCK proteins have demonstrated specificities for different Rho GTPases (**Figure 1.10, pg. 50**). Members of the DOCK-A and DOCK-B families exhibit specificity for Rac (with the exception of DOCK4 which is also a Rap1 GEF), while DOCK-C members display dual specificity for Rac and Cdc42, and the DOCK-D subfamily is confined to Cdc42 [68]. Crystallization of the DOCK9 DHR-2 in complex with Cdc42 has enlightened our mechanistic understanding of how this family of RhoGEFs activates GTPases. However, the structural determinants that bias a DOCK GEF for specific Rho GTPase remain unknown. Controversy has arisen in the literature questioning whether the DHR-2 of a DOCK GEF is necessary and sufficient for GTPase activation or whether an additional factor (ie. ELMO) is required to uncover its GEF activity. This subject will be addressed in Aim #1 (Chapter 2) of my PhD thesis.

The other well-conserved feature in DOCKs is the DHR-1. Functionally in cells, DOCK180 DHR-1 point and deletion mutants did not hinder Rac activation, but were unable to localize efficiently to the plasma membrane and showed deficiencies in cell polarization (elongation) and migration, pointing to the functional necessity of this

conserved domain [274]. Primary sequence alignment found that the DHR-1 bears similarity to C2 domains, known lipid-binding modules. Concurrently, it was demonstrated that the DHR-1 of DOCK180 binds specifically to the PI3K by-product, PtdIns(3,4,5)P_3 *in vitro* [274]. Further studies have attributed the same property to the DHR-1 of DOCK2 and DOCK4 *in vitro* [275,276]. Although the isolated DHR-1 of DOCK9 has not been tested for lipid binding, the full-length protein demonstrates affinity for PtdIns(4,5)P_2, PtdIns(3,5)P_2, and PtdIns(3,4,5)P_3 [277]. Thus, this region is reported to have both lipid-binding and membrane-targeting ability. Our recent structural study revealed the crystal structure of the DHR-1 of DOCK180 [278]. This region contains a core Type II C2 domain with important distinguishing insertions which, in the past, were likely responsible for the non-identification of the DHR-1 as a canonical C2 domain-containing region by sequence analysis. Three upper surface loops are responsible for interaction with the head group of the phospholipids PtdIns(4,5)P_2 and PtdIns(3,4,5)P_3 *in vitro*, and for localizing the protein at the cell membrane [278]. One model suggests that this dual ability to bind PtdIns(4,5)P_2 and PtdIns(3,4,5)P_3 allows for targeting to the membrane via the more abundant PtdIns(4,5)P_2, which then allows the DOCK protein to search the vicinity for the more rare and localized PI3K-generated PtdIns(3,4,5)P_3 at the leading edge of a cell [278].

In addition to the well-conserved DHR-1 and DHR-2, primary sequence alignment revealed that the DOCK subfamilies contain other well-conserved domains. All members display a C-terminally positioned proline-rich region. At the N-terminus,

members of DOCK-A and DOCK-B subfamilies have a SH3 domain, while those from subfamily DOCK-C contain a PH domain [83,266] (**Figure 1.10, pg. 50**). These regions of the DOCK proteins are typically linked in the literature with two other proteins: CrkII and ELMO. These DOCK interacting partners will be reviewed in the next section as they are pertinent for understanding DOCK function and regulation. DOCK and ELMO are inseparable in many important biological processes and will be discussed further in section 9. Physiological functions of DOCK and ELMO.

7. DOCK-interacting partners

7.1 Crk

The original discovery of DOCK180 was made in 1996 by the group of Matsuda in search of novel Crk-binding partners. Crk (*c*hicken tumour virus no. 10 [CT10] *r*egulator of *k*inase) was initially identified as a viral oncogene capable of transforming chicken embryo fibroblasts [279]. Crk was the first identified adaptor protein and is a multi-tasking scaffold that can act as a docking station for a plethora of molecules/complexes leading down to a variety of signaling highways essential for cell remodeling and migration. The Crk family includes 4 members: CrkI, CrkII, CrkIII, and Crk-like (CrkL). CrkI-CrkIII are splice variants of the same gene and CrkL is a product of a distinct gene [280-283]. These adaptor proteins feature no catalytic activity, but are able to bridge together many molecules due to well-defined modules that can initiate a cascade of signaling pathways.

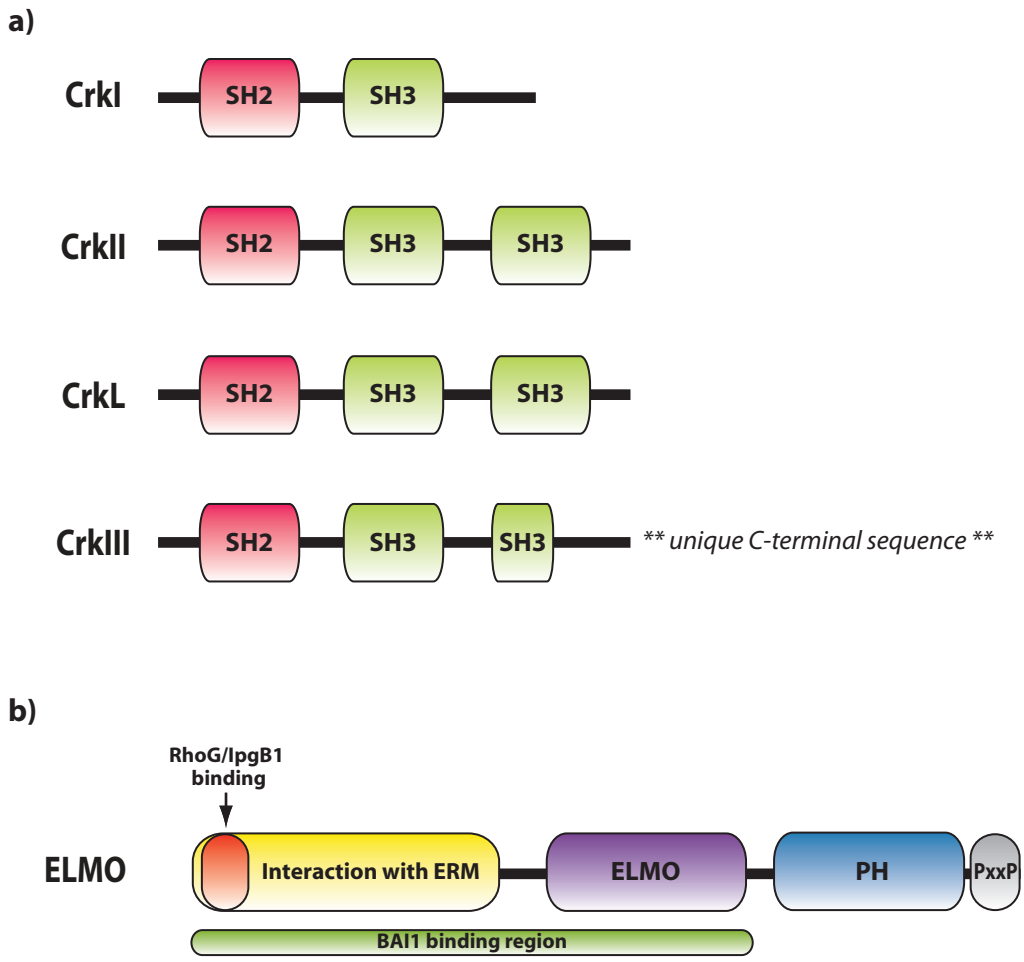

Figure 1.11. Domain architecture of mammalian Crk and ELMO proteins.
a) The Crk family. Four forms of Crk have been identified in mammals. CrkI and CrkII are products of same gene, each 28 and 40kDa, respectively. CrkL is a product of a distinct gene, but has a similar overall domain structure to CrkII. And CrkIII is similar to CrkII, but is truncated within the C-terminal SH3 domain and has a unique C-terminal sequence. **b)** The ELMO family. Although there are three form of ELMO (ELMO1-3) in mammals, most studies have focused on ELMO1 in these organisms. Structurally, ELMO has a RhoG (active form) and IpgB1 (bacterial protein) binding site at its extreme N-terminus. The N-terminus is also cited to bind ERM proteins and the phagocytosis receptor, BAI1. A conserved but unexplored ELM domain is positioned centrally, followed by a PH and proline-rich motif at its C-terminus.

Highly homologous in terms of structure, Crk proteins are composed virtually solely of SH2 and SH3 domains (**Figure 1.11, pg. 54**). SH2 domains are known to bind phosphorylated tyrosine residues and Crk has been associated to many tyrosine-phosphorylated proteins, such as, Gab1, and to the focal adhesion components, p130Cas and paxillin [284-286]. SH3 domains generally bind proline-rich motifs and are known protein-protein interaction modules. Both the GEFs C3G and DOCK180 bind Crk through the N-terminal SH3 domain [259,287,288]. In the members that contain a second SH3 domain, this region has no known binding partners. CrkII is less effective than CrkI in promoting p130Cas tyrosine phosphorylation, cell spreading and transformation, supporting a role for this domain as a negative regulator [282]. Another study found the C-terminal SH3 domain of CrkII to play a role in removal of apoptotic cells and cell spreading in *C. elegans* [289]. However, in mammals, *in vivo* gene-trap deletion of this latter SH3 domain in CrkII, while producing a truncated CrkI-like protein, does not demonstrate any obvious physiological defects in mice [290]. CrkL null mice are embryonic lethal and display defects in cranial and cardiac development [291]. These results also show that neither CrkI nor CrkII can compensate for CrkL during development. Since loss of CrkII does not induce any gross phenotypical abnormalities in mice, a knock-out mouse for CrkI and CrkII was generated and studied. These animals die before birth, with embryos presenting cardiovascular and craniofacial defects [292], leading to the conclusion that CrkL, which shares 60% primary sequence identity and significant structural homology to CrkII, is unable to compensate for both CrkI and CrkII [280,292].

7.2 ELMO

DOCK can almost never be mentioned without its binding partner ELMO (*e*ngulfment and cel*l mo*tility). Originally, ELMO/*ced-12* was identified in *C. elegans*, and studies showed that *ced-12* mutants phenocopied mutants of *ced-2*, *ced-5*, and *ced-10* [252-254]. In fact, *ced-12* was part of the same genetic cascade as *Ced-2*/*Ced-5*/*Ced-10* involved in mediating phagocytosis of apoptotic bodies and DTC migration [254]. The ELMO proteins (~82kDa) are evolutionarily conserved and include 3 mammalian members represented by ELMO1-3, with orthologs in *C. elegans* (*ced-12*) and *Drosophila* (dELMO). ELMOs are characterized by an N-terminal RhoG-binding, ERM-binding (cytoskeletal cross-linking protein) and IpgB1 (bacterial protein) binding regions [83]. A large portion of the N-terminus is also the interaction site for the Bai1 phagocytosis receptor [293]. The ELMO C-terminus houses a PH and proline-rich domain, with the proline-rich motif proposed to be the binding site for DOCK proteins [252,294,295] (**Figure 1.11, pg. 54**). Thus far, both ELMO1 and ELMO2 have demonstrated binding to DOCK1-4 [83].

The ELMO proteins possess no obvious catalytic activity and, so far, seem to function as scaffold platforms for an array of molecules. Interestingly, a very important theme has emerged surrounding the ELMO PH domain in conjunction with DOCK proteins. Many reports from the Ravichandran lab state that DOCK180 displays no Rac GEF activity alone [267,294,296]. Rather, these studies indicate that although ELMO has no enzymatic activity on its own, it functions *in trans* with DOCK180 through its PH

domain to uncover DOCK180 GEF activity towards Rac [294]. This bipartite GEF model is highly contested in the literature by other groups who have demonstrated that DOCK alone is necessary and sufficient as a Rac GEF both *in vitro* and *in cellulo* [265]. A possible explanation for this discrepancy is the difference in experimental methods employed to study DOCK180 GEF activity. Clearly, further detailed work is required to resolve this controversy to fully understand DOCK180 function and the ELMO contribution towards Rac signaling. **Part of my thesis work is dedicated to uncovering the molecular mechanism by which DOCK180 and ELMO interact and testing the importance of this partnership for DOCK180 Rac GEF activity.**

Interestingly, Bowzard and colleagues identified three proteins, ELMOD1-3, from bovine testis that share primary sequence similarity to the three mammalian ELMO proteins [169]. The region with similarity in the two sets of proteins is termed the ELMO domain and is positioned centrally in ELMO1-3 (**Figure 1.11, pg. 54**). However, no other feature is found to be conserved between the ELMO (1-3) and ELMOD (1-3) proteins. Not only is this study the first to demonstrate mammalian Arl family GAP activity, the ELMOD2 member was also shown to display GAP activity towards Arf1 and Arf6 *in vitro*, a rather surprising finding since none of the ELMOD proteins contain the canonical trademark Arf GAP domain [169]. This is an exciting discovery since Arf6 has already been linked to Rac activation and signaling in mammalian cells via the DOCK180/ELMO complex [180]. Although ELMO1-3 have been tested for Arf family GAP activity *in vitro*, no GAP function has been established to date [169].

7.2.1 The ELMO Pleckstrin Homology (PH) domain

The first PH domain was identified in the pleckstrin protein and subsequent research has revealed its existence in a myriad of proteins, such as protein kinases, GAPs, GEFs, and lipid transport proteins [297,298]. Structurally, canonical PH domains are characterized by a core three-stranded and four-stranded β-sheet 'sandwich' capped at its C-terminus by an α-helix (constitutes the PH 'superfold'), and three variable loops [79,299,300]. A trademark attributed to PH domains is the ability to bind a wide range of phosphoinositides through the phosphoinositol headgroup, and thus target proteins to cellular membranes without showing any major membrane insertion of the domain [301]. Lipid binding is credited to the heart of the variable loops region which creates a positively-charged interface [79,301,302]. The selectivity for different forms of lipid by-products is proposed to direct different PH domain-containing proteins to discrete subcellular locations. Nonetheless, although PH domains are clearly branded with this lipid-binding ability, only about 10-15% of known PH domains strongly display this characteristic. Most PH domains harbor very weak affinity and low selectivity towards PI3K by-products [79].

It is suggested that additional binding partners of PH domains and/or other domains within PH domain-containing proteins can strengthen subcellular targeting cues for these proteins. Additionally, rather than acting as localization cues, these binding partners are also proposed to effect functioning of proteins. One recent example is that of the PH domain of Bcr-Abl. This PH domain demonstrates high

specificity binding towards lipids and the proteins SMC1, DOCK9, PLCε and β–tubulin *in vitro* [303]. Clearly, further studies are required to investigate this potential function of PH domains through binding partners other than the extensively studied lipids.

To date, a defining feature of ELMO proteins is its PH domain. Although well conserved in the ELMO family, the PH domain has not been properly investigated for lipid-binding and membrane-targeting properties. *In cellulo* work with mammalian cells shows that the ELMO PH domain is necessary for DOCK180/ELMO-mediated membrane ruffling [304]. Moreover, functional studies in *C. elegans* demonstrate that the ELMO PH domain is required for proper engulfment functions, with transgenic embryos lacking this domain showing diffuse localization of the protein [253]. Whether these defects are due to mislocalization of ELMO still needs to be explored. **One goal of my thesis is to examine the lipid binding property of the ELMO PH domain and how this region is involved in DOCK180/ELMO Rac signaling during cell migration.**

8. Regulation of DOCK and ELMO

The regulation of DOCK and ELMO is quite complex. Many components have been associated in regulating these proteins and ensuing signaling cascades. As well, both post-translational modifications and the structural aspects of these molecules add another layer of complexity to DOCK/ELMO complex regulation.

8.1 Intramolecular interactions

Intramolecular contacts are said to be present in DOCK proteins. One model portrays DOCK180 to be autoinhibited at basal levels. Essentially, the DOCK180 SH3 domain is proposed to unite with the DHR-2, creating a steric clash with Rac and blocking access between the DHR-2 and Rac [295]. It is suggested that ELMO binding via its PxxP region to the DOCK180 SH3 domain releases the SH3/DHR-2 interaction, rendering the DHR-2 now accessible to Rac. This unleashing of DOCK180 is said to enable the bipartite DOCK180/ELMO to carry out its Rac GEF activity [295]. Although an interesting model of DOCK180 regulation, the steric-inhibition model lacks important elements. Firstly, the group fails to determine whether DOCK180 and ELMO are induced to form a complex only upon an extracellular stimulus or if these two proteins are always present in a complex even at basal levels. Also, if the former is true, what are the stimuli that would induce DOCK180/ELMO complex formation?

8.2 Phosphorylation

8.2.1 DOCKs

Phosphorylation of DOCK180 is seen after integrin stimulation and in *v*-Crk or *v*-Src-transformed cell lines [287]. However, the type and sites of these phosphorylation events are unclear. The functional importance of such events remains to be elucidated.

DOCK7 is richly expressed in neural Schwann cells. In these cells, the ErbB2 receptor has been directly linked to binding and phosphorylation of DOCK7 [305].

Functionally, ErbB2-stimulation resulted in an increase in DOCK7 GEF activity towards both Rac1 and Cdc42 *in cellulo*, with these cells displaying increased migratory phenotypes.

8.2.1 ELMOs

Stimulation by the Src family tyrosine kinase, HCK, induces ELMO phosphorylation [306]. Mutation of critical tyrosines in ELMO resulted in decreased phagocytic ability and cell migration of mammalian cells [306]. These ELMO mutants also caused a substantial decrease in Rac activation in cells, suggesting that ELMO phosphorylation is an important regulatory factor for DOCK180-mediated Rac activity. Mechanistically, how ELMO phosphorylation manipulates DOCK180/ELMO signaling remains a mystery. A possible answer may be that ELMO phosphorylation events 'free' an otherwise autoinhibited ELMO protein. Other possibilities include the recruitment of additional factors important for Rac signaling downstream of DOCK180.

8.3 Ubiquitylation

While DOCK180 expression alone is less stable due to ubiquitylation events, co-expression of ELMO1 hampers DOCK180 ubiquitylation *in cellulo* [307]. Interestingly, it has been mentioned that the ELMO contribution is responsible for priming DOCK180 Rac GEF activity [267,294,296]. This study offers an attractive alternative idea that ELMO stabilizes the expression of the DOCK protein rather than actually physically engaging in DOCK180-mediated Rac activation events.

8.4 Oligomerization

Certain members of the classical DH-PH RhoGEF family can oligomerize through their respective DH domains, a process often required for optimal GEF activity [308-311]. For the DOCK family, DOCK9 is reported to dimerize through the DHR-2 domain in each molecule [312]. Most recently, the crystal of the DOCK9 DHR-2 unveiled that homodimerization sites are distinct from Cdc42-binding sites leaving the GEF openly accessible to activate the GTPase [85]. However, it has yet to be determined whether dimerization via DHR-2 is a universal feature and if there are any functional consequences.

9. Physiological functions of DOCK and ELMO

Over the years, whether alone or in unison, DOCK and ELMO have been implicated in various biological processes. Initial discovery of these proteins were made in the research of cell migration *in cellulo*, phagocytosis, and myoblast fusion in model organismal systems of *Drosophila* and *C. elegans* and in mammalian cell lines. Below, we discuss the biological relevance of these proteins and downstream signaling cascades.

9.1 Phagocytosis

Phagocytosis is an effective cellular method employed to engulf and remove apoptotic cell bodies and pathogens. Efficient clearance of dying cells by phagocytes encourages healthy cellular functioning of a host. Molecular pathways that control this

process are well studied in *C. elegans* and mammalian cells. The first evidences for teamwork between *ced-5*, *ced-2* and *ced-10* were made in *C. elegans* during phagocytosis of apoptotic cells [262]. Further genetic studies identified *ced-12* to function at the same molecular step as *ced-5* during engulfment, also revealing the importance of the *ced-12* PH and proline-rich regions for *ced-12* function [252-254]. It was also found that *ced-5* and *ced-12* regulation of *ced-10* was necessary for proper cytoskeletal reorganization [252-254].

The first *bona fide* receptor found to trigger DOCK180-mediated phagocytosis is the integrin $\alpha_v\beta_5$ [263]. This integrin recruits phosphorylated p130Cas-CrkII-DOCK180 to cell surfaces for efficient Rac activation and phagosome formation by mammalian phagocytes.

Dying cells are known to expose 'eat-me' signals at their cell surface when the time is right, readying themselves for the 'clean-up crew' that will recognize these signals and proceed with their disposal [313-315]. One such signal is supplied by phosphatidylserine (PtdSer). Normally present on the inner leaflet of cells, an apoptotic cell will flip-out this 'eat-me' signal, an attractive cue for the PtdSer receptor (PSR) [316,317]. *psr-1* (ortholog of mammalian PSR) is genetically linked to the *ced-2/ced-5/ced-12/ced-10* pathway in *C. elegans*, potentially through a direct interaction via *ced-5* or *ced-12* or both proteins [318].

Opsonization of apoptotic cells refers to binding of soluble bridging signals that 'prime' a cell for detection by a phagocytosis receptor. The secreted glycoprotein milk-

fat globule EGF-factor 8 (MFG-E8) is a known opsinizing agent of PtdSer that can be recognized directly by either integrin $\alpha_v\beta_3$ or $\alpha_v\beta_5$ [319-321]. As $\alpha_v\beta_5$ has already been linked to the CrkII-DOCK180-Rac1 pathway, an interesting study found that MFG-E8 is functionally connected to $\alpha_v\beta_5$ and DOCK180 and potentiates integrin-mediated Rac activation [322]. Effectively, knockdown of DOCK180 hinders MFG-E8-$\alpha_v\beta_5$-mediated Rac activity and phagocytosis of dying cells [322].

Gas6 is another opsonizing agent of PtdSer acting through the receptor tyrosine kinase, Mer [323]. Mer stimulation by Gas6 results in activation of the Src signaling pathway, FAK phosphorylation and recruitment of the $\alpha_v\beta_5$ integrin [324]. Intriguingly, Mer and integrin $\alpha_v\beta_5$ have been linked due to the shared downstream signaling pathway. Essentially, it is suggested that these two receptors display synergy during phagocytosis in cells due to collective phosphorylation of p130Cas leading to recruitment of CrkII/DOCK180 and localized Rac1 activation [324]. Mer is unable to promote phagocytosis in cells where integrin $\alpha_v\beta_3$ and $\alpha_v\beta_5$ have been knocked down, showing the dependence of Mer on integrins during engulfment [324]. Both receptor families have been implicated in other biological processes that require versatile and dynamic cytosketelal restructuring, such as cell migration and invasion. It will be interesting to see whether these receptors also cross-talk in these processes using a similar DOCK180-signaling module.

The most recent receptor to be identified upstream of the ELMO/DOCK180/Rac unit is mammalian BAI1 (brain-specific angiogenesis inhibitor 1) [293]. BAI1 is a seven-

transmembrane GPCR that directly binds the apoptotic signaling molecule PtdSer. It was found that BAI1, through direct interaction with the N-terminal region of ELMO1, enters into a trimeric complex with ELMO1 and DOCK180 [293]. This complex formation was essential for phagocytosis by professional and non-professional phagocytes, as knockdown of BAI1 expression, hindering ELMO1/DOCK180 complex formation or inhibiting Rac GEF activity significantly reduced necrotic cell removal. BAI1 is a novel receptor now being tied to the ELMO/DOCK180 complex during uptake of apoptotic cells. BAI1 has also been linked to brain tumours and future studies will enlighten us on what roles, if any, these molecules have in ensuing signaling cascades during cancer.

The accumulated evidence pointing to the importance of the ELMO/DOCK180 configuration during engulfment of apoptotic cells is further substantiated by an *in vivo* mouse model where ELMO1-deficient mice demonstrate disrupted removal of germ cells [325]. These mice are viable and are born at Mendelian ratios. While overall gross anatomy of these animals was normal, defects were seen at the level of Sertoli cell function. One such function is the activity as disposal systems for apoptotic germ cells. This action is suggested to require ELMO, since a dominant negative ELMO1 ($ELMO1^{1-624}$) was not able to rescue phagocytosis defects of Sertoli cells as comparable to wild-type ELMO1 [325]. Interestingly, this dominant-negative ELMO1 mutant lacks the DOCK180 binding site; it is suggested that Rac activation is an important signaling event required for phagocytosis by these cells.

9.2 Gonadal development

The pioneering discovery of the *ced-2/ced-5/ced-12/ced-10* signaling pathway is much indebted to the genetically tractable system of *C. elegans*. This pathway was first simultaneously acknowledged during phagocytosis of dying cells and during gonadal tip cell (DTC) migration [252-254]. DTCs are positioned at the extremities of the two gonadal arms and steer the lengthening of each arm to form a U-shaped gonad during development in *C. elegans* [326]. Mutants of any component of this cascade will result in defective DTC migration. Moreover, just as in phagocytosis, *ced-5* and *ced-12* are positioned downstream of *ced-2* and upstream of *ced-10*, demonstrating the conserved nature of this signaling unit in different physiological processes.

9.3 Oogenesis

Another well exploited genetic tool to study directed cell migration is the model organism *Drosophila*. During fly oogenesis, the anterior of the egg chamber contains a huddle of border cells that will collectively migrate towards the oocyte at the posterior end. Duchek *et al.* show that border cells express the tyrosine kinase receptor, PVR (ortholog of mammalian PDGF and VEGF receptor), and respond to the release of the guidance molecule PVF1 by the oocyte [327]. This study also brought to light that MBC and Rac activation are important downstream components of PVR signaling during border cell migration. A few years later, this same group revealed that border cell migration occurs via distinct signaling events that direct two different modes of

migration [328]. There are two phases to border cell migration: the early and late phase. The early phase uses internal signaling cues in a 'leader' cell to direct the initial polarized migration towards the oocyte in a collective fashion. It is during this step that MBC and dELMO are found to be essential, with mutants displaying blocked migration. In the late phase, MBC/dELMO-independent cell migration is dominant where border cell migration depends rather on the assessment of signaling cues from individual units in the cluster to direct collective cell movement [328].

9.4 Muscle development

The significance of DOCK180 during muscle development was first acknowledged in *Drosophila*. In this organism, multinucleated muscle fiber formation involves fusion of two sets of muscle cell populations: founder and fusion-competent cells. Duf, Sns and Rst are the receptors that mediate fusion between the two types of cells and trigger an internal signaling cascade involving MBC [329,330]. MBC is found in both cell populations and mutant flies demonstrate a serious defect at the myoblast fusion step, with resulting single mononucleated fibers [260,329-331]. MBC is suggested to act upstream of Rac during myoblast fusion and the relationship between DOCK and Rac is exemplified *in vivo*, since loss-of-function mutations in MBC recapitulate musculature defects seen in dominant negative, constitutively active and loss-of-function mutants of Rac1 and Rac2 [142,143,332]. A structure-function study *in vivo* in *Drosophila* found that the SH3 domain, DHR-1 and DHR-2 are crucial for proper myoblast fusion [331]. However, although the DHR-1 is able to bind PIP_3, during fusion, it

seems this effect is not its primary role since MBC$^{\Delta DHR-1}$ is still membrane-targeted. It is shown that the popular DOCK180 binder, Crk, while able to bind MBC, is not required for MBC function during muscle formation [331].

dELMO has emerged as a vital component of Drosophila myoblast fusion, exhibiting binding with MBC SH3 domain and coinciding with MBC expression patterns during development. Similar to MBC, loss of dELMO results in defective myoblast fusion [333]. Intriguingly, while singly overexpressed dELMO or MBC has no phenotypic consequence, an overdose of both proteins disrupts fusion events. This effect is attributed to cooperation between dELMO and MBC in favour of Rac GEF activity [333].

A pioneering study in zebrafish suggests that DOCK180 may have a similar role to MBC in vertebrates [334]. Using morpholino-based knockdown of DOCK180 and its close homolog DOCK5, Moore *et al.* demonstrate requirement of both GEFs during fusion of fast-twitch myoblasts during zebrafish development. Interestingly, in contrast to findings in *Drosophila*, Crk proteins also play a part during this process in zebrafish [334].

Mammalian myogenesis differs from that of *Drosophila* in a distinct way. In mammals, no founder or fusion-competent cells are present. Instead, mononucleated myoblasts form syncytial muscle fibers via fusion with each other and with existing myotubes [335]. The first study to examine DOCKs in mammals found that DOCK180-null mice exhibit severe reduction in skeletal muscle formation, an effect exacerbated by knockdown of DOCK5 [336]. Deletion of DOCK180 and DOCK5 results in defective

myoblast fusion *in vitro* and *in vivo* [336]. While mammalian DOCK180 seems to mirror *Drosophila* MBC, components acting upstream and downstream of DOCK180 in muscle formation have yet to be studied in the mouse. So far, the Crk-null mouse and the recently published ELMO1-knockout mouse have not been identified to demonstrate musculature abnormalities.

9.5 Immune system

Due to its temporal location, DOCK2 is a unique DOCK member. This GEF is exclusive to the hematopoietic system and critical for lymphocyte migration [337,338]. Fukui and colleagues found that similar to DOCK180 regulation of Rac, DOCK2 is found to activate Rac in T cells and induce actin polymerization [337]. Study of DOCK2-null mice uncovered its essential role during T and B lymphocyte migration, a role dependent on Rac-mediated cytoskeletal remodeling [337]. A later study found that similar to the DOCK180/ELMO interaction, the C-terminal region of ELMO1 binds DOCK2 via its N-terminal *in cellulo* [339]. In cells, this association was required for Rac activation, however, whether ELMO is required for migratory effects of DOCK2 remains to be seen.

PI3K and Rac activity have been diagnosed as key contributing factors for neutrophil motility in the face of a chemoattractant. DOCK2 has also been shown to contribute towards stimulus-induced neutrophil migration and polarity through Rac activation. Intriguingly, an elegant study by Nishikimi and colleagues nicely shows a two-step process for instigating neutrophil migration [276]. They demonstrate that

although PIP_3 generation at the leading edge induces the initial rapid localization of DOCK2 at the cell front, a secondary production and positioning of phosphatidic acid (PA) stabilizes and focuses DOCK2 through an interaction with its polybasic C-terminal [276]. Blocking PA generation effectively blocks DOCK2 accumulation at the leading edge and subsequent neutrophil motility is hindered. While the existence of a positive-feedback loop for PIP_3 accumulation is acknowledged through interplay between PIP_3 and Rac, the mechanistic collection of PA at the leading edge remains elusive. This mode of membrane recruitment of DOCK2 has also been investigated briefly for DOCK180, which was also found to bind PA [276]. This result reveals that regulation of DOCK GEFs via sequential lipid binding properties may be a universal concept.

9.6 Cancer

As stated in previous sections, the DOCK GEFs play a part in various forms of cell migration. Understanding these events has led to key insights into understanding tumour cell motility. Cancerous cells migrate in either a mesenchymal or amoeboid fashion and some can actually transition between the two modes of migration when it is deemed convenient to promote invasive phenotypes.

Glial cells are found exclusively in the central nervous system. When they become cancerous, prognosis for patients is generally very poor with only 25% surviving two years after the initial diagnosis [340]. Concrete evidence for DOCK180 and ELMO1 in tumour progression came when both proteins were found to be highly expressed in human gliomas. The pattern of expression showed that the two proteins

were expressed almost selectively at the periphery of the tumour, while central regions were devoid of DOCK180 and ELMO1 expression [341]. Excitingly, DOCK180 and ELMO1 expression strongly correlated with the aggressiveness of invasive tumours. It was found that knockdown of either protein significantly diminished cell migration and invasion of glioma cell lines, and this was probably due to the decrease in Rac activation in these cells [341]. As well, exogenous expression of these proteins resulted in enhanced invasiveness of gliomas. Further studies are required to determine which factors trigger this distinct upregulation of DOCK180 and ELMO1 at the borders of these deadly tumours.

Overexpression of the uPAR receptor is linked to many forms of cancer [342-346]. Cancer cells hijack this receptor and downstream signaling components to promote its malignancy. Recently demonstrated, uPAR activation induces phosphorylation of p130Cas which in turn favours p130Cas-CrkII complex formation [347]. It is suggested that invasiveness of uPAR-expressing tumour cells is dependent on DOCK180-mediated Rac activation which is recruited to the membrane by CrkII. Of note, the β_3 integrin was shown to participate with uPAR to promote Rac activation in uPAR-expressing tumours [348]. It remains to be determined whether this cooperation is a result of direct or indirect interactions between the two receptors and whether this avenue of Rac activation involves DOCK180.

As mentioned, cancer cells can be extremely versatile in the face of the cellular microenvironment, switching from an amoeboid-to-mesenchymal migration mode and

vice versa in order to facilitate tumour migration and invasion. Two DOCK GEFs have been identified as important participants of these transitions. Firstly, DOCK3 is required for mesenchymal movement of melanoma cells through activation of Rac and WAVE2 [349]. However, not only does DOCK3 promote mesenchymal motion, but in the same instance it also stifles amoeboid migration due to its Rac GEF activity and reduction of MLC2 phosphorylation and ROCK activity (Rho kinase). Conversely, a transition to amoeboid movement is made by shutting off Rac activity through ROCK activation of a Rac GAP, ARHGAP22 [350].

In contrast to the DOCK3 requirement for a mesenchymal-like phenotype, DOCK10 Cdc42 GEF activity is necessary for amoeboid-type movement and invasiveness of melanoma cells [273]. The effectors N-WASP and Pak2 are critical elements of this cascade, with Pak2 leading to phosphorylation of ROCK and a rounded cell shape [273]. These findings are fascinating in the sense that DOCK family members, through their specific GEF activities for different GTPases, can control completely opposite forms of cancer cell migration.

While most DOCKs seem to be involved in the promotion of cancer, DOCK4 is identified as a potential candidate for tumour suppression. DOCK4 demonstrates specificity for both Rac1 and Rap1, a GTPase implicated in promoting tight adherens junctions [351]. DOCK4 was found to be deleted in a bone cancer mouse model. Tumour cells from these animals could be rescued by reintroducing DOCK4, displaying less invasive and growth phenotypes. Additionally, many human cancer cell lines present

frequent mutations in DOCK4. One such mutation, Pro1718Leu, causes defective Rap1-GEF activity. Rap1 activity to promote cell-cell contacts seems to be an important property for tumour suppression in these cancer cell lines. In support of this, introduction of a constitutively active form of Rap1 in these DOCK4-null cells promoted adherens junction formation and reduced tumour growth and invasiveness *in cellulo*.

10. Rationale of research

In the blueprint of cell migration, the Rho GTPases emerge as key components which filter signals from cell surface receptors and transduce the information to key regulators of the actin cytoskeleton. Rac, a member of the Rho GTPases superfamily, is a convergence point to several pathways leading to actin reorganization. DOCK180 is an atypical GEF and potent activator for Rac. A signaling pathway comprised of DOCK180 and ELMO1 demonstrates how these proteins interact biochemically and genetically to activate Rac in several important biological events. However, much controversy surrounds the molecular mechanism of interaction between the two proteins. As well, contradicting evidences in the literature have made it difficult to reconcile whether DOCK180 activity as a Rac GEF is ELMO-dependent (bipartite GEF model) or if the ELMO contribution plays some other vital role during Rac signaling events downstream of the DOCK180/ELMO complex.

Our central hypothesis, then, is that DOCK180 alone is necessary and sufficient for Rac GEF activity, and the DOCK180 interaction with ELMO is required for integration of proper Rac signaling. Specifically, we surmise that

DOCK180 binding to ELMO can spatio-temporally restrict localization of DOCK180-mediated Rac signaling and/or act as a scaffold for Rac effectors to enforce directional cell migration.

10.1 Aim #1 (Chapter 2)

In Aim #1 of my PhD thesis, *we strive to elucidate how the molecular complex between DOCK180 and ELMO is formed, and we address the question of whether complex formation contributes to Rac activation.* Because of the intricate nature of this interaction, we opted for a combination of structural and biochemical approaches to delineate the interaction surfaces on DOCK180 and ELMO. Binding-defective mutants of both proteins will be tested in functional assays for their effect in integrin-stimulated cell morphologies and for Rac activity.

10.2 Aim #2 (Chapter 3)

In Aim#2 of my PhD thesis, the question then becomes *what are the implicated domain(s) and the mechanism by which ELMO proteins facilitate Rac signaling?* Our work presented in Aim #1 (Chapter 2) supports a role for the ELMO1 N-terminus in Rac signaling by the DOCK180/ELMO1 complex. It is possible that ELMO is acting as a scaffold in this process and linking DOCK180 to downstream effectors required for cytoskeletal changes. On the other hand, it is also possible that ELMO is acting as a localization signal, through protein-protein or protein-membrane interactions, for the targeted activation of DOCK180.

To de-mystify the role of the ELMO1 N-terminus, we initiated bioinformatic analyses on various amino terminal boundaries. Our results suggest the presence of Armadillo Repeats similar to those found in Dia1, a formin. The region in the formins with homology to ELMO N-terminus is known as the Diaphanous Inhibitory Domain (DID) and is characterized to engage in intramolecular interactions with the Diaphanous Autoinhibitory Domain (DAD) to maintain these molecules in a repressed state [221,224-226]. We propose that ELMO molecules may likewise be autoinhibited by intramolecular interactions between similar modules. Such intramolecular interaction may provide regulation of the activity of the ELMO1/DOCK180 complex by masking protein-protein interaction sites or other functional domains present in proteins.

10.3 Aim #3 (Chapter 4)

In parallel to our bioinformatics query into the ELMO N-terminal (Aim #2 (Chapter 3)), our curiosity led us to Aim #3 of my PhD thesis and the *search for novel ELMO-binding partners capable of binding ELMO and releasing it from its 'dormant' state.* Aim #3 entailed a yeast two-hybrid experiment using ELMO1 as bait to screen a mouse embryo head cDNA library. A novel and alluring candidate was identified: the Arf family GTPase, Arl4A. Recent reports suggest that Arl4s are involved in cytoskeletal rearrangement through their ability to bind the Arf6 guanine exchange factor, ARNO [209,210]. Our study will investigate how Arl4A binding contributes towards DOCK180/ELMO-mediated Rac signaling and cytoskeletal remodeling. In essence, being a GTPase, Arl4A may bind the ELMO RBD, the release button that would allow

ELMO to spring open from its closed conformation, or even as a localization signal for the ELMO/DOCK180 complex at the plasma membrane.

RESULTS

CHAPTER 2

An alpha-helical extension of the ELMO1 pleckstrin homology domain mediates direct interaction to DOCK180 and is critical in Rac signaling

CHAPTER 2: Figure Acknowledgements

Figure 2.1 (A-E): Manishha Patel
Figure 2.2 (A-B): Dr. David Komander
Figure 2.3 (A-D): Dr. David Komander
Figure 2.4 (A-C): Dr. David Komander
Figure 2.4 (D-E): Manishha Patel
Figure 2.5 (A-G): Manishha Patel
Figure 2.6 (A-C): Manishha Patel
Figure 2.7 (A-E): Manishha Patel

Figure 2S1 (Table I, A-B): Manishha Patel
Figure 2S1C: Dr. Jean-François Côté
Figure 2S2 (A-C): Dr. David Komander
Figure 2S3 (A-B):Dr. David Komander
Figure 2S4 (A-B): Manishha Patel
Figure 2S5:Dr. David Komander
Figure 2S6 (A-B): Manishha Patel
Figure 2S7: Dr. David Komander
Figure 2S8: Manishha Patel

*Nadine Fradet generated multiple clones used in this study
*Mélanie Laurin and Ariane Pelletier generated data that was omitted from the final version of the manuscript
*The manuscript was written by Dr. Jean-François Côté, Dr. David Komander, and Dr. David Barford
*The manuscript was edited by Manishha Patel, Mélanie Laurin, and Ariane Pelletier

An alpha-helical extension of the ELMO1 pleckstrin homology domain mediates direct interaction to DOCK180 and is critical in Rac signaling

David Komander[‡ $ †], Manishha Patel[* †], Mélanie Laurin[*], Nadine Fradet[*],
Ariane Pelletier[*], David Barford[‡] and Jean-François Côté[* ¶ # §]

[‡]Section of Structural Biology, Chester Beatty Laboratories, Institute of Cancer Research, 237 Fulham Road, London, SW3 6JB, U.K.

[*] Institut de Recherches Cliniques de Montréal. 110 avenue des pins Ouest, Montréal (Québec) Canada, H2W 1R7.

[¶] Faculté de Médecine, Université de Montréal.

[#] Division of Experimental Medicine, McGill University

[$] Current address: Division of Protein and Nucleic Acid Chemistry, MRC Laboratory of Molecular Biology, Hills Road, Cambridge, CB2 0QH, U.K.

[†]These authors contributed equally to this work

[§]Corresponding author:
Email : Jean-François Côté
Phone: (514) 987-5647
Fax: (514) 987-5624

Running Title: α-helical extension of ELMO1 PH binds DOCK180

Abbreviations: DHR-2, DOCK Homology Region 2; GEF, guanine nucleotide exchange factor; PH, Pleckstrin Homology; Pro-rich, proline-rich

ABSTRACT

The mammalian DOCK180 protein belongs to an evolutionarily conserved protein family, which together with ELMO proteins, is essential for activation of Rac GTPase-dependent biological processes. Here, we have analyzed the DOCK180-ELMO1 interaction, and map direct interaction interfaces to the N-terminal 200 amino acids of DOCK180, and to the C-terminal 200 amino acids of ELMO1, comprising the ELMO1 PH domain. Structural and biochemical analysis of this PH domain reveals that it is incapable of phospholipid binding, but instead structurally resembles FERM domains. Moreover, the structure revealed an N-terminal amphiphatic α-helix, and point mutants of invariant hydrophobic residues in this helix disrupt ELMO1-DOCK180 complex formation. A secondary interaction between ELMO1 and DOCK180 is conferred by the DOCK180 SH3 domain and Pro-rich motifs at the ELMO1 C-terminus. Mutation of both DOCK180-interaction sites on ELMO1 is required to disrupt the DOCK180-ELMO1 complex. Significantly, although this does not affect DOCK180 GEF activity towards Rac *in vivo*, Rac signaling is impaired, implying additional roles for ELMO in mediating intracellular Rac signaling.

Keywords: DOCK180/ELMO1/Rac activation/PH domain/Cell migration

INTRODUCTION

DOCK180 family members are conserved *bona fide* guanine nucleotide exchange factors (GEFs) for Rho GTPases [83]. A subgroup of these proteins, the CDM members (*C. elegans* Ced-5, *Drosophila* Myoblast City and mammalian DOCK180), regulate several Rac-dependent biological processes including phagocytosis of apoptotic cells, cell migration, axon pathfinding and myoblast fusion *in vivo* [261,352-354]. Mechanistically, DOCK proteins rely on a conserved DOCK Homology Region (DHR)-2 domain to promote the GDP/GTP exchange of Rho GTPases [265,267]. DOCK proteins are also endowed with a conserved DHR-1 domain capable of direct interaction with phosphoinositides (PI), in particular phosphatidylinositol-(3,4,5)-trisphosphate (PtdIns(3,4,5)P_3) [274], and this activity appears to be important in Rac-mediated cell polarity and migration in addition to myoblast fusion [83].

The identification of *C. elegans Ced-12* in a screen for genes that control necrotic and apoptotic cell phagocytosis [355] led to the recognition of a unique family of highly conserved engulfment and motility (ELMO) family proteins in eukaryotes [356-358]. ELMO proteins physically interact with a subset of DOCK180-related proteins [359], including DOCK180 (DOCK1) and DOCK2-5, characterized by the presence of an amino-terminal Src Homology (SH)-3 domain [360,361]. The remaining DOCK-related proteins, including DOCK6-8 and DOCK9-11/Zizimin1-3, lack a discernable SH3 domain and have not been reported to physically interact with ELMO proteins.

Several of the biological functions of DOCK180 characterized to date have been demonstrated to also require ELMO proteins. One established model proposes the idea of a bi-partite exchange factor formed from DOCK180 and ELMO [362], supported by the finding that co-expression of ELMO was required to stimulate the Rac GEF activity of DOCK180 [362]. However, in conflict with this model, we and others have found that DOCK180 displays substantial GEF activity when it is expressed alone in cells [361,363-366].

In support of this autonomous GEF model, the purified recombinant DHR-2 domain of DOCK180 is active towards Rac *in vitro* [265]. Nevertheless, it is generally agreed that ELMO is essential for physiological DOCK180 function, since interfering with the protein's properties, such as RhoG- or ERM-binding, results in impaired Rac-dependent cell migration and phagocytosis of apoptotic cells [328,356-358,360].

The contribution of ELMO proteins for Rac signaling is poorly understood, and the mode of interaction between ELMO and DOCK proteins is not established. Some data indicate that the SH3 domain of DOCK180 binds to a proline-rich (Pro-rich) motif at the C-terminus of ELMO [356] and this interaction may regulate the activation state of DOCK180 [367]. However, since the ELMO/DOCK180 interaction is not completely blocked when either of these motifs are mutated [367], additional contact regions between the two proteins presumably facilitates the high affinity binding [359].

A second interaction site between ELMO and DOCK180 was shown to involve, indirectly, the atypical PH-domain of ELMO [368]. In agreement with this, the ELMO PH domain was reported to provide a stabilizing effect towards a complex of nucleotide-free Rac and the DOCK180 DHR-2 domain [368]. It was found that in such a complex, the ELMO PH domain does not interact with DOCK180 directly, but rather stabilizes the critical reaction intermediate in *trans*, directly increasing the GEF activity of DOCK180 towards Rac by two-fold [368].

In this study we aimed to investigate the exact mechanism of interaction between ELMO1 and DOCK180 in order to assess the contribution of these two proteins in Rac GTP-loading and signaling. In contrast to a previous report [368], we find that the atypical PH domain of ELMO1 directly interacts with DOCK180 in a Rac-independent and constitutive manner. Structural analysis of the atypical ELMO1 PH domain reveals an amphiphatic N-terminal α-helical extension, and we identify

residues in this region required for DOCK180/ELMO1 interactions. Our data reveal that whereas the Pro-rich region of ELMO1 and the SH3 domain of DOCK180 are dispensable for complex formation, these motifs are important for the physiological functions of ELMO1/DOCK180. Double mutation of both the ELMO1 amphiphatic helix and Pro-rich motif is necessary to fully abrogate signaling from this complex. Importantly, we detect no difference in DOCK180 Rac GEF activity even in cells with defective ELMO1/DOCK180 signaling, arguing against a direct role of ELMO1 in DOCK180 GEF activity. Together, our findings provide novel insight into how ELMO proteins bind to and regulate DOCK proteins.

MATERIAL AND METHODS

Additional Material and Methods. Detailed information on the plasmids used in this study is available in the **Supplementary Material (Material and Methods)**.

Antibodies, cell culture and transfections. The following antibodies were obtained commercially: anti-DOCK180 (C-19 and H-4), anti-Myc (9E10), anti-GFP (B-2) were from Santa Cruz Biotechnologies, anti-Rac was from Millipore and anti-FLAG M2 was from Sigma. A polyclonal antibody was generated against DOCK180 using a His-tagged fragment of DOCK180 as an immunogen (His-DOCK180 422-619). HEK293T cells were cultured in DMEM supplemented with 10% fetal bovine serum, penicillin and streptomycin (Gibco-BRL) and transfected by calcium phosphate or Lipofectamine 2000 (Invitrogen) using standard procedures. The CHO cell line, LR73 subclone, was maintained in alpha-MEM supplemented with 10% fetal bovine serum, penicillin and streptomycin (Gibco-BRL) and transfected using Lipofectamine 2000 (Invitrogen) according to the manufacturer's instructions. Biochemical and cell biological studies were performed 24-48 hours after transfection.

Immunoprecipitation, GST-fusion protein pulldowns and Rac-GTP assays. Cells were lysed for 10 min in a buffer consisting of 50mM Tris-HCl pH 7.5, 150mM NaCl, 1% NP-40 and 1X Complete protease inhibitor (Roche). For immunoprecipitation, clarified cell lysates were incubated with the appropriate antibody and immune complexes were allowed to form for 1 h at 4˚C. Protein A-sepharose was added for 30 min to isolate the immune complex. For GST-fusion protein pulldowns, the GST-fusion proteins were expressed in bacteria and purified on Glutathione-Sepharose 4B according to manufacturer's instruction (Amersham). Equal amounts of the various GST-fusion proteins bound to Glutathione Sepharose 4B were next incubated with cell extracts (500 μg of protein per condition). In both types of assays, the beads were

washed three times with lysis buffer and the bound proteins were analyzed by SDS-PAGE and immunoblotting. The GTP-loading status of Rac in CHO LR73 and HEK293T cells was analyzed by GST-PAK-PBD affinity precipitation as described previously [363]. Rac activation was quantified by densitometry analysis using ImageJ software. Signal for Rac-GTP was normalized to total Rac present in the cell lysate.

Cell morphology and cell migration assays. LR73 cells transfected with the indicated plasmids were subject to cell morphology or migration assays as previously described [364]. Briefly, cells were transfected with the indicated plasmids and serum starved (0.5% FBS) overnight. Cells were gently detached (0.01% trypsin and 5 mM EDTA in Hanks balanced solution), washed in fibroblast basal media supplemented with 0.5% BSA and 100 000 cells were then allowed to spread for 2 h before fixing with 4% paraformaldehyde. Cells were permeabilized with 0.2% Triton X-100 in PBS and blocked in PBS-1% BSA prior to staining with anti-DOCK180 (H4), DAPI and phalloidin. The remainder of the cells was lysed to verify the expression levels of the exogenous proteins by western blotting. For migration assays, the cells were transfected with pEGFP-C2 (0.5 μg, in addition to the indicated plasmids) as a tracker and were prepared as described above. 100 000 cells were loaded, in duplicate for each condition, in modified Boyden Chambers (COSTAR) for which the underside of the membrane was pre-coated with 10 ug/ml of fibronectin. Cells were allowed to migrate for 4 hours prior to fixation in 4% paraformaldehyde. Cell in the upper chambers were mechanically removed using cotton swabs. GFP-positive cells that migrated to the underside were counted from 3-5 independent fields on each membrane (20x magnification). The remainders of the cells were lysed to verify the expression levels of the exogenous proteins. For both assays, cells were photographed using a Leica DM4000 microscope equipped with a Retiga EXi (QImaging) camera. ANOVA and all Pairwise Multiple Comparison Procedures (Holm-Sidak method) were performed for statistical analysis (n=6 for each condition).

Lipid binding assays. GST ELMO1, ELMO1 532-707, BTK PH domain and His DOCK180 DHR-1 were produced in bacteria and purified as previously described [274]. Purified proteins were quantified and 1 µg of each was used in lipid-coated beads pull-down (Echelon Biosciences) exactly as previously described [274].

***In vitro* transcription/translation**. The T7 TnT system (Promega) and ^{35}S methionine was used, according to manufacturer's instruction, to generate the radiolabeled recombinant DOCK180 protein fragments. Interaction between DOCK180 and the ELMO1 GST-fusion proteins, performed as described above, were detected by Amplify-enhanced autoradiography (Applied Biosystem).

Protein purification for structural studies. Three C-terminal human ELMO1 constructs (532-675, 532-707, 532-727), encompassing the PH domain, were cloned into the pGEX6-P1 vector, which contains a PreScission protease-cleavable GST tag. The fusion proteins were expressed in BL21-DE3 cells overnight at 25 °C after induction with 150 µM IPTG at an OD_{600} of 0.8. Cells were lysed in Buffer A (300 mM NaCl, 25 mM Tris pH 8.50, 5 mM DTT, 1 mM EDTA) complemented with 1 mg/ml Lysozyme, 0.1 mg/ml DNAse I and Complete protease inhibitor tablets (Roche), and sonicated at 4°C. Insoluble material was removed by centrifugation for 30 min at 40000 x g, and the lysate was incubated with Glutathione Sepharose 4B resin (Amersham) for 1 hour at 4°C. The resin was washed with 100 ml Buffer A, 500 ml Buffer A with 500 mM sodium chloride, and 200 ml Buffer A with 200 mM sodium chloride. GST-PreScission protease was added (0.1 mg/ml), and the resin was incubated overnight at 4°C with agitation. The eluate, containing the ELMO1 PH domain, was collected, concentrated to 5 ml and further purified on a Superdex75 gel filtration column, coupled to a 5 ml HiTrap Glutathione Sepharose column to clear residual GST and GST-PreScission protease. The protein was concentrated in VivaSpin concentrators (VivaScience, 10000 MW cut-off) to a maximum concentration of 19

mg/ml, and dynamic light scattering indicated a monodisperse, non-aggregated sample. A two L bacterial culture produced up to 80 mg of pure ELMO1 PH for all constructs tested.

Crystallization. Crystallization screening was performed with all three ELMO1 PH proteins in a sitting drop setup by mixing 1 µl protein with 1 µl mother liquor. Although crystals were obtained from all constructs, diffracting crystals were only obtained for the shortest ELMO1 PH domain (532-675), from mother liquor containing 2.1 M sodium malonate [pH 6.75]. Hexagonal crystals grew after 2 days, and reached a maximum size of 0.3 x 0.3 x 0.3 µm after 7 days. The protein crystals were flash frozen in a nitrogen cryo-stream without further cryo-protection. For experimental phasing, ELMO1 PH domain crystals were soaked in mother liquor enriched with 1 mM EMTS (ethyl mercury thiosalicylate) for 60 minutes, and back-soaked for 20 seconds in EMTS free mother liquor prior freezing.

Data collection and structure determination. Data on ELMO1 PH crystals were collected at the European Synchrotron Radiation Facility (ESRF, Grenoble) station ID23-1. Native data were collected to 2.30 Å resolution, and derivative data with 22-fold anomalous multiplicity at the Hg edge (1.0086 Å) were collected to 3.0 Å resolution. The crystals displayed the high symmetry space group $P6_122$, which facilitated anomalous data collection (see **Table 2.1** for data collection statistics). The data was processed with Mosflm and Scala from the CCP4 suite [369]. The structure was solved in a SIRAS experiment, using SHELX / hkl2map [370], and SHARP [371]. SHARP determined a solvent content of 68 %, with 2 molecules/AU and a Matthews coefficient of 4.8. Excellent phases were obtained, and automated model building with ArpWarp [372] built ~85 % of the model. Alternating further rounds of model building in Coot [373] and refinement, initially with CNS simulated annealing [374], and subsequently using TLS restrained refinement in Refmac5 [375], were performed, leading to the final refinement statistics in **Table 2.1**.

RESULTS

The atypical PH domain of ELMO1 directly interacts with DOCK180

We initiated a detailed study to analyze which ELMO region is involved in the interaction with DOCK180. ELMO proteins contain three main conserved regions (**Figure 2.1A, pg. 93**). The N-terminal region (residues 1-280, ELMO1 numbering) binds to RhoG [361,365], ERM proteins [376,377] and *Shigella* IpgB1 [377]. The middle domain comprises an ELMO-domain (318-491), specific to ELMO proteins [169]. At the C-terminus, ELMO proteins contain an atypical PH domain (555-676) [358]. Lastly, a Pro-rich motif (707-714) typical of SH3-interacting proteins and implicated in interactions with DOCK180 [368], is located at the extreme C-terminus.

Secondary structure prediction of the C-terminal region of ELMO1 (residues 532 to 727) was performed (data not shown). In these analyses, α-helical regions were predicted both N-terminal (536-557) and C-terminal (679-697) to the annotated PH domain (**Figure 2.1A, pg. 93**, light blue regions). Using GST fusion proteins of the ELMO1 PH domain with and without the flanking regions, we tested the ability of these fragments to bind DOCK180. GST-tagged ELMO1 (532-707), containing both flanking regions, could robustly precipitate DOCK180 (**Figure 2.1B, pg. 93**). The flanking regions were crucial for the observed interaction, as deletion on the N- or C-terminal side (GST-ELMO1 555-707 and GST ELMO1-532-675, respectively) reduced DOCK180-binding significantly (**Figure 2.1B, pg. 93**). These results are in agreement with a previous report [368], with the important difference that in that study, Rac1 was required to bridge the interaction between DOCK180 and ELMO1. We find a robust interaction between DOCK180 and ELMO1 in the absence of Rac1 both *in vitro* and *in vivo*.

Figure 2.1. The atypical PH domain of ELMO1 directly interacts with DOCK180.
(A) Domain architecture of ELMO1 (following ProSite annotation) indicating known protein interaction and functional regions. The N-terminal region of ELMO1 binds to RhoG [365], ERM proteins [376], and *Shigella* IpgB1 [377]. The middle (ELMO) domain of ELMO1 has no assigned function, but is conserved in ELMO proteins. The C-terminal 200 amino acids encompassing the PH domain (blue) and flanking regions (light blue) and the Pro-rich C-terminus (purple) is the focus of this study. (B-C) The PH domain of ELMO with N- and C-terminal flanking regions interacts with DOCK180, and the flanking regions are important in the interaction. (B) GST-tagged versions of the indicated fragments of ELMO1 PH region were used to pulldown FLAG-tagged DOCK180 from HEK293T lysate. (C) Similar experiment to (B) with GFP-tagged ELMO1 variants. HEK293T cells were co-transfected with the indicated plasmids, and lysates were subjected to immunoprecipitation with an anti-DOCK180 antibody. (D) The ELMO1^{PxxP} mutant is not sufficient to abrogate DOCK180/ELMO binding *in vivo*. Lysates of HEK293T cells transfected with the indicated plasmids were immunoprecipitated with an antibody against the Myc-epitope of ELMO1. Immunoblot analysis using anti-DOCK180 rabbit polyclonal and anti-Myc antibodies established the co-precipitation of DOCK180 and ELMO proteins. (E) Disruption of a possible SH3:PxxP interaction between DOCK180 and ELMO1 is not sufficient to uncouple DOCK180/ELMO1 binding *in vitro*. Purified GST, GST-ELMO1^{WT}, or GST-ELMO1^{PxxP} were used in pulldown experiments using lysates from HEK293T cells transfected with DOCK180^{WT}, DOCK180^{W45K}, or DOCK180$^{\Delta SH3}$. The bound proteins were detected by immunoblotting with an anti-DOCK180 antibody (C-19).

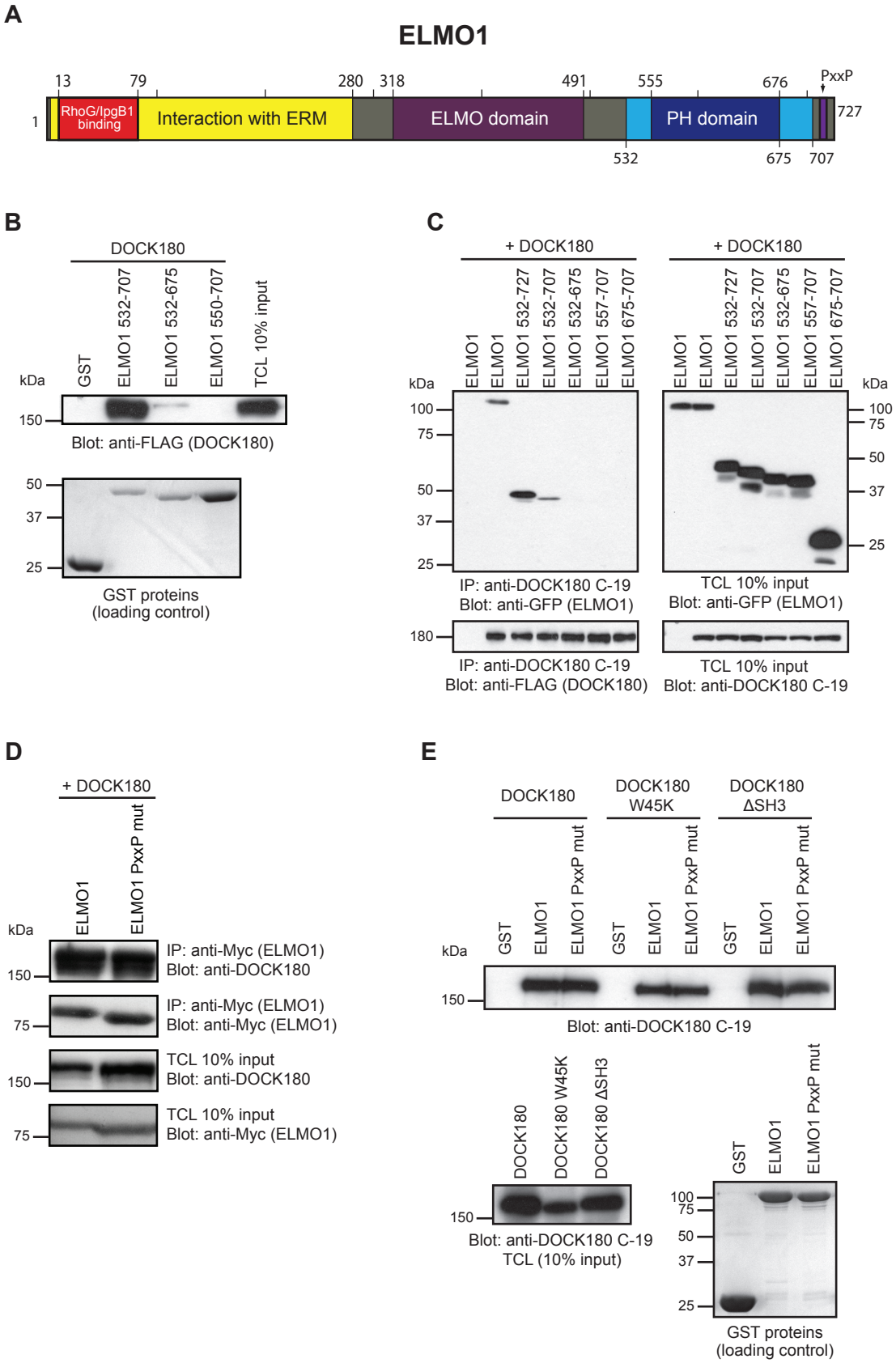
A
ELMO1
13
79
280
318
491
555
676
PxxP
1
RhoG/IpgB1 binding
Interaction with ERM
ELMO domain
PH domain
727
532
675
707
B
DOCK180
GST
ELMO1 532-707
ELMO1 532-675
ELMO1 550-707
TCL 10% input
kDa
150
Blot: anti-FLAG (DOCK180)
50
37
25
GST proteins
(loading control)
C
+ DOCK180
+ DOCK180
ELMO1
ELMO1 532-727
ELMO1 532-707
ELMO1 532-675
ELMO1 557-707
ELMO1 675-707
kDa
100
75
50
37
25
IP: anti-DOCK180 C-19
Blot: anti-GFP (ELMO1)
TCL 10% input
Blot: anti-GFP (ELMO1)
180
IP: anti-DOCK180 C-19
Blot: anti-FLAG (DOCK180)
TCL 10% input
Blot: anti-DOCK180 C-19
D
+ DOCK180
ELMO1
ELMO1 PxxP mut
kDa
150
IP: anti-Myc (ELMO1)
Blot: anti-DOCK180
75
IP: anti-Myc (ELMO1)
Blot: anti-Myc (ELMO1)
150
TCL 10% input
Blot: anti-DOCK180
75
TCL 10% input
Blot: anti-Myc (ELMO1)
E
DOCK180
DOCK180 W45K
DOCK180 ΔSH3
GST
ELMO1
ELMO1 PxxP mut
kDa
150
Blot: anti-DOCK180 C-19
DOCK180
DOCK180 W45K
DOCK180 ΔSH3
150
Blot: anti-DOCK180 C-19
TCL (10% input)
GST
ELMO1
ELMO1 PxxP mut
100
75
50
37
25
GST proteins
(loading control)

Figure 2.1

Involvement of the DOCK180 SH3 domain in ELMO1 binding

DOCK180 contains an SH3 domain at its N-terminus, and ELMO1 contains a Pro-rich motif (PxxP) at its C-terminus (**Figure 2.1A, pg. 93**). We analyzed the contribution of this potential interaction in the formation of the DOCK180/ELMO1 complex. As indicated in **Figure 2.1B**, ELMO1 (532-707), devoid of the Pro-rich motif, robustly interacted with DOCK180, indicating that a SH3/PxxP interaction is dispensable for complex formation. Furthermore, GFP-fusion proteins of the ELMO1 PH domain, with or without the PxxP motif, were tested for their ability to co-immunoprecipitate with DOCK180. These experiments revealed that, in cells, the PH domain of ELMO1 (residues 532-707) is the minimal domain capable of binding to DOCK180 (**Figure 2.1C, pg. 93**). However, the addition of the Pro-rich region of ELMO1 PH seemed to enhance its ability to interact with DOCK180 (**Figure 2.1C, pg. 93**).

To understand the contribution of the DOCK180 SH3 domain in the interaction with ELMO1, the proline residues 707, 710-712, 714 and 727 of ELMO1 were mutated to alanines ($ELMO1^{PxxP}$). Co-immunoprecipitation experiments of myc-tagged $ELMO1^{WT}$ and $ELMO1^{PxxP}$ in HEK293T cells indicated that both proteins interacted to an equivalent extent with exogenously expressed DOCK180 (**Figure 2.1D, pg. 93**). For the reverse experiment, DOCK180 lacking the SH3 domain ($DOCK180^{\Delta SH3}$) and a mutant in which a conserved Trp residue in the SH3 domain of DOCK180 was mutated to Lys ($DOCK180^{W45K}$), abolishing the binding of the SH3 domain to PxxP sequences [378], were tested for their ability to bind $ELMO1^{WT}$ or $ELMO1^{PxxP}$. GST-tagged full-length $ELMO1^{WT}$ and $ELMO1^{PxxP}$ bound equally well to DOCK180, $DOCK180^{\Delta SH3}$ and $DOCK180^{W45K}$ in pulldown experiments (**Figure 2.1E, pg. 93**). These results indicate that the DOCK180/ELMO1 interaction is not dependent on the additional SH3/PxxP interaction, although *in vivo*, such an interaction might well exist. However, it is also

possible that both motifs have additional functions and/or binding partners in cells that contribute to the cellular function of the DOCK180/ELMO complex (see below).

Structural analysis of the ELMO1/DOCK180 interaction

Our data indicated that on ELMO1, the PH domain and its flanking regions mediate the principle interactions responsible for complex formation with DOCK180. To understand the interaction between ELMO1 and DOCK180 in molecular detail, we initiated structural studies of the ELMO1 PH domain (**Figure 2.2A, pg. 97**). The ELMO1 PH domain is classified as a false-negative PH domain in ProSite (PS50003, [379]), as it does not fit the canonical PH domain profile, and therefore sequence comparison with crystallized PH domains is of limited value to aid domain boundary definition. Another crystallized member of this subgroup of PH domains is that of PDK1 which was found to form a unique N-terminal helical extension [380]. This prompted us to include the N-terminal flanking region of the ELMO1 PH domain in our constructs for crystallization. Three ELMO1 PH domain constructs were analyzed, comprising residues 532-675, 532-707 and 532-727. Diffraction quality protein crystals could only be obtained for the shortest construct, lacking the C-terminal flanking region (532-675). Diffraction data were collected to 2.3 Å resolution at the ESRF, and the structure was solved by SAD phasing using a mercury derivative. Excellent experimental phases were obtained and the structure was built and refined to a final R-factor of 0.208 (R_{free} 0.239) (**Table 2.1, pg. 98**). Two molecules of the ELMO1 PH domain are present per asymmetric unit, which superpose with an RMSD of 1.0 Å (over 132 Cα atoms). In the subsequent analysis we will focus on one molecule only.

Figure 2.2. Structure of the ELMO PH domain and conservation in the ELMO family.

(A) The structure of the ELMO1 PH domain (residues 532-675) is shown in cartoon representation. The αN helix is shown in green, the PH domain fold in teal, the VL1 region in yellow, and the β5/β6 loop is shown in orange. (B) A sequence alignment of the crystallized ELMO1 PH domain region and C-terminal residues from various species, as well as the ELMO2 and ELMO3 isoforms is shown. Secondary structure elements are indicated and labeled according to (A), and a black line indicates the end of the crystallized construct. Boxes indicate the VL1 and β5-β6 loop regions highlighted in (A). At the C-terminus, the SH3 binding region is boxed and the predicted helical region (αC2), which is not part of the structure, is indicated.

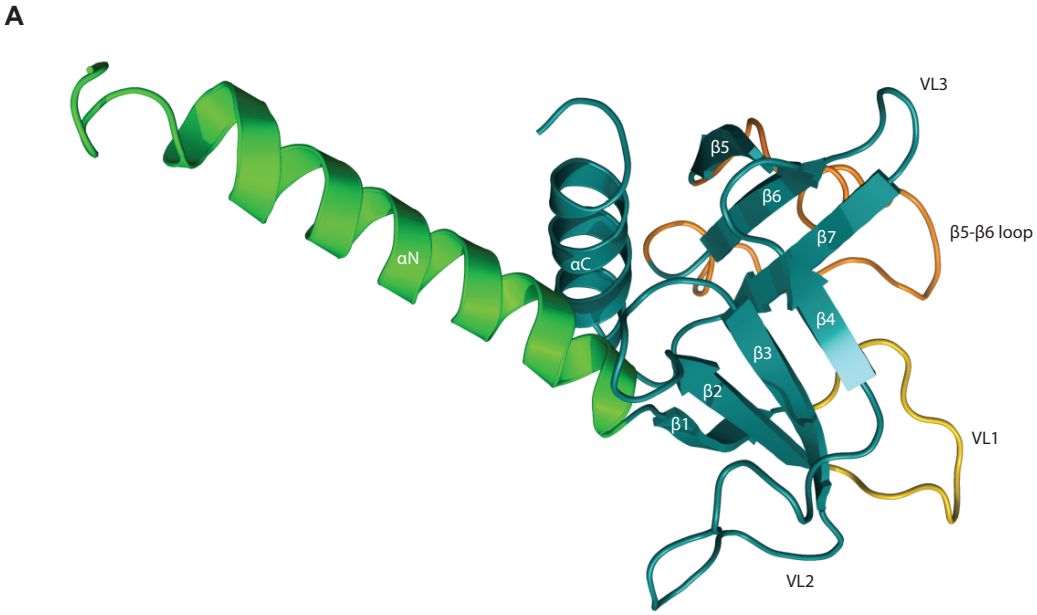
A
VL3
β5
β6
β7
β5-β6 loop
αN
αC
β4
β3
β2
β1
VL1
VL2

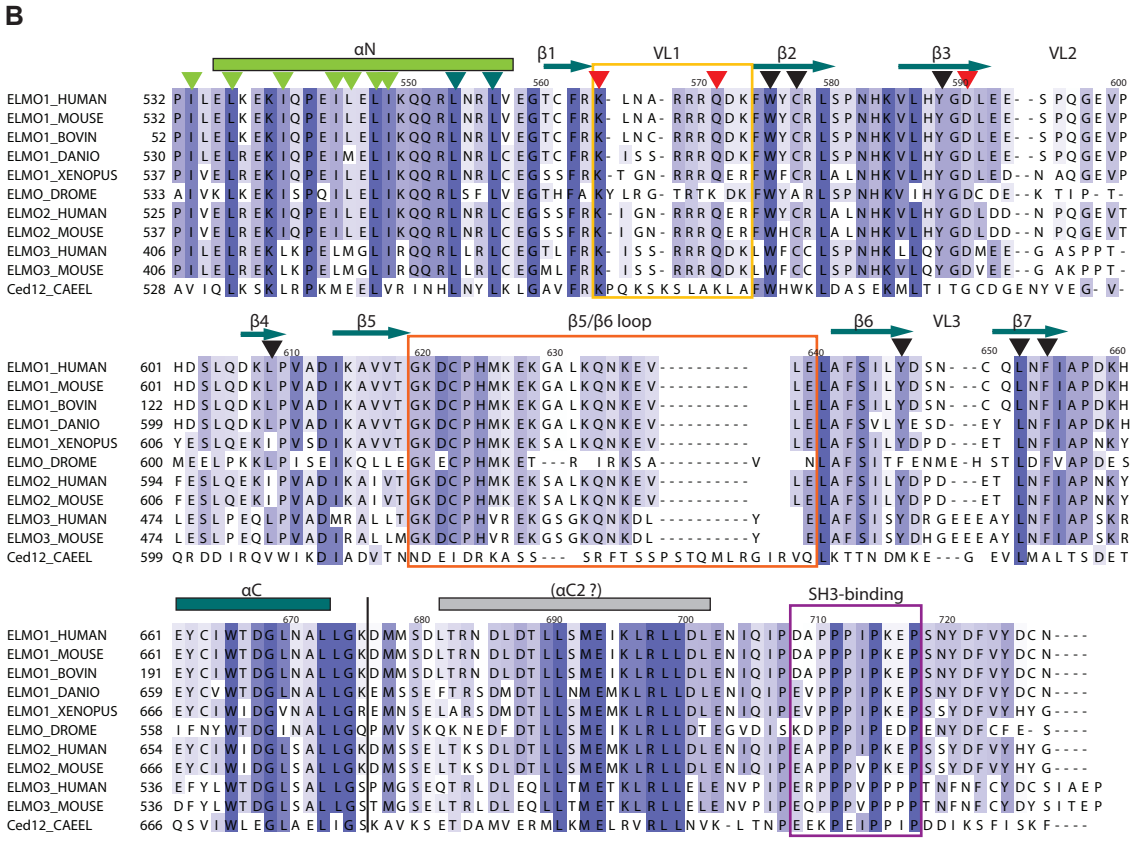
B
αN
β1
VL1
β2
β3
VL2
β4
β5
β5/β6 loop
β6
VL3
β7
αC
(αC2 ?)
SH3-binding
ELMO1_HUMAN
ELMO1_MOUSE
ELMO1_BOVIN
ELMO1_DANIO
ELMO1_XENOPUS
ELMO_DROME
ELMO2_HUMAN
ELMO2_MOUSE
ELMO3_HUMAN
ELMO3_MOUSE
Ced12_CAEEL

Figure 2.2

Table 2.1 Data collection, phasing and refinement statistics.

Values in brackets are for the highest resolution bin. All measured data were included in structure refinement.

	ELMO1 PH domain EMTS	ELMO1 PH domain Native
Data collection		
Beamline	ID23-2	ID23-2
Wavelength (Å)	1.0086	1.0000
Space Group	$P6_122$	$P6_122$
Unit Cell (Å)	a,b = 165.47, c = 81.47	a,b = 166.02, c =81.70
Resolution (Å)	80.0-3.00 (3.16-3.00)	40.0-2.30 (2.42-2.30)
Observed reflections	555933 (82449)	188356 (28101)
Unique reflections	13668 (1941)	29960 (4298)
Multiplicity	40.7 (42.5)	6.3 (6.5)
Completeness (%)	100.0 (100.0)	99.9 (100.0)
R_{merge}	0.124 (0.537)	0.058 (0.229)
<I> / σI	35.5 (8.7)	22.7 (8.3)
Phasing statistics		
Anomalous completeness (%)	100.0 (100.0)	
Anomalous multiplicity	22.2 (22.5)	
<FOM> before/after DM	0.26 / 0.83	
Phasing power anomalous	1.96	
Phasing power isomorphous	1.55	
Refinement		
Reflections in test set		1504 (5%)
R_{cryst}		0.208
R_{free}		0.239
Number of groups		
Protein residues		288
Water		150
Wilson B (Å^2)		43.1
<B> protein (Å^2)		19.1
<B> water (Å^2)		23.0
RMSD from ideal geometry		
Bond length (Å)		0.020
Bond angles (°)		1.9
Main chain B (Å^2)		1.3

Structure and evolutionarily conserved features of the ELMO1 PH domain

The crystallized ELMO1 construct contains two main structural features. The N-terminal 23 residues form a single extended α-helix (αN, residues 532-554), which, without break leads into the β1-strand of a following canonical PH domain fold (residues 555-675,) (**Figure 2.2A, pg. 97**). This fold is defined by a three-stranded and a four-stranded β-sheet forming a sandwich structure that is capped on one side by a C-terminal α-helix (αC) [79] (**Figure 2.2A, pg. 97**). The C-terminal helix of the ELMO1 PH domain interacts with invariant hydrophobic residues of the N-terminal helix (Leu553, Leu558), which stabilizes the striking 70° angle between helices (**Figure 2.2A and B, pg. 97**). Notably, the extended N-terminal helix in the ELMO1 PH domain is a unique feature of ELMO proteins, bearing no resemblance to the extension seen in the PDK1 PH domain [380], nor has it been observed in any other PH domain structurally characterized to date.

We performed sequence analysis of ELMO1 PH domains from different species and also compared the three mammalian ELMO isoforms for conserved features in their PH domain region (**Figure 2.2B, pg. 97**). The PH domain including the N-terminal helix extension is well conserved throughout species from *Drosophila melanogaster* to *Homo sapiens* and contains a large number of invariable residues. Strong sequence conservation within the three isoforms of human and mouse ELMO proteins suggests very similar structures of the PH domain regions of ELMO proteins (**Figure 2.2B, pg. 97**). The sequence similarity, length and conservation of loop insertions (VL) and the large number of invariant residues indicates that the ELMO PH domain fold is conserved in all ELMO isoforms, indicating a general functional equivalence of this region in ELMO proteins.

The ELMO1 PH domain is unable to bind phosphoinositides

In order to identify similar structures in the protein data bank, we performed a DALI search [381] with the PH domain region of ELMO1 (residues 554-675) (**Table 2.2, pg. 101**). The highest similarity to the ELMO PH domain was found with the PH domain of phospholipase C δ (PLCδ) in complex with inositol (1,4,5)-trisphosphate (Ins(1,4,5)P_3) (pdb-id 1mai, Z-score 10.5) [301] (**Figure 2.3B, pg. 103**), and with the PH domain of Dual Adaptor of Phosphotyrosine and 3-Phosphoinositides (DAPP1) in complex with inositol (1,3,4,5)-tetrakisphosphate (Ins(1,3,4,5)P_4) (pdb-id 1fao, Z-score 9.0) [382] (**Figure 2.3C, pg. 103**, **Table 2.2, pg. 101**). DAPP1 and PLCδ both contain insertions in the β5/β6 loop similar to ELMO1, probably accounting for the high Z-scores. Notably, DALI analysis did not detect similarities of the ELMO1 PH domain with PH domains from the other large family of Rho family GEFs that contain a catalytic Dbl-Homology (DH)/PH domain tandem.

The overall structural similarity of ELMO1 with PLCδ and DAPP1 suggested that the phospholipid-binding properties might be conserved, and that the ELMO1 PH domain might have a role in localizing the ELMO1/DOCK180 complex to membranes. The common site of interaction with phosphoinositides (PI) in PH domains is created by three Variable Loops, connecting β1/β2 (VL1), β3/β4 (VL2), and β6/β7 (VL3), respectively, located opposite of the α-helices at the open side of the β-sheet sandwich [382]. The Variable Loops create a positively charged pocket for interaction with the negatively charged phosphoinositides (**Figure 2.3, pg. 103**). Two key basic residues are conserved in this pocket of PI-binding PH domains [382], namely a Lys residue on β1 located in the back of the pocket, which interacts with the D4-phosphates of Ins(1,4,5)P_3 or Ins(1,3,4,5)P_4, and an Arg residue in the β2-strand, which interacts with the adjacent phosphate group of the ligand (**Figure 2.3B and C, pg. 103**). In

Table 2.2 DALI analysis of the ELMO1 PH domain fold.

PH domain	**PDB-ID**	**Z-score**	**RMSD**	**aligned residues**
PLCδ-IP3	1mai	10.5	2.4 Å	96
DAPP1-IP4	1fao	9.0	2.5 Å	86
Moesin	1ef1	8.8	2.3 Å	83

Figure 2.3. Comparison of the PH domain fold of ELMO with other PH domains

(A) Representation of the ELMO1 PH domain structure. On the left hand side, the PH domain fold is shown with an orientation looking into the putative ligand binding site. In the middle image, the β1- and β2-strands and VL1 region is shown in cartoon representation, and key residues involved in PI-binding and ligands are drawn. Hydrogen bonds are indicated as black dotted lines. The right hand image is an electrostatic surface potential calculated with APBS of the same view as to the left. Blue regions indicate positive surface potential, red regions indicate negative surface potential and white indicates uncharged regions. Key residues, loop regions and ligands are labeled. (B) PLCδ PH domain in complex with Ins(1,4,5)P_3 (1mai, [301]), shown as in (A). The ligand is shown in stick representation with red oxygens and purple phosphorous atoms. (C) DAPP1 PH domain in complex with Ins(1,3,4,5)P_4 (1fao, [382]). (D) F3 subdomain of Moesin bound to its C-terminal tail peptide in yellow (1ef1, [383]).

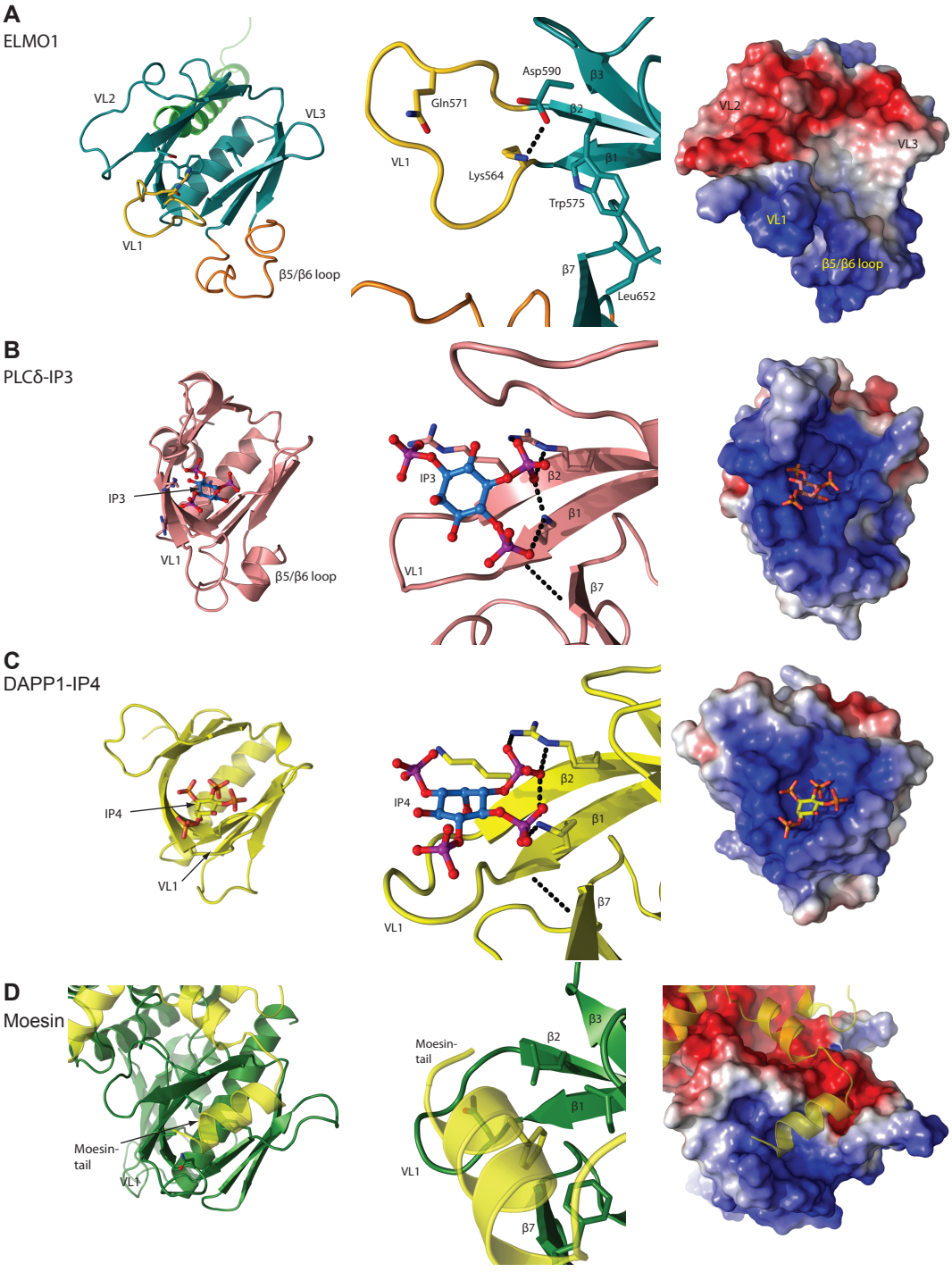
A
ELMO1
VL2
VL3
VL1
β5/β6 loop
Asp590
β3
Gln571
β2
VL1
Lys564
β1
Trp575
β7
Leu652
VL2
VL3
VL1
β5/β6 loop
B
PLCδ-IP3
IP3
VL1
β5/β6 loop
IP3
β2
β1
VL1
β7
C
DAPP1-IP4
IP4
VL1
IP4
β2
β1
β7
VL1
D
Moesin
Moesin-
tail
VL1
Moesin-
tail
β3
β2
β1
VL1
β7

Figure 2.3

ELMO1, Lys residue is conserved (Lys564), however, the Arg-equivalent residue is substituted by a Trp (Trp575), forming a hydrophobic rather than a positively charged base of the pocket (**Figure 2.3A, pg. 103**). More strikingly, the position of the guanidine-group of the conserved Arg residue is structurally replaced by the sidechain carboxy-group of Asp590, which neutralizes the charge of Lys564, and in addition would repel a phosphate group of a bound PI-ligand (**Figure 2.3A, pg. 103**). Notably, residues Lys564, Trp575 and Asp590 are invariant in all ELMO PH domains (**Figure 2.2B, pg. 97**). Hence, ELMO PH domains display structural features incompatible with PI-binding analogously to PLCδ or DAPP1 (**Figure 2.3, pg. 103**, further analysis in **Supplementary Material**). In agreement with the structural results, we found that neither full length ELMO1 nor the isolated ELMO1 PH domain were capable of specific binding to any phosphorylated PI *in vitro,* in lipid-coated beads pulldown experiments or phospholipid overlay assays (**Supplementary Figure 2S1, pg. 130**). We conclude that ELMO1 does not serve as a phospholipid-targeting module in the ELMO1/DOCK180 complex.

Further analysis of the ELMO1 PH domain fold revealed significant similarity with the F3 subdomain of FERM (band **F**our point one, **E**zrin, **R**adixin, **M**oesin) domains (see **Figure 2.3D, pg. 103**, **Supplementary Material**, and **Supplementary Figure 2S2, pg. 132**). Interestingly, in the context of FERM domains, the PI-binding site equivalent region is utilized as a protein-protein interaction site [383]. Future work will address whether the similarly shaped ELMO PH domain interacts with protein motifs through this site.

Analysis of the N-terminal helical extension of the ELMO1 PH domain

The N-terminal helical extension is a defining feature of the ELMO1 PH domain, and this region is involved in several crystal lattice contacts, forming a tight dimer

interaction with the second molecule in the asymmetric unit, and with a crystallographically related second dimer in the crystal lattice (**Figure 2.4A, pg. 107**, **Supplementary Material** and **Supplementary Figure 2S3, pg. 134**). These prominent helix-helix interactions suggest that the N-terminal α-helix might be involved in protein-protein interactions.

Further analysis shows that the N-terminal α-helix is amphiphatic in nature: hydrophobic Leu and Ile residues (Ile533, Leu536, Ile540, Ile544, Leu545, Leu547, Ile548) are all located to one side of the helix, while the opposite surface shows a hydrophilic character (**Figure 2.4A and B, pg. 107**). This pattern of Leu/Ile residues with a spacing of four amino acids is reminiscent of coiled-coil-proteins, which often interact in a well-described coiled-coil or Leu-zipper fashion. Examination of the electrostatic potential and conservation of this region indeed reveals a hydrophobic ridge spanning the entire length (27 Å) of the protruding helix (**Figure 2.4B, pg. 107**). Importantly, the involved Leu and Ile residues are fully conserved in ELMO proteins and Ced-12 (**Figure 2.4C, pg. 107**), indicating potential functional relevance.

The hydrophobic side of the ELMO1 αN helix is a DOCK180-binding surface

We tested whether the strikingly conserved hydrophobic residues of the αN helix were involved in DOCK180-binding. Fully conserved hydrophobic residues in ELMO1 were mutated to negatively charged residues (L536D, I544D, L545E, L547E and I548D, termed ELMO$^{\alpha N}$ hereafter) and the resulting Myc-tagged or GST fusion proteins expressed at similar levels with the wild-type proteins. The mutant proteins were tested for their ability to co-immunoprecipitate DOCK180. While full-length ELMO1^{WT} and ELMO1^{PxxP} bound to DOCK180 (**Figure 2.4D, pg. 107**), ELMO1$^{\alpha N}$ and the ELMO$^{\alpha N/PxxP}$ double mutant completely lost their ability to interact with DOCK180 (**Figure 2.4D, pg. 107**). The same ELMO1 mutants (ELMO$^{\alpha N}$, ELMO1^{PxxP} and

Figure 2.4. The extended N-terminal α-helix of ELMO1 PH domains is a DOCK180 binding site.

(A) Cartoon representation of the N-terminal α-helix colored according to Figure 2.2A. Hydrophobic Leu and Ile residues are shown and labeled (see **Figure 2.2B, pg. 97**). The second molecule of the asymmetric unit is shown in yellow, interacting through the helix in an anti-parallel fashion but not employing the hydrophobic Leu/Ile residues; the Leu/Ile sidechains of both molecules point towards the same side, generating a large hydrophobic platform which interacts with the same α-helical region of a crystallographically related dimer (also see **Supplementary Figure 2S3, pg. 134**). (B) Electrostatic surface potential calculated with APBS. Blue regions indicate positive surface potential, red regions indicate negative surface potential and white indicates hydrophobic regions. (C) The surface of the ELMO1 PH domain is colored from white (fully conserved) to black (no conservation). (D-E) Mutation of conserved hydrophobic residues in the αN-helix of the ELMO1 PH domain abolishes the DOCK180/ELMO1 interaction. (D) Lysates of HEK293T cells transfected with the indicated plasmids were immunoprecipitated with an antibody against the Myc-epitope (ELMO1). The co-precipitation of the various ELMO1 proteins and DOCK180 was analyzed via immunoblotting with anti-Myc (ELMO) and anti-FLAG (DOCK180) antibodies, respectively. (E) Lysates of HEK293T cells transfected with FLAG-DOCK180 were subjected to pulldown assays with GST-ELMO1 proteins. The precipitation of DOCK180 by the various ELMO1 fusion proteins was detected via immunoblotting with anti-FLAG (DOCK180).

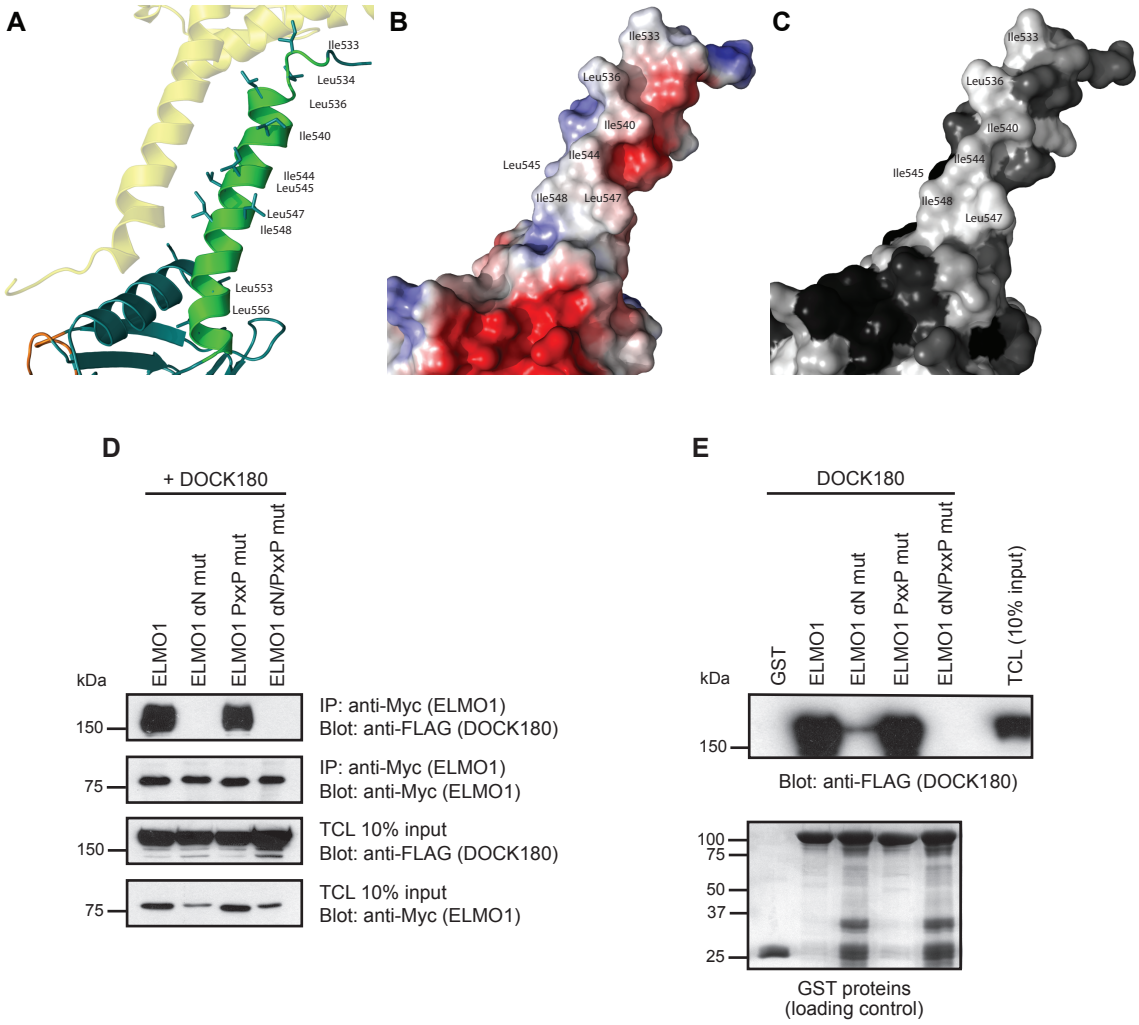
A
Ile533
Leu534
Leu536
Ile540
Ile544
Leu545
Leu547
Ile548
Leu553
Leu556
B
Ile533
Leu536
Ile540
Ile544
Leu545
Ile548
Leu547
C
Ile533
Leu536
Ile540
Ile544
Ile545
Ile548
Leu547
D
+ DOCK180
ELMO1
ELMO1 αN mut
ELMO1 PxxP mut
ELMO1 αN/PxxP mut
kDa
150
IP: anti-Myc (ELMO1)
Blot: anti-FLAG (DOCK180)
75
IP: anti-Myc (ELMO1)
Blot: anti-Myc (ELMO1)
150
TCL 10% input
Blot: anti-FLAG (DOCK180)
75
TCL 10% input
Blot: anti-Myc (ELMO1)
E
DOCK180
GST
ELMO1
ELMO1 αN mut
ELMO1 PxxP mut
ELMO1 αN/PxxP mut
TCL (10% input)
kDa
150
Blot: anti-FLAG (DOCK180)
100
75
50
37
25
GST proteins
(loading control)

Figure 2.4

ELMO$^{\alpha N/PxxP}$) expressed as GST proteins were also tested for their ability to precipitate with DOCK180 from cell lysates. In agreement with the above data, the ELMO1^{WT} and ELMO1^{PxxP} bound equally well to DOCK180 in pulldown experiments (**Figure 2.4E, pg. 107**). However, minimal but reproducible binding to DOCK180 could be observed for the ELMO1$^{\alpha N}$ while the double mutant ELMO1$^{\alpha N/PxxP}$ completely lost the ability to interact with DOCK180 (**Figure 2.4E, pg. 107**). To confirm these results, we also generated similar mutants of ELMO1 with minimal mutations in the αN helix (ELMO1$^{L547E/I548D}$ and ELMO1$^{L547E/I548D/PxxP}$) and obtained identical results with respect to DOCK180 binding (**Supplementary Figure 2S4, pg. 136**). In addition, we also created an ELMO1 mutant in which the hydrophobic residues were mutated to alanine (ELMO1$^{L547A/I548A}$), instead of charged residues, and we demonstrated that this mutant lacks DOCK180-binding activity (**Supplementary Figure 2S4, pg. 136**). We conclude that we have identified a single helix on ELMO proteins, preceding the PH domain, which mediates direct hydrophobic interactions with DOCK180.

Identification of ELMO1-binding sites on DOCK180

Having identified crucial regions within ELMO1 for DOCK180 binding, we attempted to map the reciprocal interaction sites on DOCK180. DOCK180 contains three annotated domains: an N-terminal SH3 domain, and DHR-1 and DHR-2 domains which function as PI-binding and GDP/GTP exchange domains, respectively [363,364] (**Figure 2.5A, pg. 110**). At its C-terminus, several Pro-rich regions implicated in interactions with SH3 domains are found [83]. As mentioned above and in agreement with a previous study [360], we found that DOCK180$^{\Delta SH3}$ interacts with ELMO1 (**Figure 2.5B, pg. 110**) in co-transfection experiments using HEK293T cells. However, deletion of the N-terminal 536 amino acids of DOCK180 (DOCK180$^{\Delta 1-536}$) completely abrogated its ability to interact with ELMO1 (**Figure 2.5B, pg. 110**), suggesting the

Figure 2.5. Identification of a novel ELMO1-binding region on DOCK180.

(A) Schematic representation of DOCK180. The SH3 domain (red), DHR-1 (yellow) and DHR-2 (green) domains mediate protein-interaction, PI-binding and Rac GDP/GTP exchange, respectively [363,364]. Pro-rich motifs at the C-terminus (purple) bind in *trans* to SH3 domains [83]. The N-terminal 200 amino acids encompass the ELMO-binding region [83] (pink). (B) The N-terminal region of DOCK180 is essential for ELMO binding. HEK293T cells were transfected with $DOCK180^{WT}$, $DOCK180^{\Delta SH3}$ or $DOCK180^{\Delta 1\text{-}536}$, and cell lysates were subjected to immunoprecipitation against Myc-tagged ELMO1. Bound proteins were analyzed by immunoblotting using anti-DOCK180 and anti-Myc antibodies. (C) The first 200 amino acids of DOCK180 harbor the ELMO binding domain. A panel of N-terminal GST-DOCK180 constructs was used in a pulldown assay with a lysate from Myc-ELMO1 transfected HEK293T cells. Bound proteins were detected by immunoblotting with an anti-Myc antibody. (D) The SH3 domain of DOCK180 contributes in ELMO1 binding. GST-fusion proteins of the residues 1-200 of $DOCK180^{WT}$ or $DOCK180^{W45K}$ were used in a pulldown assay with a lysate of Myc-ELMO1 transfected HEK293T cells. Bound proteins were detected by immunoblotting with an anti-Myc antibody. (E-F) Residues 69-187 of DOCK180 are sufficient for binding to ELMO while the SH3 domain provides a stabilizing effect in the formation of DOCK180/ELMO complex. (E) $DOCK180^{1\text{-}187}$, $DOCK180^{1\text{-}422}$ and (F) $DOCK180^{69\text{-}187}$ fragments specifically interact with ELMO1 and were visualized by autoradiography according to Material and Methods. (G) Hydrophobic residues of a predicted alpha-helical region between the SH3 and DHR-1 domain of DOCK180 are involved in ELMO1-binding (also see (A) and **Supplementary Figure 2S4**). GST-fusion proteins of the residues 1-200 of $DOCK180^{WT}$, $DOCK180^{L96D/W99E}$ and $DOCK180^{I132D/L133D}$ were used in a pulldown assay with a lysate of Myc-ELMO1 transfected HEK293T cells. Bound proteins were detected by immunoblotting with an anti-Myc antibody.

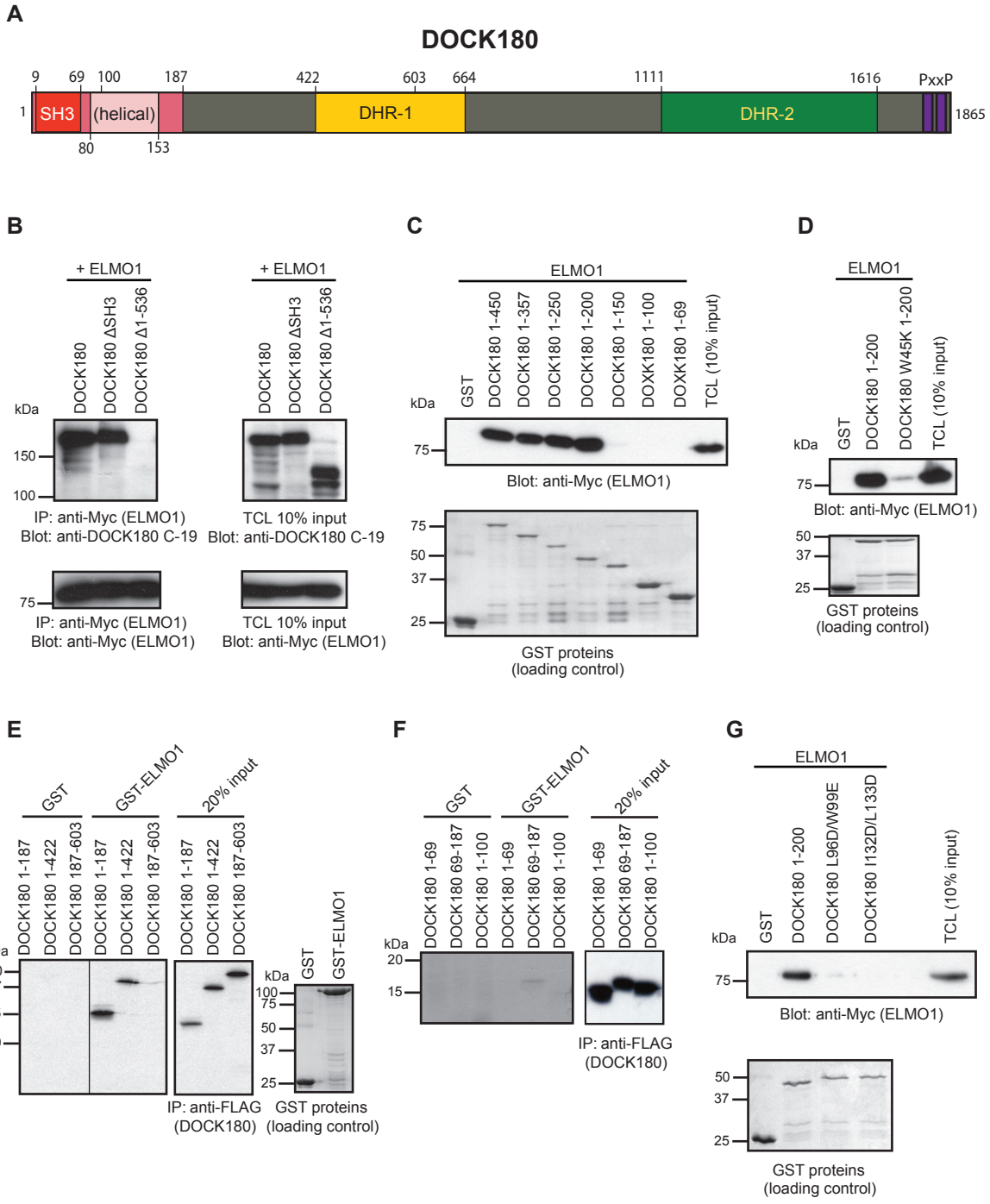
A
DOCK180
9
69
100
187
422
603
664
1111
1616
PxxP
1
SH3
(helical)
DHR-1
DHR-2
1865
80
153
B
+ ELMO1
DOCK180
DOCK180 ΔSH3
DOCK180 Δ1-536
kDa
150
100
IP: anti-Myc (ELMO1)
Blot: anti-DOCK180 C-19
TCL 10% input
Blot: anti-DOCK180 C-19
75
IP: anti-Myc (ELMO1)
Blot: anti-Myc (ELMO1)
TCL 10% input
Blot: anti-Myc (ELMO1)
C
ELMO1
GST
DOCK180 1-450
DOCK180 1-357
DOCK180 1-250
DOCK180 1-200
DOCK180 1-150
DOXK180 1-100
DOXK180 1-69
TCL (10% input)
kDa
75
Blot: anti-Myc (ELMO1)
75
50
37
25
GST proteins
(loading control)
D
ELMO1
GST
DOCK180 1-200
DOCK180 W45K 1-200
TCL (10% input)
kDa
75
Blot: anti-Myc (ELMO1)
50
37
25
GST proteins
(loading control)
E
GST
GST-ELMO1
20% input
DOCK180 1-187
DOCK180 1-422
DOCK180 187-603
kDa
50
37
25
20
IP: anti-FLAG
(DOCK180)
kDa
100
75
50
37
25
GST
GST-ELMO1
GST proteins
(loading control)
F
GST
GST-ELMO1
20% input
DOCK180 1-69
DOCK180 69-187
DOCK180 1-100
kDa
20
15
IP: anti-FLAG
(DOCK180)
G
ELMO1
GST
DOCK180 1-200
DOCK180 L96D/W99E
DOCK180 I132D/L133D
TCL (10% input)
kDa
75
Blot: anti-Myc (ELMO1)
50
37
25
GST proteins
(loading control)

Figure 2.5

presence of an ELMO1 binding site within the N-terminal region of DOCK180. A series of GST fusion proteins of N-terminal fragments of DOCK180 (1-450, 1-357, 1-250, 1-200, 1-150, 1-100, 1-69) were generated to delineate this ELMO1-binding site. These studies revealed that the first two hundred amino acids of DOCK180 are required to efficiently pulldown ELMO1 from cell extracts (**Figure 2.5C, pg. 110**, colored pink in **Figure 2.5A, pg. 110**). Interestingly, in the context of DOCK180 1-200, the W45K mutation in the SH3 domain significantly impairs its ability to precipitate ELMO1 (**Figure 2.5D, pg. 110**).

In reverse experiments, we studied whether N-terminal fragments of DOCK180, expressed by *in vitro* transcription/translation (IVT), were able to associate with GST ELMO1. While both DOCK180 1-422 and 1-187 were active in binding ELMO1, a DOCK180 fragment comprising residues 187-603 was incapable of such association (**Figure 2.5E, pg. 110**). Next, we tested the ability of GST-ELMO1 to precipitate the IVT DOCK180 fragments 1-69, 1-100 and 69-187. While no interaction of the SH3 domain-containing fragments of DOCK180 (1-69 and 1-100) to ELMO1 could be detected (**Figure 2.5F, pg. 110**), ELMO1 specifically precipitated albeit weakly the DOCK180 69-187 protein (**Figure 2.5F, pg. 110**). We conclude that the N-terminal 187 amino acids of DOCK180 harbor the binding site for ELMO proteins, with a primary binding site between residues 69-187. Importantly, we note that in the latter experiments, Rac1 is absent, highlighting that DOCK180/ELMO1 complex formation is Rac1 independent. Interestingly, in these *in vitro* experiments, more efficient association was observed in the DOCK180 fragment containing the SH3 domain (residues 1-69, **Figure 2.5E**) **, pg. 110**, in contrast to some of our co-immunoprecipitation and pulldown experiments. It therefore appears that in the IVT system, the DOCK180/ELMO1 interaction is stabilized by the SH3/PxxP interaction of the two molecules.

Secondary structure prediction of the first 200 amino acids of ELMO-interacting DOCK proteins (DOCK1/DOCK180, 2,3,4 and 5) from multiple species uncovered a helical region from residues 80-153 in DOCK180, which overlaps with a highly conserved region in these proteins (**Figure 2.5A, pg. 110**, **Supplementary Figure 2S5, pg. 138**). We speculated that these predicted helical/coiled-coil regions of DOCK180 might interact directly with the αN-helix of the ELMO1 PH domain in a coiled-coil fashion, and hence we designed mutations in two hydrophobic patches within this region in GST-DOCK180 1-200. The mutant proteins were soluble and expressed to similar levels with the WT counterpart. Significantly, both resulting proteins, DOCK180 $^{L96D/W99E}$ and DOCK180 $^{I132D/L133D}$, were unable to precipitate ELMO1 from cell extracts (**Figure 2.5G, pg. 110**). Hence, within the minimal ELMO1 binding domain of DOCK180, both hydrophobic and SH3-mediated interactions are utilized, and as for ELMO1, mutation of a few hydrophobic amino acids completely disrupts DOCK180/ELMO complex formation.

ELMO1 does not contribute towards DOCK180-mediated Rac activation

Previous findings indicated that complex formation between ELMO1 and DOCK180 promotes the GEF activity of DOCK180 towards Rac by two-fold [362,368]. In contrast, we demonstrated that DOCK180 alone activates Rac, and that the DHR-2 domain of DOCK180 is necessary and sufficient for this activity [363,364]. In order to clarify this ambiguity, we precipitated the GTP-bound form of Rac1 using the p21 binding domain of PAK1 (PBD-assay) [363]. We found that DOCK180 is indispensable for promoting Rac GTP-loading in CHO LR73 cells, and the presence of ELMO1^{WT} did not increase Rac activation (**Figure 2.6A, pg. 114**). Furthermore, the ELMO1$^{\alpha N/PxxP}$ double mutant defective in DOCK180 binding did not alter Rac GTP-loading in comparison to ELMO1^{WT} (**Figure 2.6A, pg. 114**). To ascertain that we performed these Rac activation measurements in the linear range of the assay, we included a condition

Figure 2.6. ELMO1 does not contribute towards DOCK180-mediated Rac activation

(A) Rac activation by DOCK180 is independent of ELMO1 in CHO LR73cells. Cells were transfected with the indicated plasmids and GTP-loaded Rac was pulled down from cell lysates using the p21-binding domain of PAK fused to GST (PBD-assay). The amount of Rac in pulldowns and in total cell lysates (TCL) was detected by immunoblotting with an anti-Rac antibody. Expression levels of the various proteins, and equal loading of Rac in all samples, were analyzed by immunoblotting of the TCL using anti- FLAG, anti-Myc and anti-Rac antibodies. This is a representative experiments from four independent assays. (B) Quantification of Rac activation by the various proteins was performed by densitometry from the experiment in (A). (C) A form of DOCK180 lacking the ELMO1 binding region robustly activates Rac. HEK293T cells were transfected with the indicated plasmids and GTP-loaded Rac was pulled down from cell lysates in a PBD-assay. The amount of Rac in pulldowns and in total cell lysates (TCL) was detected by immunoblotting with an anti-Rac antibody. Expression levels of the various DOCK180 proteins, and equal loading of Rac in all samples, were analyzed by immunoblotting of the TCL using anti-DOCK180 and anti-Rac antibodies.

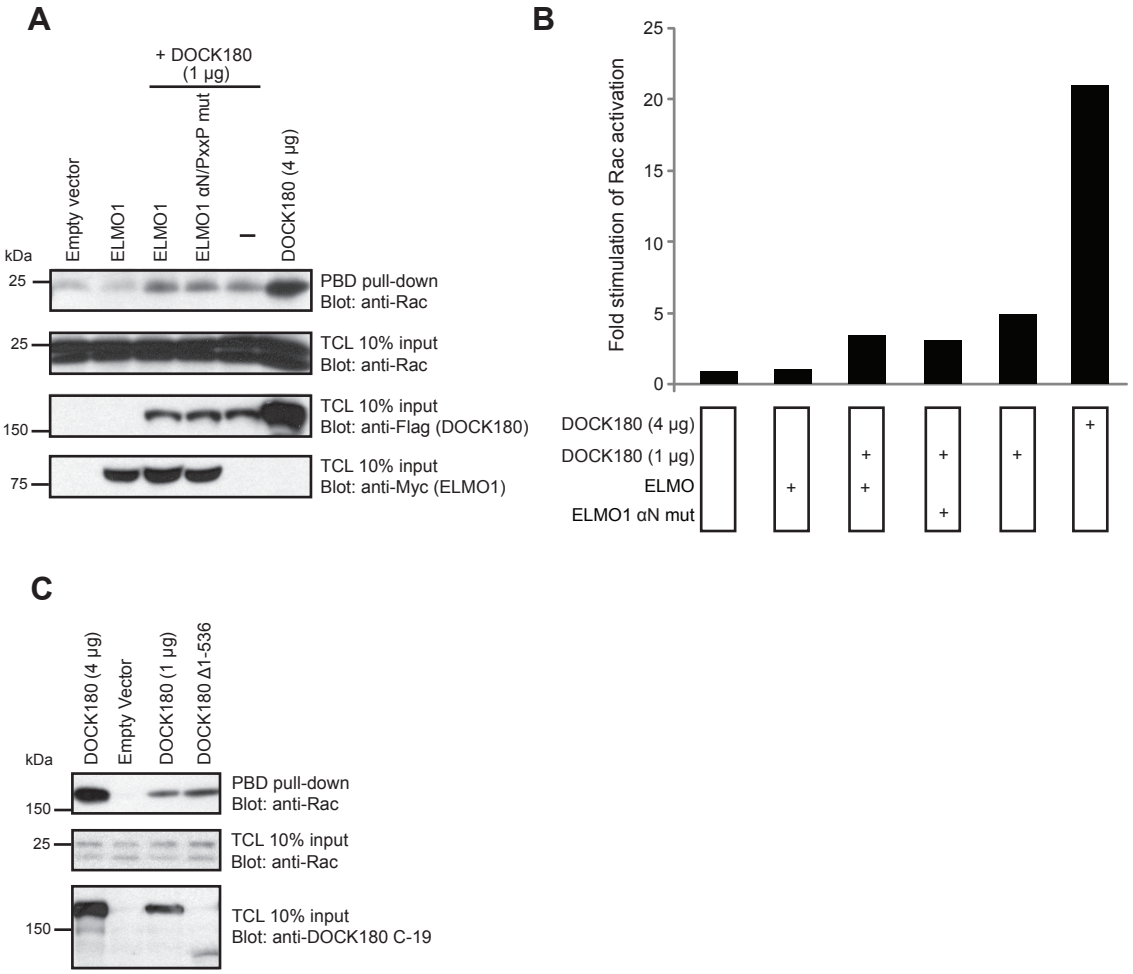
A
+ DOCK180 (1 µg)
Empty vector
ELMO1
ELMO1
ELMO1 αN/PxxP mut
–
DOCK180 (4 µg)
kDa
25
PBD pull-down
Blot: anti-Rac
25
TCL 10% input
Blot: anti-Rac
150
TCL 10% input
Blot: anti-Flag (DOCK180)
75
TCL 10% input
Blot: anti-Myc (ELMO1)
B
Fold stimulation of Rac activation
25
20
15
10
5
0
DOCK180 (4 µg)
DOCK180 (1 µg)
ELMO
ELMO1 αN mut
C
DOCK180 (4 µg)
Empty Vector
DOCK180 (1 µg)
DOCK180 Δ1-536
kDa
150
PBD pull-down
Blot: anti-Rac
25
TCL 10% input
Blot: anti-Rac
150
TCL 10% input
Blot: anti-DOCK180 C-19

Figure 2.6

with saturating amount of DOCK180 (4 μg instead of 1 μg of plasmid). We noted a further increase in Rac activation in comparison to the samples expressing DOCK180 at lower levels, therefore, proving the linearity of the Rac-PBD assay in these conditions (**Figure 2.6A, pg. 114**). Similar results were obtained in HEK293T cells (data not shown). To test if DOCK180 can activate Rac in an ELMO independent manner, a DOCK180 mutant incapable of binding to ELMO1 ($DOCK180^{\Delta 1\text{-}536}$) was expressed in HEK293T cells and Rac activity was measured. We found that much like $DOCK180^{WT}$, $DOCK180^{\Delta 1\text{-}536}$ robustly activated Rac when expressed alone in cells (**Figure 2.6B, pg. 114**). As above, we added a control where DOCK180 is expressed to saturation in order to demonstrate that the activities of $DOCK180^{WT}$ and $DOCK180^{\Delta 1\text{-}536}$ toward Rac were measured in the linear range of the assay. These results emphasize an intrinsic GEF activity in DOCK180 which is independent of ELMO binding.

Both the PH domain and PxxP motifs of ELMO1 contribute to DOCK180/ELMO1 signaling

We tested our model of DOCK180/ELMO1 interaction on Rac signaling using functional cell spreading and migration assays in CHO LR73 cells. These cells express endogenous ELMO proteins and DOCK180 (data not shown). We found that exogenous expression of $ELMO1^{WT}$ or $ELMO1^{\alpha N/PxxP}$ had no effect on spreading of LR73 cells on fibronectin when expressed alone (data not shown and [274]). However, when $ELMO1^{WT}$ or $ELMO1^{\alpha N/PxxP}$ were overexpressed in LR73 cells (2 μg instead of 0.3 μg of plasmids), we noted that both proteins could partially interfere with cell spreading, probably by sequestering essential components for Rac signaling (**Supplementary Figure 2S6, pg. 140**).

Co-expression of DOCK180/ELMO1/CrkII results in cell elongation when LR73 cells are replated on fibronectin-coated dishes [364]. We co-expressed $ELMO1^{WT}$ and

mutants together with DOCK180 and CrkII and examined the morphology of the transfected cells. In agreement with our biochemical characterization, ELMO1^{PxxP} had no effect on the ability of the ELMO1 protein to promote the elongation of cells when co-expressed with DOCK180 and CrkII (**Figure 2.7A-C, pg. 118**). ELMO1$^{\alpha N}$ prevented signaling from this complex to a small extent, as judged by morphological differences in elongated cells in comparison to the control conditions (**Figure 2.7A and B, pg. 118**). Interestingly, the double mutation ELMO1$^{\alpha N/PxxP}$ markedly prevented cell elongation on fibronectin (**Figure 2.7A and B, pg. 118**).

When the cells were tested for their ability to migrate, similar results were obtained. As reported earlier [364], LR73 expressing ELMO1^{WT}/DOCK180/CrkII had an increased capacity to migrate towards fibronectin in a boyden-chamber (**Figure 2.7D and E, pg. 118**) and ELMO1^{PxxP} promoted cell migration just as well as its wild-type counterpart (**Figure 2.7D and E, pg. 118**). ELMO1$^{\alpha N}$ led to a slight reduction in the ability of LR73 cells to migrate towards fibronectin (**Figure 2.7D and E, pg. 118**). Mutations in both the αN helix and in the PxxP motif of ELMO1 were required to abrogate the ability of this protein to support cell migration (**Figure 2.7D and E, pg. 118**). These results show that ELMO1/DOCK180 complex formation is required for DOCK180 function in cells. Furthermore, the functional data indicate that ectopic expression of ELMO1 mutants display dominant effects without affecting Rac activation. These results strengthen our notion that DHR-2 mediated Rac GEF activity of DOCK180 is ELMO independent.

Figure 2.7. Abrogating DOCK180/ELMO1 interaction *in vivo* results in defective cell elongation and migration. (A-E) DOCK180/ELMO1 binding is required for proper cell elongation. (A) Serum-starved LR73 cells transfected with the indicated plasmids were detached and plated on fibronectin–coated chambers for 1 h. Cells in the top panels were stained with an antibody against DOCK180 (H-4), while bottom panels represent an overlay of the anti-DOCK180, rhodamine-phalloidin and DAPI stains. Cells were photographed at 100X magnification. A scale bar represents 10 μm. (B) Quantification of the effect on cell elongation in response to disruption of the DOCK180/ELMO1 interaction. Several independent fields of the experiments from (A) were photographed at a magnification of 20X, and cells were scored for three phenotypes: round (attached and minimally spread), spread (clearly spread and flat cells) and elongated (elongated cells with polarity). (C) Expression levels of the transfected proteins for spreading assays were analyzed by immunoblotting cell lysates with anti-FLAG and anti-Myc (ELMO1 and CrkII) antibodies, as indicated. (D) Serum-starved LR73 cells transfected with a GFP vector in addition to the indicated plasmids were detached and placed in the upper compartment of a Boyden chamber. Cells were allowed to migrate for 4 h towards fibronectin and then fixed and stained with DAPI. GFP/DAPI double-positive cells that migrated to the underside of the membrane were counted from photographs taken at 20X magnification. The migration assay was performed in triplicate and data is shown as mean $\pm$ s.d. $^*P < 0.002$; one-way ANOVA. (E) Expression levels of the transfected proteins for migration assays were analyzed by immunoblotting cell lysates with anti-FLAG and anti-Myc antibodies, as indicated.

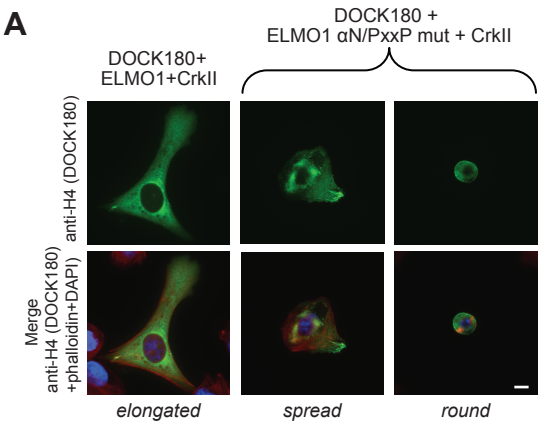

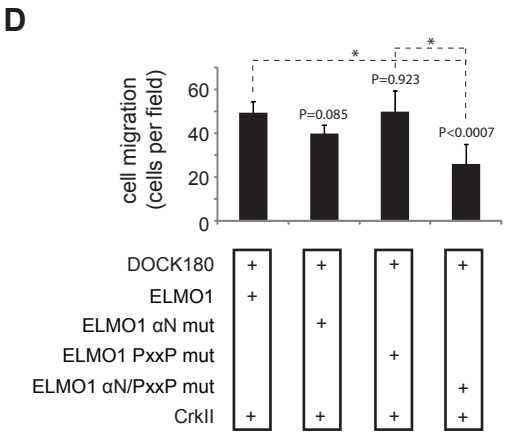

B

Transfection	Observed phenotypes
ELMO1 (n=53)	Elongated: 53% Spread: 43% Round: 4%
ELMO1 αN mut (n=53)	Elongated: 51% Spread: 45% Round: 4%
ELMO1 PxxP mut (n=49)	Elongated: 47% Spread: 47% Round: 6%
ELMO1 αN/PxxP mut (n=42)	Elongated: 26% Spread: 72% Round 2%

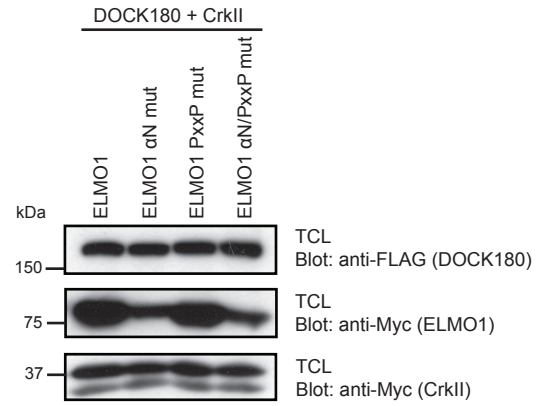

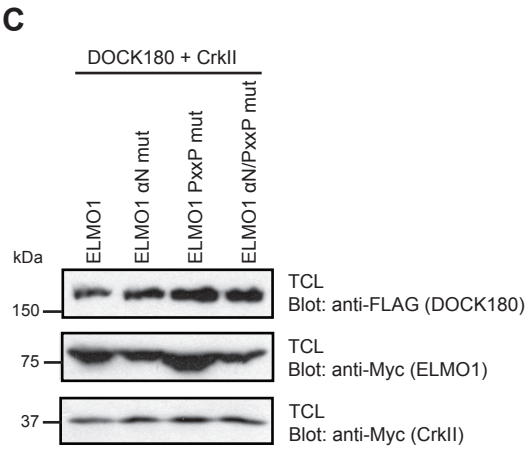

Figure 2.7

DISCUSSION

Two contact regions between DOCK180 and ELMO1

Analysis of the molecular details of the DOCK180 and ELMO1 interaction has highlighted some inconsistencies [83,359], however, definitive information is essential for the understanding of Rac activation and signaling mediated by this complex. Here we present data that DOCK180 and ELMO1 interact directly through the N-terminal 187 amino acids of DOCK180 and the C-terminal 195 amino acids of ELMO1 (residues 532-727). The primary interaction between these two regions involves the atypical ELMO1 PH domain (residues 532-707), especially the αN-helix (residues 532-555), and, on DOCK180, a previously uncharacterized region between the SH3 and DHR-1 domains (residues 69-187). Further analysis revealed the existence of an evolutionarily conserved alpha-helical region (residues 80-153) in DOCK180, which is likely to mediate direct contacts with the atypical hydrophobic αN-helix of the ELMO1 PH domain. A second interaction involves the N-terminal SH3 domain of DOCK180 and the C-terminal PxxP motifs of ELMO1. Our biochemical results support a mechanism whereby the PH domain of ELMO1 and its flanking regions, especially the αN helix, is the main determinant for binding to DOCK180, whereas the secondary SH3/PxxP interaction is not sufficient to promote complex formation. In cells however, functional analyses revealed that the PxxP motifs in ELMO1 also contribute in promoting efficient cell spreading and cell migration. Our findings in cells correlate with *in vivo* data in *C. elegans* where both the PH domain and Pro-rich region were necessary for the engulfment function of Ced-12 [358]. The functional, but not biochemical necessity of the DOCK180 SH3 domain and ELMO1 PxxP motif, might indicate other uncharacterized binding partners for these regions. CrkII and $p130^{Cas}$ are other components that have been implicated to signal to the DOCK180 complex, and these proteins also contain

SH3 domains and PxxP motifs. Further structural characterization and identification of additional components of the signaling complexes will be required.

Additional functions of the PH domain of ELMO?

The structural analysis of the ELMO1 PH domain enabled a detailed characterization and comparison with other PH domains. We were able to confidently exclude an involvement of the PH domain in PI-binding, as the common PI binding site in ELMO1 is not capable of interacting with such positively charged ligands. Recently, structural analyses of the ESCRT-II GLUE domain [384], Tiam1 and ArhGAP9 [385] have revealed a second mode of PH domain - PI interactions through conserved regions outside of the common PI binding site. In ELMO1 however, this binding site is also different, both at a structural and sequence level.

Instead, we have found strong similarities with FERM domains that contain within their F3 subdomain a PH-like fold, and which use the common PI binding site instead as a protein interaction interface [383]. Further functional and structural characterization of this putative protein interaction interface is required, but it is tempting to speculate that ELMO may also interact with proteins through this surface.

PH domains appear essential in DOCK GEFs. DOCK1, 2, 5 and DOCK3 and 4 bind to ELMO and utilize its PH domain, while Zizimin1/DOCK9, 10 and 11 contain PH domains themselves in their N-termini [83]. A structure of the DOCK9 PH domain has recently been deposited in the protein databank (**Supplementary Figure 2S5, pg. 138**). This PH domain does not resemble the ELMO1 PH domain, and analysis of the surface potential suggests that it might interact with PIs (**Figure 2.3, pg. 103** and **Supplementary Material**). Indeed, it was recently reported that the DOCK9 PH domain binds to PI ligands and may target DOCK9 to membranes [277]. Hence, it appears

that PH domains of the DOCK GEFs may function in various ways (protein-protein interaction in ELMO/DOCK180 as opposed to membrane interaction in DOCK9), and future research will need to address their roles in more details.

PH domain of ELMO1: Direct or indirect binding to DOCK180 and the implications for Rac GTP-loading?

A previous study highlighted a fragment of ELMO1, virtually identical to the one characterized here, that was unable to bind DOCK180 directly, but could only interact with a pre-formed complex between DOCK180 and nucleotide-free Rac [368]. Mechanistically, these findings were proposed to regulate the catalytic GEF-activity of DOCK180 towards Rac and at least partially explained the bi-partite GEF model [368], in which DOCK180 and ELMO act somehow together in GDP/GTP exchange. Our detailed mapping of the respective binding sites conflicts with such a '*trans*' binding mode, as we observe direct interaction independent of Rac. Our structure-based mutagenesis identified key conserved hydrophobic residues in ELMO1 that mediate the direct interaction with DOCK180, and point mutations disrupt this binding. We found that ELMO1 does not affect GTP loading of Rac by DOCK180, however it is required for signaling to or from the DOCK180/ELMO1 complex. However, as these studies were performed in cells expressing endogenous ELMO1, further studies and knockout models for ELMO family members are required to fully comprehend a contribution of ELMO proteins in DOCK180 mediated Rac GEF activity. The ability of ELMO1 to signal to the actin cytoskeleton likely resides in its N-terminal region where it can bind to ERM proteins and RhoG. These ELMO1-mediated interactions might also play a targeting role (e.g. RhoG resides at the plasma membrane), and in fact point to a role of ELMO1 as an interaction platform for other molecules involved in the pathway. We are now investigating the exciting possibility that ELMO proteins may have a scaffolding function in connecting Rac activators and Rac effectors.

ACKNOWLEDGEMENTS

We thank Dr M. Matsuda for gifts of reagents. Drs. M. Roe and O. Opaleye are acknowledged for data collection and O. Opaleye also for help in protein purification and crystallization. D. Komander is supported by a Beit Memorial Fellowship for Medical Research. M. Patel and M. Laurin are supported by CIHR funded scholarships from the IRCM Cancer Training Program. This work was supported by a CIHR operating grant (J-F Côté) and Cancer Research UK (D. Barford). J-F Côté holds a CIHR New Investigator Award.

Coordinates and structure factors have been deposited with the protein data bank, accession number 2vsz.

SUPPLEMENTARY MATERIAL

SUPPLEMENTARY TEXT

Detailed structural analysis of the PH domain fold of ELMO1

In the main text, we focused our analysis of the ELMO1 PH on the putative PI binding site and the αN helix. Here we extend the structural analysis, highlighting additional interesting features of ELMO1 PH domains, which account for the classification of the ELMO1 PH domain as an outlier to the classical PH domain fold. The ELMO1 PH domain varies from the canonical PH domain fold in two regions: the VL2 loop region (residues 592-604) is unusually long compared to other PH domains and folds back over the four-stranded β-sheet (**Figure 2.2A, pg. 97**). The interactions between VL2 and the outer side of the four-stranded β-sheet are mainly hydrophobic (Cys561, Phe574, and Tyr 576 on strands β1 and β2; Leu591, Pro595, Val599 and Leu604 in VL2), and hence are unlikely to allow a large degree of movement of VL2. Another insertion of 20 amino acids exists between β-strands β5 and β6 (residues 619-639), and folds over the three-stranded β-sheet, forming an additional fourth loop shaping the putative ligand-binding site. Overall, the insertions cover a large surface on the β-sheets, thereby determining surface features of the ELMO PH domain.

Further analysis of the PI-binding region of the ELMO1 PH domain reveals similarity to FERM domains

We noted in the main text, that the ELMO PH domain is incapable of PI-binding due to replacement of key conserved residues. In addition to this, other differences between ELMO PH domains and PI-binding PH domains can be found. The β1-strand in ELMO1 does not contact the β7-strand as observed in PI-binding PH domains, resulting

in a parallel orientation of the β-sheets rather than a barrel-like structure. This markedly shapes the surface of this region, and alters the electrostatic potential of the ELMO1 PH domain dramatically compared to PI-binding family members (**Figure 2.3, pg. 103**). ELMO1 features a large hydrophobic platform (formed by the highly conserved residues Trp575, Cys577, Tyr588, Leu608, Tyr646, Leu652 and Phe654), which is confined on one side by VL1 and the β5/β6 insertion, and on the other side by the VL3 region (**Figure 2.2B, pg. 97 and 2.3A, pg. 103**). Both VL1 and the β5/β6-insertion show positive electrostatic potential, whilst VL2 is negatively charged (**Figure 2.3A, pg. 103**).

Nevertheless, the conserved nature of this common PH domain interaction surface suggests a different functionality. Interestingly, further examination of the DALI analysis indicated significant similarity with another class of PH domain folds occurring in FERM domains. FERM domains consist of three subdomains F1, F2 and F3, with the F3 subdomain comprising a PH domain fold. The ELMO1 PH domain and the FERM domain of Moesin (pdb-id 1ef1, [383]) share a Z-score of 8.8 (**Table 2.2, pg. 101**) and superimpose with an RMSD of 2.4 Å over 83 Cα atoms (**Figure 2.3D, pg. 103**).

Importantly, the F3 subdomain in FERM proteins is a protein-interaction domain, and utilizes the common PI-binding site for interaction with the tail-region of the ERM protein via an intramolecular contact (**Figure 2.3D, pg. 103** and **Supplementary Figure 2S2, pg. 132**). The last ten amino acids of Moesin form a short helix, which occupies the largely hydrophobic PI-equivalent binding pocket in the F3 subdomain of Moesin (**Figure 2.3D, pg. 103**). Superposition of Moesin and the ELMO1 PH domain places this Moesin tail-helix onto the hydrophobic patch of ELMO1, and the single Phe residue in the Moesin tail is located in a complementary hydrophobic pocket on ELMO1, reminiscent of the intramolecular Moesin interaction (**Supplementary Figure 2S2, pg. 132**). In contrast, the Gln571 and Asp590 of ELMO1 overlap with the C-terminal Met residue of Moesin (**Supplementary Figure 2S2, pg. 132**). ELMO1 has been reported to bind to ERM proteins, but this was attributed to N-terminal regions of

ELMO1 [360,377]. The similarity of ELMO PH domains with the F3 subdomain of ERM proteins nevertheless suggests that this site in ELMO1 could be utilized for peptide/protein binding in an analogous manner to FERM domains. DOCK180 itself does not contain sequences similar to the ERM tail region, and hence, such an interaction is unlikely to be utilized in DOCK180/ELMO complex formation. Further research will be required to determine the potential protein ligand(s) for this conserved putative protein interaction surface in the ELMO PH domain.

Conserved hydrophobic residues C-terminally to the ELMO PH domain are not involved in DOCK180 interaction

To achieve robust complex formation with DOCK180, the PH domain of ELMO1 had to be extended on both the N- and C-terminus. While we identified key interacting residues in the αN-helix, the contribution of the C-terminal extension is not clear. This region is not included in the crystal structure (**Figure 2.1B, pg. 93**); however, secondary structure prediction and conservation analysis identifies a putative helical/coil-coil signature comprising several invariant hydrophobic residues (**Figure 2.2B, pg. 97**). We tested whether mutation of such residues had a similar effect in abrogating complex formation as mutation of the αN helix did. GST-fusion proteins of ELMO1$^{L689A/L690A}$ and ELMO1$^{R697A/L698A/L699A}$ did not affect complex formation significantly (**Supplementary Figure 2S1, pg. 130**). Therefore, structural consequences of the C-terminal extension of the ELMO PH domain, and its position in relation to the PH domain fold and αN helix, are currently unclear, and further structural studies on full-length ELMO and complexes between ELMO and DOCK proteins will be required.

ELMO1 is a monomer in solution and in cells

The ELMO1 PH domain crystallized by tight packing of the αN-helix, forming a four-helix bundle (**Supplementary Figure 2S3, pg. 134**). Although this is often a crystallization artifact, the possibility existed that ELMO dimerizes/oligomerizes *in vivo*, and that the αN-helix functions as a dimerization/oligomerization domain. However, in gel filtration analysis of the ELMO1 PH domain and of full-length ELMO1, the proteins elute at the expected molecular weight for monomers (data not shown). Hence, the oligomerization is likely to be induced during formation of the crystal lattice. Additionally, the ability of full length Myc- and GFP-tagged ELMO1 to dimerize could not be supported experimentally in co-immunoprecipitation experiments (**Supplementary Figures 2S8, pg. 144**). We conclude that the α-helical extension of the ELMO1 PH domain does not support dimerization of the ELMO1 PH or ELMO1 molecules in solution. Interestingly, DOCK proteins have been shown to be dimeric in cells, and the stoichiometry of a DOCK180/ELMO complex hence requires further analysis.

A PI-binding PH domain in Zizimin-1/DOCK9

Another member of the DOCK180-family of RhoGEFs is the Cdc42-specific DOCK9/Zizimin1 protein [386]. DOCK9 contains the DHR-1 and DHR-2 regions also found in DOCK180, but differs from DOCK180 in a different domain organization [386]. Instead of an N-terminal SH3 domain and ELMO-interaction region in DOCK180, DOCK9 contains a PH domain at its N-terminus [83,359].

Having identified unique features in the PH domain of ELMO proteins, we wondered whether these are also present in other DOCK180-related Rho-family GEFs. A structure of the DOCK9/Zizimin1 PH domain solved by an NMR structural genomics

consortium (RIKEN) has been deposited in the protein data bank (pdb-id 1wg7, **Supplementary Figure 2S6, pg. 140**). Compared to the ELMO1 PH domain, it lacks the N-terminal helical extension, and contains shorter versions of the VL2-flap and the β5-β6 insertion. In contrast to the ELMO1 PH domain, the DOCK9 PH domain structure shows all features of PI-binding PH domains (**Supplementary Figure 2S7, pg. 142**). It displays a similar, strongly positively charged PI-binding pocket, and features the conserved Lys (Lys26 in DOCK9), and Arg (Arg43 in DOCK9) residues, as well as further positively charged residues (Lys41, Lys70) required for PI-binding. Based on the structure, we suspect the PH domain of DOCK9 to be a PI binding domain. Recent data indeed suggest the possibility that the DOCK9 PH domain is able to contribute directly to membrane localization of DOCK9 by interacting with phosphoinositides [277]. This highlights yet again the remarkable versatility of PH domains, which in the case of the DOCK180-related RhoGEFs seem to have evolved to take part in entirely different regulatory processes.

SUPPLEMENTARY MATERIAL AND METHODS

Plasmid Constructs. pCNX2 Flag-DOCK180, pCNX2 Flag-DOCK180$^{\Delta SH3}$, pCAGGS DOCK180$^{\Delta 1-536}$ and pCAGGS Myc-CrkII were gifts from M. Matsuda. pcDNA3.1 Myc-ELMO1 and pEBB ELMO1-GFP were previously described [363]. Plasmids coding for DOCK180 GST-fusion proteins (residues 1-450, 1-357, 1-250, 1-200, 1-150, 1-100 and 1-69) were generated by PCR using the DOCK180 cDNA as a template and cloned into the SalI/NotI sites of pGEX4T-1. The pGEX4T-1 DOCK180^{W45K} (1-200), DOCK180$^{L96D/W99E}$ (1-200) and DOCK180$^{I132D/L133D}$ (1-200) were generated by site-directed mutagenesis (QuickChange; Stratagene). The pcDNA3.1 ELMO1^{PxxP} (P707A/P710A/P711A/P712A/P714A/P717A) and the ELMO1$^{\alpha N}$ (L536D/I544D/L545E/L547E/I548D) were generated by site-directed mutagenesis. To construct ELMO1$^{\alpha N/PxxP}$ double mutant of Myc-ELMO1 in pcDNA3.1, the EcoRV/BamHI fragment of the αN mutant cDNA was subcloned into the same sites of the ELMO1 PxxP mutant. A similar strategy was used to generate the pcDNA3.1 ELMO1$^{\alpha N/PxxP}$ and ELMO1$^{L547E/I548D/PxxP}$. Full length ELMO1 GST-fusion constructs (αN, PxxP, αN/PxxP, L547E/I548D and L547E/I548D/PxxP mutants) were generated by subcloning the BamH1/XhoI fragment of the ELMO1 cDNA in pcDNA3.1 into the BamHI/SalI sites of pGEX4T1. GST ELMO$^{L547A/I548A}$ was generated by site directed mutagenesis. The various ELMO1 PH GST-fusion and GFP-fusion constructs were generated by PCR using the ELMO1 cDNA as a template and cloned into the XhoI/EcoRI sites of pGEX4T-1 and EcoRI/SalI sites of pEGFP-C2, respectively. The plasmids used for expression of the N-terminus of DOCK180 (residues 1-69, 1-100, 1-187, 1-422, 69-187 and 187-603) by *in vitro* transcription/translation were constructed as followed: corresponding cDNA was amplified by PCR and cloned in the BglII/XhoI sites of pCMVTag-1 (Promega) downstream of the T7 RNA polymerase promoter. pET28a DOCK180 DHR-1 and pGEX4T1 BMX/Etk PH were previously reported [274].

Supplementary Figure 2S1. List of ELMO1 constructs tested for binding with DOCK180 and phosphoinositides. Table. Summary of the various ELMO1 constructs which were generated and tested for DOCK180- and PI-binding in this study. (A) ELMO1 is incapable of binding to lipids *in vitro*. Purified recombinant GST-ELMO1 or GST-ELMO1 PH proteins (1 μg each) were incubated with beads coated with the indicated phosphoinositides, or as a control, with beads alone. The bound proteins were detected by immunoblotting with anti-GST antibodies. (B-C) As positive controls, the DHR-1 domain of DOCK180 (B) and the PH domain of BMX/Etk (C) were purified and subjected to binding to various phosphoinositides, as in (A).

Table I

Construct	Figure No.	Dock180-binding capability
GST-ELMO1	1e	+++ [a]
GST- ELMO1 532-675	1b	+ [a]
GST- ELMO1 550-707	1b	- [a]
GST- ELMO1 532-707	1b	+++ [a]
Myc- ELMO1	1d, 5b	+++ [b]
Myc- ELMO1^{G559A}	Not shown	+++ [b]
Myc- ELMO1$^{F641A/S642A/I643A}$	Not shown	+++ [b]
Myc- ELMO1^{W665A}	Not shown	+++ [b]
GFP- ELMO1	1c	+++ [b]
GFP- ELMO1 532-727	1c	+++ [b]
GFP- ELMO1 532-707	1c	++ [b]
GFP- ELMO1 532-675	1c	- [b]
GFP- ELMO1 557-707	1c	- [b]
GFP- ELMO1 566-707	1c	- [b]
GFP- ELMO1 675-707	1c	- [b]
Myc- ELMO1$^{L689A/L690A}$	Not shown	+++ [b]
Myc- ELMO1$^{R697A/L698A/L699A}$	Not shown	+++ [b]
Myc- ELMO1^{L536E}	Not shown	+++ [b]
Myc- ELMO1^{I544D}	Not shown	+++ [b]
Myc- ELMO1^{I548D}	Not shown	+ [b]
Myc- ELMO1$^{L547E/I548D}$	S4a	- [b]
Myc- ELMO1$^{L547E/I548D/PxxP}$	S4a	- [b]
GST- ELMO1$^{L547A/I548A}$	S4b	- [a]
Myc- ELMO1 $^{\alpha N}$	4d	- [b]
Myc- ELMO1 ^{PxxP}	1d, 4d	+++ [b]
Myc- ELMO1 $^{\alpha N/PxxP}$	4d	- [b]
GST- ELMO1 $^{\alpha N}$	4e	+ [a]
GST- ELMO1 ^{PxxP}	1e, 4e	+++ [a]
GST- ELMO1 $^{\alpha N/PxxP}$	4e	- [a]
Myc- ELMO1 $^{\Delta 548-727}$	Not shown	- [b]

a: GST-pulldown experiment

b: co-immunoprecipitation experiment

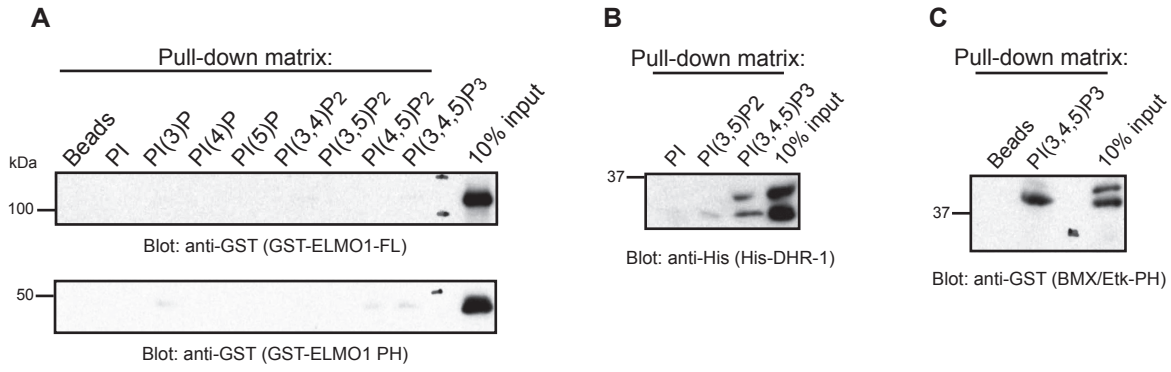

Supplementary Figure 2S1

Supplementary Figure 2S2. Comparison of conserved features between Moesin-tail interaction and ELMO1 PH domain.

(A) A detailed view of the interactions between the Moesin F3-subdomain (under a grey surface) and the Moesin tail helix (in yellow). Hydrophobic residues (shown as sticks under the surface) are labeled and form a pocket for the interaction with Phe574. (B) Similar conserved, hydrophobic residues in the ELMO1 PH domain form a similarly sized pocket. (C) Superposition of the ELMO1 PH domain and Moesin places the tail region and Phe574 neatly into the hydrophobic pocket on ELMO1. However, steric clashes are present with the C-terminus of the tail region (Met577) on Moesin and Asp590/Gln571 on ELMO1.

Moesin

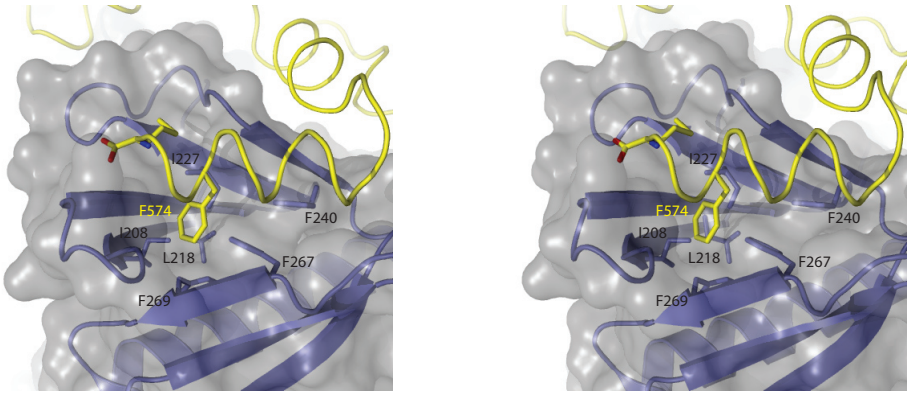

ELMO1

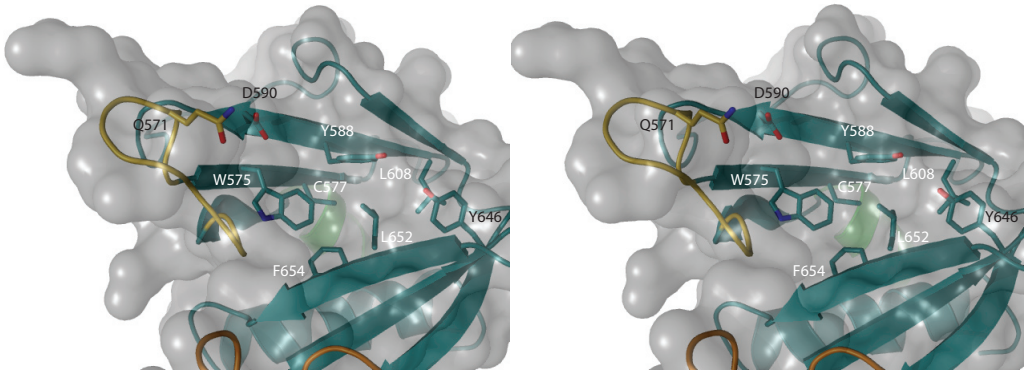

ELMO1 / Moesin C-terminus (model)

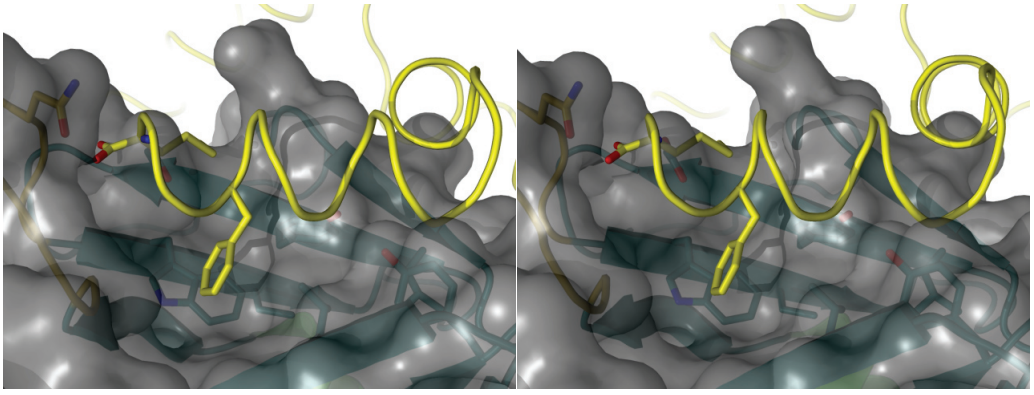

Supplementary Figure 2S2

Supplementary Figure 2S3. Involvement of the N-terminal helical extension of the ELMO1 PH domain in crystal packing.

(**A**) The asymmetric unit of the crystals contains a dimer of the ELMO1 PH domain, in which the N-terminal helices pack against each other in an anti-parallel fashion. This exposes the conserved hydrophobic residues to one side of the dimer. (B) A dimer-dimer interaction is created by a two-fold crystallographic axis. A four-helix bundle is formed by hydrophobic helix interactions. The oligomerisation is likely to be induced during formation of the crystal lattice, as the analyzed proteins are monomeric in solution (judged by gel filtration analysis, data not shown). Additionally, the ability of full length Myc- and GFP-tagged ELMO1 proteins to dimerize could not be supported experimentally in co-immunoprecipitation experiments (**Supplementary Figure 2S6**).

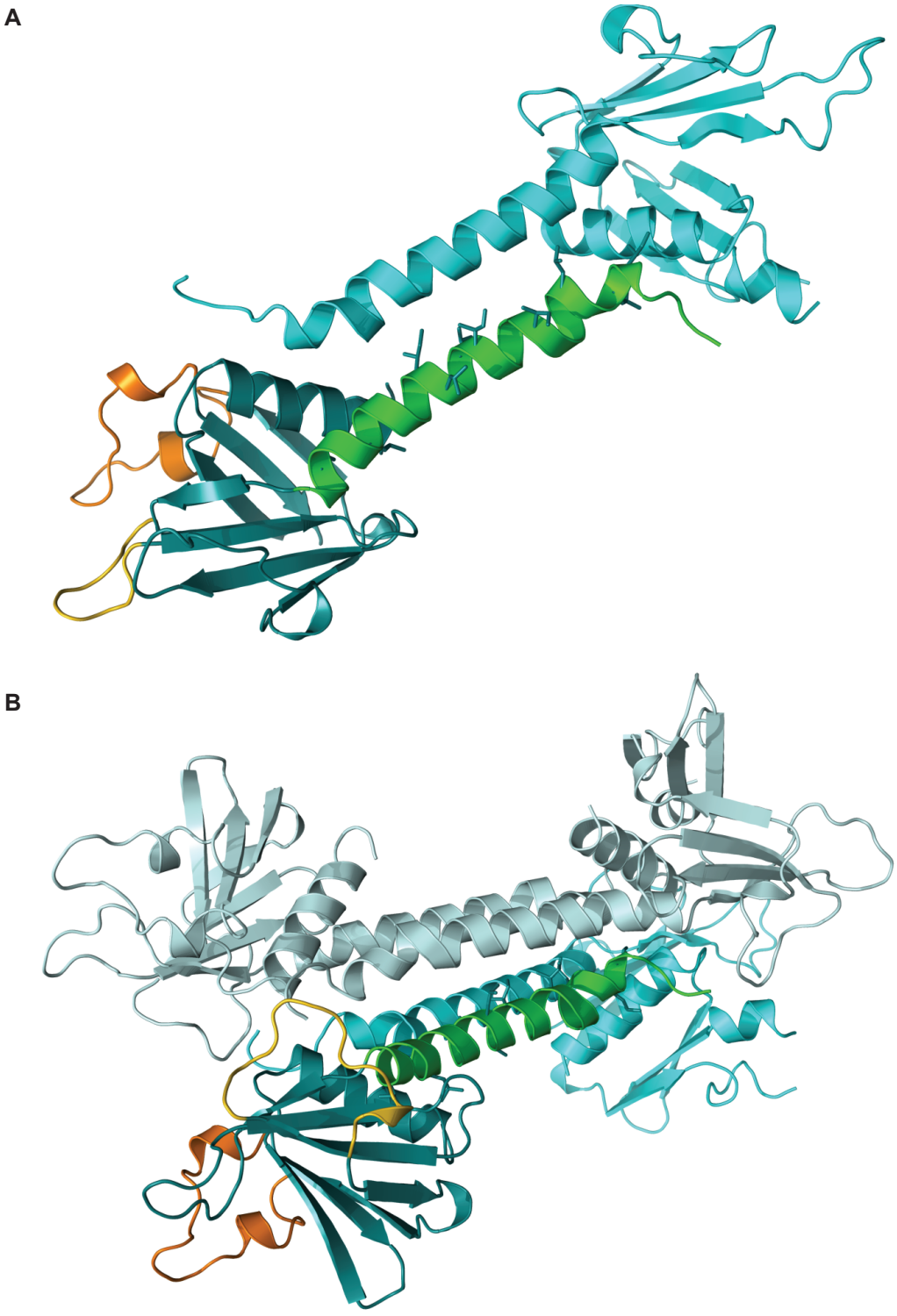

Supplementary Figure 2S3

Supplementary Figure 2S4. Mutations in conserved hydrophobic residues in the αN-helix of the ELMO1 PH domain abolishes the DOCK180/ELMO1 interaction. (A) Lysates of HEK293T cells transfected with the indicated plasmids were immunoprecipitated with an antibody against the Myc-epitope (ELMO1). The co-precipitation of the various ELMO1 proteins and DOCK180 was analyzed via immunoblotting with anti-Myc (ELMO1) and anti-FLAG (DOCK180) antibodies, respectively. (B) Lysates of HEK293T cells transfected with the FLAG DOCK180 were subjected to pulldown assays with GST ELMO1^{WT}, ELMO1$^{L547E/I548D}$, ELMO1$^{L547E/I548D/PxxP}$ and ELMO1$^{L547A/I548A}$ proteins. The precipitation of DOCK180 by the various ELMO1 fusion proteins was detected via immunoblotting with anti-FLAG (DOCK180).

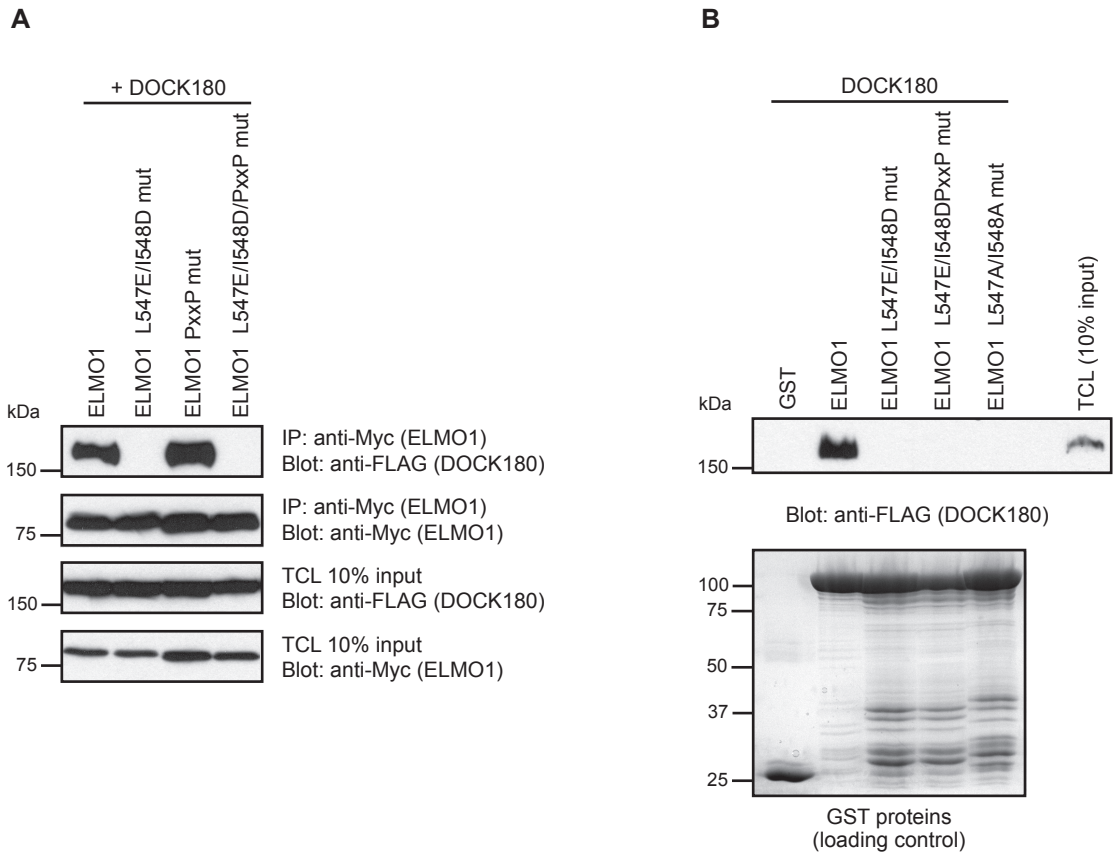

Supplementary Figure 2S4

Supplementary Figure 2S5. Sequence alignment and secondary structure prediction of the minimal ELMO-binding region of DOCK180 uncover a conserved alpha-helical region.

A sequence alignment, of the minimal ELMO-binding region in DOCK180, from several DOCK180-family members and multiple species is shown. Predicted alpha-helical regions are shown in red. Hydrophobic amino acids that were mutated in Figure 2.5G are indicated by arrows. Notably, the mutations of these amino acids in GST DOCK180 1-200 completely abolished binding to Myc-ELMO1.

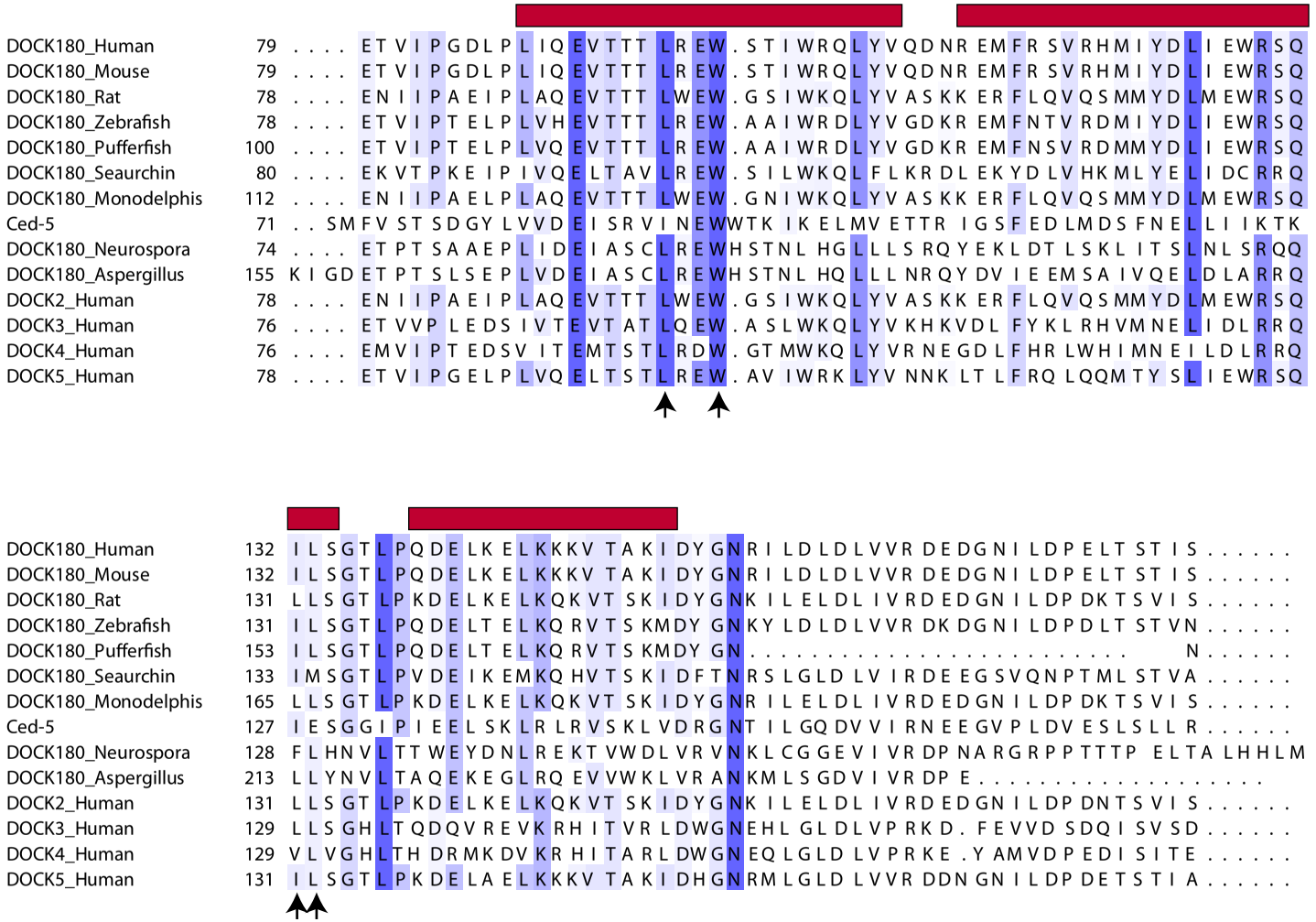

Supplementary Figure 2S5

Supplementary Figure 2S6. Overexpression of dominant-negative Rac, ELMO1^{WT} or ELMO1$^{\alpha N/PxxP}$ mutant alone in LR73 cells interferes with cell spreading. (A) Quantification of the effect on cell spreading in response to overexpression of the indicated proteins. RacN17 was used as a dominant-negative mutant to interfere with cell spreading. Several independent fields were photographed at a magnification of 20X and cells were scored for three phenotypes: round (attached and minimally spread), spread (clearly spread and flat cells) and elongated (elongated cells with polarity). (B) Expression levels of the indicated overexpressed proteins for spreading assays were analyzed by immunoblotting cell lysates with anti-Myc (ELMO) and anti-FLAG (RacN17) antibodies, as indicated.

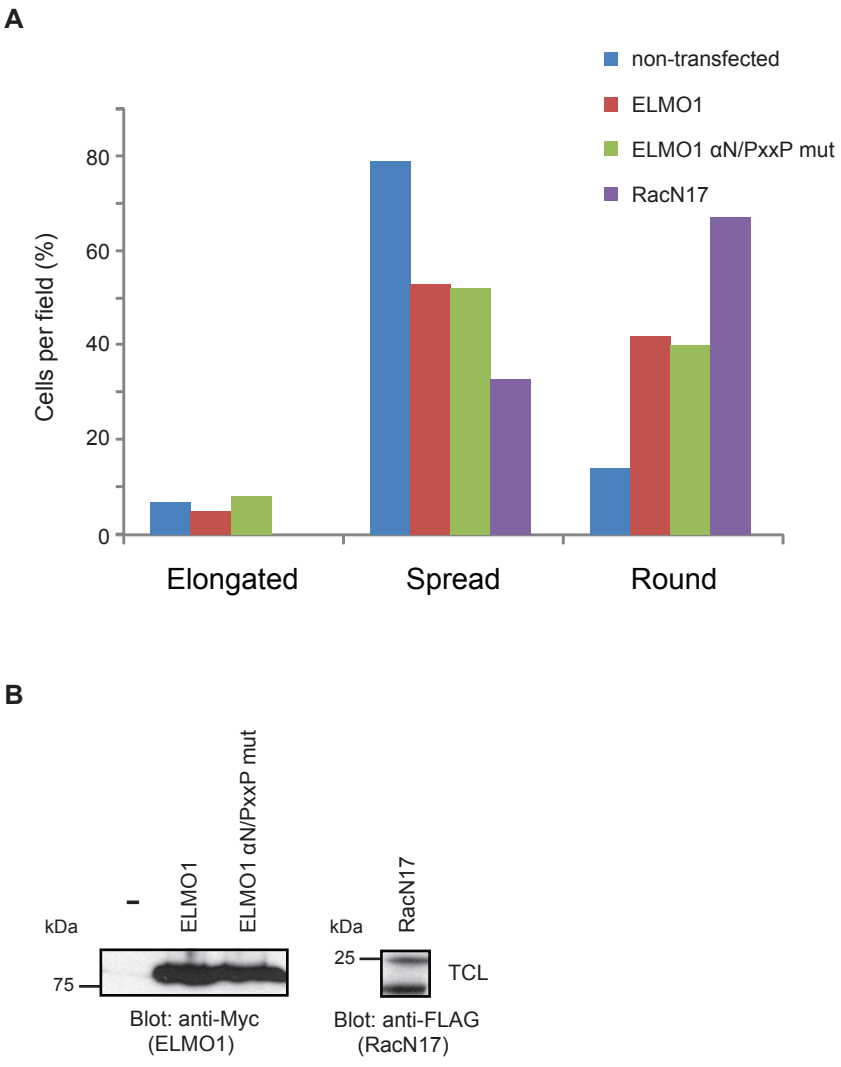

Supplementary Figure 2S6

Supplementary Figure 2S7. A PI-binding PH domain in other DOCK proteins.

Structure of the DOCK9/Zizimin1 PH domain solved by NMR (1wg7, unpublished), which shows all features of a phosphoinositide-binding PH domain. The view is shown as in Figure 2.3.

DOCK9

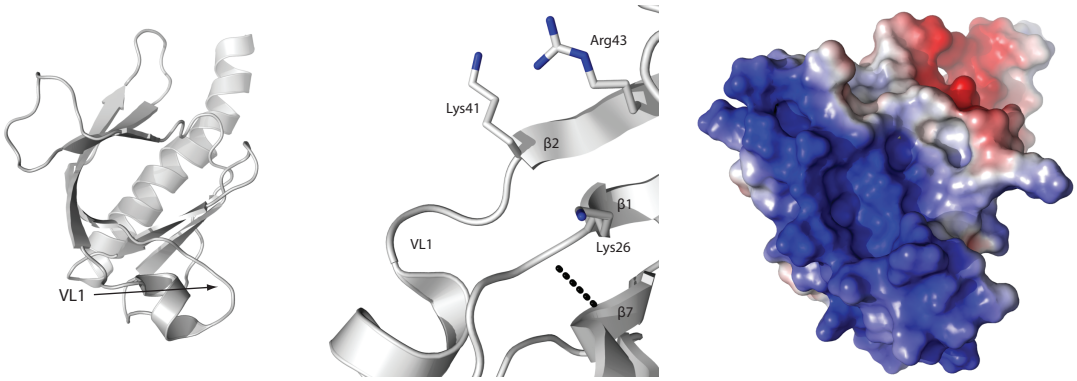

Supplementary Figure 2S7

Supplementary Figure 2S8. ELMO1 proteins do not dimerize in cells.

Differentially tagged ELMO1 constructs with GFP- and Myc-tags were co-expressed in HEK293T cells and cell lysates were subjected to immunoprecipitation against Myc (ELMO1). Immunoblot analysis detected no co-precipitation of ELMO1 (GFP) with ELMO1 (Myc). Reverse experiments were also performed (GFP IP) and no interaction with Myc-ELMO1 were detected (not shown).

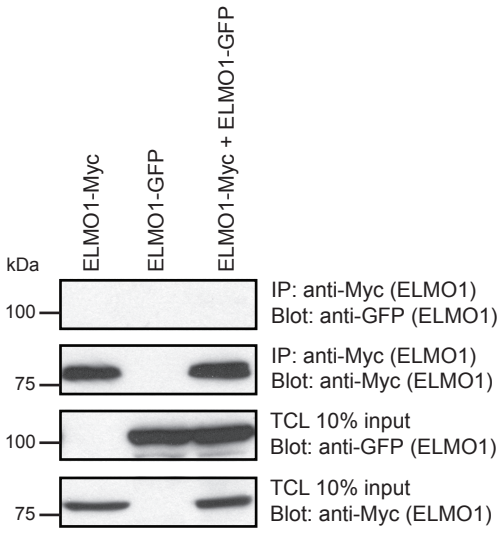

Supplementary Figure 2S8

CHAPTER 3

An evolutionarily conserved auto-inhibitory molecular switch in ELMO proteins regulates Rac signaling

CHAPTER 3: Figure Acknowledgements

Figure 3.1 (A-C) Dr. Jean-François Côté and Manishha Patel

Figure 3.1 (D-F): Manishha Patel

Figure 3.2 (A): Dr. Kay Hofmann

Figure 3.2 (B-D): Manishha Patel

Figure 3.3 (A): Dr. Yoran Margaron

Figure 3.3 (B-C): Manishha Patel

Figure 3.3 (D): Nadine Fradet

Figure 3.4 (A-D): Dr. Yoran Margaron

Figure 3S1 (A,C): Dr. Jean-François Côté and Manishha Patel

Figure 3S1 (B,E-F): Manishha Patel

Figure 3S1 (D): Dr. Brian Wilkes

Figure 3S2 (A): Dr. Yoran Margaron

Figure 3S2 (B,E): Nadine Fradet

Figure 3S2 (C): Qi Yang

Figure 3S2 (D): Manishha Patel

Figure 3S3 (A-C): Dr. Yoran Margaron

Figure 3S3 (D): Manishha Patel

*Nadine Fradet generated many clones used in this study

*Dr. Michel Bouvier contributed plasmids and expert advice for BRET^2 experiments

*The manuscript was written by Dr. Jean-François Côté

*The manuscript was edited by Manishha Patel and Dr. Yoran Margaron

An evolutionarily conserved auto-inhibitory molecular switch in ELMO proteins regulates Rac signaling

Manishha Patel[1,7], Yoran Margaron[1,7], Nadine Fradet[1], Qi Yang[1], Brian Wilkes[1], Michel Bouvier[2,3], Kay Hofmann[4] and Jean-François Côté[1,3,5,6]

[1] Institut de Recherches Cliniques de Montréal. 110 avenue des pins ouest, Montréal (Québec) Canada, H2W 1R7.
[2]Institut de Recherches en Immunologie et en Cancérologie. 2950 chemin Polytechnique, Montréal (Québec) Canada, H3T 1J4.
[3] Faculté de Médecine, Université de Montréal.
[4] Milteny Biotec GmbH, D-51428 Bergisch Gladbach, Germany.
[5] Division of Experimental Medicine, McGill University

[6]Corresponding author:
Email: Jean-François Côté
Phone: (514) 987-5647
Fax: (514) 987-5624

[7]These authors contributed equally.

Running Title: Regulation of ELMO proteins by auto-inhibition

Summary

DOCK proteins encompass a family of guanine nucleotide exchange factors (GEFs) controling the spatiotemporal activity of Rac1/Cdc42 GTPases during polarity, migration, phagocytosis and myoblast fusion [83,293,336,387]. ELMO proteins physically associate with a subset of DOCK members and are emerging as critical regulators of Rac signaling [252,267,357,358,360,365]. While formation of a DOCK180/ELMO complex is not essential for Rac1 activation, ELMO mutants deficient in binding to DOCK180 were unable to promote cytoskeleton-remodeling [388]. Exactly how ELMO regulates signaling through DOCK GEFs is poorly understood. Here, we identify an auto-inhibitory switch in ELMO presenting structural homology to an analogous regulatory unit described for Dia-family formins. One part of the switch, composed of tandem canonical Ras-Binding Domain (RBD) and Armadillo repeats, is positioned N-terminally while the other is housed in the C-terminus. We demonstrate physical interaction between these fragments suggesting auto-inhibition of ELMO at the basal state. Using a BRET^2 intra-molecular biosensor, we establish that ELMO undergoes conformational changes upon disruption of auto-inhibitory contacts. We found that engagement of ELMO to active RhoG, via the RBD, or with DOCK180, promoted the relief of auto-inhibition in ELMO. Functionally, ELMO mutants with impaired auto-regulatory activity were found to promote both cell elongation and migration. These results demonstrate an unsuspected level of regulation for DOCK180-mediated Rac1 signaling via auto-inhibition of ELMO.

Results and Discussion

The GEF activity of DOCK proteins is mediated by the DOCK homology region-2, a module exclusive to this family of GEFs [85,267,272,363]. The identification of upstream regulators of the DOCK180-Rac pathway revealed a role for this GEF in developmental and pathological processes [293,328,347,389,390]. Previous studies demonstrated a total requirement for ELMO proteins in biological processes controlled by DOCK180 [83,388]. Nevertheless, the molecular mechanisms by which ELMO orchestrate Rac signaling in concert with DOCK180 remain to be established. We used bioinformatics to search for novel structural elements in ELMO that could regulate Rac signaling. Threading analysis performed with the Phyre algorithm identified Armadillo Repeats (ARR), in ELMO1,2,3 and *Drosophila* ELMO, bearing structural homology to ARR found in the formin Dia1 [226] (**Figure 3S1A, pg. 167**). Structural homology between ELMO1 and the formins Dia1 [221,224] and FHOD1 [391] was also detected using the 3D-Jury structure prediction algorithm (**Figure 3S1B, pg. 167**). Finally, BLAST searches uncovered primary amino acid sequence similarity between ELMO1 and FHOD1 (**Figure 3S1C, pg. 167**). The region in Dia1 and FHOD1 sharing homology to ELMO is the Diaphanous Inhibitory Domain (DID) and is characterized to engage in intra-molecular interactions with a Diaphanous Auto-regulatory Domain (DAD) to maintain these proteins in a repressed state [392]. A hallmark of this regulatory switch is the presence of a GTPase binding site N-terminal to the DID. Mechanistically, engagement of GTPases to auto-inhibited formins disrupts the inhibitory DID-DAD interactions, therefore exposing their actin polymerization activity [224,391]. As the region in ELMO preceding the ARR interacts with RhoG [365], this led us to hypothesize that the N-terminus of ELMO may constitute part of a similar auto-inhibitory module. We therefore termed the ARR in ELMO as the ELMO Inhibitory Domain (EID) (**Figure 3.1A, pg. 151**). Based on sequence alignment with FHOD1, the EID is defined by one

Figure 3.1. Intra-molecular interactions in ELMO1 through novel domains. (**A**) Schematic representation of the structural homology between ELMO and Dia-family formins. (**B**) The ELMO1 EID domain is composed of HEAT and Armadillo Repeats (ARR). Predicted α-helices (grey); Hydrophobic residues of the ARR consensus sequence (yellow); Polar residues (blue and red); I204 in ARR-3 is a conserved residue of ELMO proteins (green). (**C**) Sequence alignment of the auto-regulatory domains of ELMO (EAD) and Dia-related formins (DAD). Red arrows indicate highly conserved residues forming the core motif. Mutation of critical EID or EAD residues disrupts EID/EAD interaction in co-immunoprecipitation (**D**) and yeast two-hybrid system (**E**). (**D**) Lysates of HEK293T cells transfected with the indicated plasmids were subjected to immunoprecipitation with an anti-FLAG (lane 1-4) or anti-DOCK180 H-70 (lane 5-8) antibody. Immunoblots were analyzed using anti-Myc (ELMO1) and anti-DOCK180 (H-70) antibodies. HC=IgG heavy chain. (**E**) Yeasts co-transformed with LexA fusion construct of ELMO1$^{1\text{-}315}$ and B42 fusion constructs of ELMO1$^{315\text{-}727}$ were grown on non-selective and selective (-Leucine) medium for a nutrient selective growth assay. (**F**) Mapping of critical EAD region boundaries. Yeasts co-transformed with the indicated plasmids were assayed as in (**E**). See also Figure 3S1.

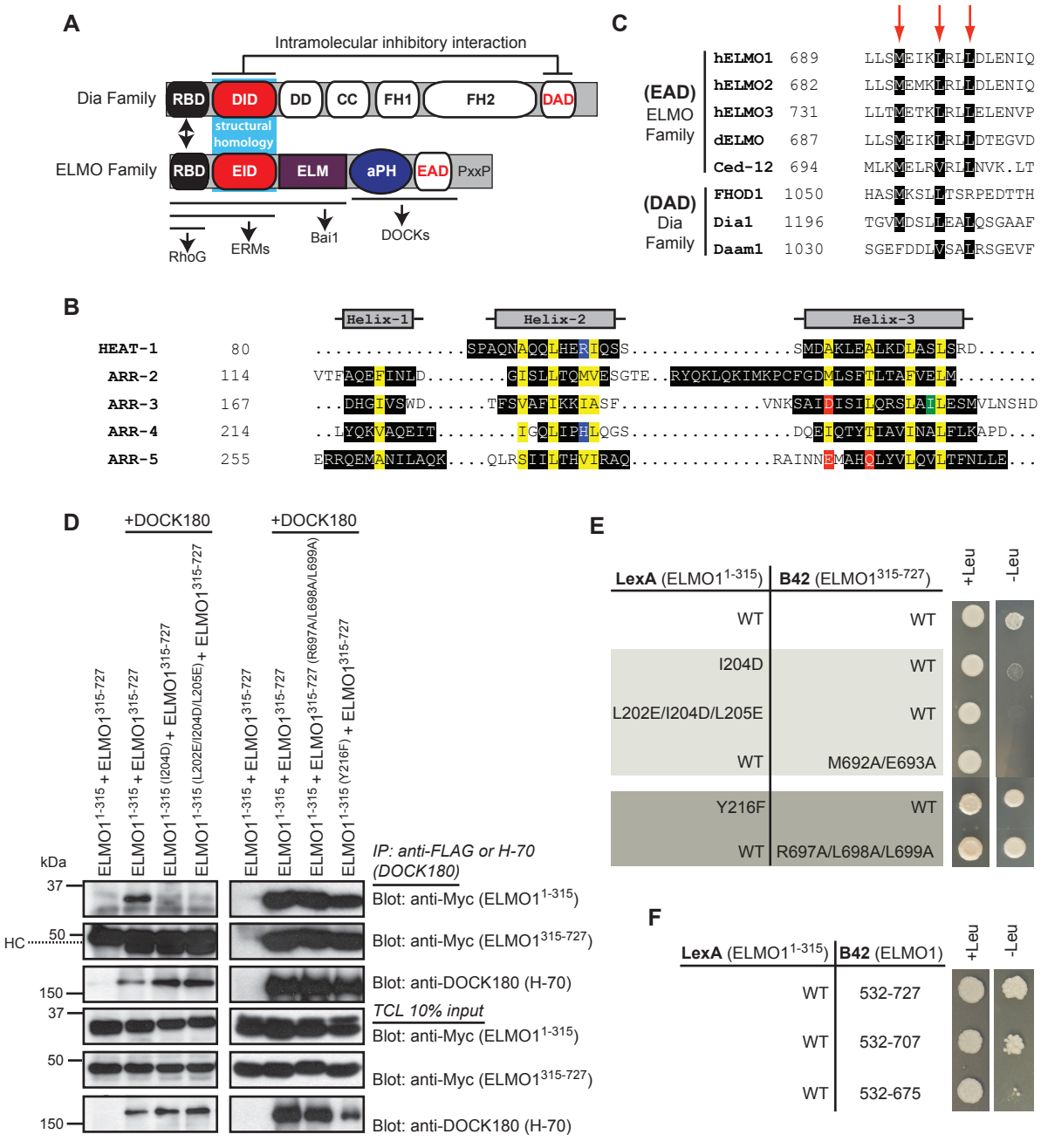
A
Intramolecular inhibitory interaction
Dia Family
RBD
DID
DD
CC
FH1
FH2
DAD
structural homology
ELMO Family
RBD
EID
ELM
aPH
EAD
PxxP
RhoG
ERMs
Bai1
DOCKs
C
(EAD) ELMO Family
hELMO1 689 LLSMEIKLRLLDLENIQ
hELMO2 682 LLSMEMKLRLLDLENIQ
hELMO3 731 LLTMETKLRLLELENVP
dELMO 687 LLSMEIKLRLLDTEGVD
Ced-12 694 MLKMELRVRLLNVK.LT
(DAD) Dia Family
FHOD1 1050 HASMKSLLTSRPEDTTH
Dia1 1196 TGVMDSLLEALQSGAAF
Daam1 1030 SGEFDDLVSALRSGEVF
B
Helix-1
Helix-2
Helix-3
HEAT-1 80 .....SPAQNAQQLHERIQSS.....SMDAKLEALKDLASLSRD.....
ARR-2 114 VTFAQEFINLD.....GISLLTQMVESGTE..RYQKLQKIMKPCFGDMLSFTLTAFVELM.....
ARR-3 167 ...DHGIVSWD.....TFSVAFIKKIASF.....VNKSAIDISILQRSLAILESMVLNSHD
ARR-4 214 ..IYQKVAQEIT.....IGQLIPHLQGS.....DQEIQTYTIAVINALFLKAPD...
ARR-5 255 ERRQEMANILAQK....QLRSIILTHVIRAQ.....RAINNFMAHQLYVLQVLTFNLLE...
D
+DOCK180
+DOCK180
ELMO1 1-315 + ELMO1 315-727
ELMO1 1-315 + ELMO1 315-727
ELMO1 1-315 (I204D) + ELMO1 315-727
ELMO1 1-315 (L202E/I204D/L205E) + ELMO1 315-727
ELMO1 1-315 + ELMO1 315-727
ELMO1 1-315 + ELMO1 315-727 (R697A/L698A/L699A)
ELMO1 1-315 + ELMO1 315-727 (Y216F) + ELMO1 315-727
kDa
37
HC
50
150
37
50
150
IP: anti-FLAG or H-70 (DOCK180)
Blot: anti-Myc (ELMO1 1-315)
Blot: anti-Myc (ELMO1 315-727)
Blot: anti-DOCK180 (H-70)
TCL 10% input
Blot: anti-Myc (ELMO1 1-315)
Blot: anti-Myc (ELMO1 315-727)
Blot: anti-DOCK180 (H-70)
E
LexA (ELMO1 1-315)
B42 (ELMO1 315-727)
+Leu
-Leu
WT WT
I204D WT
L202E/I204D/L205E WT
WT M692A/E693A
Y216F WT
WT R697A/L698A/L699A
F
LexA (ELMO1 1-315)
B42 (ELMO1)
+Leu
-Leu
WT 532-727
WT 532-707
WT 532-675

Figure 3.1

HEAT domain followed by four ARR (**Figure 3.1B, pg. 151**). Searching for the equivalent of the formins' DAD in ELMO is not straightforward since this functional region is not a domain but rather, a short amphipatic helix. We nevertheless identified a C-terminal region in ELMO that resembles the formins DAD [225,226], and we named it the ELMO Auto-Regulatory Domain (EAD) (**Figure 3.1A, C, pg. 151**).

If the EID and EAD of ELMO behave like the analogous domains in formins, they should interact directly. We tested whether ELMO1$^{1\text{-}315}$ can interact with ELMO1$^{315\text{-}727}$ and found that these two ELMO1 fragments specifically co-precipitated with DOCK180 (**Figure 3.1D, pg. 151**). The critical residues of Dia1 and FHOD1 DIDs involved in binding the DAD, Alanine 256 and Valine 228, respectively, are located in a hydrophobic region of the last helix of the third ARR [226,391]. Structure-based alignment of the ELMO EID with the DIDs of Dia1 and FHOD1 suggested L202, I204 and L205 as candidate residues potentially important for the function of the ELMO EID. By analyzing the Phyre generated 3D-model of the ELMO1 EID and comparing it to the structures of Dia1 and FHOD1, I204 was found to be surface exposed and is thus likely to contribute to EAD binding (**Figure 3S1D, pg. 167**). We found that two mutants in this hydrophobic patch, ELMO1$^{1\text{-}315(I204D)}$ and ELMO1$^{1\text{-}315(L202E/I204D/L205E)}$, lost the ability to interact with ELMO1$^{315\text{-}727}$ both in co-immunoprecipitation and yeast two-hybrid assays (**Figure 3.1D,E, pg. 151**). Mutation of another close by residue in the ELMO1 EID, Y216F, did not affect the EID/EAD interaction (**Figure 3.1D,E, pg. 151**). Next, we investigated which residues in the EAD are critical in EID binding. To provide evidence that the EAD is included in the predicted α-helix located between aas 681-701 of ELMO1 (Figure 3.1C), we used the yeast two-hybrid system. We found that nested C-terminal truncations (ELMO1$^{532\text{-}727}$ and ELMO1$^{532\text{-}707}$) maintained interaction with ELMO1$^{1\text{-}315}$ whereas further deletion of the region containing the predicted EAD (ELMO1$^{532\text{-}675}$) diminished the binding (**Figure 3.1F, pg. 151**). In both FHOD1 and Dia1, the conserved Methionine of the DAD is responsible for extensive contacts with

the DID [225,226] (**Figure 3.1C, pg. 151**). Therefore, the equivalent Methionine 692, in addition to the highly conserved Glutamate 693, of ELMO1 were both mutated to Alanine. We found that ELMO1$^{1\text{-}315}$ was incapable of binding ELMO1$^{315\text{-}727(M692A/E693A)}$ in a yeast two-hybrid interaction assay, yet this mutant retained the ability to bind DOCK180 (**Figure 3.1E, pg. 151** and **3S1E, pg. 167**). Importantly, mutation of other residues in this region, namely R697A/L698A/L699A, had no effect on the EID/EAD interaction (**Figure 3.1D,E, pg. 151**).

The presence of GTPase-binding activity at the N-terminus of ELMO proteins [365] suggest that the EID/EAD interactions could be regulated by engagement of active RhoG in a model suggestive of Dia-family formin activation [392]. Despite similarity in their DIDs, the GTPase binding domains of Dia1 and FHOD1 are structurally unrelated [393]. In Dia1 it is solely α-helical and Rho-selective while in FHOD1 it is composed of an ubiquitin-fold found in Ras-Binding Domains (RBD) and is Rac-specific [224,391]. Our bioinformatic analyses uncovered that the GTPase-binding boundary of ELMO proteins belongs to the family of RBDs [394]. We found homology between ELMO, FHOD1 and c-Raf RBDs. Superimposition of FHOD1 and c-Raf RBD structures results in the alignment with ELMO shown in **Figure 3.2A (pg. 155)**, allowing us to narrow in on Leucine 43 as a likely candidate in the ELMO1 RBD to mediate contact to active RhoG on the basis that the analogous residue in c-Raf is in contact with Ras [394]. In GST pull-down assays, both ELMO1^{L43A} and ELMO1$^{1\text{-}315(L43A)}$ were incapable of binding RhoG^{V12} (**Figure 3.2B, pg. 155**). Similarly, ELMO1$^{1\text{-}315(L43A)}$ was impaired in RhoG^{V12}-binding in co-immunoprecipitation assays (**Figure 3.2C, pg. 155**). Functionally, we found that ELMO1 mutants lacking RBD activity failed to synergize with DOCK180 and CrkII in promoting cell elongation (**Figure 3.2D, pg. 155**) suggesting that this domain is essential for biological activity of the complex.

Figure 3.2. The N-Terminus ELMO1 contains a Ras-Binding Domain. (**A**) Secondary structure and sequence comparison between ELMO-family proteins, FHOD1, and Raf1 indicates an evolutionarily conserved RBD characterized by the presence of an ubiquitin-like subdomain. ELMO secondary structure was predicted with Jpred3. FHOD1 PBD=3dad and Raf1 PBD=1gua. Residues potentially involved in contacting RhoG are shown in red. E=β-strand, H=α-helical. (**B-C**) L43A mutation in ELMO1 RBD abolishes the interaction with $RhoG^{V12}$. (**B**) GST-tagged versions of the indicated ELMO1 proteins were used to pulldown HA-tagged $RhoG^{V12}$ from HEK293T lysates. Bound proteins were detected by immunoblotting with an anti-HA antibody. (**C**) Transfected HEK293T cells were subjected to immunoprecipitation against Myc-tagged ELMO1. Bound proteins were analyzed by immunoblotting using anti-HA ($RhoG^{V12}$) and anti-Myc (ELMO1) antibodies. (**D**) Mutational inactivation or deletion of the ELMO1 RBD results in defective cell elongation. Images represent an overlay of anti-H-4 (DOCK180), rhodamine-phalloidin and DAPI stains. Scale bar, 10 μm. Several independent fields of the experiments were scored for the indicated phenotypes.

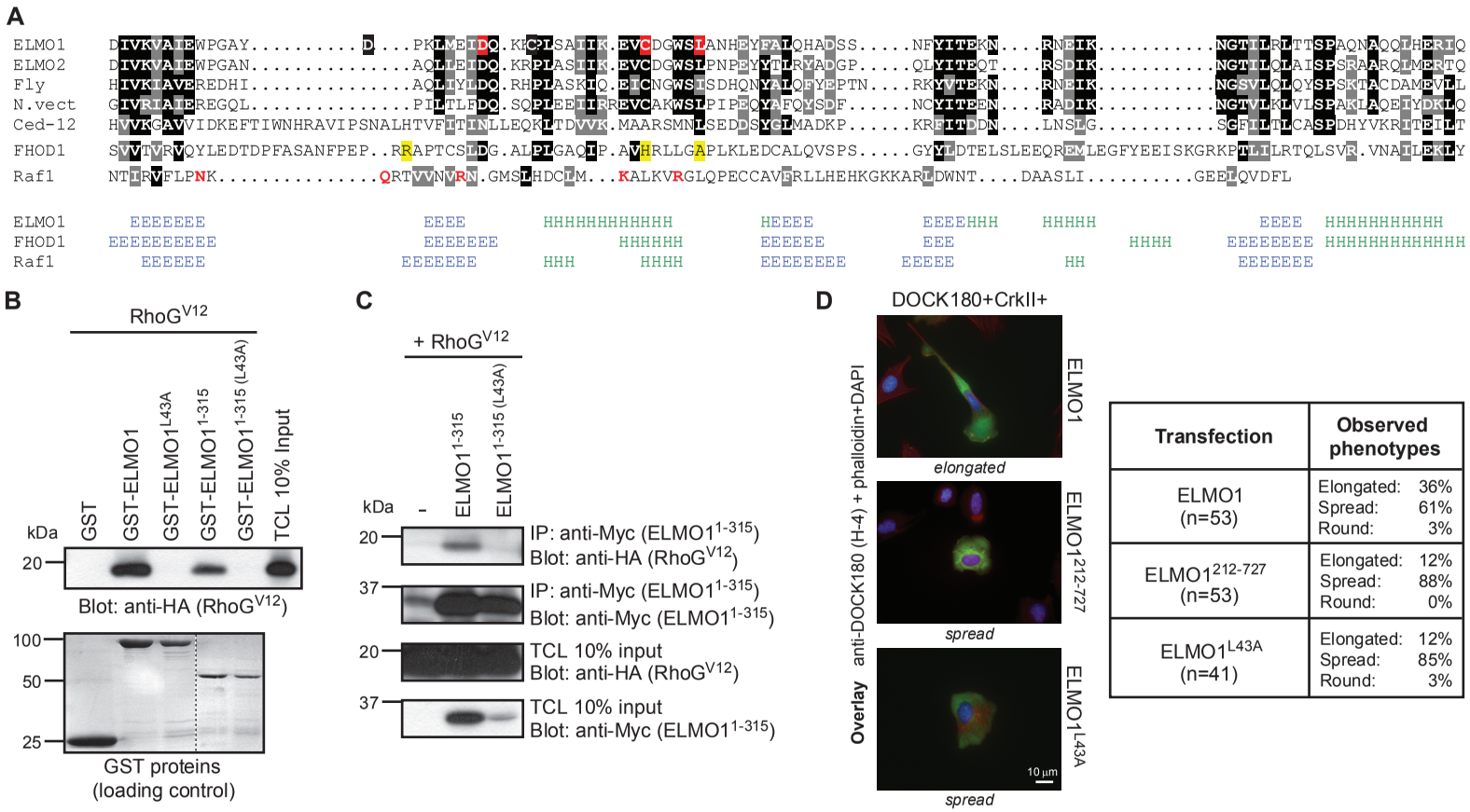

Transfection	Observed phenotypes	
ELMO1 (n=53)	Elongated:	36%
	Spread:	61%
	Round:	3%
ELMO1$^{212-727}$ (n=53)	Elongated:	12%
	Spread:	88%
	Round:	0%
ELMO1^{L43A} (n=41)	Elongated:	12%
	Spread:	85%
	Round:	3%

Figure 3.2

Although ELMO associates with RhoG [365], the minimal protein surface responsible for the interaction is poorly characterized. We investigated whether the RBD of ELMO is sufficient for membrane targeting by RhoG. We found that both the RBD (Myc-ELMO1$^{1-113}$) and the RBD-EID unit (Myc-ELMO1$^{1-315}$), but not the L43A mutant counterparts, re-localized to the membrane when co-expressed with RhoG^{V12} (**Figure 3.3A, pg. 158** and **3S2A, pg. 169**). ELMO1 lacking the RBD, ELMO1$^{113-727}$, also failed to re-localize to the membrane when co-expressed with RhoG^{V12} (**Figure 3.3A, pg. 158**). These results support the hypothesis that engagement of the RBD of ELMO proteins to GTPase(s) may be a key event to localize and anchor the ELMO/DOCK complex at the membrane. To test whether the engagement of active RhoG to the RBD competes with the EID/EAD interaction, we performed a biochemical cell fractionation assay. We observed that the RBD-EID unit of ELMO (Myc-ELMO1$^{1-315}$) is, as expected, enriched in the membrane fraction when expressed with RhoG^{V12} (**Figure 3.3B,C, pg. 158**). Co-expression of an ELMO fragment containing the EAD (Myc-ELMO1$^{315-727}$) in this system coerced the RBD-EID fragment away from RhoG^{V12} at the membrane, increasing the proportion of Myc-ELMO1$^{1-315}$ in the cytosol (**Figure 3.3B,C, pg. 158**).

To address whether intra-molecular interactions would take place in full-length ELMO, we developed a bioluminescence resonance energy transfer (BRET^2) ELMO conformation biosensor. We tagged ELMO2 at its extremities with GFP^{10} and *Renilla* Luciferase (RlucII) tags (**Figure 3.3D, pg. 158**). ELMO2 was chosen, as it is compatible for cloning in the BRET^2 vector and shares 88% similarity with ELMO1. Since our model predicts spatial proximity between the N- and C-terminal ends of ELMO proteins, BRET^2 signal should occur in the auto-inhibited state and decrease in the active conformation. Indeed, BRET^2 signal is detected when GFP^{10}-ELMO2-RlucII is expressed alone (**Figure 3.3D, pg. 158**). Importantly, the BRET^2 signal observed is independent of the concentration of ELMO2 indicating that intra-molecular

Figure 3.3. Full length ELMO2 is auto-inhibited and regulated by RhoG-binding to the RBD. (**A**) Membrane recruitment of ELMO1 RBD by RhoG. HeLa cells were transfected with the indicated plasmids and ELMO1 and $RhoG^{V12}$ localization was analyzed using anti-Myc and anti-HA antibodies, respectively. Scale bar, 20 μm. (**B-C**) In the presence of $RhoG^{V12}$, ELMO1 EAD-containing fragment coerces ELMO1 RBD-EID away from the membrane and into the cytosol. HEK293T cells were transfected with the indicated plasmids and cytosolic and membrane fractions were biochemically purified and analyzed via immunoblotting with the indicated antibodies. Quantification of band intensity was used to calculate the ratio of protein found in the membrane vs. the cytosol; error bars represent s.d., *n*=3. (**D**) Disrupting the EID/EAD interaction leads to conformational changes in ELMO2. Schematic model of the GFP^{10}-ELMO2-RlucII conformation biosensor. Luminescence at 400 nm and fluorescence at 510 nm were measured upon addition of DeepBlueC in HEK293T cells expressing indicated proteins, *n*=3. ANOVA tests and Bonferroni's multiple comparison were performed to compare each condition (***, $P<0.001$; error bars represent s.e.m, *n*=3). See also Figures 3S2.

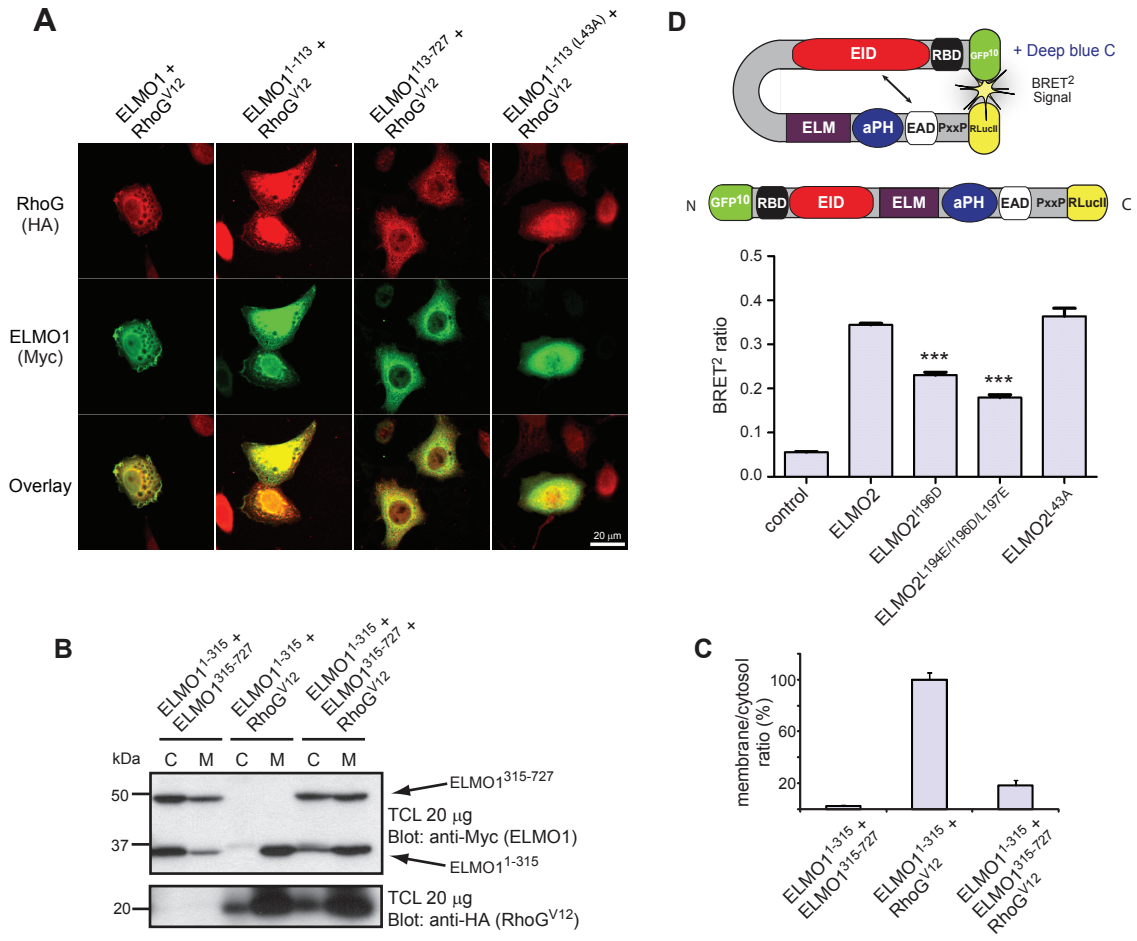
A
ELMO1 + RhoG^{V12}
ELMO1$^{1-113}$ + RhoG^{V12}
ELMO1$^{113-727}$ + RhoG^{V12}
ELMO1$^{1-113\ (L43A)}$ + RhoG^{V12}
RhoG (HA)
ELMO1 (Myc)
Overlay
20 μm
B
ELMO1$^{1-315}$ + ELMO1$^{315-727}$
ELMO1$^{1-315}$ + RhoG^{V12}
ELMO1$^{1-315}$ + ELMO1$^{315-727}$ + RhoG^{V12}
kDa
C M C M C M
50
37
20
ELMO1$^{315-727}$
TCL 20 μg
Blot: anti-Myc (ELMO1)
ELMO1$^{1-315}$
TCL 20 μg
Blot: anti-HA (RhoG^{V12})
C
membrane/cytosol ratio (%)
100
60
20
ELMO1$^{1-315}$ + ELMO1$^{315-727}$
ELMO1$^{1-315}$ + RhoG^{V12}
ELMO1$^{1-315}$ + ELMO1$^{315-727}$ + RhoG^{V12}
D
EID
RBD
GFP^{10}
+ Deep blue C
BRET^2 Signal
ELM
aPH
EAD
PxxP
RLucII
N
C
BRET^2 ratio
0.5
0.4
0.3
0.2
0.1
0.0
***
***
control
ELMO2
ELMO2^{I196D}
ELMO2$^{L194E/I196D/L197E}$
ELMO2^{L43A}

Figure 3.3

interactions instead of oligomerization events are observed (**Figure 3S2B, pg. 169**). To test if disturbing the EID/EAD interaction in ELMO2 leads to conformational changes, we expressed GFP^{10}-ELMO2-RlucII with function inactivating mutations in the EID (I196D or L194E/I196D/L197E) and detected a decrease in $BRET^2$ signal suggesting that these mutants are in an open conformation (**Figure 3.3D, pg. 158**). Mutation of residue L43A in the RBD did not affect $BRET^2$ signal (**Figure 3.3D, pg. 158**). We used this probe to test if interaction of ELMO2 with its binding partners $RhoG^{V12}$ and DOCK180 could affect the conformation state of ELMO2. Unfortunately, the bulky tags on the GFP^{10}-ELMO2-RlucII almost totally abolished the interaction with $RhoG^{V12}$ (**Figure 3S2C, pg. 169**) preventing us to conclusively determine if this GTPase can alter ELMO2 conformation in this assay. Interestingly, the binding of DOCK180 to GFP^{10}-ELMO2-RlucII, which still occurs, promoted conformational changes in ELMO2 suggesting that DOCK180 can participate in promoting the open conformation of ELMO (**Figure 3S2D,E, pg. 169**).

A previous report highlighted that ELMO can induce stress fibers [358] while other studies noted that ELMO has no effect on the cytoskeleton [252,360,364,388]. We reasoned that if ELMO auto-inhibition is important for regulating Rac signaling, activated mutants of ELMO1 should promote cytoskeletal changes. We studied the impact of ELMO1 in the presence/absence of $RhoG^{V12}$ on the morphology of HeLa cells grown on poly-L-lysine. Expression of $ELMO1^{WT}$, $ELMO1^{I204D}$, $ELMO1^{M692A/E693A}$ or $ELMO1^{L43A}$ did not induce morphological alteration in comparison to control cells (**Figure 3S3A, pg. 171**). In contrast, expression of $RhoG^{V12}$ amplified cell spreading as judged by morphology and quantification of the Feret's diameter (**Figure 3.4A, B, pg. 161**). When $RhoG^{V12}$ was co-expressed with $ELMO1^{WT}$ and $ELMO1^{L43A}$, membrane ruffles additionally characterized the cells but, notably, their Feret diameters were unchanged with respect to cells expressing $RhoG^{V12}$ (**Figure 3.4A, B, pg. 161**). Strikingly, the active ELMO mutants $ELMO1^{I204D}$ and $ELMO1^{M692A/E693A}$ distinctly

Figure 3.4. The EID/EAD intra-molecular interaction is a regulatory feature of ELMO in cells. (**A**) Activated ELMO1 mutants synergize with RhoG to promote cell elongation. HeLa cells were transfected with the indicated plasmids and ELMO1 and $RhoG^{V12}$ localization was observed with anti-Myc and anti-HA antibodies, respectively. Scale bar, 20 μm. (**B**) Quantification of the effect of ELMO1 mutations on cell elongation. The morphology of cells in (**A**) was analyzed using anti-Myc antibodies. For each condition, the Feret's diameter of >40 cells was measured (bars represents lowest and highest values; see method). (**C**) Activated ELMO1 mutants promote cell elongation on fibronectin. Serum-starved LR73 cells transfected with the indicated ELMO1 plasmids were detached and plated on fibronectin-coated chambers for 2 h. Cells were stained for ELMO1 (anti-Myc) and DOCK180 (H-70). Scale bar, 20 μm. (**D**) Quantification of cell morphology (see Materials and Methods). >More than 100 cells were analyzed for each condition. In both set of experiments, ANOVA tests and Bonferroni's multiple comparison were performed to compare each condition (*, $P<0.05$; **, $P<0.005$; ***, $P<0.001$; error bars represent s.e.m, $n=3$). See also Figure 3S3.

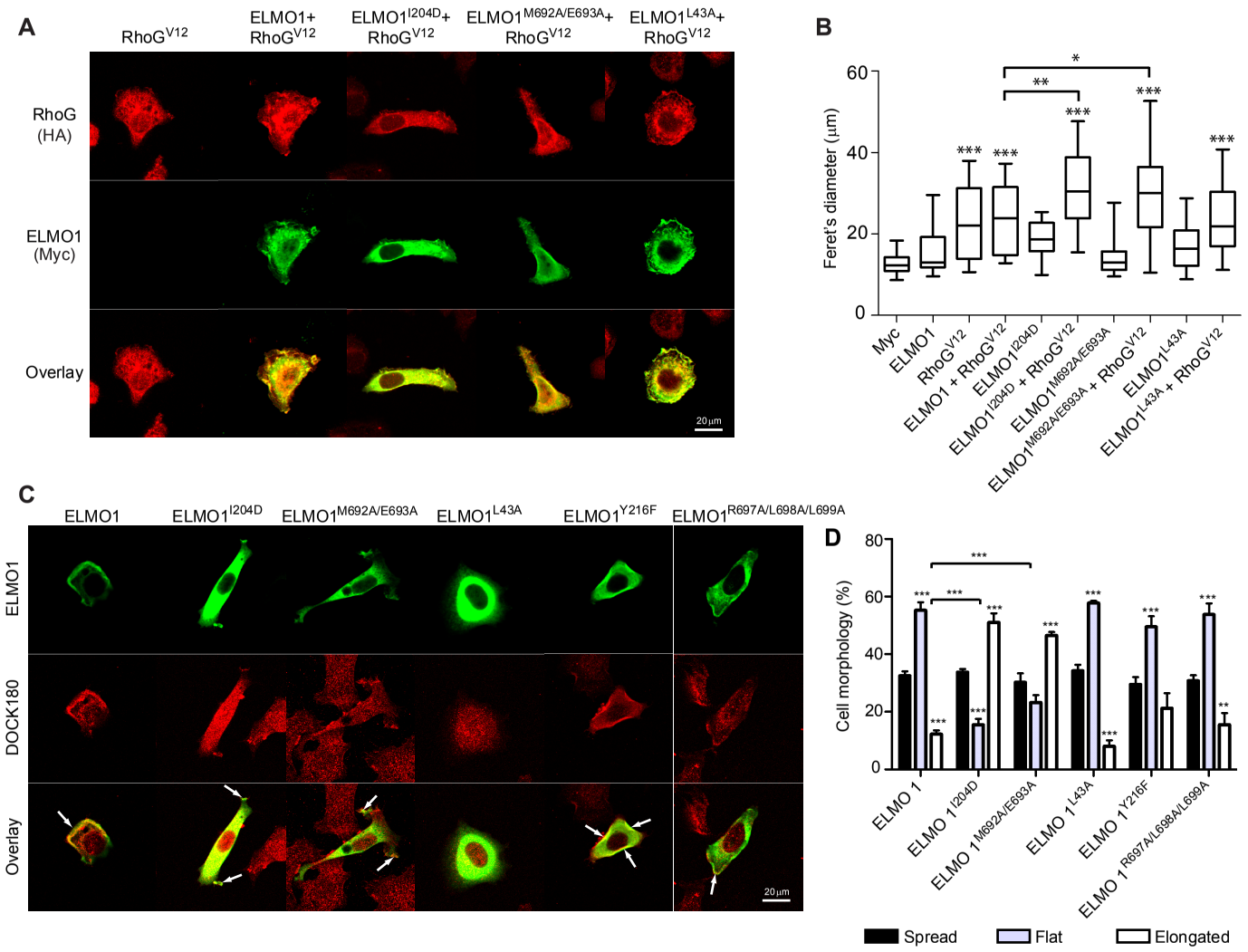
A
RhoG^V12
ELMO1+ RhoG^V12
ELMO1^I204D+ RhoG^V12
ELMO1^M692A/E693A+ RhoG^V12
ELMO1^L43A+ RhoG^V12
RhoG (HA)
ELMO1 (Myc)
Overlay
20 µm
B
Feret's diameter (µm)
0
20
40
60
*
**
***
Myc
ELMO1
RhoG^V12
ELMO1 + RhoG^V12
ELMO1^I204D
ELMO1^I204D + RhoG^V12
ELMO1^M692A/E693A
ELMO1^M692A/E693A + RhoG^V12
ELMO1^L43A
ELMO1^L43A + RhoG^V12
C
ELMO1
ELMO1^I204D
ELMO1^M692A/E693A
ELMO1^L43A
ELMO1^Y216F
ELMO1^R697A/L698A/L699A
ELMO1
DOCK180
Overlay
20 µm
D
Cell morphology (%)
0
20
40
60
80
***
**
ELMO 1
ELMO 1^I204D
ELMO 1^M692A/E693A
ELMO 1^L43A
ELMO 1^Y216F
ELMO 1^R697A/L698A/L699A
Spread
Flat
Elongated

Figure 3.4

promoted cell elongation when expressed with RhoG^{V12} (**Figure 3.4A, B, pg. 161**). We next analyzed the morphology of integrin-activated HeLa cells expressing ELMO1 and found that ELMO1^{WT} and ELMO1^{L43A} failed to induce cytoskeletal changes (**Figure 3.4C, D, pg. 161**). In agreement with our data suggesting a central role for the RBD in localizing ELMO at the membrane during integrin signaling, we noted that ELMO1^{L43A} remained cytosolic (**Figure 3.4C, pg. 161**). Notably, ELMO1 mutants lacking auto-regulatory properties (ELMO1^{I204D} and ELMO1$^{M692A/E693A}$) efficiently accumulated at cell extremities and induced cell elongation (**Figure 3.4C,D, pg. 161**). As a control, we found that mutants in which the EID/EAD interaction is not abrogated, ELMO1^{Y216F} and ELMO1$^{R697A/L698A/L699A}$, behaved like ELMO1^{WT} (**Figure 3.4C,D, pg. 161**). Furthermore, we found that constitutively activated ELMO1 variants (ELMO1^{I204D} and ELMO1$^{M692A/E693A}$) were sufficient to induce more than two-fold increase in cell motility (**Figure 3S3B, pg. 171**). Significantly, uncoupling DOCK180-binding from these constitutively activated ELMO1 mutants abrogated the cell elongation phenotype indicating that they are dependent on DOCK180-mediated activation of Rac (**Figure 3S3C, pg. 171**). Finally, we observed little impact on the global Rac activation in either 293T or LR73 cells expressing active ELMO1 mutants (**Figure 3S3D, pg. 171**). Instead, we found that these mutants promote cell elongation by localizing DOCK180 at the membrane (**Figure 3.4C, pg. 161**).

In this study, we identified three novel domains in ELMOs: the RBD, EID and EAD. We propose that the activation state of ELMO proteins is regulated, much like in Dia-family formins, via interaction with other proteins. We provided biochemical evidence that active RhoG and the ELMO EAD are competing for binding to the ELMO RBD-EID unit suggesting that RhoG could actively participate in unleashing the EID/EAD negative regulation. Alternatively, we cannot rule out the hypothesis that RhoG recruits “inactive” ELMO to the membrane where an additional interaction partner comes into play to stabilize ELMO in an active conformation. We also found

that DOCK180 binding to ELMO promotes conformational changes in ELMO. This result is in agreement with several reports suggesting that co-expression of ELMO and DOCK180 is essential for optimal activity of the complex and we now propose that this may be a consequence of favoring the open conformation of ELMO.

The physiological relevance of the RhoG/ELMO/DOCK180 interaction is not clear. In fact, new lines of evidence suggest that RhoG may modestly contribute to the regulation of this pathway. First, while DOCK180 mutant mice suffer from defects in myoblast fusion [336], mice lacking RhoG undergo normal development [395] suggesting that this GTPase cannot be a master regulator of DOCK180 signaling. Second, while RhoG is a *bona fide* ELMO binder, it is not activated by integrin engagement and is not an essential component upstream of DOCK180 in cell spreading [153]. Here, we demonstrated that ELMO recruitment at the membrane is dependent on the activity of the RBD during integrin signaling suggesting that additional GTPase(s), activated by integrins, must bind ELMO. The exact mechanism whereby open ELMO mutants are able to promote polarity is not understood. Our model is that ELMO may enter in a repressed state to mask an intrinsic enzymatic activity much like formins do to control their actin nucleation potential. The central region of ELMO contains an uncharacterized ELM domain suspected to house GAP activity toward Arf GTPases [169]. Our structure/function analysis suggests that the ELM is essential for the polarization activity of the ELMO/DOCK180 complex (not shown). We are currently testing if the ELM carries GAP enzymatic activity and most importantly if the auto-inhibitory switch regulates it.

MATERIALS AND METHODS

All experimental procedures are described in the Supplemental Material section.

ACKNOWLEDGEMENTS

We are grateful to Dr P. Schiller for his support with *in silico* structure analyses. We thank members of the Côté laboratory for helpful comments and Drs V. Braga and J.M. Di Noia for critical reading of the manuscript. We also thank members of the lab of Dr Archambault for help with yeast work. This work was supported by CIHR operating grants MOP-77591 (to J.-F. Côté) and MOP-89716 (to P. Schiller and supporting B. Wilkes). J.-F. Côté holds a CIHR New Investigator award.

Figure 3S1. Identification of the ELMO Inhibitory Domain (EID) and its homology to Dia-family Formins; Related to Figure 3.1. (**A**) Threading analysis using the Phyre Server [396] on ELMO1 aas 79-305 uncovers ARRs structurally similar to ARRs of Dia family formins. Shown is the top hit retrieved by the server: corresponds to the DID domain of Dia1 in complex with the DAD [225,226] (PDB=2bap). Similar analyses of ELMO2, ELMO3 and Drosophila ELMO produce equivalent results (data not shown). (**B**) 3D-Jury [397] predictions of ARRs in ELMO N-Terminus. The top 7 hits obtained after submitting ELMO1 N-Terminus (aas 1-340) to 3D-Jury prediction are all ARRs present in Dia and FHOD1 formins. 3D-Jury generates meta-predictions based on several prediction algorithms (RPSB_01, FFAS_03, BASI_01, BASI_02, BASI_04, PSIB_01) and scores models by their similarity to other models. Jscores above 50 indicate correct fold assignment with >90% probability. (1), (4) and (6) correspond to the DID domain of FHOD1 [391,393] (PDB=3dada) and were predicted by the RPSB_01, BASI_01 and PSIB_01 servers, respectively. (2) and (3) correspond to the unbound DID domain of Dia1 [224] (PDB=1z2cb) and were predicted by the FFAS_03 and BASI_02 servers, respectively. (5) and (7) correspond to the dimeric DID domain of Dia1 [221] (PDB=2bxa) and were predicted by FF3A_07 and BASI_04 servers, respectively. (**C**) BLAST analysis using ELMO1 aas 74-279 reveals primary sequence amino acid similarity between ELMO1 and the FHOD1 N-Terminal region corresponding to the DID domain of FHOD1. (**D**) Volume contour models of the ELMO1 EID (aas 80-305, generated by Phyre), DID of FHOD1 (aas 115-339; PBD=3dad) and DID of Dia1 (aas 135-435; PBD=2bap). I204 of ELMO1 is surface exposed and was predicted as the equivalent of the critical DID residues (indicated in orange) of FHOD1 (V228) and Dia (A256) implicated in binding the DAD. (**E**) Lysates of HEK293T cells transfected with the indicated plasmids were immunoprecipitated with an anti-Myc antibody. Immunoblot analysis using anti-FLAG (DOCK180) and anti-Myc (ELMO1) antibodies demonstrates that the ELMO EAD mutation (M692A/E693A) does not hinder co-precipitation with DOCK180. (**F**) Schematic representation of all ELMO constructs used in this study.

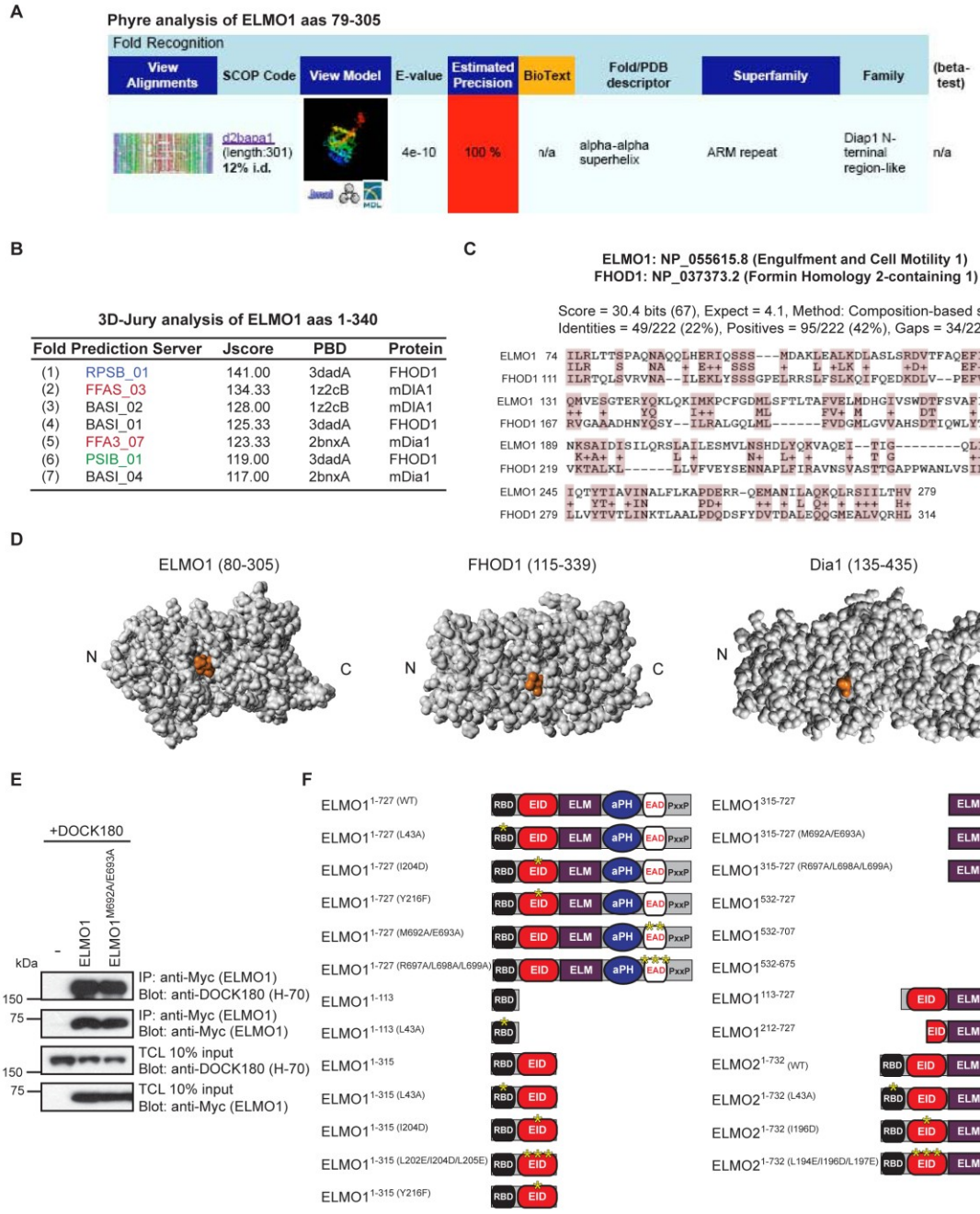

Supplementary Figure 3S1

Figure 3S2. Characterization of the ELMO1 RBD and of an ELMO2 conformation biosensor, and demonstration of conformational changes in ELMO following binding to DOCK180; Related to Figure 3.3. (**A**) Shown are the complementary controls to Figure 3.3A. HeLa cells were transfected with the indicated plasmids. After 24 h, the localization of ELMO1 and $RhoG^{V12}$ was analyzed using anti-Myc and anti-HA antibodies, respectively, by laser scanning microscopy. Scale bar, 20 μm. (**B**) The $BRET^2$ ratio of the GFP^{10}-ELMO2-RlucII biosensor is independent of protein expression levels. 100 ng to 800 ng of plasmid coding for the ELMO2 $BRET^2$ biosensor were transfected in HEK293T. RLucII activity and $BRET^2$ ratios were experimentally obtained and plotted. Importantly, similar $BRET^2$ ratios were obtained independent of protein expression levels. These results denote that the GFP^{10}-ELMO2-RlucII biosensor acts autonomously and not via protein oligomerization and/or aggregation. (**C**) GFP^{10}-ELMO2-RlucII biosensor is unable to bind RhoG as compared to Myc-ELMO2. Lysates of HEK293T cells transfected with the indicated plasmids were subject to pulldowns with streptavidin-Dynabeads (RhoG). Immunoblot analysis was performed with anti-ELMO2 and streptavidin-HRP (RhoG). (**D**) Lysates of HEK293T cells transfected with the indicated plasmids were immunoprecipitated with an anti-FLAG antibody. Immunoblot analysis using anti-ELMO2 and anti-FLAG (DOCK180) antibodies demonstrates the co-precipitation of DOCK180 with Myc-ELMO2 and GFP^{10}-ELMO2-RLucII. (**E**) Binding of DOCK180 to ELMO2 alters ELMO2 conformation. $BRET^2$ signal (400 nm luminescence and 510 nm fluorescence) measurements after DeepBlueC addition in HEK293T cells expressing indicated proteins (***, $P<0.001$, by ANOVA test and Bonferroni's multiple comparison; error bars represent s.e.m, $n=6$).

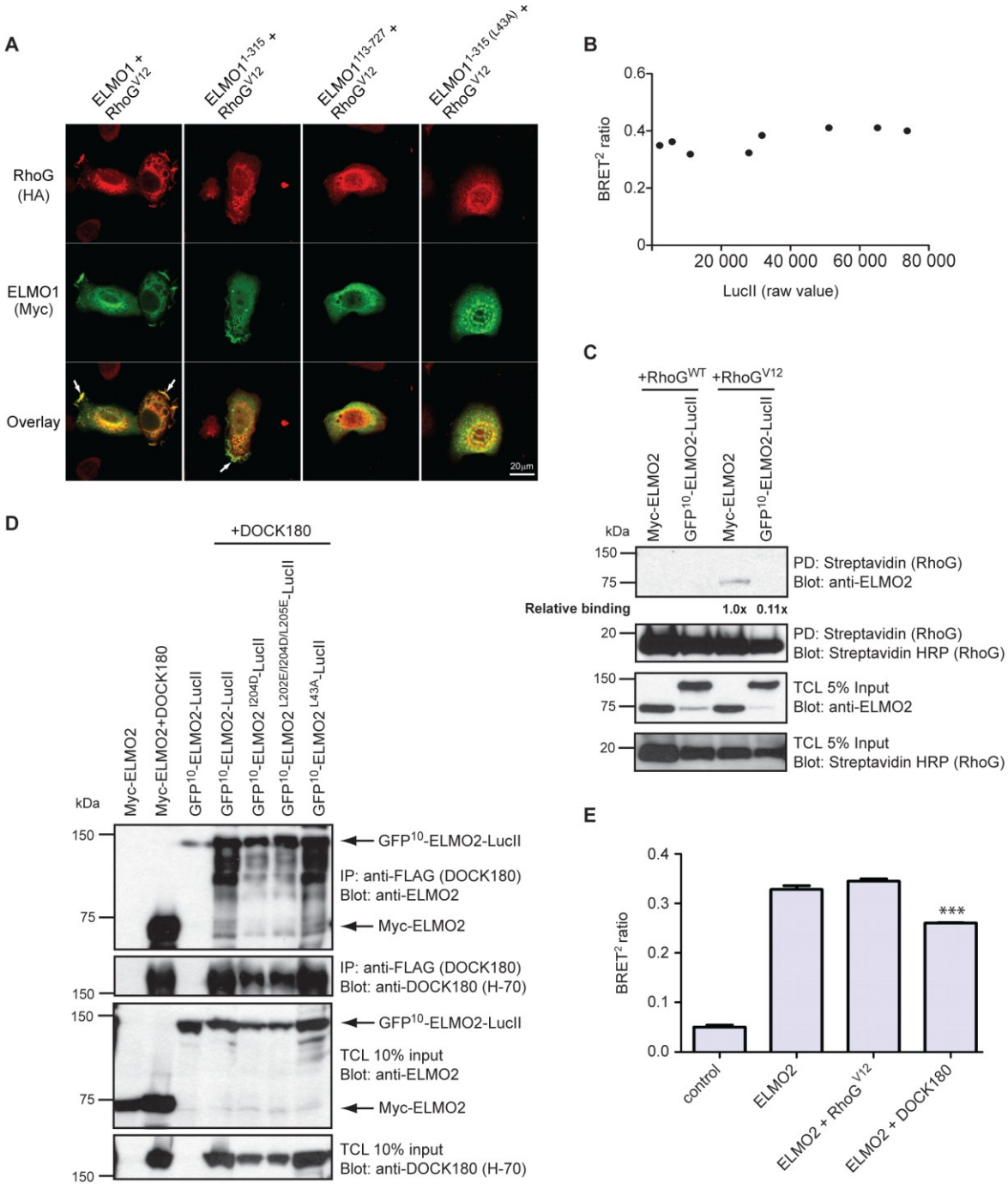

Supplementary Figure 3S2

Figure 3S3. Auto-regulatory defective ELMO mutants promote migration and cytoskeletal changes in a DOCK180-dependant manner; Related to Figure 3.4. (**A**) Shown are the complementary control conditions of Figure 3.4A. HeLa cells were transfected with the indicated plasmids. After 24h incubation, the localization of ELMO1 and $RhoG^{V12}$ was observed with anti-Myc and anti-HA antibodies, respectively, using a laser scanning microscope. Scale bar, 20 μm. (**B**) Left Panel: Activated ELMO1 mutants promote cell motility. Right Panel: Activated ELMO1 mutants synergize with DOCK180 and CrkII to promote cell motility. Migration of LR73 cells was evaluated by Transwell migration assays. Relative cell migration was determined by the number of migrated cells normalized to ELMO alone (Left panel) or ELMO1+DOCK180+CrkII (Right panel) conditions which were arbitrarily set at 100% (*, $P<0.05$; **, $P<0.005$; ***, $P<0.001$, by ANOVA test and Bonferroni's multiple comparison; error bars represent s.e.m, $n=4$). Expression levels of the transfected proteins for migration assays were analyzed by immunoblotting cell lysates with anti-DOCK180 (H-70) and anti-Myc (ELMO1 and CrkII) antibodies, as indicated. (**C**) Activated mutants of ELMO1 are dependant on DOCK180 for their biological activity. Upper panel: serum-starved LR73 cells transfected with the indicated ELMO1 plasmids were detached and plated on fibronectin-coated chambers for 2 h. Cells were stained for ELMO1 (anti-Myc) and phalloidin-Alexa 633. Scale bar, 20 μm. Bottom: quantification of cell morphology. More than 100 cells were analyzed for each condition (***, $P<0.001$, by ANOVA test and Bonferroni's multiple comparison; error bars represent s.e.m, $n=3$). (**D**) Active ELMO1 mutants do not promote global Rac activation. HEK293T and CHO LR73 cells were transfected with the indicated plasmids and GTP-loaded Rac was pulled down from cell lysates using the p21-binding domain of PAK fused to GST (PBD-assay). The amount of Rac in pulldowns and in total cell lysates (TCL) was detected by immunoblotting with an anti-Rac antibody. Expression levels of the various proteins, and equal loading of Rac in all samples, were analyzed by immunoblotting of the TCL using anti-FLAG (DOCK180), anti-Myc (ELMO1) and anti-Rac antibodies.

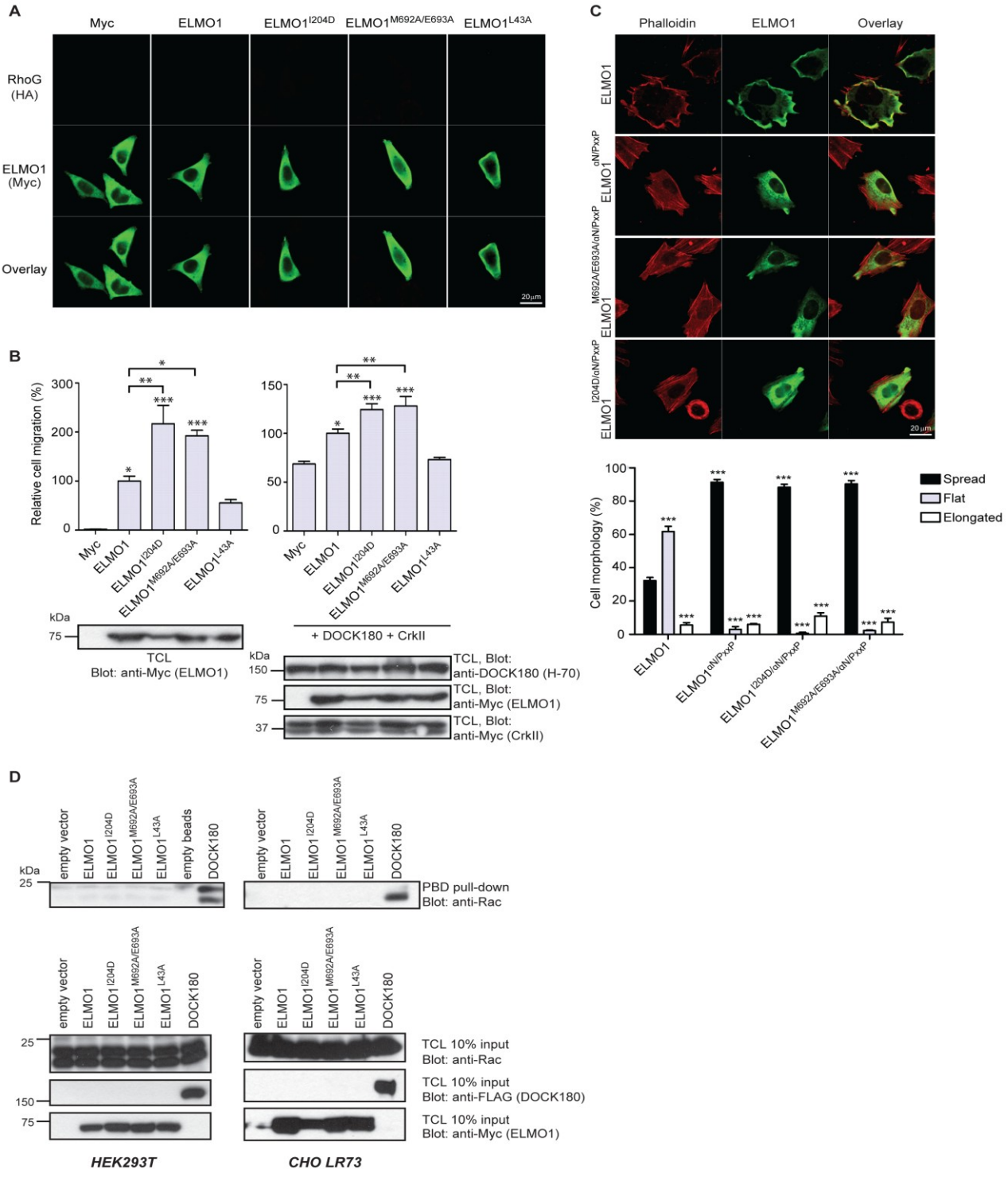

Supplementary Figure 3S3

MATERIALS AND METHODS

Antibodies, cell culture and transfections. Anti-DOCK180 (H-4 and H-70), anti-Myc (9E10), and anti-HA (Y-11) were from Santa Cruz Biotechnologies. HEK293T and HeLa cells were cultured in DMEM supplemented with 10% fetal bovine serum, penicillin and streptomycin (Gibco-BRL) and transfected by calcium phosphate or Lipofectamine 2000 (Invitrogen) using standard procedures. The CHO cell line, LR73 subclone, was maintained in alpha-MEM supplemented with 10% fetal bovine serum, penicillin and streptomycin (Gibco-BRL) and transfected using Lipofectamine 2000 (Invitrogen) according to the manufacturer's instructions. Biochemical and cell biological studies were performed 24-48 hours after transfection.

Plasmid Constructs. pCNX2 Flag-DOCK180 and pCAGGS Myc-CrkII were donated by Dr M. Matsuda. HA-RhoG was kindly provided by Dr P. Fort. pcDNA3.1 Myc-ELMO1 was previously described [363]. Plasmids coding for Myc-ELMO1 proteins (aas 1-113, 1-315, 113-727, 212-727 and 315-727) were generated by PCR using Myc-ELMO1 as a template and cloned into the BamHI/XhoI sites of pcDNA3. HA-RhoG^{V12}, Myc-ELMO1^{I204D} (WT, 1-315), Myc-ELMO1$^{L202E/1204D/L205E}$ (WT, 1-315), Myc-ELMO1^{Y216F} (WT, 1-315), Myc-ELMO1$^{M692A/E693A}$ (WT, 315-727), ELMO1$^{R697A/L698A/L699A}$ (WT, 315-727), and Myc-ELMO1^{L43A} (WT, 1-113, 1-315) were generated by site-directed mutagenesis (QuickChange; Stratagene). pEG202 and pJG4-5alt were obtained from Dr. J. Archambault. Yeast constructs for ELMO1 (WT, 1-315, 1-315^{I204D} and 1-315$^{L202E/1204D/L205E}$) were generated via PCR using the Myc-ELMO1 as a template and cloned into the BamHI/XhoI sites of pEG202 (LexA-tagged vector). pEG202-ELMO1$^{1-315\ (Y216F)}$ was generated by site-directed mutagenesis. ELMO1$^{532-727,\ 532-707\ and\ 532-675}$ were generated via PCR using the Myc-ELMO1 as a template and cloned into the BglII/XhoI sites of pJG4-5alt (B42-tagged vector). pJG4-5alt-ELMO1$^{315-727\ (M692A/E693A)}$ and ELMO1$^{315-727\ (R697A/L698A/L699A)}$ were generated via site-directed mutagenesis. pcDNA3.1 GFP^{10}-ELMO2-RLucII was generated by subcloning ELMO2 Kpn1/HindIII into

pcDNA3.1 GFP^{10}-EPAC1-RLucII whereby replacing the EPAC1 coding sequence by ELMO2 while keeping identical linkers. ELMO2, ELMO2^{L43A}, ELMO1^{I196D} and ELMO1$^{L194E/I196D/L197E}$ mutants were generated by site-directed mutagenesis and were tagged with GFP^{10} and LucII with the same aforementioned cloning strategy. The pBABE rtTA and pOZ hBirA plasmids were gifts from Dr. Paul Jolicoeur and Dr. Vasily Ogryzko, respectively. Plasmids coding for RhoG^{WT} were generated via PCR, cloned into the EcoRI/BamHI sites of (pTRE-Biotag-TEV), and finally subcloned into the XhoI site of CMV-deleted pcDNA3. To create RhoG^{V12}, a site-directed mutagenesis was done using pcDNA3-TRE-Biotag- RhoG^{WT}.

Immunoprecipitation, GST-fusion protein and streptavidin pulldowns. GST-fusion protein pulldowns and immunoprecipitation experiments were performed as previously described [388]. In **Figure 3.1D (pg. 151)**, cells were first treated with the reversible DSP cross-linker (Pierce; 2 μM final) for 30 min prior to lysis and immunoprecipitation. Streptavidin pulldowns were performed as suggested by the manufacturer. Briefly, transfected cells were lysed with MLB buffer (1% NP-40, 25mM Hepes pH 7.5, 150mM NaCl, 10mM MgCl2, 1mM EDTA, 10% glycerol) and incubated with washed Streptavidin-beads (Dynabeads M-280 Streptavidin; Invitrogen) for 30 min at 4°C. Beads were collected using a magnet and washed three times with MLB buffer followed by fractionation of bound material by SDS-PAGE.

Rac-GTP assays. The GTP-loading status of Rac in HEK293T cells was analyzed by GST-PAK-PBD affinity precipitation as described previously [363].

Yeast Two-Hybrid Interaction Assay. The genotype of the yeast reporter strain EGY48 is MATα ura3 trp1 his3 6lexAop-LEU2, auxotrophic for tryptophan (Trp), uracil (Ura), histidine (His), with LEU2 as a reporter gene. Yeast were grown in rich medium (1% yeast, 2% Bacto-peptone, 2% glucose) or in synthetic minimal medium with appropriate supplements. Yeasts were transformed by the lithium acetate method

using standard protocol, with LexA-tagged ELMO1 constructs (HIS3) screening B42-tagged ELMO1 constructs (TRP1) for interaction. Double transformants were plated on non-selective (-Histidine, -Tryptophan) and selective (-Histidine, -Tryptophan, -Leucine) medium containing galactose. Plates were incubated at 30°C for 3-5 days.

Cell fractionation assay. Cell fractionation was performed as previously described [364]. Equal amounts of proteins (20 μg) were resolved by SDS-PAGE and proteins of interest were analyzed via immunoblotting with appropriate antibodies.

Cell spreading and colocalization assays. For integrin independent assays, HeLa and LR73 cells were grown for 24 h in 4-well LabTeck chambers (25,000 cells per well, Falcon) coated with poly-L-lysine (26 μg/cm^2, Sigma). Cells were then transfected with the indicated plasmids and grown for an additional 24 h. Cell were fixed by 4% paraformaldehyde treatment. Immunofluorescence was performed and Feret diameters of more than 40 cells were analyzed using the threshold function of Image-J software (NIH) (*n*=3 for each condition). Diameters are presented as "box and whisker" plots showing means, quartile, and highest and lowest values. For the cell-spreading assay on fibronectin, LR73 cells were transfected with the indicated plasmids and were subjected to cell morphology analysis as previously described [364]. Briefly, serum starved cells (0.5% FBS, overnight) were gently detached (0.01% trypsin and 5 mM EDTA, in Hanks balanced solution, Gibco), washed in Fibroblast Basal Medium (Clonetics) supplemented with 0.5% BSA (Sigma) and 40,000 cells were allowed to spread on fibronectin (10 μg/cm^2) for 2 h before fixing with 4% paraformaldehyde. Morphology of the cells expressing the various ELMO1 mutants was analyzed by immunofluorescence. Cells were scored for three phenotypes: spread (normal), flat (increased spreading and rounder) and elongated (polarized-like) (more than 100 cells per condition were analyzed, *n*=3).

Immunofluorescence. Cells were fixed with 4% paraformaldehyde, permeabilized with 0.2% Triton X-100 (Sigma) in PBS and blocked in PBS-1% BSA (United States Biological). Cells were incubated with anti-Myc and anti-HA antibodies (1:200 and 1:100 dilution, respectively) for 45 min, and then incubated with goat anti-mouse Alexa488 and goat anti-rabbit Alexa 633 (Invitrogen) (both 1:1,000 dilution) for 30 min. After one wash in Tween 0.2% (Sigma) in PBS and three in PBS alone, the chambers slides were mounted with coverslips using *Slow Fade*® Gold antifade reagent with DAPI mounting medium (Invitrogen). Fluorescence images were captured with a Zeiss LSM510 confocal microscope, and the quantitative cell morphology analysis was performed using images taken with a Leica DM4000 epifluorescence microscope (Deerfield, IL) equipped with a Retiga EXi (QImaging, Burnaby, BC, Canada) camera.

Cell migration assay. Cell migration assays were performed using modified Boyden chambers as previously described [364]. Briefly, 6.5 mm-diameter transwell inserts with 8-µm pores were used in 24-well plates (Corning, CA). LR73 cells were transfected, using Lipofectamine 2000 (Invitrogen), with the indicated plasmids and were serum starved (0.5% FBS) overnight. Cells were prepared as for spreading assays on fibronectin and 100,000 cells were seeded in transwells inserts precoated with fibronectin (90 µg/cm^2). Cells were allowed to migrate for 4 h prior to fixation in 4% paraformaldehyde. Then, the top surface of the chamber was wiped using a cotton swab and chambers were stained with anti-Myc and anti-mouse Alexa488 antibodies (1:200 and 1:1,000 dilution, respectively). Fluorescence images were acquired with a Leica DM4000 epifluorescence microscope (Deerfield, IL) equipped with a Retiga EXi camera (QImaging, Burnaby, BC, Canada), for 15 fields per insert using a 10X lens. The number of positive cells was counted using the threshold function of Image-J software (NIH). Migration was normalized to ELMO1 alone or to the ELMO1+DOCK180+CrkII condition that was arbitrarily set at 100%. Expression levels of the exogenous proteins were verified by western blotting using the remaining cells. Measurements were done in duplicate (n=4).

BRET² Assay. HEK293T cells were transfected with the ELMO2 biosensor or pcDNA3.1 RlucII alone using Lipofectamine 2000. 24-48h post-transfection, cells were harvested in DMEM and washed once with PBS. For each sample, 50,000 or 100,000 cells in PBS were distributed in 96-well white opaque plate (Optiplate, Perkin Elmer). The luciferase substrate, DeepBlueC (Biotium), was added at a final concentration of 5 μM. The luminescence at 400 nm and fluorescence at 510 nm were measured with the PHERAstar (BMG Labtech). The BRET² ratios were calculated as described [398] (*n*=3).

Statistical analysis. Statistical differences between two groups of data were analyzed using ANOVA test and Bonferroni's multiple comparison procedures (minimum of *n*=3).

CHAPTER 4

The Arf family GTPase, Arl4A, complexes with ELMO and reveals a polyvalent Ras-Binding Domain in ELMO

CHAPTER 4: Figure Acknowledgements

Figure 4.1 (A-C): Manishha Patel

Figure 4.2 (A-D): Manishha Patel

Figure 4.3: Tsai-Chen Chiang

Figure 4.4 (A-D): Tsai-Chen Chiang

Figure 4.5 (A-C): Manishha Patel

Figure 4.6: Tsai-Chen Chiang

Supplementary Figure 4S1: Tsai-Chen Chiang

Supplementary Figure 4S2: Tsai-Chen Chiang

*The manuscript was written by Manishha Patel and edited by Dr. Jean-François Côté

The Arf family GTPase, Arl4A, complexes with ELMO and reveals a polyvalent Ras-Binding Domain in ELMO

Manishha Patel[*†], Tsai-Chen Chiang[‡†], Fang-Jen S. Lee[‡] and Jean-François Côté[* ¶ # §]

[*]Institut de Recherches Cliniques de Montréal. 110 avenue des pins ouest, Montréal (Québec) Canada, H2W 1R7.

[‡]Institute of Molecular Medicine, College of Medicine, National Taiwan University, and Department of Medical Research, National Taiwan University Hospital, Taipei 100, Taiwan.

[¶]Faculté de Médicine, Université de Montréal, Montréal, PQ H3C 3J7, Canada

[#]Division of Experimental Medicine, McGill University, Montréal, PQ H3A 1A3, Canada

[§]Corresponding author:

Email: Jean-François Côté

Phone: (514) 987-5647

Fax: (514) 987-5624

[†] These authors contributed equally

Running Title: Arl4A interacts with the RBD of ELMO

Abstract

Directed cell migration is integral during various biological processes, such as, embryonic development, immune response, and cancer metastasis. Tight control of the Rho GTPase Rac is a key molecular event underlying spatio-temporal coordination of Rac activation and ensuing signaling pathways. The DOCK family members of guanine nucleotide exchange factors (GEFs) have emerged as important positive regulators of Rho GTPases. The prototypical DOCK protein, DOCK180, is linked to ELMO during cell migration, phagocytosis, and myoblast fusion. Until recently, the role of ELMO during DOCK180-mediated Rac activation and signaling was poorly understood. We found that ELMO was not required for DOCK180 Rac GEF activity, but rather for the proceeding Rac signaling cascade. Specifically, at basal state, our work revealed ELMO to be regulated via intramolecular contacts similar to an autoinhibitory module found in formins. In formins, release of this autoinhibition comes via GTPase binding a GTPase binding domain (GBD). We also found that ELMO contains a GBD similar in structure to that of the formin FHOD1, and is referred to as a Ras-binding domain (RBD). The ELMO RBD was found to be important for membrane targeting and autoinhibition relief of ELMO.

This study identifies Arl4A, an Arf-related GTPase, as a novel ELMO binding partner. Specifically, Arl4A binds the ELMO RBD and acts as a membrane recruitment signal for the ELMO/DOCK180/Rac module to induce cytoskeletal changes. Our data reveals that ELMO is proficient for interaction with GTPases from divergent families, leading to the conclusion that ELMO contains a polyvalent RBD. This is the first study to identify an RBD with dual specificity for Rho and Arf family GTPases. Our results may have broad implications in the activation and localization of this pathway by additional GTPases.

Introduction

An elaborate cast of players are directed to coordinate Rho GTPases during numerous basic biological processes such as cell migration, polarity and adhesion. The evolutionarily conserved family of DOCK proteins mediates guanine nucleotide exchange on a subset of these Rho GTPases to control active remodeling of the actin cytoskeleton [83]. Amongst the eleven mammalian proteins, DOCK180 (also known as DOCK1)-5 and DOCK9-11 are characterized as specific activators of Rac and Cdc42 GTPases, respectively [83,266]. Deviants of the distinctive DH-PH Rho GEFs, the DOCK proteins rely on the DOCK homology region-2 (DHR-2) for guanine nucleotide exchange activity, and a lipid-binding DHR-1 for membrane targeting [265,274].

Amid the DOCK proteins, the CDM members (*C. elegans* ced-5*, Drosophila* Myoblast City and mammalian DOCK1/2/5) have been reported to regulate a number of Rac-dependent biological events including cell migration, cell polarization, myoblast fusion and engulfment of apoptotic cells [180,253,336,399]. The interaction of DOCK180 with various proteins is critical in regulating Rac signaling. One major protein family interacting with DOCK180 is the ELMO family. Genetic analyses in worms and flies suggest that ELMO is crucial for all studied biological functions of DOCK180 [83,266]. Cell biology studies in mammalian cells suggest that disrupting the ELMO/DOCK180 interaction blocks signaling from this complex.

Until recently, the implicated domain(s) and the mechanism by which ELMO proteins facilitate Rac signaling were obscure. Our findings identified three previously uncharacterized modules of ELMO proteins: Ras-Binding Domain (RBD), ELMO Inhibitory Domain (EID), and ELMO Autoregulatory Domain (EAD) [400]. We discovered an autoinhibitory switch in ELMO presenting structural homology to an analogous regulatory unit described for Dia-family formins [220,231,400,401]. The switch is organized via physical bridging of a tandem RBD-EID at the N-terminus, and an EAD at the C-terminus. At basal levels, the intramolecular interaction between these fragments is suggested to sequester ELMO in a closed conformation, and it is hypothesized that

additional binding partners will alleviate this autoinhibited state once the cell is stimulated. Functionally, ELMO1 mutants with defective autoregulatory activity were found to promote cell elongation and migration, highlighting the importance of tight conformational regulation of ELMO [400].

An indication that proper membrane targeting of ELMO is an important event in DOCK180-Rac activation came from the demonstration that expression of myristoylated ELMO2 induces uncontrolled membrane ruffles [402]. Due to its ability to interact with membrane-localized and signaling proteins, the N-terminus of ELMO is a strong candidate for proper targeting of the ELMO/DOCK180 complex [152,293,402,403]. RhoG, in its active GTP-bound state, was demonstrated to recruit ELMO/DOCK180 to the membrane and induce Rac-dependent cytoskeletal changes promoting efficient cell migration, phagocytosis and neurite outgrowth [152,250,251,255,404]. However, a later study demonstrated that RhoG is not required for integrin-mediated Rac signaling and motility [153]. It is evident that understanding the molecular events that regulate ELMO/DOCK180 recruitment to the membrane is an important area of investigation to fully comprehend how these proteins are controlled.

This study investigates a novel molecular event capable of controling ELMO recruitment to the membrane. We initiated a screen to identify unknown ELMO binding proteins and identified an Arf-related GTPase, Arl4A, as a candidate to promote signaling by the ELMO/DOCK180/Rac pathway via a membrane recruitment mechanism. Our data reveal that the ELMO N-terminus is capable of interacting with GTPases from divergent families, leading to the conclusion that ELMO contains a polyvalent RBD. To our knowledge, this is the first study to identify an RBD with dual specificity for Rho and Arf family GTPases. Our results may have broad implications in the activation and localization of this pathway by additional GTPases.

Results

An Arf-related GTPases, Arl4A, binds the ELMO1 Ras Binding Domain (RBD)

We previously reported that the formation of an ELMO/DOCK180 complex is essential for Rac GTP-induced cytoskeletal changes but not for Rac GTP-loading *per se,* the latter being solely dependent on the intrinsic GEF activity of DOCK180 [388]. The C-terminal atypical PH domain of ELMO1 was found to mediate binding to DOCK180 and we proposed that the N-terminal region is likely to contain either membrane targeting and/or Rac effector recruitment activity to promote efficient Rac signaling.

Since ELMO proteins are repressed via intramolecular interactions, we reasoned that molecules that interact with the RBD might activate or spatially position the ELMO/DOCK180 complex for activation. To identify novel partners of the N-terminus of ELMO1, we performed a yeast-two hybrid screen using ELMO1 as bait and an embryonic mouse brain cDNA library as prey. Among the novel candidate ELMO1 partners, we decided to study in more detail Arl4A, a small GTPase of the Arf family. The Arf family member, Arf6, is heavily implicated in cytoskeletal reorganization via numerous signaling events [180-182,209,210]. One such pathway places Arf6 upstream of DOCK180 and ELMO and ensuing Rac activation and signaling [180]. However, the exact mechanism by which Arf6 controls ELMO/DOCK180-mediated Rac signaling is poorly understood. Arl4A belongs to the large family of Arf-related proteins. The Arl4 family consists of three closely related members: A, C, and D [156]. Unlike the other members of this family, Arl4s are preferentially GTP-loaded due to their weak affinity for nucleotides and therefore exhibit high spontaneous nucleotide exchange rates [212]. Recent reports suggest that Arl4s are involved in cytoskeletal rearrangement through their ability to bind the Arf6 guanine exchange factor ARNO and localize it to the cell periphery for Arf6 activation [209,210].

We used the yeast two-hybrid system to verify which isoforms of Arl4s interact with ELMO proteins. Using ELMO1 as bait revealed specificity for the Arl4A protein since no interaction was noted for Arl4C or Arl4D **(Figure 4.1A, pg. 187)**. Moreover,

ELMO1 binding to Arl4A was nucleotide-state dependent, with ELMO1 selectively interacting with the WT and constitutively active (Q79L) forms but not with dominant negative (T34N) Arl4A **(Figure 4.1A, pg. 187)**. To validate these results in a mammalian cell context, we co-expressed Myc-ELMO1 with the WT, Q79L and T34N forms of Arl4A in 293T cells. Similar to what was observed in yeast, specific interaction between ELMO1 and both $Arl4A^{WT}$ and $Arl4A^{Q79L}$ was observed **(Figure 4.1B, pg. 187)**. Finally, we could generalize the binding of Arl4A to all isoforms of ELMO since we found a specific interaction in co-immunoprecipitation between Arl4A and Myc-ELMO1, Myc-ELMO2 and Myc-ELMO3 **(Figure 4.1C, pg. 187)**.

To map the active ELMO1 binding interface for Arl4A, we used a panel of ELMO1 truncation mutants **(Figure 4.2A, pg. 189)** in the yeast two-hybrid system. Our data suggests that the first 113 amino acids of ELMO1 have the ability to complex with Arl4A **(Figure 4.2B, pg. 189)**. Similarly, deletion of the first 113 amino acids was sufficient to abrogate binding of ELMO1 to Arl4A. Moreover, we also found that $ELMO1^{1\text{-}113}$ was sufficient to bind Arl4A in 293T cells **(Figure 4.2C, pg. 189)**. A mutant of ELMO1 lacking the first 113 amino acids was difficult to express, but we could demonstrate that the first 212 amino acids of ELMO1 are required for interacting with Arl4A since $ELMO1^{212\text{-}727}$ is unable to co-precipitate Arl4A **(Figure 4.2C, pg. 189)**. Together, these results demonstrate that Arl4A interacts specifically with the RBD of ELMO that was previously identified for the interaction with RhoG-GTP. Consistent with our original hypothesis, active Arl4A would be a good candidate to relieve the inhibitory EID-EAD interaction in ELMO and localize ELMO/DOCK180 to the membrane for Rac activation.

Our discovery that the Arl4A binding site encompasses the ELMO RBD led to an exciting possibility. Similar to active RhoG, Arl4A may also have specific affinity for this protein module. Our prior findings disclosed ELMO1 residue Leucine 43 as the cornerstone for forging the ELMO1 RBD/RhoG-GTP contact [400]. In a yeast two-hybrid assay, we found that both $Arl4A^{WT}$ and $Arl4A^{Q79L}$ were unable to interact with

Figure 4.1. Arl4A is a novel ELMO-interacting partner binding the extreme N-terminal region of ELMO. (**A**) Arl4A WT and Q79L interact with ELMO1 in a yeast two-hybrid system. Yeast strain EGY48 co-transformed with LexA BD fusion construct of $ELMO1^{WT}$ and the B42 fusion constructs of the indicated Arl4s were grown on selective (-Histidine, -Trytophan, -Leucine) and non-selective (-Histidine, -Trytophan) medium for a nutrient selective growth assay. (**B**) Arl4A and ELMO1 interact *in vivo* in cells. HEK293T cells transfected with the indicated plasmids were subject to a crosslinker, lysed and immunoprecipitated with an anti-Myc antibody (ELMO1). Immunoblot analysis using anti-Myc and FLAG-HRP antibodies established the co-precipitation of ELMO and Arl4A proteins. (**C**) Arl4A interacts with all forms of ELMO. HEK293T cells transfected with the indicated plasmids were crosslinked, lysed and immunoprecipitated with an antibody against the Myc-epitope (ELMO1-3). The co-precipitation of the various ELMO proteins and Arl4A was analyzed via immunoblotting with anti-Myc (ELMO1-3) and anti-FLAG-HRP (Arl4A) antibodies, respectively.

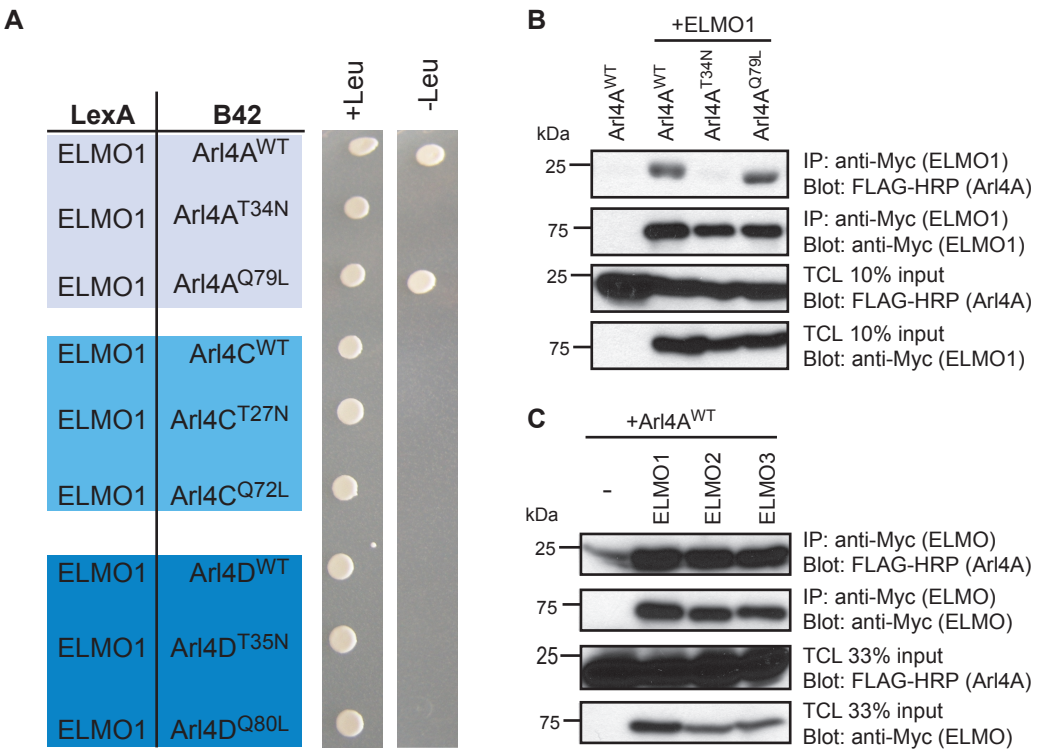
A
LexA
B42
+Leu
-Leu
ELMO1
Arl4A^WT
ELMO1
Arl4A^T34N
ELMO1
Arl4A^Q79L
ELMO1
Arl4C^WT
ELMO1
Arl4C^T27N
ELMO1
Arl4C^Q72L
ELMO1
Arl4D^WT
ELMO1
Arl4D^T35N
ELMO1
Arl4D^Q80L
B
+ELMO1
Arl4A^WT
Arl4A^WT
Arl4A^T34N
Arl4A^Q79L
kDa
25
IP: anti-Myc (ELMO1)
Blot: FLAG-HRP (Arl4A)
75
IP: anti-Myc (ELMO1)
Blot: anti-Myc (ELMO1)
25
TCL 10% input
Blot: FLAG-HRP (Arl4A)
75
TCL 10% input
Blot: anti-Myc (ELMO1)
C
+Arl4A^WT
-
ELMO1
ELMO2
ELMO3
kDa
25
IP: anti-Myc (ELMO)
Blot: FLAG-HRP (Arl4A)
75
IP: anti-Myc (ELMO)
Blot: anti-Myc (ELMO)
25
TCL 33% input
Blot: FLAG-HRP (Arl4A)
75
TCL 33% input
Blot: anti-Myc (ELMO)

Figure 4.1

Figure 4.2. Arl4A binds the ELMO1 RBD through a key evolutionarily conserved RBD residue. (**A**) Schematic representation of ELMO1 deletion mutants used in yeast two-hybrid experiments. (**B**) The ELMO1 N-Terminus is required for Arl4A binding. Yeast strain EGY48 co-transformed with LexA BD fusion construct of ELMO1^{WT} and deletion mutants and the B42 fusion constructs of the indicated Arl4As were grown on selective (-Histidine, -Trytophan, -Leucine) and non-selective (-Histidine, -Trytophan) medium for a nutrient selective growth assay. (**C**) The Arl4A/ELMO1 interaction *in cellulo* requires the ELMO1 RBD. HEK293T cells transfected with the indicated plasmids were crosslinked, lysed and immunoprecipitated with an antibody against the Myc-epitope (ELMO1). The co-precipitation of the various ELMO1 proteins and Arl4A was analyzed via immunoblotting with anti-Myc (ELMO) and anti-FLAG-HRP (Arl4A) antibodies, respectively. (**D**) Mutation of a key conserved residue in the ELMO RBD (L43A) abolishes Arl4A binding. Yeast strain EGY48 co-transformed with LexA BD fusion construct of ELMO1 (WT or L43A) and the B42 fusion construct of Arl4A (WT or Q79L) were grown on selective (-Histidine, -Trytophan, -Leucine) and non-selective (-Histidine, -Trytophan) medium for a nutrient selective growth assay.

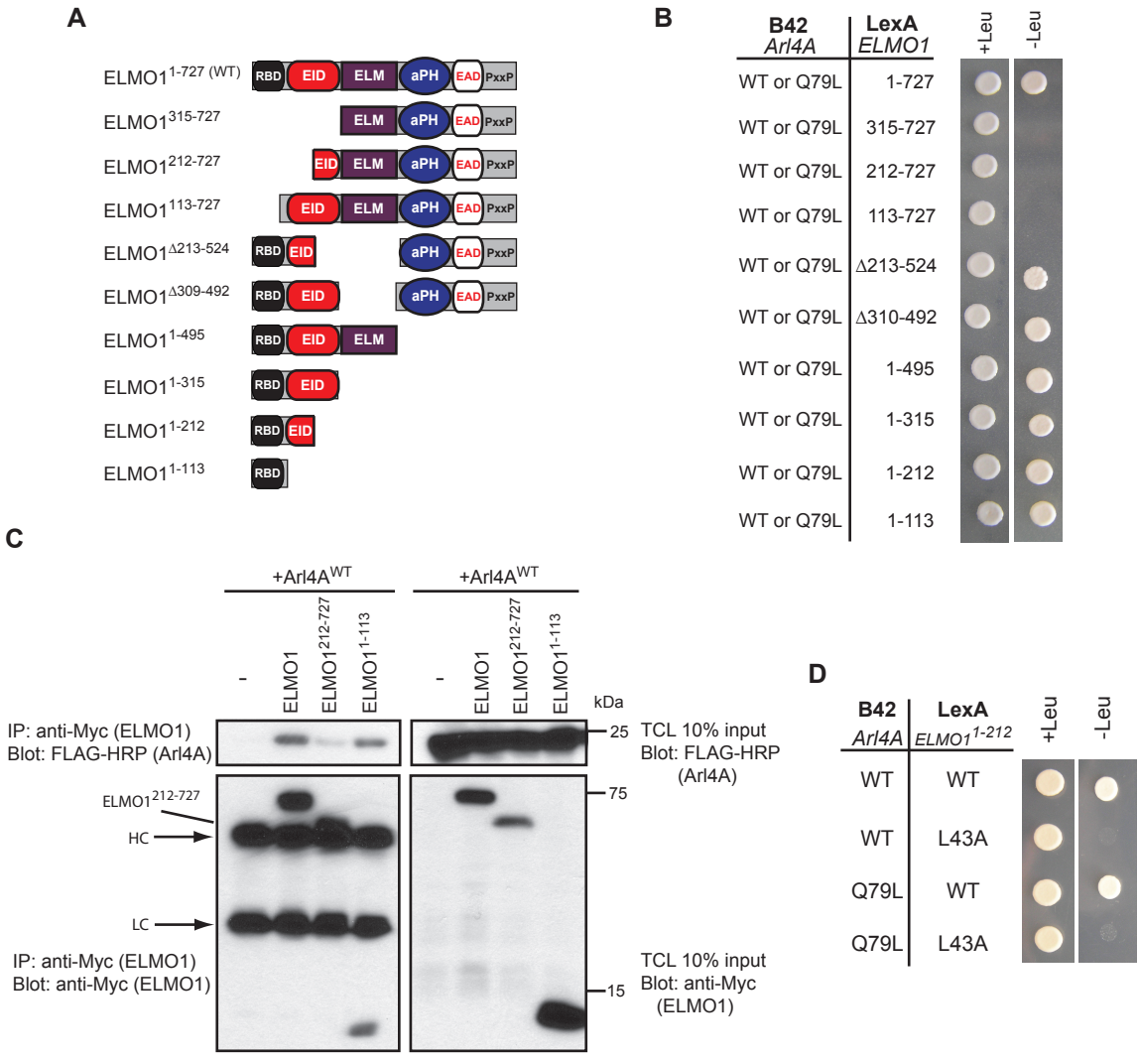
A
ELMO1 1-727 (WT)
ELMO1 315-727
ELMO1 212-727
ELMO1 113-727
ELMO1 Δ213-524
ELMO1 Δ309-492
ELMO1 1-495
ELMO1 1-315
ELMO1 1-212
ELMO1 1-113
RBD
EID
ELM
aPH
EAD
PxxP
B
B42 Arl4A
LexA ELMO1
+Leu
-Leu
WT or Q79L 1-727
WT or Q79L 315-727
WT or Q79L 212-727
WT or Q79L 113-727
WT or Q79L Δ213-524
WT or Q79L Δ310-492
WT or Q79L 1-495
WT or Q79L 1-315
WT or Q79L 1-212
WT or Q79L 1-113
C
+Arl4A WT
+Arl4A WT
-
ELMO1
ELMO1 212-727
ELMO1 1-113
kDa
IP: anti-Myc (ELMO1)
Blot: FLAG-HRP (Arl4A)
TCL 10% input
Blot: FLAG-HRP
(Arl4A)
25
75
15
ELMO1 212-727
HC
LC
IP: anti-Myc (ELMO1)
Blot: anti-Myc (ELMO1)
TCL 10% input
Blot: anti-Myc
(ELMO1)
D
B42 Arl4A
LexA ELMO1 1-212
+Leu
-Leu
WT WT
WT L43A
Q79L WT
Q79L L43A

Figure 4.2

ELMO1$^{1\text{-}212\ (L43A)}$ in comparison to its wild-type counterpart **(Figure 4.2D, pg. 189)**. This result validates our previous finding that ELMO proteins contain a previously unrecognized canonical RBD. Furthermore, our data supports the notion that the ELMO RBD, similar to other ubiquitin superfold RBDs, has the potential to attract GTPases of different families. Our study identifies, for the first time, an RBD with the ability to interact with both Rho and Arf family GTPases.

Arl4A targets ELMO to the membrane

Our results are consistent with the model that Arl4A interacts with the RBD of ELMO proteins to relieve the ELMO intramolecular interaction and/or favor membrane recruitment. RhoG was previously reported to activate the ELMO/DOCK180 pathway by localizing ELMO to the membrane in a manner dependent on its nucleotide-state [251]. To test if Arl4A also promotes membrane recruitement of ELMO1, we analyzed the cellular distribution of ELMO1 in cells expressing the various forms of Arl4A (WT, Q79L and T34N). While Myc-ELMO1 expressed alone is cytoplasmic, co-expression with WT and active Arl4A led to its membrane recruitment **(Figure 4.3, pg. 192)**. The specificity of ELMO-binding to Arl4A was further demonstrated by colocalization experiments that revealed that ELMO1 does not colocalize at the membrane with either Arl4C or Arl4D, with these cells showing a less protrusive phenotype (data not shown). This suggests that ELMO proteins are *bona fide* effectors of Arl4A and act by localizing ELMO/DOCK180 to the membrane for Rac activation.

Arl4A induces actin cytoskeleton remodeling in an Arf6-independent manner

Previous studies demonstrated that activated Arl4A, C, and D could recruit ARNO GEFs to the membrane [209,210]. Arl4D was studied in more detail and was reported to induce actin stress fiber disassembly through an ARNO-Arf6 dependent pathway [209,210]. Independent work also reported that the ARNO-Arf6 pathway might facilitate membrane recruitment of ELMO/DOCK180 and promote Rac-dependent

Figure 4.3. ELMO1 colocalizes with Arl4A at membrane protrusions. In adherent HeLa cells, expression of Myc-ELMO1 alone displays a cytosolic distribution. Co-

expression of Arl4A^{WT} with Myc-ELMO1^{WT} promotes membrane ruffling and localization of ELMO1 to membrane protrusions. HeLa cells were stained for Arl4A (red) and ELMO1 (green) using anti-Arl4A and anti-Myc antibodies, respectively.

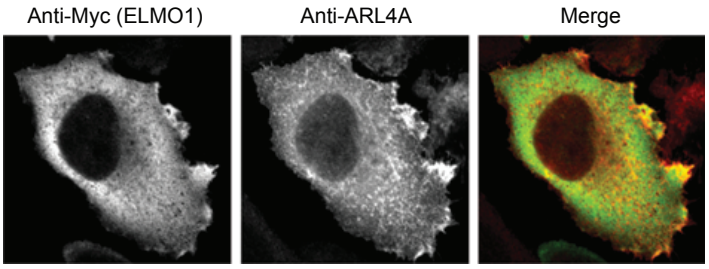

Figure 4.3

migration [180]. Similar to what was reported for expression of Arl4D^{Q80L} in HeLa cells, we found that Arl4A^{Q79L} promotes actin stress fiber disassembly (**Figure 4.4A, pg. 195**). Additionally, to determine whether Arl4A is stimulated downstream of integrin signaling, we plated transfected cells on fibronectin and found that cells expressing Arl4A^{WT} demonstrated cell spreading and membrane ruffling at a higher level compared to control cells (**Figure 4.4B, pg. 195**). Incidently, in marked contrast to what was observed with Arl4D, co-expression of Arf6^{T27N} did not block Arl4A-induced stress fiber disassembly (**Figure 4.4C, pg. 195**). Furthermore, compared to exogenous expression of Arl4A^{T34N}, Arl4A^{WT} expression in Arf6-depleted HeLa cells demonstrated actin stress fiber disassembly (**Supplementary Figure 4S1, pg. 209**). These results suggest that Arl4A may be signaling via an alternative pathway to regulate remodeling of the actin cytoskeleton.

We next investigated if Arl4A can regulate localization and activity of Rac in HeLa cells. We found that exogenous Arl4A^{Q79L} co-localizes with GFP-Rac1 in HeLa cells (**Figure 4.4D, pg. 195**). Moreover, we noted a more cytosolic distribution of GFP-Rac1 with a marked decrease in membrane protrusiveness in cells co-expressing Rac1 and the dominant-negative form of Arl4A (**Figure 4.4D, pg. 195**). In addition, downregulation of Arl4A protein levels with a specific Arl4A RNAi decreased the level of active Rac when compared with HeLa cells transfected with a non-targeting RNAi (**Supplementary Figure 4S2, pg. 211**). Cells treated with RNAi against Arf6 did not lead to decreased active Rac levels, suggesting that here, at least in this context, Rac activation is Arf6-independent (**Supplementary Figure 4S2, pg. 211**). Together, these results suggest that active Arl4A can impact the actin cytoskeleton, Rac localization and Rac GTP-loading in an Arf6-independent manner.

Figure 4.4. Arl4A induces cytoskeletal changes and membrane ruffling in an Arf6-independent manner. (**A**) Overexpression of Arl4A^{WT} and Arl4A^{Q79L} alters actin structure in HeLa cells, but Alr4A^{T34N} does not. Active Arl4A was overexpressed in HeLa cells and stained for Arl4A (red) and phalloidin (green) using anti-Arl4A and Fluor 488 phalloidin, respectively. The bar chart indicates quantification results for each condition. The area of each cell was delineated and the mean fluorescence intensity of Fluor 488 phalloidin was measured in pixels using Image J (NIH). About 50 cells were assessed in each experiment, and data are means $\pm$ s.e.m. of triplicate experiments. (**B**) Arl4A induces membrane ruffling when cells are subject to integrin stimulation. HeLa cells were transfected with empty vector or ARL4A^{WT}. Cells were plated on fibronectin for 50 min and fixed and stained with anti-ARL4A and Alexa Fluor 488 phalloidin. Cells expressing ARL4A show membrane ruffling, and sometimes, polarized morphology. Compared to mock cells, ARL4A expression also induces cell spreading. For quantification, the area of each cell was delineated and about 100 cells were estimated for each condition. Scale bar = 10 μm. (**C**) Co-expression of dominant-negative Arf6 (Arf6^{T27N}) with Arl4A^{WT} or Arl4A^{Q79L} does not hinder actin cytoskeletal reorganization. HeLa cells were co-transfected with Arf6^{T27N} and either Arl4A^{WT} or Arl4A^{Q79L}. (**D**) Constitutively active Rac-induced membrane ruffling is suppressed by co-expression of dominant-negative Arl4A. GFP-Rac1WT and V12 were expressed alone in HeLa cells, or GFP-Rac1^{V12} was co-expressed with wild type, constitutively active and inactive mutants of Arl4A. Cells were fixed and stained with anti-Arl4A.

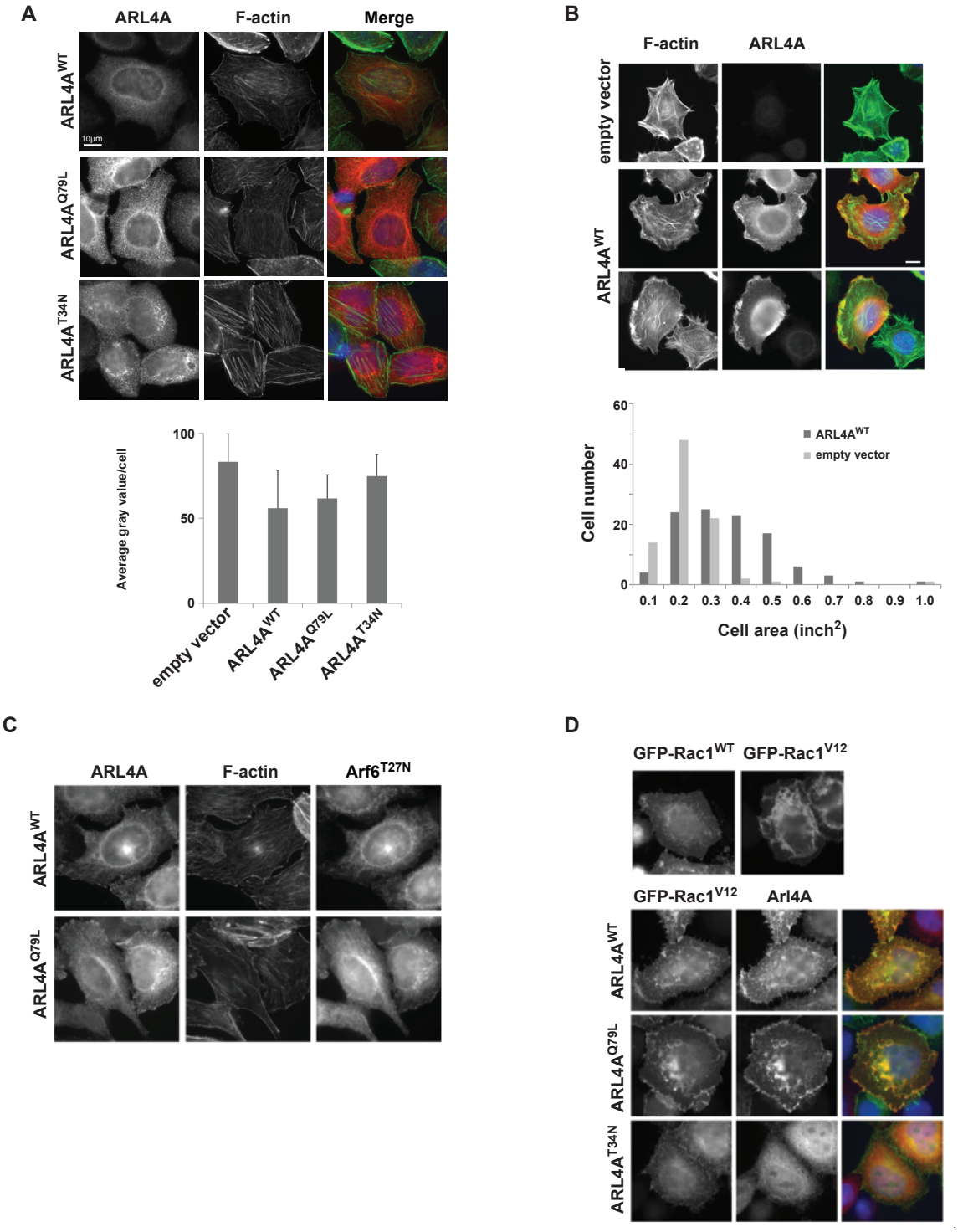
A
ARL4A
F-actin
Merge
ARL4A^WT
ARL4A^Q79L
ARL4A^T34N
10μm
Average gray value/cell
100
50
0
empty vector
ARL4A^WT
ARL4A^Q79L
ARL4A^T34N
B
F-actin
ARL4A
empty vector
ARL4A^WT
Cell number
60
40
20
0
ARL4A^WT
empty vector
0.1 0.2 0.3 0.4 0.5 0.6 0.7 0.8 0.9 1.0
Cell area (inch^2)
C
ARL4A
F-actin
Arf6^T27N
ARL4A^WT
ARL4A^Q79L
D
GFP-Rac1^WT
GFP-Rac1^V12
GFP-Rac1^V12
Arl4A
ARL4A^WT
ARL4A^Q79L
ARL4A^T34N

Figure 4.4

Arl4A-mediated actin cytoskeleton reorganization occurs through ELMO/DOCK180 and Rac

To investigate whether Arl4A modulates the actin cytoskeleton via the ELMO/DOCK180/Rac signaling pathway, we first tested if Arl4A/ELMO can enter into a trimolecular complex with the atypical Rac GEF, DOCK180. We found that Arl4A, alongside ELMO1, can be specifically co-precipitated with DOCK180 (**Figure 4.5A, pg. 199**). In order to test the role of Rac and ELMO1 in Arl4A-mediated cytoskeleton rearrangements, we developed an assay using HeLa cell-spreading on fibronectin (expressing either GFP alone or co-expressed with $Arl4A^{WT}$, $Arl4A^{Q79L}$, or $Arl4A^{T34N}$). While $Arl4A^{T34N}$ did not affect HeLa cell morphology, two major phenotypes were identified in $Arl4A^{WT}$ and $Arl4A^{Q79L}$ spreading cells. We found that 50-55% of the cells expressing the active GTPases (WT or Q79L) displayed: 1-formation of neurite-like extension or 2- membrane ruffles (**Figure 4.5B, pg. 199**). For quantification purposes, these two phenotypes were pooled and termed "protrusive" (**Figure 4.5B, pg. 199**). In contrast, the dominant negative Arl4A expressing cells looked identical to GFP expressing controls (**Figure 4.5B, pg. 199**). We next tested whether Arl4A is mediating cytoskeletal changes via ELMO and Rac. Co-expression of either a dominant negative Rac1 or ELMO1 lacking Arl4A binding activity ($ELMO1^{212-727}$ or $ELMO1^{L43A}$) with $Arl4A^{WT}$ prevented cytoskeletal re-organization in HeLa cells (**Figure 4.5C, pg. 199**). Together, these results suggest that the ELMO/DOCK180/Rac pathway mediates Arl4A-induced remodeling of the actin cytoskeleton.

Moreover, we used a stress fiber disassembly assay to examine the contribution of ELMO1 during Arl4A-induced cytoskeletal rearrangement. Exogenous expression of ELMO1 alone did not induce any cytoskeletal remodeling, while co-expression of ELMO1 and $Arl4A^{WT}$ led to a decrease in stress fiber formation (**Figure 4.6A, pg. 200**). Furthermore, ELMO1 mutants defective in Arl4A binding ($ELMO1^{315-727}$ and $ELMO1^{L43A}$) were unable to recapitulate results with wildtype conditions (**Figure 4.6B, pg. 200**). These results highlight the importance of Arl4A-binding via the ELMO RBD

for ELMO-induced re-structuring of the actin cytoskeleton, possibly via the DOCK180/Rac pathway.

Figure 4.5. Arl4A induces cellular protrusions through an ELMO/DOCK180/Rac signaling module. (**A**) ELMO is the common denominator for DOCK180/ELMO1/Arl4A trimeric complex formation. HEK293T cells transfected with the indicated plasmids were subject to a crosslinker, lysed and immunoprecipitated with H-70 (DOCK180). The co-precipitation of DOCK180, ELMO1 WT and mutants, and Arl4A was analyzed via immunoblotting with anti-H-70 (DOCK180), anti-Myc (ELMO) and anti-FLAG-HRP (Arl4A) antibodies, respectively. (**B**) Arl4A-induced membrane protrusions are dependent on ELMO1 and a Rac signaling pathway. Serum-starved HeLa cells transfected with the indicated plasmids were detached and plated on fibronectin–coated chambers for 2 h. Panels represent an overlay of GFP, rhodamine-phalloidin and DAPI stains. Cells were photographed at 100X magnification. Scale bar = 10 μm. (**C**) Quantification of the effect on cell morphology in response to overexpression of Arl4A and other proteins. Several independent fields of the experiments from (B) were photographed at a magnification of 40X, and cells were scored for two phenotypes: spread (clearly spread and flat cells) and spread with protrusions (subdivided into (i) protrusive and (ii) neurite-like elongated cells).

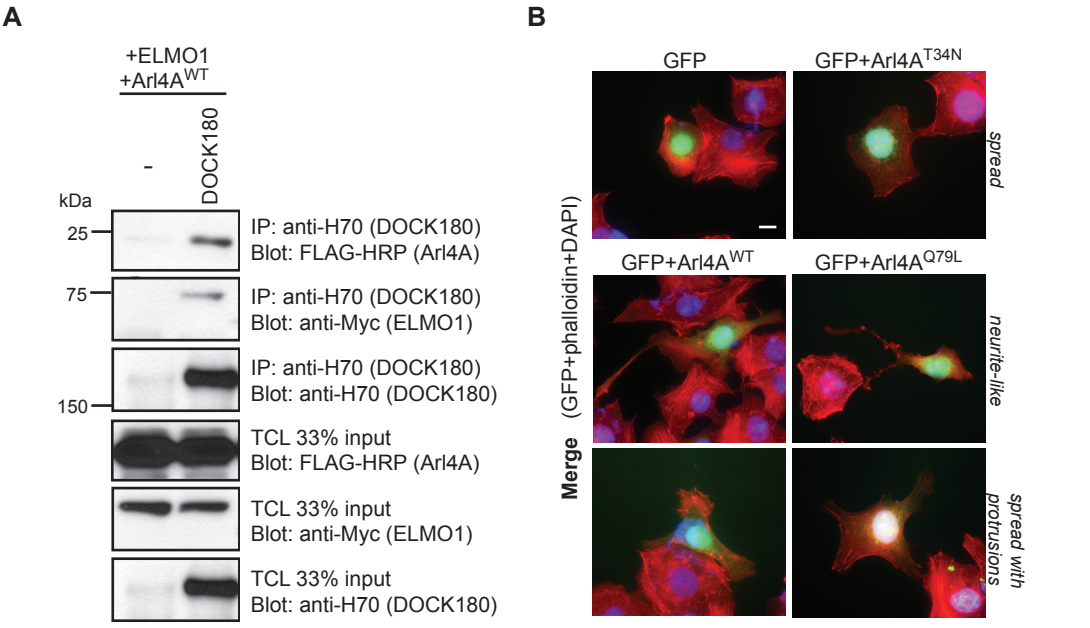

C

Transfection	Observed phenotypes
control **(n=40)**	Protrusive: 20% Spread: 80%
Arl4A^{WT} **(n=44)**	Protrusive: 44% Spread: 56%
Arl4A^{T34N} **(n=40)**	Protrusive: 15% Spread: 85%
Arl4A^{Q79L} **(n=52)**	Protrusive: 50% Spread: 50%

Transfection	Observed phenotypes
control **(n=33)**	Protrusive: 30% Spread: 70%
Arl4A^{WT} **(n=36)**	Protrusive: 53% Spread: 47%
Arl4A^{WT}+ELMO$^{212-727}$ **(n=43)**	Protrusive: 26% Spread: 74%
Arl4A^{WT}+Rac1^{T17N} **(n=31)**	Protrusive: 0% Spread: 100%

Transfection	Observed phenotypes
control **(n=31)**	Protrusive: 16% Spread: 84%
Arl4A^{Q79L}+ELMO1^{WT} **(n=60)**	Protrusive: 48% Spread: 52%
Arl4A^{Q79L} +ELMO1^{L43A} **(n=61)**	Protrusive: 18% Spread: 82%

Figure 4.5

Figure 4.6. Hindrance of the Arl4A/ELMO1 complex reduces stress fiber disassembly. (**A** and **B**) HeLa cells transfected with Arl4A^{WT} and Myc-ELMO1 or indicated mutants were fixed and stained with anti-Arl4A (red), anti-Myc antibody (ELMO) (blue), and fluo-phalloidin (green). Expression of full-length proteins and indicated mutants alone did not significantly affect actin organization. Co-expression of either Myc-ELMO1 full-length or ELMO1$^{1-315}$ and Arl4A^{WT} reduced F-actin intensity, indicating stress fiber disassembly. Arl4A-binding defective mutants (ELMO1$^{315-727}$ and ELMO1^{L43A}) did not induce substantial stress fiber disassembly.

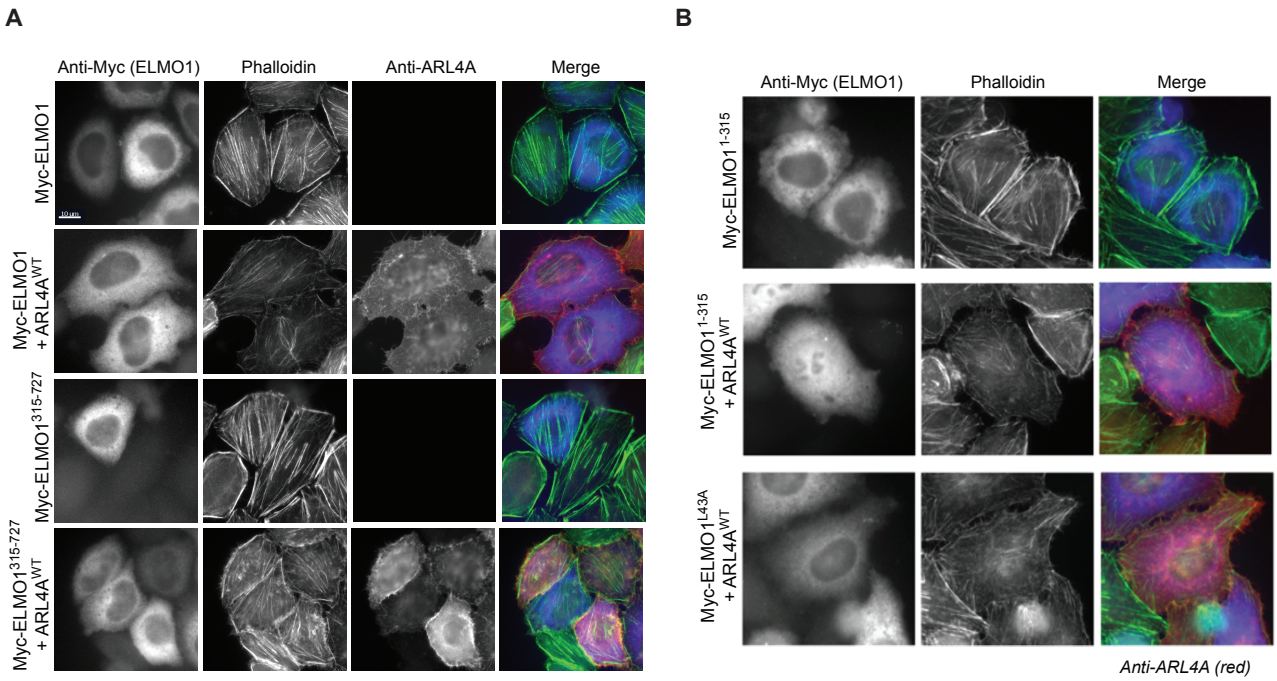
A
Anti-Myc (ELMO1)
Phalloidin
Anti-ARL4A
Merge
Myc-ELMO1
Myc-ELMO1 + ARL4A^WT
Myc-ELMO1^315-727
Myc-ELMO1^315-727 + ARL4A^WT
B
Anti-Myc (ELMO1)
Phalloidin
Merge
Myc-ELMO1^1-315
Myc-ELMO1^1-315 + ARL4A^WT
Myc-ELMO1^L43A + ARL4A^WT
Anti-ARL4A (red)

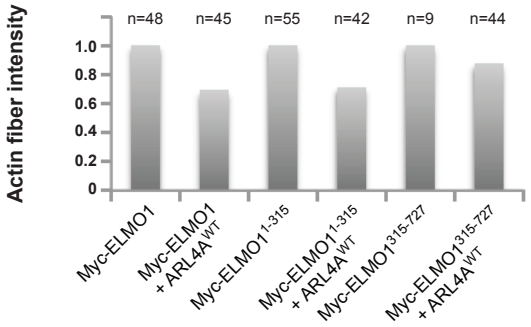
Actin fiber intensity
n=48
n=45
n=55
n=42
n=9
n=44
1.0
0.8
0.6
0.4
0.2
0
Myc-ELMO1
Myc-ELMO1 + ARL4A^WT
Myc-ELMO1^1-315
Myc-ELMO1^1-315 + ARL4A^WT
Myc-ELMO1^315-727
Myc-ELMO1^315-727 + ARL4A^WT

Figure 4.6

Discussion

The role of ELMO during DOCK180 Rac GEF activity and cellular restructuring is not completely understood. Our recent work demonstrated that ELMO, via intramolecular interactions between its newly identified EID and EAD regions, exists as an autoinhibited molecule at basal level, requiring RBD engagement for autoinhibition relief and subsequent localized DOCK180-mediated Rac signaling [400]. Here, we identify the RBD of ELMO as a polyvalent GTPase binding region capable of interacting with different Ras GTPase family members. While it was well-known that ELMO has the ability to bind RhoG-GTP through its extreme N-terminus, our recent work revealed that the minimal RhoG binding site was an evolutionarily conserved RBD [400]. The work from the present study identifies Arl4A, a member of the Arf subfamily of Ras GTPases, as a novel ELMO RBD binding partner, and the evolutionarily conserved feature of the GTPase/ELMO interaction is demonstrated by critical point mutation of a conserved residue in the ELMO RBD. This discovery opens up a gateway of possibilities where various Ras superfamily GTPases may converge to regulate ELMO membrane localization and/or relief of ELMO autoinhibition.

Membrane targeting of the DOCK180/ELMO complex

Targeting of the ELMO/DOCK180 complex to the membrane may be fine-tuned by various inputs. While initial studies pointed to a role for the PH domain of ELMO as being instrumental for the targeting of the ELMO/DOCK180 complex to the plasma membrane, we uncovered that the ELMO PH domain displays no such activity [388]. Membrane targeting of this complex has also been attributed to the lipid-binding properties of the DHR-1 of DOCK180 [274]. As well, the localization of DOCK2 to the neutrophil pseudopod requires sequential binding of two signaling lipids: first a global recruitment to the membrane via the DHR-1 domain engaging phosphatidylinositol-3,4,5-phosphates, followed by polybasic region binding to phosphatidic acid [276].

Further studies are required to expose whether localization of DOCK180 can be regulated in a similar manner.

We and others have highlighted the functional importance of the N-terminal of ELMO1 for ELMO/DOCK180 subcellular localization [152,293,400]. Now, with the discovery of active Arl4A as a novel binding partner of the ELMO RBD, our study demonstrates for the first time a RBD that can bind both a Rho and Arf family GTPase. The Arl4 proteins (Arl4A, Arl4C, and Arl4D) have recently emerged as important cytoskeletal regulators. In terms of structure, these three proteins are similar to other Arf family members, yet are unique by virtue of a short basic extension at the C-terminus [157]. Interestingly, the N-terminal amphipathic helices of the Arl4 proteins are shorter and less hydrophobic than those of other Arf family members. Deletion of this basic extension in cells results in displacement of Arl4A from the plasma membrane, advocating that the C-terminal basic extension may function as a support system for the N-terminal amphipathic helices and aid in the localization of Arl4 proteins to membranes [405].

Our findings demonstrate that ELMO1 alone is cytoplasmic, and co-expression specifically with active Arl4A leads to its membrane recruitment to sites of membrane ruffling, while expression with either Arl4C or Arl4D did not induce a protrusive phenotype (data not shown). We therefore propose ELMO proteins as *bona fide* effectors of Arl4A that can target the ELMO/DOCK180 module to the membrane for localized Rac activation and signaling.

Structural features of the ELMO RBD: Insights from the FHOD1 RBD

The ELMO RBD is structurally similar to the RBD of the Dia-family formin, FHOD1. FHOD1 is an outlier of this family in terms of its GBD structure and reveals an ubiquitin superfold very similar to that of the Ras-binding domains (RBDs) of c-Raf1 and PI3 kinase, and has the characteristic of binding the Rac GTPase and not Rho nor Cdc42 GTPases [391]. As demonstrated for other formin members, the GBD is viewed as a

key GTPase docking site that, when engaged, releases and activates the protein. The unusual nature of the FHOD1 RBD is illustrated by deletion experiments that demonstrate removal of the RBD does not activate the formin as in Dia [391]. Rather, the interaction with Rac seems to be a recruitment signal and is insufficient in activating the protein. Notably, phosphorylation events by ROCK at three specific sites within the DAD unlock the compressed autoinhibited state and induce F-actin stress fiber assembly [242,406]. This data points to potential alternative roles of the formin RBD that have yet to be defined. As such, we speculate that the ELMO RBD may function in a manner reminiscent of the RBD of FHOD1. Specifically, we hypothesize that the spatio-temporal positioning of various GTPases able to interact with the ELMO RBD will conduct selective regulation of autoinhibited ELMO and/or targeting of ELMO/DOCK180-induced Rac signaling.

Arl4A induces cytoskeletal remodeling through ELMO/DOCK180 and Rac

Our findings support a role for Arl4A in actin cytoskeleton rearrangement through a pathway that stimulates DOCK180/ELMO-induced Rac signaling. Studies have already demonstrated that Arl4A and its close relatives Arl4C and Arl4D promote actin restructuring through recruitment of ARNO, an Arf6 GEF, to the plasma membrane [209,210]. Interestingly, Arf6 is positioned upstream of Rac activation in various biological processes. One model advocates that Arf6 activation will recruit the DOCK180/ELMO complex to the leading edge of a cell [180-182]. Here, however, our research demonstrates that Arl4A-induced cytoskeletal remodeling occurs via an Arf6-independent pathway. Intriguingly, this may signify that Arl4A can act as a central signaling nodule for two divergent GTPase pathways.

In conclusion, we identify a novel RBD in ELMO displaying, for the first time, selectivity for both Arf and Rho GTPases. In contrast to the Dia formins, effector-binding to the ELMO RBD is not proven to be a release mechanism for the autoinhibited ELMO molecule. Rather, similar to the FHOD1 protein, this signal seems to target ELMO to distinct areas of the plasma membrane. It will be interesting to

investigate if additional members of the Ras superfamily bind the ELMO RBD and whether they also act as membrane localization signals and/or relieve ELMO autoinhibition. It is possible that the ELMO RBD is strictly required for subcellular localization while binding of additional partners at distinct sites (ie. EID or EAD) act to release the closed conformation of ELMO. The unleashing of ELMO can result in the exposure of otherwise masked regions of ELMO, such as the ELM domain. The work from Bowzard and colleagues shows that the ELMOD family of proteins demonstrates GAP activity on selective Arf family members, and they attribute this enzymatic function to the ELM domain [169]. To date, the ELM region of ELMO has been poorly investigated and has no ascribed function. Clearly, further studies are required to identify components that will open up the ELMO molecule and illuminate how its hidden regions contribute towards actin cytoskeleton remodeling.

MATERIAL AND METHODS

Antibodies, cell culture and transfections. The following antibodies were obtained commercially: anti-DOCK180 (C-19, H-4, and H-70) and anti-Myc (9E10) were from Santa Cruz Biotechnologies, anti-Rac was from Millipore, and anti-FLAG M2 and anti-FLAG-M2-HRP were from Sigma. The Arl4A antibody was described previously [210]. HEK293T and HeLa cells were cultured in DMEM supplemented with 10% fetal bovine serum, penicillin and streptomycin (Gibco-BRL) and transfected by calcium phosphate or Lipofectamine 2000 (Invitrogen) using standard procedures. Biochemical and cell biological studies were performed 24-48 hours after transfection.

Plasmid Constructs. pCNX2 Flag-DOCK180 was a gift from M. Matsuda. pcDNA3.1 Myc-ELMO1 and was previously described [363]. Plasmids coding for Myc-ELMO1 proteins (residues 1-113, 1-315, 315-727, 212-727) were generated by PCR using Myc-ELMO1 as a template and cloned into the BamHI/XhoI sites of pcDNA3Myc. The yeast constructs for ELMO1 (WT and residues 1-113, 1-212, 1-315, 1-495, 315-727, 212-727, 113-727, Δ114-524, Δ213-524, and Δ310-492) were generated via PCR using the Myc-ELMO1 as a template and cloned into the BamHI/XhoI sites of pEG202 (LexA tagged vector). Myc-ELMO1$^{1\text{-}212\ (L43A)}$ has been described previously [400]. FLAG-Arl4A (WT, T34N, and Q79L) were generated via PCR and cloned into the EcoRI/XhoI sites of the pcDNA-FLAG vector. Non-tagged ARL4A (WT, T34N, and Q79L) constructs have been described previously [210].

Immunoprecipitation and GST-fusion protein pulldowns. Immunoprecipitation and pulldown experiment protocols have been described previously [388]. Briefly, cells were lysed for 10 min in a buffer consisting of 50mM Tris-HCl pH 7.5, 150mM NaCl, 1% NP-40 and 1X Complete protease inhibitor (Roche). For immunoprecipitation, clarified cell lysates were incubated with the appropriate antibody and immune complexes were allowed to form for 1 h at 4˚C. Protein A-sepharose was added for 30 min to isolate the immune complex. For cross-linking prior to immunoprecipitation, cells were treated with DSP (2uM) (Pierce) for 30 min according to the manufacturer's instructions. For GST-fusion protein pulldowns, the GST-fusion proteins were expressed in bacteria and purified on Glutathione-Sepharose

4B according to manufacturer's instruction (Amersham). Equal amounts of the various GST-fusion proteins bound to Glutathione Sepharose 4B were next incubated with cell extracts (500 μg of protein per condition). In both types of assays, the beads were washed three times with lysis buffer and the bound proteins were analyzed by SDS-PAGE and immunoblotting.

Yeast Two-Hybrid Interaction Assay. The genotype of the yeast reporter strain EGY48 is MATα ura3 trp1 his3 6lexAop-LEU2, auxotrophic for tryptophan (Trp), uracil (Ura), histidine (His), with LEU2 as a reporter gene. Yeast were grown in rich medium (1% yeast, 2% Bacto-peptone, 2% glucose) or in synthetic minimal medium with appropriate supplements. Yeasts were transformed by the lithium acetate method using standard protocol, with LexA-tagged ELMO1 constructs (HIS3) screening B42-tagged Arl4 constructs (TRP1) for interaction. Double transformants were plated on non-selective (-Histidine, -Tryptophan) and selective (-Histidine, -Tryptophan, -Leucine) medium containing galactose. Plates were incubated at 30°C for 3-5 days.

Cell morphology assay. For the cell-spreading assay on fibronectin, HeLa cells transfected with the indicated plasmids were subject to cell morphology as previously described [364]. Briefly, cells were transfected with the indicated plasmids and serum starved (0.5% FBS) overnight. Cells were gently detached (0.01% trypsin and 5 mM EDTA in Hanks balanced solution), washed in DMEM supplemented with 0.5% BSA and 40 000 cells were then allowed to spread for the indicated time (50 min or 2h) before fixing with 4% paraformaldehyde. Cells were permeabilized with 0.2% Triton X-100 in PBS and blocked in PBS-1% BSA prior to staining with DAPI and phalloidin. The remainder of the cells was lysed to verify the expression levels of the exogenous proteins by western blotting. For integrin independent assays, experiments were performed as previously described [210].

Stress fiber disassembly assay. Stress fiber disassembly assays were performed as previously described [210].

PAK pulldowns. PAK-PBD pulldown assays were performed as previously described [388].

Supplementary Figure 4S1. Knockdown of Arf6 does not hinder Arl4A^{WT}-induced actin cytoskeleton rearrangement. HeLa cells expressing constitutively active Arl4A (Arl4A^{Q79L}) or dominant-negative Arl4A (Arl4A^{T34N}) were transfected with control scramble RNAi or Arf6 RNAi. Cells were then subject to stress fiber disassembly analysis. The bar chart indicates quantification results for each condition. The area of each cell was delineated and the mean fluorescence intensity of Fluor 488 phalloidin was measured in pixels using Image J (NIH). About 50 cells were assessed in each experiment, and data are means $\pm$ s.e.m. of triplicate experiments.

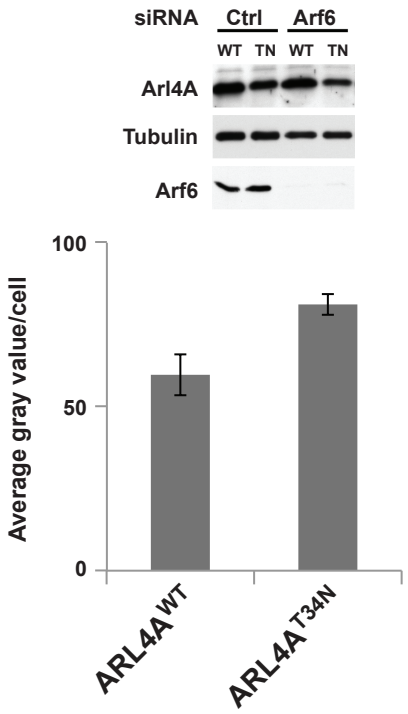

Supplementary Figure 4S1

Supplementary Figure 4S2. Knockdown of Arl4A decreases Rac activation levels in HeLa cells. (A) ARL4A expression was depleted by pSuper RNAi system. HeLa cells were transfected with pSUPER.neo+gfp, or pSUPER.neo+gfp containing sequences specific against ARL4A (shARL4A#1 and #2) or ARF6 (shARF6). After 72 h of transfection, the cells were harvested and the RNA was extracted for detection by RT-PCR. (B) HeLa cells were treated with shArl4A#1, #2,#1+2 (2X, two-fold DNA content) and shArf6. After 72 h, cell lysates were collected and the Rac-GTP level was detected by PAK-PBD pulldown assays. Rac1 protein levels were detected by immunoblot using anti-Rac1 antibody. The protein level of EGFP indicated the transfection efficiency of each group.

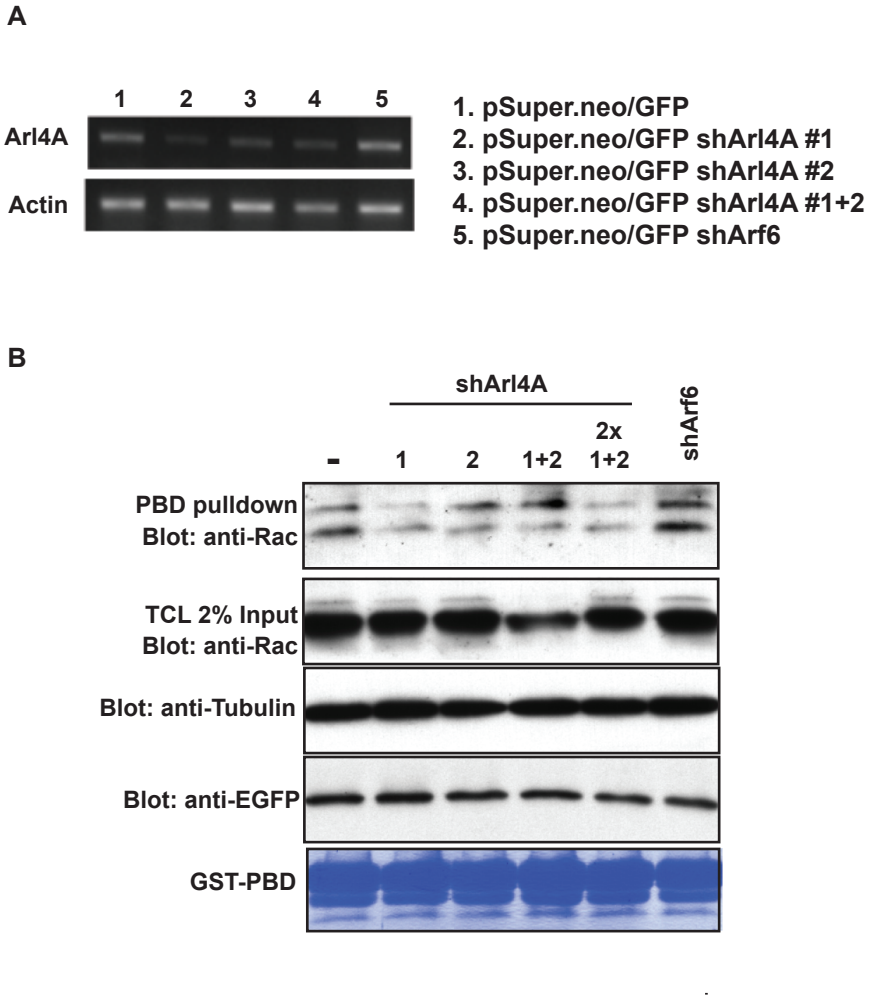

Supplementary Figure 4S2

DISCUSSION

Directional cell migration is a fundamental attribute of various cell types during various biological processes. The control of a key player, the Rac GTPase, via the DOCK180/ELMO module has quickly become a pivotal factor that guides cell motility. To reiterate, the central hypothesis of this thesis is that DOCK180 functions as a Rac GEF, with ELMO binding to DOCK180 being required for integration of proper Rac signaling rather than Rac activation *per se*. We postulated that ELMO may act as a subcellular targeting signal for spatio-temporal restriction of DOCK180-mediated Rac signaling and/or act as a scaffold for Rac effectors to enforce directional cell migration.

The ELMO/DOCK180 interface: Novel discovery of an atypical PH domain in ELMO and an evolutionarily conserved helical structure in DOCK180

Previous reports are marked with inconsistencies regarding the molecular mechanism of DOCK180/ELMO interaction [252,294,295]. To properly investigate the importance of the DOCK180/ELMO connection during biological processes, we needed to clearly dissect the molecular mechanism of interaction between the two proteins. In Aim #1 (Chapter 2) of my thesis, through biochemical and structural work, we report a previously uncharacterized atypical PH domain of ELMO1 [388].

The ELMO1 PH domain was originally annotated as residues 555-676 [253]. When compared to other PH domains on ProSite (protein families and domains database), ELMO1$^{555\text{-}676}$ was cataloged as a false-positive. Our investigation into secondary structure prediction of this region and its immediate N- and C-termini uncovered

potential flanking helices at these extremities [388]. Our collaborators attempted to crystallize this entire region (ELMO1$^{532-707}$), but were only able to produce diffracting crystals with ELMO1$^{532-675}$. Nevertheless, what we found was distinctively unique for the ELMO PH. First, similar to other well-known PH structures, the core of the ELMO1 PH forms an anti-parallel β-sheet sandwich which is capped off at its C-terminus by an α-helix. Uniquely, the flanking N-terminal (ELMO1$^{536-557}$) portion forms an α–helix, which has not been characterized in any other PH domain to date. The only other documented PH domain to display such a structure is that of 3-phosphoinositide-dependent protein kinase 1 (PDK1), which also does not fall into the category of canonical PH domains due to its distinctive N-terminal 'bud' [380]. However, although both ELMO and PDK1 display N-terminal α–helical extensions, these structures differ strongly. In the case of PDK1, the α–helical extension continues from its core β-sheet sandwich (β_1-β_4) followed by two additional β-sheets (β_5-β_6) ('bud'). Through various hydrophobic interactions, the bud collapses against the β sheets (β_1- β_6) and creates a hydrophobic core [380]. In ELMO1, an N-terminal α-helix leads straight from the β_1-sheet and projects stably outward from the rest of the structure due to hydrophobic contacts with the C-terminal helix of the ELMO1 PH domain. To date, no function has been ascribed to this region of PDK1.

Our crystallization data revealed that the unique N-terminal extension of the ELMO1 PH domain is an amphipathic structure, with one side having hydrophilic properties, and the other lined with invariant hydrophobic residues that serve as the

primary interface for DOCK180 binding. Duly noted is the fact that ELMO1 PH crystals form tight dimers due to packing of N-terminal α-helices against each other. Although this is probably an artifact of the crystallization process (in our hands, no such dimers or oligomers are found in solution or *in cellulo*), our data proposed that the N-terminal extension may play host to other protein-protein (helix/helix) interactions. We subsequently analyzed the primary sequence of DOCK proteins' N-terminal region and exposed a putative evolutionarily conserved helical region (N-terminal α-helical region of DOCK180, herein referred to as DOCK180$^{80\text{-}153}$). Invariant hydrophobic patches in this DOCK180 helical region were responsible for ELMO1 interaction [388], reinforcing the notion that the ELMO N-terminal α-helix extension serves as a protein-protein interface.

Previous studies have proposed that the ELMO C-terminus is required to bind to the DOCK180 N-terminus, with a classical SH3/PxxP interaction as the basis of complex formation [252,294,295]. Regions adjacent to these domains have also been suggested to contribute to the binding, however, no clear interaction sites had been established. We found that the DOCK180 SH3/ELMO1 PxxP interaction biochemically offers a stabilizing effect to the primary contact site between DOCK180$^{69\text{-}187}$/ELMO1 PH domain [388]. Functionally, this secondary binding interface is essential for cell elongation and migration *in cellulo* [388], supporting previous findings citing its importance in cells and *in vivo* in *C. elegans* during cell migration and phagocytosis [252,253,295].

Lu and colleagues proposed that the ELMO1 PH domain binds DOCK180 *in trans* through Rac, forming a trimeric complex that is essential for uncovering DOCK180 Rac GEF activity [294] (discussed further below). In contrast, our findings reveal a direct DOCK180$^{69\text{-}187}$/ELMO1 PH domain interaction rather than an indirect coupling [388]. It would be of interest to co-crystallize the ELMO1 PH/PxxP and DOCK180 SH3/helical region as analyses of this crystal would validate our published biological interaction sites and enlighten the structural aspect of how the SH3/PxxP contact sites contribute towards the primary DOCK180 helical region/ELMO PH interface. Furthermore, with these crystals, we could further corroborate whether our mutational analyses warrants a true complex abolishment between DOCK180 and ELMO or if these mutations simply lead to significant misfolding of proteins.

While our work cleanly breaks down the molecular interfaces and key residues arbitrating the ELMO1/DOCK180 interaction, many interesting questions remain. To date, studies advocate a scaffolding role for ELMO. It is quite possible ELMO acts as a bridge for DOCK180 to Rac effectors (enforced proximity) [407]. Also, DOCK180 binding to ELMO may endorse a conformational change in either or both proteins that allows for uncovering additional modular domains important for Rac signaling. Undoubtedly, from a structural perspective, a crystallization of ELMO in complex with DOCK180 would be of interest to answer some of these questions.

The atypical PH domain in ELMO is not a lipid-binding module

Contrary to popular belief, only a minority of PH domains display lipid-binding characteristics [408-410]. Structurally, this phosphoinositide binding is attributed mostly to the variable loop regions of the PH domain. In these cases, the variable loops (VL1, VL2 and VL3) create a positively charged surface that binds negatively charged phosphoinositides. It is these loops that generate the electrostatic polarization shown and required by lipid-binding PH domains [79]. While many reports suggest that the ELMO PH domain may also display this characteristic, no direct evidence supports this claim. We clearly demonstrated that the ELMO1 PH domain falls into the major category of PH domains, with no lipid affinity noted *in vitro* [388]. Concluded from our crystallography data, this is most likely due to marked differences between the ELMO1 PH domain variable loops and the same regions in PH domains known to bind strongly and specifically to phosphoinositides. In ELMO1, VL2 is longer than in conventional lipid binding PH domains, and demonstrates an overall negative charge, with the result of no electrostatic polarization in the variable loops region [388]. Thus, the ELMO1 PH domain variable loops do not create the required positively-charged pocket to accommodate phospholipid binding.

Rather than lipid-binding PH domains, we found structural similarities between the ELMO1 PH domain and the F3 subdomain of FERM. This latter domain is well documented as a protein-protein interaction interface [383], which leads to the speculation that the core of the ELMO PH domain may also function in a similar manner. It would be interesting to see whether there are yet undiscovered partners

that bind to this region and hinder or support the DOCK180 interaction in such close proximity. (As we will discuss further below, we are highly interested in discovering if any novel interactions occur at the ELMO C-terminus that can relieve ELMO autoinhibition).

ELMO is not required for DOCK180-mediated Rac activation, but rather for Rac signaling ensuing from this complex

We also attempted to resolve the mechanistics behind DOCK180-mediated Rac activation. Specifically, we wanted to clarify the much debated bipartite GEF model and the *in trans* requirement of ELMO for uncovering DOCK180 Rac GEF activity [294]. Our results conclude that DOCK180 alone is necessary and sufficient for Rac activation [388], supporting previously published reports where the isolated catalytic unit of DOCK180 (and other DOCK proteins), the DHR-2, demonstrates Rac GEF activity *in vitro* and shows comparable Rac activation to full-length DOCK180 in cells [265]. A possible set-back to our *in cellulo* Rac activation assays may be the contribution of endogenous proteins towards DOCK180 Rac GEF activity. Therefore, we tried an *in vitro* GEF assay using the fluorescent *mant* molecule linked to GDP. When *mant*-GDP is bound to Rac, the GTPase will emit fluorescence; when *mant*-GDP is released from Rac, it becomes quenched in the solution resulting in low fluorescence. Theoretically, in the presence of DOCK180 full-length, Rac should become GTP-loaded and we expected to see a concomitant decrease in fluorescence. We had opted for a baculovirus system so as to produce a high concentration of tag-purified full-length DOCK180. Unfortunately, we

were not able to produce sufficient functional purified DOCK180 protein to perform this assay. Thus, an *in vitro* GEF assay with purified DOCK180 (wild-type and the newly uncovered ELMO-binding defective mutants) would be desirable to concretely prove the independence of DOCK proteins for Rac activation.

While the ELMO component is not essential for Rac activation, we found that it is vital for Rac signaling ensuing from the DOCK180/ELMO1 complex during cell spreading and migration. How ELMO is factoring into DOCK180-mediated Rac signaling became the focus of Aim #2 (Chapter 3) of my project. The literature on ELMO regulation of DOCK proteins points towards a role for ELMO in subcellular targeting of the complex. Specifically, numerous ELMO binding partners of the N-terminal region, such as active RhoG, the bacterial protein IpgB1, and the phagocytosis receptor BAI1 have all been implicated in coaxing and/or tethering ELMO and DOCK180 to the plasma membrane [152,250,293,402]. Therefore, the N-terminal portion of ELMO proteins has been fitted as a membrane localizing signal, while the C-terminus bridges the DOCK proteins to Rac signaling pathways.

Our interests lie in 'homing' signals downstream of integrins that will direct the ELMO/DOCK180 module to discrete areas of a migrating cell to promote directional cell movement. While active RhoG has been endorsed as one of these key integrin-dependent 'homing' signals, the group of Dr. Schwartz plainly negate these claims by demonstrating that RhoG is not activated via integrin stimulation nor is its expression required to promote cell migration [153]. Rather, their results show that Rac activation

via integrin stimulation is important for this process, and DOCK180 is an important factor for integrin-mediated Rac activation and cell spreading [153]. Our study and others have shown ELMO is critical for integrin-mediated DOCK180/Rac signaling, however, the exact role of ELMO here is still poorly understood. Clearly, greater attention is required in this field. Results from Aim #2 (Chapter 3) and #3 (Chapter 4) of my thesis allow us to better understand the function(s) of ELMO and are discussed below.

ELMO is an autoinhibited molecule via EID/EAD intramolecular interactions: Discovery of how three novel modules in ELMO regulate its activity

Aim #2 (Chapter 3) of my thesis led to the discovery of novel domains in ELMO and insights into the function of these proteins during cell migration. Thus far, ELMO was endowed with only a scaffolding role in Rac signaling. Our query into how ELMO plays into DOCK180-mediated Rac signaling led us to unearth domains in ELMO that are defined in the DRFs. In these formins, these modules collaborate for autoinhibition of the formins' actin nucleation activity and specific release of this catalytic function in a space and time-dependent manner. We revealed an autoinhibitory node between the EID and EAD, homologous to the DRFs' DID/DAD interaction [400]. Release of the formin DID/DAD connection is proposed to come in the form of GTPase binding to the formin GBD, although in some cases this interaction only leads to partial release of autoinhibition (ie. RhoA-binding to the Dia1) [224,226] or not at all (ie. Rac1 binding to FHOD1 [391]. See below for further discussion).

Although primary sequence analysis showed low sequence similarity, a structural superimposition model found that the ELMO GBD structurally resembles the GBD of the formin FHOD1. While all known DRFs contain a GBD, these domains can differ in terms of structure and effector binding. In comparison to the Dia1 GBD binding to Rho, the GBD of FHOD1 has only been shown to bind selectively to Rac, and is classed as a RBD due to its structural similarity to the RBD of c-Raf1[391]. Structurally, the FHOD1 RBD is distinguished from Dia proteins by virtue of a ubiquitin-like fold [391]; rather than the fold, it is usually the amino acid sequence of the GBD that decides which GTPase(s) to bind [411]. We found a similar superfold at the extreme N-terminus of mammalian ELMO and its orthologs in *Drosophila* and *C. elegans* [400], showing its evolutionarily conserved nature in these proteins.

While we demonstrate 'opening' of ELMO is integral for cell elongation and migration, and that RhoG binds the RBD and localizes ELMO to the membrane, it remains to be determined what signals lead to the unhinging of the closed ELMO conformation. It is quite possible that a repertoire of unidentified GTPases are waiting to be unmasked as novel ELMO RBD partners. Multiple effector binding is a feature of many GBDs. As yet, no signature has been revealed that will allow us to identify which GTPase(s) will bind a given GBD. Therefore, a screen of all known Ras family GTPases against the ELMO RBD may uncover vital partners involved in opening the intramolecular ELMO complex. Currently, we are examining the entire Ras superfamily of GTPases against the ELMO1 RBD and ELMO1 full-length proteins via yeast two-

hybrid experiments to identify potential candidates. Studies with isolated RBD domains can produce misleading data since additional domains in the effector protein are sometimes required for RBD engagement via the GTPase. This point is exemplified by the RBD of Tiam1 which requires its DH/PH domain to bind Rap [412]. In this way, other domains of ELMO may be required by binding partners in order to engage the RBD.

As mentioned, the ELMO RBD resembles the FHOD1 RBD; in this formin, RBD engagement does not structurally reform the DID/DAD interaction, and thus, does not result in the release of its catalytic function [242,391]. This is also partly true for the formin Dia, where only a partial release of autoinhibition is seen with GTPase binding. It is suggested that additional factors are required to fully activate the formin. Therefore, it is possible that in ELMO, the RBD serves only to localize the protein to discrete areas of the cell and binding partners in the vicinity of the EID or EAD serve to release the autoinihibited molecule. An example of this form of regulation is portrayed by the formin DAAM1 which binds Dvl at its C-terminus [237]. In this regard, we found exogenous expression of DOCK180 with ELMO2 results in a partial opening of the ELMO2 molecule (as visualized by a BRET^2 biosensor) [400]. We have found that endogenous ELMO and DOCK180 are always in a complex, both in non-stimulated and integrin-stimulated cells (data not shown). Therefore, we suggest that, endogenously in these complexes, ELMO is already 'primed' by DOCK180 for full autoinhibition relief. Additionally, it is possible that yet unidentified binders of the C-terminal region of

ELMO, perhaps via the ELMO PH domain, will serve as a release switch. Moreover, it would be interesting to test already identified partners whose binding sites overlap with the ELMO RBD and EID regions (ie: IpgB1, BAI1, and ERM proteins [293,402,403]) for promotion of conformational changes in ELMO that induce or contribute towards ELMO autoinhibition relief. Finally, ELMO has been shown to be phosphorylated downstream of HCK signaling [306]. It would be interesting to see whether ELMO phosphorylation could also lead to autoinhibition relief. The identification of novel ELMO partners, as well as, investigation into its post-translational modification(s) will increase our understanding of ELMO regulation.

Autoinhibitory regulation of ELMO: insights into the function of ELMO proteins

ELMO proteins are conserved throughout evolution, with orthologs ranging from fungi to humans [413]. The human network consists of 6 members divided into two groups based on primary sequence similarity and biological function(s). The one common feature between members is a region termed the ELMO domain (herein referred to as the ELM domain). While a subset of these proteins display DOCK180-binding and a part in Rac signaling pathways (ELMO1-3), the other half demonstrates GAP activity towards Arf GTPases, specifically Arl2 (ELMOD1-3). Although not clearly demonstrated, this latter family's Arf GAP activity is attributed to the ELM domain [169]. This domain in the ELMO1-3 members shows no activity on Arf GTPases and has yet to demonstrate any GAP activity at all.

Intriguingly, while mammalian, *Drosophila* and *C. elegans* ELMO orthologs have always been correlated with promoting migratory events, in *Dictyostelium discoideum*, the ELMO-like protein ElmoA is associated with a negative regulatory role during phagocytosis and cell migration [414]. In terms of phylogeny, ElmoA is closer to the ELMOD orthologs than to mammalian, fly and worm ELMOs [413]. The reason for this deviant physiological output may reside in the fact that ElmoA contains a yet undiscovered GAP activity that shuts off important GTPase(s) that stimulate cell polarization. In this way, autoinhibitory regulation of ELMO may be a means to mask regions host to untapped GAP activity (ie: ELM domain). It is also possible that these masked areas have a completely novel role, such as, binding of Rac effectors or other proteins important for cytoskeletal transformation. Probing for specific ELM domain binding partners in cells by mass spectrometry would answer some of the questions we have on the functions of ELMO.

We are particularly interested in the ELM region of ELMO because its primary sequence is highly conserved from worms to humans, and points to evolutionarily conserved functions. The fact that its binding surface is very likely masked at dormant states by autoregulation makes it even more intriguing. Clearly, the next big step will be to investigate the ELM domain with closer scrutiny; we postulate that discovering the function(s) of the ELMO ELM domain will be essential for understanding how the ELMO/DOCK180 complex regulates directed cell motility.

Identification of a polyvalent Ras-Binding Domain (RBD) in ELMO proteins

Almost since its discovery, ELMO proteins have been associated with a scaffolding role in DOCK180-mediated Rac signaling. The early discovery of RhoG binding to the N-terminus of ELMO found it acts as a membrane-localizing signal of the ELMO/DOCK180 module [152,250]. Characterization of the RhoG-binding site is poor. One study claimed this region of ELMO to contain conserved armadillo repeats (ARRs) [255]. However, our analyses failed to identify any such region in the RhoG-binding site ($ELMO1^{1-79}$) (data not shown).

In Aim #3 (Chapter 4) of my thesis, our attempt to identify novel *bona fide* partners of ELMO with the potential to act as membrane localization signals identified Arl4A, an Arf family GTPase, as a novel interactor of the ELMO N-terminus. The fact that the Arl4A binding site coincided with that of RhoG led to the discovery of a polyvalent RBD in ELMO (Patel et al, *in preparation*). ELMO1 RBD binding of both RhoG (Rho family) and Arl4A (Arf family) demonstrates for the first time, as far as we know, a RBD with cross-selectivity for the Rho and Arf family GTPases.

Complexing the ELMO RBD: a membrane localization signal?

RhoG binding to the N-terminus of ELMO was the first membrane targeting signal identified for ELMO [152]. Since then, the bacterial release of IpgB1 into a host mammalian cell has been shown to act as a cytosolic signal recruiting the ELMO/DOCK180 complex to the plasma membrane via interaction with the RhoG-binding interface on ELMO [402]. As well, mammalian BAI1 has demonstrated ELMO N-

terminal-binding and concomitant localization of ELMO to the periphery [293]. Therefore, the ELMO N-terminus is associated with a variety of membrane localization signals. With our recent discovery of Arl4A as a novel ELMO partner, we identify that the ELMO RBD, via active GTPase binding, can act as a shuttling system for ELMO to the plasma membrane.

Our discovery of a polyvalent RBD in ELMO reveals a probable membrane localization signal for this protein. In Aim #2 (Chapter 3) of my thesis, a conserved residue in the ELMO RBD (Leucine 43) was found to be critical for GTPase binding and integrin-dependent membrane targeting [400]. This key residue was also found to be important for Arl4A binding to the ELMO1 RBD. It would be interesting to see whether the ability of the aforementioned ELMO N-terminal partners to localize ELMO is in any way dependent on the RBD and the conserved L43 residue.

RBDs of many proteins have been branded with membrane-targeting properties. Examples include membrane targeting of phospholipase C (PLC)ε and PI3K through Ras [415,416]. In the case of PI3K, it is still debated whether the sole function of this interaction is to direct PI3K to the periphery or if it is an activation signal for PI3K lipid-kinase activity [416]. As in the case of PI3K RBD/Ras interaction, the ELMO RBD/GTPase interaction may serve not only as a membrane targeting signal, but as an autoinihibition relief cue. In support of this, our data from cell fractionation assays demonstrate that RhoG competes with the EAD for the RBD-EID module to coerce it to the membrane [400]. However, our results also lead to the important conclusion that

RhoG does not fully activate ELMO, since its co-expression does not induce 'active' ELMO cellular phenotypes (ie. cell elongation). Clearly, other factors are required here to unleash the ELMO protein. It will be interesting to see whether other GTPases can fully activate the ELMO proteins via binding the RBD.

Arl4A is an effector of the ELMO RBD that induces cytoskeletal modulation

The identification of Arl4A as an ELMO effector revealed three main concepts. As discussed, Arl4A binding to ELMO disclosed (i) a polyvalent RBD in ELMO, (ii) a novel membrane targeting signal for ELMO, and finally, (iii) a novel GTPase signaling cascade of Arl4A-Rac1 that controls actin cytoskeleton dynamics. Prior studies have uncovered that the Arl4 family are instrumental guiding signals for ARNO, an Arf6 GEF, and subsequent Arf6-dependent membrane reorganization and membrane ruffling [209,210]. In Aim #3 (Chapter 4) of my thesis, we demonstrate that Arl4A can stimulate actin modulation through ELMO/DOCK180/Rac, and this through an Arf6-independent pathway (Patel et al, *in preparation*). Other studies have linked Arf6 to Rac signaling and localization [180-183]. However, while the mechanistic connection between Arf6 and Rac remains obscure, our study identifies the ELMO RBD as a direct partner for active Arl4A, and that Arl4A-dependent cytoskeletal remodeling relies on DOCK180-mediated Rac signaling. The transient nature of the Arl4A/ELMO interaction did not allow us to conclude whether Arl4A can open the dormant ELMO molecule. Further studies will be required to determine if Arl4A has a dual role as a targeting and activating signal for ELMO.

What role, if any, does ELMO play in vivo in mammals?

From the literature, we see that ELMO has diverse implications during cell migration in myoblast fusion, apoptosis, and phagocytosis. However, all these studies have focused *in cellulo* and *in vivo* in the fly and worm. One very recent paper reveals that ELMO1-deficient mice display defects in clearance of apoptotic germ cells, but are otherwise phenotypically normal and viable. There are three forms of ELMO in mammals: ELMO1-3. It is possible that loss of one form of ELMO can be compensated for by the other forms. As well, restrictive protein expression patterns of ELMO proteins may explain why ELMO1-deficient mice are phenotypically normal. In this respect, knockout mice of the other ELMO proteins and double knockouts would be interesting to analyze.

As we are interested in how ELMO influences DOCK180 during various biological processes, knock-in mice may be insightful. Specifically, a knock-in mouse of ELMO-defective in binding DOCK180 (ELMO PH/PxxP mutant) would help us understand the implications of the ELMO/DOCK180 interaction *in vivo* in mammals, and whether this complex formation is important during known biological functions of DOCK180, such as, myoblast fusion and phagocytosis.

We have demonstrated that ELMO is autoinhibited via intramolecular interactions, the tight regulation of which is important for cell spreading and migration. To dissect whether this form of regulation is important *in vivo* in a whole system, we propose that knock-in mice with mutations in the autoregulatory EID

region would be informative. Equally revealing would be an ELMO knock-in of the RBD (L43A in ELMO1). From our *in cellulo* results, we deduce that autoregulation of ELMO is critical to prevent promiscuous Rac signaling. Therefore, *in vivo*, we expect that the EID knock-in animals may reflect unregulated Rac activation events, with illicit cell migration and spreading during processes such as cancer metastasis and phagocytosis. Conversely, we expect RBD knock-in animals to have improper targeting of ELMO and misdirection of ELMO effects, and thus, a decrease of cellular spreading and migratory processes.

Conclusions

In conclusion, I would like to remark that research into the DOCK180/ELMO interaction has revealed an intricate relationship between the two proteins. An interesting proposition involves the steric-inhibition model for DOCK180. Here, it is proposed that a DOCK180 SH3/DHR-2 interaction blocks its Rac GEF activity at basal levels, and cell stimulation and ELMO binding to DOCK180 relieves this autoinhibition [295]. In our model, we suggest that in unstimulated conditions, ELMO and DOCK180 are already in a complex through its primary interaction interface, ELMO PH/DOCK180$^{80\text{-}153}$ (**Figure 5.1, pg.232**). A stimuli will then lead to ELMO activation and induce conformational changes in this molecule that lead to a stabilizing of the DOCK180/ELMO complex through the DOCK180 SH3/ELMO PxxP (**Figure 5.1, pg. 232**).

We demonstrate that ELMO binding to DOCK180 is not required for Rac activation, but rather, for ensuing Rac signaling events. We propose that ELMO is autoinhibited at basal levels via intramolecular interactions between its newly discovered EID and EAD, relief of which occurs through cell stimulation. Cell stimulation will lead to ELMO RBD engagement (via a GTPase or other novel binding partner) that then anchors the ELMO/DOCK180 complex for localized Rac activation. It is also possible that cell stimulation leads to ELMO binding of yet unknown partners that relieve autoinhibition. Thus, the masked region of ELMO, the ELM domain, becomes exposed. Some probable roles of the ELM domain include: i) binding of Rac effectors and/or ii) GAP activity on yet unidentified GTPases that impede cell migration and/or directionality (**Figure 5.1, pg. 232**).

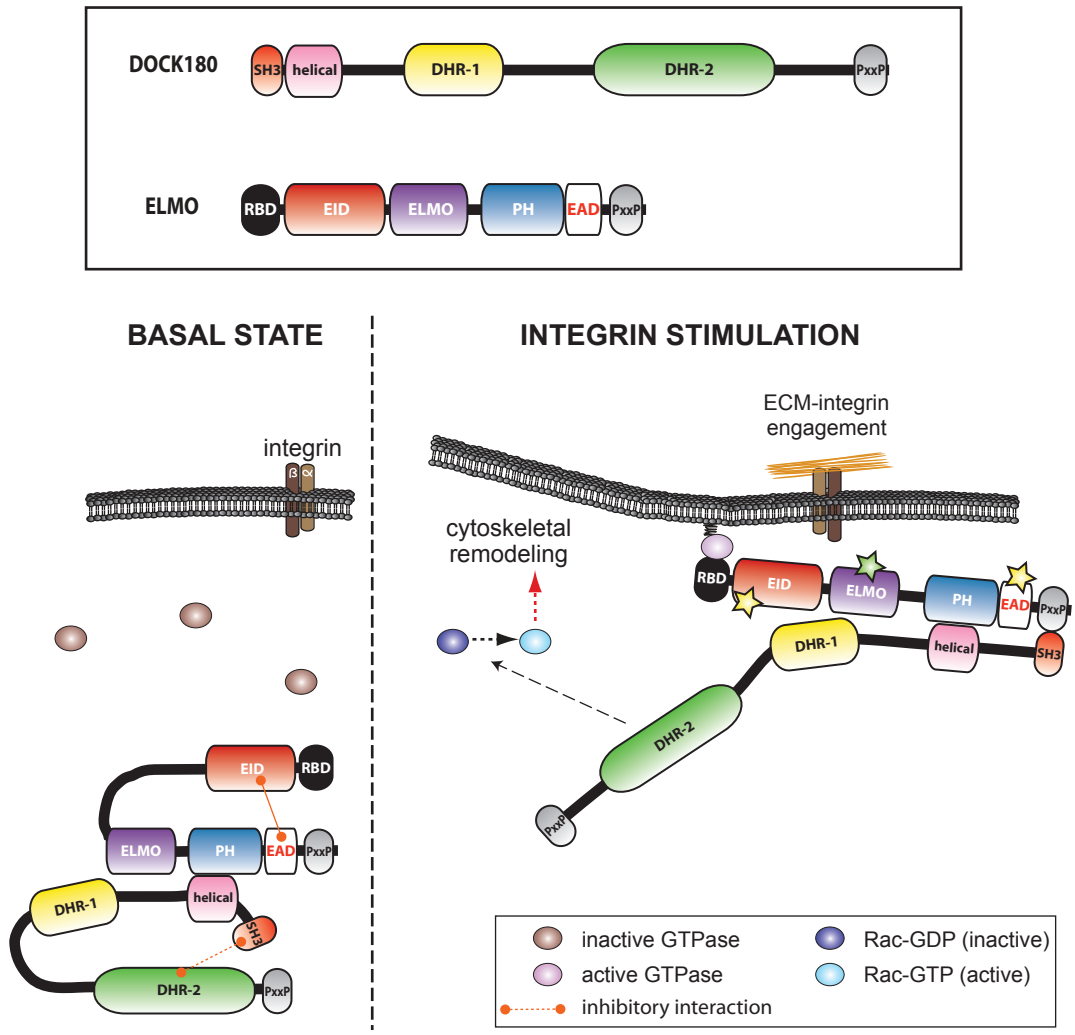

Figure 5.1. Proposed model for regulation of the ELMO/DOCK180 complex.
In this model, ELMO is autoinhibited at basal levels via intramolecular EID/EAD interactions, relief of which occurs through cell stimulation and ELMO RBD engagement (via a GTPase or other novel binding partner). The ELMO/DOCK180 complex is then anchored to the membrane for localized Rac activation. It is also possible that cell stimulation leads to ELMO binding of yet unknown partners that bind the EID or EAD and relieve autoinhibition (yellow stars). Thus, masked regions of ELMO, the ELM domain, become exposed. A few probable roles of the ELM include: i) binding of Rac effectors or ii) GAP activity on yet unidentified GTPases that impede cell migration and/or directionality (green star).

Also proposed here is that in unstimulated conditions, ELMO and DOCK180 are already in a complex through its primary interaction interface, ELMO PH/DOCK180$^{80\text{-}153,}$ and DOCK180 GEF activity is hindered through a DHR-2/SH3 interaction. Cell stimulation will then lead to ELMO activation and induce conformational changes in this molecule that lead to a stabilizing of the DOCK180/ELMO complex through DOCK180 SH3/ELMO PxxP.

Bibliography

1 (WHO), W. H. O. <http://www.who.int/mediacentre/factsheets/fs297/en/> (2009).

2 Canada, C. C. S. a. t. N. C. I. o. *Canadian cancer statistics 2008*, < www.cancer.ca/Canada-wide/About%20cancer/Cancer%20statistics/Canadian%20Cancer%20Statistics.aspx?sc_lang=en > (2008).

3 Steeg, P. S. Tumor metastasis: mechanistic insights and clinical challenges. *Nat Med* **12**, 895-904, doi:nm1469 [pii]

10.1038/nm1469 [doi] (2006).

4 Friedl, P. & Wolf, K. Plasticity of cell migration: a multiscale tuning model. *J Cell Biol* **188**, 11-19, doi:jcb.200909003 [pii]

10.1083/jcb.200909003 [doi] (2010).

5 Biname, F., Pawlak, G., Roux, P. & Hibner, U. What makes cells move: requirements and obstacles for spontaneous cell motility. *Mol Biosyst* **6**, 648-661, doi:10.1039/b915591k [doi] (2010).

6 Kaur, C., Dheen, S. T. & Ling, E. A. From blood to brain: amoeboid microglial cell, a nascent macrophage and its functions in developing brain. *Acta Pharmacol Sin* **28**, 1087-1096, doi:10.1111/j.1745-7254.2007.00625.x [doi] (2007).

7 Friedl, P., Borgmann, S. & Brocker, E. B. Amoeboid leukocyte crawling through extracellular matrix: lessons from the Dictyostelium paradigm of cell movement. *J Leukoc Biol* **70**, 491-509 (2001).

8 Lammermann, T. & Sixt, M. Mechanical modes of 'amoeboid' cell migration. *Curr Opin Cell Biol* **21**, 636-644, doi:S0955-0674(09)00114-8 [pii]

10.1016/j.ceb.2009.05.003 [doi] (2009).

9 Lauffenburger, D. A. & Horwitz, A. F. Cell migration: a physically integrated molecular process. *Cell* **84**, 359-369, doi:S0092-8674(00)81280-5 [pii] (1996).

10 Ananthakrishnan, R. & Ehrlicher, A. The forces behind cell movement. *Int J Biol Sci* **3**, 303-317 (2007).

11 Coates, T. D., Watts, R. G., Hartman, R. & Howard, T. H. Relationship of F-actin distribution to development of polar shape in human polymorphonuclear neutrophils. *J Cell Biol* **117**, 765-774 (1992).

12 Sullivan, S. J., Daukas, G. & Zigmond, S. H. Asymmetric distribution of the chemotactic peptide receptor on polymorphonuclear leukocytes. *J Cell Biol* **99**, 1461-1467 (1984).

13 Lawson, M. A. & Maxfield, F. R. Ca(2+)- and calcineurin-dependent recycling of an integrin to the front of migrating neutrophils. *Nature* **377**, 75-79, doi:10.1038/377075a0 [doi] (1995).

14 Schmidt, C. E., Horwitz, A. F., Lauffenburger, D. A. & Sheetz, M. P. Integrin-cytoskeletal interactions in migrating fibroblasts are dynamic, asymmetric, and regulated. *J Cell Biol* **123**, 977-991 (1993).

15 Cain, R. J. & Ridley, A. J. Phosphoinositide 3-kinases in cell migration. *Biol Cell* **101**, 13-29, doi:BC20080079 [pii]

10.1042/BC20080079 [doi] (2009).

16 Funamoto, S., Meili, R., Lee, S., Parry, L. & Firtel, R. A. Spatial and temporal regulation of 3-phosphoinositides by PI 3-kinase and PTEN mediates chemotaxis. *Cell* **109**, 611-623, doi:S0092867402007559 [pii] (2002).

17 Iijima, M., Huang, Y. E. & Devreotes, P. Temporal and spatial regulation of chemotaxis. *Dev Cell* **3**, 469-478, doi:S1534580702002927 [pii] (2002).

18 Leslie, N. R., Yang, X., Downes, C. P. & Weijer, C. J. The regulation of cell migration by PTEN. *Biochem Soc Trans* **33**, 1507-1508, doi:BST20051507 [pii]

10.1042/BST20051507 [doi] (2005).

19 Wang, F. *et al.* Lipid products of PI(3)Ks maintain persistent cell polarity and directed motility in neutrophils. *Nat Cell Biol* **4**, 513-518, doi:10.1038/ncb810 [doi]

ncb810 [pii] (2002).

20 Weiner, O. D. *et al.* A PtdInsP(3)- and Rho GTPase-mediated positive feedback loop regulates neutrophil polarity. *Nat Cell Biol* **4**, 509-513, doi:10.1038/ncb811 [doi]

ncb811 [pii] (2002).

21 Innocenti, M. *et al.* Phosphoinositide 3-kinase activates Rac by entering in a complex with Eps8, Abi1, and Sos-1. *J Cell Biol* **160**, 17-23, doi:10.1083/jcb.200206079 [doi]

jcb.200206079 [pii] (2003).

22 Felder, S. & Elson, E. L. Mechanics of fibroblast locomotion: quantitative analysis of forces and motions at the leading lamellas of fibroblasts. *J Cell Biol* **111**, 2513-2526 (1990).

23 Pollard, T. D. & Borisy, G. G. Cellular motility driven by assembly and disassembly of actin filaments. *Cell* **112**, 453-465, doi:S009286740300120X [pii] (2003).

24 dos Remedios, C. G. *et al.* Actin binding proteins: regulation of cytoskeletal microfilaments. *Physiol Rev* **83**, 433-473, doi:10.1152/physrev.00026.2002 [doi] (2003).

25 Bershadsky, A. D., Balaban, N. Q. & Geiger, B. Adhesion-dependent cell mechanosensitivity. *Annu Rev Cell Dev Biol* **19**, 677-695, doi:10.1146/annurev.cellbio.19.111301.153011 [doi] (2003).

26 Rid, R., Schiefermeier, N., Grigoriev, I., Small, J. V. & Kaverina, I. The last but not the least: the origin and significance of trailing adhesions in fibroblastic cells. *Cell Motil Cytoskeleton* **61**, 161-171, doi:10.1002/cm.20076 [doi] (2005).

27 Zamir, E. *et al.* Dynamics and segregation of cell-matrix adhesions in cultured fibroblasts. *Nat Cell Biol* **2**, 191-196, doi:10.1038/35008607 [doi] (2000).

28 Ridley, A. J. *et al.* Cell migration: integrating signals from front to back. *Science* **302**, 1704-1709, doi:10.1126/science.1092053 [doi]

302/5651/1704 [pii] (2003).

29 Wu, D. Y. & Goldberg, D. J. Regulated tyrosine phosphorylation at the tips of growth cone filopodia. *J Cell Biol* **123**, 653-664 (1993).

30 Mitra, S. K. & Schlaepfer, D. D. Integrin-regulated FAK-Src signaling in normal and cancer cells. *Curr Opin Cell Biol* **18**, 516-523, doi:S0955-0674(06)00122-0 [pii]

10.1016/j.ceb.2006.08.011 [doi] (2006).

31 Shattil, S. J., Kim, C. & Ginsberg, M. H. The final steps of integrin activation: the end game. *Nat Rev Mol Cell Biol* **11**, 288-300, doi:nrm2871 [pii]

10.1038/nrm2871 [doi] (2010).

32 Mitchison, T. J. & Cramer, L. P. Actin-based cell motility and cell locomotion. *Cell* **84**, 371-379, doi:S0092-8674(00)81281-7 [pii] (1996).

33 Ridley, A. J. Rho GTPases and cell migration. *J Cell Sci* **114**, 2713-2722 (2001).

34 Regen, C. M. & Horwitz, A. F. Dynamics of beta 1 integrin-mediated adhesive contacts in motile fibroblasts. *J Cell Biol* **119**, 1347-1359 (1992).

35 Pantaloni, D., Le Clainche, C. & Carlier, M. F. Mechanism of actin-based motility. *Science* **292**, 1502-1506 (2001).

36 Stossel, T. P., Fenteany, G. & Hartwig, J. H. Cell surface actin remodeling. *J Cell Sci* **119**, 3261-3264, doi:119/16/3261 [pii]

10.1242/jcs.02994 [doi] (2006).

37 Chhabra, E. S. & Higgs, H. N. The many faces of actin: matching assembly factors with cellular structures. *Nat Cell Biol* **9**, 1110-1121, doi:ncb1007-1110 [pii]

10.1038/ncb1007-1110 [doi] (2007).

38 Pollard, T. D. & Cooper, J. A. Actin, a central player in cell shape and movement. *Science* **326**, 1208-1212, doi:326/5957/1208 [pii]

10.1126/science.1175862 [doi] (2009).

39 Insall, R. H. & Machesky, L. M. Actin dynamics at the leading edge: from simple machinery to complex networks. *Dev Cell* **17**, 310-322, doi:S1534-5807(09)00348-7 [pii]

10.1016/j.devcel.2009.08.012 [doi] (2009).

40 Rafelski, S. M. & Theriot, J. A. Crawling toward a unified model of cell mobility: spatial and temporal regulation of actin dynamics. *Annu Rev Biochem* **73**, 209-239, doi:10.1146/annurev.biochem.73.011303.073844 [doi] (2004).

41 Nicholson-Dykstra, S., Higgs, H. N. & Harris, E. S. Actin dynamics: growth from dendritic branches. *Curr Biol* **15**, R346-357, doi:S0960-9822(05)00429-X [pii]

10.1016/j.cub.2005.04.029 [doi] (2005).

42 Campellone, K. G. & Welch, M. D. A nucleator arms race: cellular control of actin assembly. *Nat Rev Mol Cell Biol* **11**, 237-251, doi:nrm2867 [pii]

10.1038/nrm2867 [doi] (2010).

43 Goley, E. D. & Welch, M. D. The ARP2/3 complex: an actin nucleator comes of age. *Nat Rev Mol Cell Biol* **7**, 713-726, doi:nrm2026 [pii]

10.1038/nrm2026 [doi] (2006).

44 Goode, B. L. & Eck, M. J. Mechanism and function of formins in the control of actin assembly. *Annu Rev Biochem* **76**, 593-627, doi:10.1146/annurev.biochem.75.103004.142647 [doi] (2007).

45 Pruyne, D. *et al.* Role of formins in actin assembly: nucleation and barbed-end association. *Science* **297**, 612-615, doi:10.1126/science.1072309 [doi]

1072309 [pii] (2002).

46 Sagot, I., Rodal, A. A., Moseley, J., Goode, B. L. & Pellman, D. An actin nucleation mechanism mediated by Bni1 and profilin. *Nat Cell Biol* **4**, 626-631, doi:10.1038/ncb834 [doi]

ncb834 [pii] (2002).

47 Kovar, D. R. Molecular details of formin-mediated actin assembly. *Curr Opin Cell Biol* **18**, 11-17, doi:S0955-0674(05)00191-2 [pii]

10.1016/j.ceb.2005.12.011 [doi] (2006).

48 Shimada, A. *et al.* The core FH2 domain of diaphanous-related formins is an elongated actin binding protein that inhibits polymerization. *Mol Cell* **13**, 511-522, doi:S1097276504000590 [pii] (2004).

49 Harris, E. S. & Higgs, H. N. Actin cytoskeleton: formins lead the way. *Curr Biol* **14**, R520-522, doi:10.1016/j.cub.2004.06.043 [doi]

S0960982204004488 [pii] (2004).

50 Moseley, J. B. & Goode, B. L. Differential activities and regulation of Saccharomyces cerevisiae formin proteins Bni1 and Bnr1 by Bud6. *J Biol Chem* **280**, 28023-28033, doi:M503094200 [pii]

10.1074/jbc.M503094200 [doi] (2005).

51 Chhabra, E. S. & Higgs, H. N. INF2 Is a WASP homology 2 motif-containing formin that severs actin filaments and accelerates both polymerization and depolymerization. *J Biol Chem* **281**, 26754-26767, doi:M604666200 [pii]

10.1074/jbc.M604666200 [doi] (2006).

52 Wen, Y. *et al.* EB1 and APC bind to mDia to stabilize microtubules downstream of Rho and promote cell migration. *Nat Cell Biol* **6**, 820-830, doi:10.1038/ncb1160 [doi]

ncb1160 [pii] (2004).

53 Lewkowicz, E. *et al.* The microtubule-binding protein CLIP-170 coordinates mDia1 and actin reorganization during CR3-mediated phagocytosis. *J Cell Biol* **183**, 1287-1298, doi:jcb.200807023 [pii]

10.1083/jcb.200807023 [doi] (2008).

54 Bartolini, F. *et al.* The formin mDia2 stabilizes microtubules independently of its actin nucleation activity. *J Cell Biol* **181**, 523-536, doi:jcb.200709029 [pii]

10.1083/jcb.200709029 [doi] (2008).

55 Bartolini, F. & Gundersen, G. G. Formins and microtubules. *Biochim Biophys Acta* **1803**, 164-173, doi:S0167-4889(09)00183-9 [pii]

10.1016/j.bbamcr.2009.07.006 [doi] (2010).

56 Quinlan, M. E., Heuser, J. E., Kerkhoff, E. & Mullins, R. D. Drosophila Spire is an actin nucleation factor. *Nature* **433**, 382-388, doi:nature03241 [pii]

10.1038/nature03241 [doi] (2005).

57 LeClaire, L. L., 3rd, Baumgartner, M., Iwasa, J. H., Mullins, R. D. & Barber, D. L. Phosphorylation of the Arp2/3 complex is necessary to nucleate actin filaments. *J Cell Biol* **182**, 647-654, doi:jcb.200802145 [pii]

10.1083/jcb.200802145 [doi] (2008).

58 Padrick, S. B. & Rosen, M. K. Physical mechanisms of signal integration by WASP family proteins. *Annu Rev Biochem* **79**, 707-735, doi:10.1146/annurev.biochem.77.060407.135452 [doi] (2010).

59 Machesky, L. M. & Insall, R. H. Scar1 and the related Wiskott-Aldrich syndrome protein, WASP, regulate the actin cytoskeleton through the Arp2/3 complex. *Curr Biol* **8**, 1347-1356, doi:S0960-9822(98)00015-3 [pii] (1998).

60 Marchand, J. B., Kaiser, D. A., Pollard, T. D. & Higgs, H. N. Interaction of WASP/Scar proteins with actin and vertebrate Arp2/3 complex. *Nat Cell Biol* **3**, 76-82, doi:10.1038/35050590 [doi] (2001).

61 Prehoda, K. E., Scott, J. A., Mullins, R. D. & Lim, W. A. Integration of multiple signals through cooperative regulation of the N-WASP-Arp2/3 complex. *Science* **290**, 801-806, doi:8938 [pii] (2000).

62 Anton, I. M. *et al.* WIP deficiency reveals a differential role for WIP and the actin cytoskeleton in T and B cell activation. *Immunity* **16**, 193-204, doi:S1074761302002686 [pii] (2002).

63 Ho, H. Y. *et al.* Toca-1 mediates Cdc42-dependent actin nucleation by activating the N-WASP-WIP complex. *Cell* **118**, 203-216, doi:10.1016/j.cell.2004.06.027 [doi]

S0092867404006294 [pii] (2004).

64 Eden, S., Rohatgi, R., Podtelejnikov, A. V., Mann, M. & Kirschner, M. W. Mechanism of regulation of WAVE1-induced actin nucleation by Rac1 and Nck. *Nature* **418**, 790-793, doi:10.1038/nature00859 [doi]

nature00859 [pii] (2002).

65 Takenawa, T. & Suetsugu, S. The WASP-WAVE protein network: connecting the membrane to the cytoskeleton. *Nat Rev Mol Cell Biol* **8**, 37-48, doi:nrm2069 [pii]

10.1038/nrm2069 [doi] (2007).

66 Colicelli, J. Human RAS superfamily proteins and related GTPases. *Sci STKE* **2004**, RE13, doi:10.1126/stke.2502004re13 [doi]

stke.2502004re13 [pii] (2004).

67 Heasman, S. J. & Ridley, A. J. Mammalian Rho GTPases: new insights into their functions from in vivo studies. *Nat Rev Mol Cell Biol* **9**, 690-701, doi:nrm2476 [pii]

10.1038/nrm2476 [doi] (2008).

68 Cote, J. F. a. V., K. in *Discovery of DOCK180 Superfamily of Exchange Factors* (ed Renata and Wadih Arap. Pasqualini) 171-189 (CRC Press / Taylor & Francis 2009).

69 Vetter, I. R. & Wittinghofer, A. The guanine nucleotide-binding switch in three dimensions. *Science* **294**, 1299-1304, doi:10.1126/science.1062023 [doi]

294/5545/1299 [pii] (2001).

70 Magee, T. & Seabra, M. C. Fatty acylation and prenylation of proteins: what's hot in fat. *Curr Opin Cell Biol* **17**, 190-196, doi:S0955-0674(05)00016-5 [pii]

10.1016/j.ceb.2005.02.003 [doi] (2005).

71 Wright, L. P. & Philips, M. R. Thematic review series: lipid posttranslational modifications. CAAX modification and membrane targeting of Ras. *J Lipid Res* **47**, 883-891, doi:R600004-JLR200 [pii]

10.1194/jlr.R600004-JLR200 [doi] (2006).

72 Aspenstrom, P., Ruusala, A. & Pacholsky, D. Taking Rho GTPases to the next level: the cellular functions of atypical Rho GTPases. *Exp Cell Res* **313**, 3673-3679, doi:S0014-4827(07)00358-8 [pii]

10.1016/j.yexcr.2007.07.022 [doi] (2007).

73 Chardin, P. Function and regulation of Rnd proteins. *Nat Rev Mol Cell Biol* **7**, 54-62, doi:nrm1788 [pii]

10.1038/nrm1788 [doi] (2006).

74 Symons, M. & Settleman, J. Rho family GTPases: more than simple switches. *Trends Cell Biol* **10**, 415-419, doi:S0962-8924(00)01832-8 [pii] (2000).

75 Rossman, K. L., Der, C. J. & Sondek, J. GEF means go: turning on RHO GTPases with guanine nucleotide-exchange factors. *Nat Rev Mol Cell Biol* **6**, 167-180, doi:nrm1587 [pii]

10.1038/nrm1587 [doi] (2005).

76 Eva, A. & Aaronson, S. A. Isolation of a new human oncogene from a diffuse B-cell lymphoma. *Nature* **316**, 273-275 (1985).

77 Hart, M. J., Eva, A., Evans, T., Aaronson, S. A. & Cerione, R. A. Catalysis of guanine nucleotide exchange on the CDC42Hs protein by the dbl oncogene product. *Nature* **354**, 311-314, doi:10.1038/354311a0 [doi] (1991).

78 Rebecchi, M. J. & Scarlata, S. Pleckstrin homology domains: a common fold with diverse functions. *Annu Rev Biophys Biomol Struct* **27**, 503-528, doi:10.1146/annurev.biophys.27.1.503 [doi] (1998).

79 Lemmon, M. A. & Ferguson, K. M. Signal-dependent membrane targeting by pleckstrin homology (PH) domains. *Biochem J* **350 Pt 1**, 1-18 (2000).

80 Liu, X. *et al.* NMR structure and mutagenesis of the N-terminal Dbl homology domain of the nucleotide exchange factor Trio. *Cell* **95**, 269-277, doi:S0092-8674(00)81757-2 [pii] (1998).

81 Rossman, K. L. & Campbell, S. L. Bacterial expressed DH and DH/PH domains. *Methods Enzymol* **325**, 25-38, doi:S0076-6879(00)25428-1 [pii] (2000).

82 Rossman, K. L. *et al.* Multifunctional roles for the PH domain of Dbs in regulating Rho GTPase activation. *J Biol Chem* **278**, 18393-18400, doi:10.1074/jbc.M300127200 [doi]

M300127200 [pii] (2003).

83 Cote, J. F. & Vuori, K. GEF what? Dock180 and related proteins help Rac to polarize cells in new ways. *Trends Cell Biol* **17**, 383-393, doi:S0962-8924(07)00157-2 [pii]

10.1016/j.tcb.2007.05.001 (2007).

84 Erickson, J. W. & Cerione, R. A. Structural elements, mechanism, and evolutionary convergence of Rho protein-guanine nucleotide exchange factor complexes. *Biochemistry* **43**, 837-842, doi:10.1021/bi036026v [doi] (2004).

85 Yang, J., Zhang, Z., Roe, S. M., Marshall, C. J. & Barford, D. Activation of Rho GTPases by DOCK exchange factors is mediated by a nucleotide sensor. *Science* **325**, 1398-1402, doi:325/5946/1398 [pii]

10.1126/science.1174468 (2009).

86 Schmidt, A. & Hall, A. Guanine nucleotide exchange factors for Rho GTPases: turning on the switch. *Genes Dev* **16**, 1587-1609, doi:10.1101/gad.1003302 [doi] (2002).

87 Das, B. *et al.* Control of intramolecular interactions between the pleckstrin homology and Dbl homology domains of Vav and Sos1 regulates Rac binding. *J Biol Chem* **275**, 15074-15081, doi:10.1074/jbc.M907269199 [doi]

M907269199 [pii] (2000).

88 Bustelo, X. R. Regulatory and signaling properties of the Vav family. *Mol Cell Biol* **20**, 1461-1477 (2000).

89 Sprang, S. R. G proteins, effectors and GAPs: structure and mechanism. *Curr Opin Struct Biol* **7**, 849-856, doi:S0959-440X(97)80157-1 [pii] (1997).

90 Moon, S. Y. & Zheng, Y. Rho GTPase-activating proteins in cell regulation. *Trends Cell Biol* **13**, 13-22, doi:S0962892402000041 [pii] (2003).

91 Bos, J. L., Rehmann, H. & Wittinghofer, A. GEFs and GAPs: critical elements in the control of small G proteins. *Cell* **129**, 865-877, doi:S0092-8674(07)00655-1 [pii]

10.1016/j.cell.2007.05.018 [doi] (2007).

92 Brandao, M. M., Silva-Brandao, K. L., Costa, F. F. & Saad, S. T. Phylogenetic analysis of RhoGAP domain-containing proteins. *Genomics Proteomics Bioinformatics* **4**, 182-188, doi:S1672-0229(06)60031-4 [pii]

10.1016/S1672-0229(06)60031-4 [doi] (2006).

93 Nassar, N., Hoffman, G. R., Manor, D., Clardy, J. C. & Cerione, R. A. Structures of Cdc42 bound to the active and catalytically compromised forms of Cdc42GAP. *Nat Struct Biol* **5**, 1047-1052, doi:10.1038/4156 [doi] (1998).

94 Dovas, A. & Couchman, J. R. RhoGDI: multiple functions in the regulation of Rho family GTPase activities. *Biochem J* **390**, 1-9, doi:BJ20050104 [pii]

10.1042/BJ20050104 [doi] (2005).

95 DerMardirossian, C. & Bokoch, G. M. GDIs: central regulatory molecules in Rho GTPase activation. *Trends Cell Biol* **15**, 356-363, doi:S0962-8924(05)00127-3 [pii]

10.1016/j.tcb.2005.05.001 [doi] (2005).

96 Hoffman, G. R., Nassar, N. & Cerione, R. A. Structure of the Rho family GTP-binding protein Cdc42 in complex with the multifunctional regulator RhoGDI. *Cell* **100**, 345-356, doi:S0092-8674(00)80670-4 [pii] (2000).

97 Longenecker, K. *et al.* How RhoGDI binds Rho. *Acta Crystallogr D Biol Crystallogr* **55**, 1503-1515, doi:GR0936 [pii] (1999).

98 Olofsson, B. Rho guanine dissociation inhibitors: pivotal molecules in cellular signalling. *Cell Signal* **11**, 545-554, doi:S0898-6568(98)00063-1 [pii] (1999).

99 Chuang, T. H., Bohl, B. P. & Bokoch, G. M. Biologically active lipids are regulators of Rac.GDI complexation. *J Biol Chem* **268**, 26206-26211 (1993).

100 Takahashi, K. *et al.* Direct interaction of the Rho GDP dissociation inhibitor with ezrin/radixin/moesin initiates the activation of the Rho small G protein. *J Biol Chem* **272**, 23371-23375 (1997).

101 Yamashita, T. & Tohyama, M. The p75 receptor acts as a displacement factor that releases Rho from Rho-GDI. *Nat Neurosci* **6**, 461-467, doi:10.1038/nn1045 [doi]

nn1045 [pii] (2003).

102 Tolias, K. F., Couvillon, A. D., Cantley, L. C. & Carpenter, C. L. Characterization of a Rac1- and RhoGDI-associated lipid kinase signaling complex. *Mol Cell Biol* **18**, 762-770 (1998).

103 Bourmeyster, N. & Vignais, P. V. Phosphorylation of Rho GDI stabilizes the Rho A-Rho GDI complex in neutrophil cytosol. *Biochem Biophys Res Commun* **218**, 54-60, doi:S0006-291X(96)90011-X [pii]

10.1006/bbrc.1996.0011 [doi] (1996).

104 Forget, M. A., Desrosiers, R. R., Gingras, D. & Beliveau, R. Phosphorylation states of Cdc42 and RhoA regulate their interactions with Rho GDP dissociation inhibitor and their extraction from biological membranes. *Biochem J* **361**, 243-254 (2002).

105 Hancock, J. F. & Hall, A. A novel role for RhoGDI as an inhibitor of GAP proteins. *EMBO J* **12**, 1915-1921 (1993).

106 Scita, G. *et al.* Signaling from Ras to Rac and beyond: not just a matter of GEFs. *EMBO J* **19**, 2393-2398, doi:10.1093/emboj/19.11.2393 [doi] (2000).

107 Rittinger, K. *et al.* Crystal structure of a small G protein in complex with the GTPase-activating protein rhoGAP. *Nature* **388**, 693-697, doi:10.1038/41805 [doi] (1997).

108 Ihara, K. *et al.* Crystal structure of human RhoA in a dominantly active form complexed with a GTP analogue. *J Biol Chem* **273**, 9656-9666 (1998).

109 Lin, R., Bagrodia, S., Cerione, R. & Manor, D. A novel Cdc42Hs mutant induces cellular transformation. *Curr Biol* **7**, 794-797, doi:S0960-9822(06)00338-1 [pii] (1997).

110 Reinstein, J., Schlichting, I., Frech, M., Goody, R. S. & Wittinghofer, A. p21 with a phenylalanine 28----leucine mutation reacts normally with the GTPase activating protein GAP but nevertheless has transforming properties. *J Biol Chem* **266**, 17700-17706 (1991).

111 Feig, L. A. Tools of the trade: use of dominant-inhibitory mutants of Ras-family GTPases. *Nat Cell Biol* **1**, E25-27, doi:10.1038/10018 [doi] (1999).

112 Brunsveld, L., Waldmann, H. & Huster, D. Membrane binding of lipidated Ras peptides and proteins--the structural point of view. *Biochim Biophys Acta* **1788**, 273-288, doi:S0005-2736(08)00244-7 [pii]

10.1016/j.bbamem.2008.08.006 [doi] (2009).

113 Gomes, A. Q. *et al.* Membrane targeting of Rab GTPases is influenced by the prenylation motif. *Mol Biol Cell* **14**, 1882-1899, doi:10.1091/mbc.E02-10-0639 [doi]

E02-10-0639 [pii] (2003).

114 Westwick, J. K. *et al.* Rac regulation of transformation, gene expression, and actin organization by multiple, PAK-independent pathways. *Mol Cell Biol* **17**, 1324-1335 (1997).

115 Sahai, E., Alberts, A. S. & Treisman, R. RhoA effector mutants reveal distinct effector pathways for cytoskeletal reorganization, SRF activation and transformation. *EMBO J* **17**, 1350-1361, doi:10.1093/emboj/17.5.1350 [doi] (1998).

116 Wang, L. & Zheng, Y. Cell type-specific functions of Rho GTPases revealed by gene targeting in mice. *Trends Cell Biol* **17**, 58-64, doi:S0962-8924(06)00336-9 [pii]

10.1016/j.tcb.2006.11.009 [doi] (2007).

117 Zheng, Y. Dbl family guanine nucleotide exchange factors. *Trends Biochem Sci* **26**, 724-732, doi:S0968-0004(01)01973-9 [pii] (2001).

118 Debreceni, B. *et al.* Mechanisms of guanine nucleotide exchange and Rac-mediated signaling revealed by a dominant negative trio mutant. *J Biol Chem* **279**, 3777-3786, doi:10.1074/jbc.M308282200 [doi]

M308282200 [pii] (2004).

119 Chan, A. Y. *et al.* Roles of the Rac1 and Rac3 GTPases in human tumor cell invasion. *Oncogene* **24**, 7821-7829, doi:1208909 [pii]

10.1038/sj.onc.1208909 [doi] (2005).

120 Bruce Alberts, A. J., Julian Lewis, Martin Raff, Keith Roberts, and Peter Walter. (Garland Science., New York., 2002).

121 Wennerberg, K. & Der, C. J. Rho-family GTPases: it's not only Rac and Rho (and I like it). *J Cell Sci* **117**, 1301-1312, doi:10.1242/jcs.01118 [doi]

117/8/1301 [pii] (2004).

122 ten Klooster, J. P. & Hordijk, P. L. Targeting and localized signalling by small GTPases. *Biol Cell* **99**, 1-12, doi:BC20060071 [pii]

10.1042/BC20060071 [doi] (2007).

123 Jaffe, A. B. & Hall, A. Rho GTPases: biochemistry and biology. *Annu Rev Cell Dev Biol* **21**, 247-269, doi:10.1146/annurev.cellbio.21.020604.150721 [doi] (2005).

124 Gardiner, E. M. *et al.* Spatial and temporal analysis of Rac activation during live neutrophil chemotaxis. *Curr Biol* **12**, 2029-2034, doi:S0960982202013349 [pii] (2002).

125 Manser, E. *et al.* Molecular cloning of a new member of the p21-Cdc42/Rac-activated kinase (PAK) family. *J Biol Chem* **270**, 25070-25078 (1995).

126 Bagrodia, S. & Cerione, R. A. Pak to the future. *Trends Cell Biol* **9**, 350-355, doi:S0962-8924(99)01618-9 [pii] (1999).

127 Bokoch, G. M. Biology of the p21-activated kinases. *Annu Rev Biochem* **72**, 743-781, doi:10.1146/annurev.biochem.72.121801.161742 [doi]

121801.161742 [pii] (2003).

128 Szczepanowska, J. Involvement of Rac/Cdc42/PAK pathway in cytoskeletal rearrangements. *Acta Biochim Pol* **56**, 225-234, doi:20091831 [pii] (2009).

129 Innocenti, M. *et al.* Abi1 is essential for the formation and activation of a WAVE2 signalling complex. *Nat Cell Biol* **6**, 319-327, doi:10.1038/ncb1105 [doi]

ncb1105 [pii] (2004).

130 Knaus, U. G., Wang, Y., Reilly, A. M., Warnock, D. & Jackson, J. H. Structural requirements for PAK activation by Rac GTPases. *J Biol Chem* **273**, 21512-21518 (1998).

131 Haeusler, L. C. *et al.* Purification and biochemical properties of Rac1, 2, 3 and the splice variant Rac1b. *Methods Enzymol* **406**, 1-11, doi:S0076-6879(06)06001-0 [pii]

10.1016/S0076-6879(06)06001-0 [doi] (2006).

132 Michaelson, D. *et al.* Differential localization of Rho GTPases in live cells: regulation by hypervariable regions and RhoGDI binding. *J Cell Biol* **152**, 111-126 (2001).

133 Williams, C. L. The polybasic region of Ras and Rho family small GTPases: a regulator of protein interactions and membrane association and a site of nuclear

localization signal sequences. *Cell Signal* **15**, 1071-1080, doi:S0898656803000986 [pii] (2003).

134 ten Klooster, J. P., Jaffer, Z. M., Chernoff, J. & Hordijk, P. L. Targeting and activation of Rac1 are mediated by the exchange factor beta-Pix. *J Cell Biol* **172**, 759-769, doi:jcb.200509096 [pii]

10.1083/jcb.200509096 [doi] (2006).

135 Moll, J., Sansig, G., Fattori, E. & van der Putten, H. The murine rac1 gene: cDNA cloning, tissue distribution and regulated expression of rac1 mRNA by disassembly of actin microfilaments. *Oncogene* **6**, 863-866 (1991).

136 Shirsat, N. V., Pignolo, R. J., Kreider, B. L. & Rovera, G. A member of the ras gene superfamily is expressed specifically in T, B and myeloid hemopoietic cells. *Oncogene* **5**, 769-772 (1990).

137 Malosio, M. L., Gilardelli, D., Paris, S., Albertinazzi, C. & de Curtis, I. Differential expression of distinct members of Rho family GTP-binding proteins during neuronal development: identification of Rac1B, a new neural-specific member of the family. *J Neurosci* **17**, 6717-6728 (1997).

138 Haataja, L., Groffen, J. & Heisterkamp, N. Characterization of RAC3, a novel member of the Rho family. *J Biol Chem* **272**, 20384-20388 (1997).

139 Sugihara, K. *et al.* Rac1 is required for the formation of three germ layers during gastrulation. *Oncogene* **17**, 3427-3433, doi:10.1038/sj.onc.1202595 [doi] (1998).

140 Tahirovic, S. *et al.* Rac1 regulates neuronal polarization through the WAVE complex. *J Neurosci* **30**, 6930-6943, doi:30/20/6930 [pii]

10.1523/JNEUROSCI.5395-09.2010 [doi] (2010).

141 Vasyutina, E., Martarelli, B., Brakebusch, C., Wende, H. & Birchmeier, C. The small G-proteins Rac1 and Cdc42 are essential for myoblast fusion in the mouse. *Proc Natl Acad Sci U S A* **106**, 8935-8940, doi:0902501106 [pii]

10.1073/pnas.0902501106 [doi] (2009).

142 Luo, L., Liao, Y. J., Jan, L. Y. & Jan, Y. N. Distinct morphogenetic functions of similar small GTPases: Drosophila Drac1 is involved in axonal outgrowth and myoblast fusion. *Genes Dev* **8**, 1787-1802 (1994).

143 Hakeda-Suzuki, S. *et al.* Rac function and regulation during Drosophila development. *Nature* **416**, 438-442, doi:10.1038/416438a [doi]

416438a [pii] (2002).

144 Roberts, A. W. *et al.* Deficiency of the hematopoietic cell-specific Rho family GTPase Rac2 is characterized by abnormalities in neutrophil function and host defense. *Immunity* **10**, 183-196, doi:S1074-7613(00)80019-9 [pii] (1999).

145 Walmsley, M. J. *et al.* Critical roles for Rac1 and Rac2 GTPases in B cell development and signaling. *Science* **302**, 459-462, doi:10.1126/science.1089709 [doi]

302/5644/459 [pii] (2003).

146 Gu, Y. *et al.* Hematopoietic cell regulation by Rac1 and Rac2 guanosine triphosphatases. *Science* **302**, 445-449, doi:10.1126/science.1088485 [doi]

302/5644/445 [pii] (2003).

147 Corbetta, S. *et al.* Generation and characterization of Rac3 knockout mice. *Mol Cell Biol* **25**, 5763-5776, doi:25/13/5763 [pii]

10.1128/MCB.25.13.5763-5776.2005 [doi] (2005).

148 Corbetta, S. *et al.* Essential role of Rac1 and Rac3 GTPases in neuronal development. *FASEB J* **23**, 1347-1357, doi:fj.08-121574 [pii]

10.1096/fj.08-121574 [doi] (2009).

149 Hajdo-Milasinovic, A., Ellenbroek, S. I., van Es, S., van der Vaart, B. & Collard, J. G. Rac1 and Rac3 have opposing functions in cell adhesion and differentiation of neuronal cells. *J Cell Sci* **120**, 555-566, doi:jcs.03364 [pii]

10.1242/jcs.03364 [doi] (2007).

150 Hajdo-Milasinovic, A., van der Kammen, R. A., Moneva, Z. & Collard, J. G. Rac3 inhibits adhesion and differentiation of neuronal cells by modifying GIT1 downstream signaling. *J Cell Sci* **122**, 2127-2136, doi:122/12/2127 [pii]

10.1242/jcs.039958 [doi] (2009).

151 Gauthier-Rouviere, C. *et al.* RhoG GTPase controls a pathway that independently activates Rac1 and Cdc42Hs. *Mol Biol Cell* **9**, 1379-1394 (1998).

152 Katoh, H. & Negishi, M. RhoG activates Rac1 by direct interaction with the Dock180-binding protein Elmo. *Nature* **424**, 461-464, doi:10.1038/nature01817 [doi]

nature01817 [pii] (2003).

153 Meller, J., Vidali, L. & Schwartz, M. A. Endogenous RhoG is dispensable for integrin-mediated cell spreading but contributes to Rac-independent migration. *J Cell Sci* **121**, 1981-1989, doi:jcs.025130 [pii]

10.1242/jcs.025130 [doi] (2008).

154 Chen, F. *et al.* Cdc42 is required for PIP(2)-induced actin polymerization and early development but not for cell viability. *Curr Biol* **10**, 758-765, doi:S0960-9822(00)00571-6 [pii] (2000).

155 Vigorito, E. *et al.* Immunological function in mice lacking the Rac-related GTPase RhoG. *Mol Cell Biol* **24**, 719-729 (2004).

156 Kahn, R. A. *et al.* Nomenclature for the human Arf family of GTP-binding proteins: ARF, ARL, and SAR proteins. *J Cell Biol* **172**, 645-650, doi:jcb.200512057 [pii]

10.1083/jcb.200512057 [doi] (2006).

157 Gillingham, A. K. & Munro, S. The small G proteins of the Arf family and their regulators. *Annu Rev Cell Dev Biol* **23**, 579-611, doi:10.1146/annurev.cellbio.23.090506.123209 [doi] (2007).

158 Kahn, R. A., Goddard, C. & Newkirk, M. Chemical and immunological characterization of the 21-kDa ADP-ribosylation factor of adenylate cyclase. *J Biol Chem* **263**, 8282-8287 (1988).

159 Casanova, J. E. Regulation of Arf activation: the Sec7 family of guanine nucleotide exchange factors. *Traffic* **8**, 1476-1485, doi:TRA634 [pii]

10.1111/j.1600-0854.2007.00634.x [doi] (2007).

160 Goldberg, J. Structural basis for activation of ARF GTPase: mechanisms of guanine nucleotide exchange and GTP-myristoyl switching. *Cell* **95**, 237-248, doi:S0092-8674(00)81754-7 [pii] (1998).

161 Pasqualato, S., Renault, L. & Cherfils, J. Arf, Arl, Arp and Sar proteins: a family of GTP-binding proteins with a structural device for 'front-back' communication. *EMBO Rep* **3**, 1035-1041, doi:10.1093/embo-reports/kvf221 [doi]

3/11/1035 [pii] (2002).

162 Antonny, B., Beraud-Dufour, S., Chardin, P. & Chabre, M. N-terminal hydrophobic residues of the G-protein ADP-ribosylation factor-1 insert into membrane

phospholipids upon GDP to GTP exchange. *Biochemistry* **36**, 4675-4684, doi:10.1021/bi962252b [doi]

bi962252b [pii] (1997).

163 Cox, R., Mason-Gamer, R. J., Jackson, C. L. & Segev, N. Phylogenetic analysis of Sec7-domain-containing Arf nucleotide exchangers. *Mol Biol Cell* **15**, 1487-1505, doi:10.1091/mbc.E03-06-0443 [doi]

E03-06-0443 [pii] (2004).

164 Jackson, C. L. & Casanova, J. E. Turning on ARF: the Sec7 family of guanine-nucleotide-exchange factors. *Trends Cell Biol* **10**, 60-67, doi:S0962-8924(99)01699-2 [pii] (2000).

165 Nakano, A. & Muramatsu, M. A novel GTP-binding protein, Sar1p, is involved in transport from the endoplasmic reticulum to the Golgi apparatus. *J Cell Biol* **109**, 2677-2691 (1989).

166 Chardin, P. & Callebaut, I. The yeast Sar exchange factor Sec12, and its higher organism orthologs, fold as beta-propellers. *FEBS Lett* **525**, 171-173, doi:S0014579302030685 [pii] (2002).

167 Kahn, R. A. *et al.* Consensus nomenclature for the human ArfGAP domain-containing proteins. *J Cell Biol* **182**, 1039-1044, doi:jcb.200806041 [pii]

10.1083/jcb.200806041 [doi] (2008).

168 Randazzo, P. A., Inoue, H. & Bharti, S. Arf GAPs as regulators of the actin cytoskeleton. *Biol Cell* **99**, 583-600 (2007).

169 Bowzard, J. B., Cheng, D., Peng, J. & Kahn, R. A. ELMOD2 is an Arl2 GTPase-activating protein that also acts on Arfs. *The Journal of biological chemistry* **282**, 17568-17580 (2007).

170 Moss, J. & Vaughan, M. Molecules in the ARF orbit. *J Biol Chem* **273**, 21431-21434 (1998).

171 Donaldson, J. G. & Honda, A. Localization and function of Arf family GTPases. *Biochem Soc Trans* **33**, 639-642, doi:BST0330639 [pii]

10.1042/BST0330639 [doi] (2005).

172 Randazzo, P. A., Nie, Z., Miura, K. & Hsu, V. W. Molecular aspects of the cellular activities of ADP-ribosylation factors. *Sci STKE* **2000**, re1, doi:10.1126/stke.2000.59.re1 [doi]

2000/59/re1 [pii] (2000).

173 D'Souza-Schorey, C. & Chavrier, P. ARF proteins: roles in membrane traffic and beyond. *Nat Rev Mol Cell Biol* **7**, 347-358, doi:nrm1910 [pii]

10.1038/nrm1910 [doi] (2006).

174 Lenhard, J. M., Kahn, R. A. & Stahl, P. D. Evidence for ADP-ribosylation factor (ARF) as a regulator of in vitro endosome-endosome fusion. *J Biol Chem* **267**, 13047-13052 (1992).

175 Norman, J. C. *et al.* ARF1 mediates paxillin recruitment to focal adhesions and potentiates Rho-stimulated stress fiber formation in intact and permeabilized Swiss 3T3 fibroblasts. *J Cell Biol* **143**, 1981-1995 (1998).

176 Balch, W. E., Kahn, R. A. & Schwaninger, R. ADP-ribosylation factor is required for vesicular trafficking between the endoplasmic reticulum and the cis-Golgi compartment. *J Biol Chem* **267**, 13053-13061 (1992).

177 Kahn, R. A. *et al.* The amino terminus of ADP-ribosylation factor (ARF) is a critical determinant of ARF activities and is a potent and specific inhibitor of protein transport. *J Biol Chem* **267**, 13039-13046 (1992).

178 Serafini, T. *et al.* ADP-ribosylation factor is a subunit of the coat of Golgi-derived COP-coated vesicles: a novel role for a GTP-binding protein. *Cell* **67**, 239-253, doi:0092-8674(91)90176-Y [pii] (1991).

179 Donaldson, J. G. Multiple roles for Arf6: sorting, structuring, and signaling at the plasma membrane. *J Biol Chem* **278**, 41573-41576, doi:10.1074/jbc.R300026200 [doi]

R300026200 [pii] (2003).

180 Santy, L. C., Ravichandran, K. S. & Casanova, J. E. The DOCK180/Elmo complex couples ARNO-mediated Arf6 activation to the downstream activation of Rac1. *Curr Biol* **15**, 1749-1754, doi:S0960-9822(05)01011-0 [pii]

10.1016/j.cub.2005.08.052 [doi] (2005).

181 Santy, L. C. & Casanova, J. E. Activation of ARF6 by ARNO stimulates epithelial cell migration through downstream activation of both Rac1 and phospholipase D. *J Cell Biol* **154**, 599-610, doi:10.1083/jcb.200104019 [doi]

jcb.200104019 [pii] (2001).

182 White, D. T., McShea, K. M., Attar, M. A. & Santy, L. C. GRASP and IPCEF promote ARF-to-Rac signaling and cell migration by coordinating the association of ARNO/cytohesin 2 with Dock180. *Mol Biol Cell* **21**, 562-571, doi:E09-03-0217 [pii]

10.1091/mbc.E09-03-0217 [doi] (2010).

183 Radhakrishna, H., Al-Awar, O., Khachikian, Z. & Donaldson, J. G. ARF6 requirement for Rac ruffling suggests a role for membrane trafficking in cortical actin rearrangements. *J Cell Sci* **112 (Pt 6)**, 855-866 (1999).

184 Cotton, M. *et al.* Endogenous ARF6 interacts with Rac1 upon angiotensin II stimulation to regulate membrane ruffling and cell migration. *Mol Biol Cell* **18**, 501-511, doi:E06-06-0567 [pii]

10.1091/mbc.E06-06-0567 [doi] (2007).

185 Honda, A. *et al.* Phosphatidylinositol 4-phosphate 5-kinase alpha is a downstream effector of the small G protein ARF6 in membrane ruffle formation. *Cell* **99**, 521-532, doi:S0092-8674(00)81540-8 [pii] (1999).

186 O'Luanaigh, N. *et al.* Continual production of phosphatidic acid by phospholipase D is essential for antigen-stimulated membrane ruffling in cultured mast cells. *Mol Biol Cell* **13**, 3730-3746, doi:10.1091/mbc.E02-04-0213 [doi] (2002).

187 Jones, D. H. *et al.* Type I phosphatidylinositol 4-phosphate 5-kinase directly interacts with ADP-ribosylation factor 1 and is responsible for phosphatidylinositol 4,5-bisphosphate synthesis in the golgi compartment. *J Biol Chem* **275**, 13962-13966, doi:C901019199 [pii] (2000).

188 Bach, A. S. *et al.* ADP-ribosylation factor 6 regulates mammalian myoblast fusion through phospholipase D1 and phosphatidylinositol 4,5-bisphosphate signaling pathways. *Mol Biol Cell* **21**, 2412-2424, doi:E09-12-1063 [pii]

10.1091/mbc.E09-12-1063 [doi] (2010).

189 Chen, E. H., Pryce, B. A., Tzeng, J. A., Gonzalez, G. A. & Olson, E. N. Control of myoblast fusion by a guanine nucleotide exchange factor, loner, and its effector ARF6. *Cell* **114**, 751-762, doi:S0092867403007207 [pii] (2003).

190 Suzuki, T. *et al.* Crucial role of the small GTPase ARF6 in hepatic cord formation during liver development. *Mol Cell Biol* **26**, 6149-6156, doi:26/16/6149 [pii]

10.1128/MCB.00298-06 [doi] (2006).

191 Tamkun, J. W. *et al.* The arflike gene encodes an essential GTP-binding protein in Drosophila. *Proc Natl Acad Sci U S A* **88**, 3120-3124 (1991).

192 Clark, J. *et al.* Selective amplification of additional members of the ADP-ribosylation factor (ARF) family: cloning of additional human and Drosophila ARF-like genes. *Proc Natl Acad Sci U S A* **90**, 8952-8956 (1993).

193 Burd, C. G., Strochlic, T. I. & Gangi Setty, S. R. Arf-like GTPases: not so Arf-like after all. *Trends Cell Biol* **14**, 687-694, doi:S0962-8924(04)00283-1 [pii]

10.1016/j.tcb.2004.10.004 [doi] (2004).

194 Bhamidipati, A., Lewis, S. A. & Cowan, N. J. ADP ribosylation factor-like protein 2 (Arl2) regulates the interaction of tubulin-folding cofactor D with native tubulin. *J Cell Biol* **149**, 1087-1096 (2000).

195 Hoyt, M. A., Stearns, T. & Botstein, D. Chromosome instability mutants of Saccharomyces cerevisiae that are defective in microtubule-mediated processes. *Mol Cell Biol* **10**, 223-234 (1990).

196 Li, Y. *et al.* Functional genomic analysis of the ADP-ribosylation factor family of GTPases: phylogeny among diverse eukaryotes and function in C. elegans. *FASEB J* **18**, 1834-1850, doi:18/15/1834 [pii]

10.1096/fj.04-2273com [doi] (2004).

197 Sharer, J. D., Shern, J. F., Van Valkenburgh, H., Wallace, D. C. & Kahn, R. A. ARL2 and BART enter mitochondria and bind the adenine nucleotide transporter. *Mol Biol Cell* **13**, 71-83, doi:10.1091/mbc.01-05-0245 [doi] (2002).

198 Zhou, C., Cunningham, L., Marcus, A. I., Li, Y. & Kahn, R. A. Arl2 and Arl3 regulate different microtubule-dependent processes. *Mol Biol Cell* **17**, 2476-2487, doi:E05-10-0929 [pii]

10.1091/mbc.E05-10-0929 [doi] (2006).

199 Hofmann, I. & Munro, S. An N-terminally acetylated Arf-like GTPase is localised to lysosomes and affects their motility. *J Cell Sci* **119**, 1494-1503, doi:jcs.02958 [pii]

10.1242/jcs.02958 [doi] (2006).

200 Okai, T. *et al.* Novel small GTPase subfamily capable of associating with tubulin is required for chromosome segregation. *J Cell Sci* **117**, 4705-4715, doi:10.1242/jcs.01347 [doi]

jcs.01347 [pii] (2004).

201 Avidor-Reiss, T. *et al.* Decoding cilia function: defining specialized genes required for compartmentalized cilia biogenesis. *Cell* **117**, 527-539, doi:S009286740400412X [pii] (2004).

202 Chiang, A. P. *et al.* Comparative genomic analysis identifies an ADP-ribosylation factor-like gene as the cause of Bardet-Biedl syndrome (BBS3). *Am J Hum Genet* **75**, 475-484, doi:10.1086/423903 [doi]

S0002-9297(07)63318-7 [pii] (2004).

203 Fan, Y. *et al.* Mutations in a member of the Ras superfamily of small GTP-binding proteins causes Bardet-Biedl syndrome. *Nat Genet* **36**, 989-993, doi:10.1038/ng1414 [doi]

ng1414 [pii] (2004).

204 Li, J. B. *et al.* Comparative genomics identifies a flagellar and basal body proteome that includes the BBS5 human disease gene. *Cell* **117**, 541-552, doi:S0092867404004507 [pii] (2004).

205 Pazour, G. J., Agrin, N., Leszyk, J. & Witman, G. B. Proteomic analysis of a eukaryotic cilium. *J Cell Biol* **170**, 103-113, doi:jcb.200504008 [pii]

10.1083/jcb.200504008 [doi] (2005).

206 Schrick, J. J., Vogel, P., Abuin, A., Hampton, B. & Rice, D. S. ADP-ribosylation factor-like 3 is involved in kidney and photoreceptor development. *Am J Pathol* **168**, 1288-1298, doi:168/4/1288 [pii] (2006).

207 Calin, G. A. *et al.* Familial cancer associated with a polymorphism in ARLTS1. *N Engl J Med* **352**, 1667-1676, doi:352/16/1667 [pii]

10.1056/NEJMoa042280 [doi] (2005).

208 Petrocca, F. *et al.* Alterations of the tumor suppressor gene ARLTS1 in ovarian cancer. *Cancer Res* **66**, 10287-10291, doi:66/21/10287 [pii]

10.1158/0008-5472.CAN-06-2289 [doi] (2006).

209 Hofmann, I., Thompson, A., Sanderson, C. M. & Munro, S. The Arl4 family of small G proteins can recruit the cytohesin Arf6 exchange factors to the plasma membrane. *Curr Biol* **17**, 711-716, doi:S0960-9822(07)01074-3 [pii]

10.1016/j.cub.2007.03.007 [doi] (2007).

210 Li, C. C. *et al.* ARL4D recruits cytohesin-2/ARNO to modulate actin remodeling. *Mol Biol Cell* **18**, 4420-4437, doi:E07-02-0149 [pii]

10.1091/mbc.E07-02-0149 [doi] (2007).

211 Dingwall, C. & Laskey, R. A. Nuclear targeting sequences--a consensus? *Trends Biochem Sci* **16**, 478-481 (1991).

212 Jacobs, S. *et al.* ADP-ribosylation factor (ARF)-like 4, 6, and 7 represent a subgroup of the ARF family characterization by rapid nucleotide exchange and a nuclear localization signal. *FEBS Lett* **456**, 384-388, doi:S0014579399007590 [pii] (1999).

213 Lin, C. Y. *et al.* ARL4, an ARF-like protein that is developmentally regulated and localized to nuclei and nucleoli. *J Biol Chem* **275**, 37815-37823, doi:10.1074/jbc.M002470200 [doi]

M002470200 [pii] (2000).

214 Schurmann, A. *et al.* Reduced sperm count and normal fertility in male mice with targeted disruption of the ADP-ribosylation factor-like 4 (Arl4) gene. *Mol Cell Biol* **22**, 2761-2768 (2002).

215 Shen, H. M., Dai, J., Chia, S. E., Lim, A. & Ong, C. N. Detection of apoptotic alterations in sperm in subfertile patients and their correlations with sperm quality. *Hum Reprod* **17**, 1266-1273 (2002).

216 Chardin, P. *et al.* A human exchange factor for ARF contains Sec7- and pleckstrin-homology domains. *Nature* **384**, 481-484, doi:10.1038/384481a0 [doi] (1996).

217 Cohen, L. A. *et al.* Active Arf6 recruits ARNO/cytohesin GEFs to the PM by binding their PH domains. *Mol Biol Cell* **18**, 2244-2253, doi:E06-11-0998 [pii]

10.1091/mbc.E06-11-0998 [doi] (2007).

218 Klarlund, J. K., Tsiaras, W., Holik, J. J., Chawla, A. & Czech, M. P. Distinct polyphosphoinositide binding selectivities for pleckstrin homology domains of GRP1-like proteins based on diglycine versus triglycine motifs. *J Biol Chem* **275**, 32816-32821, doi:10.1074/jbc.M002435200 [doi]

M002435200 [pii] (2000).

219 Wallar, B. J. & Alberts, A. S. The formins: active scaffolds that remodel the cytoskeleton. *Trends Cell Biol* **13**, 435-446, doi:S0962892403001533 [pii] (2003).

220 Aspenstrom, P. Formin-binding proteins: modulators of formin-dependent actin polymerization. *Biochim Biophys Acta* **1803**, 174-182, doi:S0167-4889(09)00168-2 [pii]

10.1016/j.bbamcr.2009.06.002 [doi] (2010).

221 Otomo, T., Otomo, C., Tomchick, D. R., Machius, M. & Rosen, M. K. Structural basis of Rho GTPase-mediated activation of the formin mDia1. *Mol Cell* **18**, 273-281, doi:S1097-2765(05)01226-8 [pii]

10.1016/j.molcel.2005.04.002 (2005).

222 Schonichen, A. *et al.* Biochemical characterization of the diaphanous autoregulatory interaction in the formin homology protein FHOD1. *J Biol Chem* **281**, 5084-5093, doi:M509226200 [pii]

10.1074/jbc.M509226200 [doi] (2006).

223 Wallar, B. J. *et al.* The basic region of the diaphanous-autoregulatory domain (DAD) is required for autoregulatory interactions with the diaphanous-related formin inhibitory domain. *J Biol Chem* **281**, 4300-4307, doi:M510277200 [pii]

10.1074/jbc.M510277200 [doi] (2006).

224 Rose, R. *et al.* Structural and mechanistic insights into the interaction between Rho and mammalian Dia. *Nature* **435**, 513-518, doi:nature03604 [pii]

10.1038/nature03604 [doi] (2005).

225 Nezami, A. G., Poy, F. & Eck, M. J. Structure of the autoinhibitory switch in formin mDia1. *Structure* **14**, 257-263, doi:S0969-2126(06)00045-1 [pii]

10.1016/j.str.2005.12.003 (2006).

226 Lammers, M., Rose, R., Scrima, A. & Wittinghofer, A. The regulation of mDia1 by autoinhibition and its release by Rho*GTP. *EMBO J* **24**, 4176-4187, doi:7600879 [pii]

10.1038/sj.emboj.7600879 (2005).

227 Alberts, A. S. Identification of a carboxyl-terminal diaphanous-related formin homology protein autoregulatory domain. *J Biol Chem* **276**, 2824-2830, doi:10.1074/jbc.M006205200 [doi]

M006205200 [pii] (2001).

228 Li, F. & Higgs, H. N. The mouse Formin mDia1 is a potent actin nucleation factor regulated by autoinhibition. *Curr Biol* **13**, 1335-1340, doi:S0960982203005402 [pii] (2003).

229 Watanabe, N., Kato, T., Fujita, A., Ishizaki, T. & Narumiya, S. Cooperation between mDia1 and ROCK in Rho-induced actin reorganization. *Nat Cell Biol* **1**, 136-143, doi:10.1038/11056 [doi] (1999).

230 Xu, Y. *et al.* Crystal structures of a Formin Homology-2 domain reveal a tethered dimer architecture. *Cell* **116**, 711-723, doi:S0092867404002107 [pii] (2004).

231 Schonichen, A. & Geyer, M. Fifteen formins for an actin filament: a molecular view on the regulation of human formins. *Biochim Biophys Acta* **1803**, 152-163, doi:S0167-4889(10)00015-7 [pii]

10.1016/j.bbamcr.2010.01.014 [doi] (2010).

232 Watanabe, N. *et al.* p140mDia, a mammalian homolog of Drosophila diaphanous, is a target protein for Rho small GTPase and is a ligand for profilin. *EMBO J* **16**, 3044-3056, doi:10.1093/emboj/16.11.3044 [doi] (1997).

233 Pellegrin, S. & Mellor, H. The Rho family GTPase Rif induces filopodia through mDia2. *Curr Biol* **15**, 129-133, doi:S096098220500031X [pii]

10.1016/j.cub.2005.01.011 [doi] (2005).

234 Fan, L., Pellegrin, S., Scott, A. & Mellor, H. The small GTPase Rif is an alternative trigger for the formation of actin stress fibers in epithelial cells. *J Cell Sci* **123**, 1247-1252, doi:jcs.061754 [pii]

10.1242/jcs.061754 [doi] (2010).

235 Brandt, D. T. *et al.* Dia1 and IQGAP1 interact in cell migration and phagocytic cup formation. *J Cell Biol* **178**, 193-200, doi:jcb.200612071 [pii]

10.1083/jcb.200612071 [doi] (2007).

236 Habas, R., Kato, Y. & He, X. Wnt/Frizzled activation of Rho regulates vertebrate gastrulation and requires a novel Formin homology protein Daam1. *Cell* **107**, 843-854, doi:S0092-8674(01)00614-6 [pii] (2001).

237 Liu, W. *et al.* Mechanism of activation of the Formin protein Daam1. *Proc Natl Acad Sci U S A* **105**, 210-215, doi:0707277105 [pii]

10.1073/pnas.0707277105 [doi] (2008).

238 Li, F. & Higgs, H. N. Dissecting requirements for auto-inhibition of actin nucleation by the formin, mDia1. *J Biol Chem* **280**, 6986-6992, doi:M411605200 [pii]

10.1074/jbc.M411605200 [doi] (2005).

239 Seth, A., Otomo, C. & Rosen, M. K. Autoinhibition regulates cellular localization and actin assembly activity of the diaphanous-related formins FRLalpha and mDia1. *J Cell Biol* **174**, 701-713, doi:jcb.200605006 [pii]

10.1083/jcb.200605006 [doi] (2006).

240 Westendorf, J. J. The formin/diaphanous-related protein, FHOS, interacts with Rac1 and activates transcription from the serum response element. *J Biol Chem* **276**, 46453-46459, doi:10.1074/jbc.M105162200 [doi]

M105162200 [pii] (2001).

241 Gasteier, J. E. *et al.* Activation of the Rac-binding partner FHOD1 induces actin stress fibers via a ROCK-dependent mechanism. *J Biol Chem* **278**, 38902-38912, doi:10.1074/jbc.M306229200 [doi]

M306229200 [pii] (2003).

242 Takeya, R., Taniguchi, K., Narumiya, S. & Sumimoto, H. The mammalian formin FHOD1 is activated through phosphorylation by ROCK and mediates thrombin-induced stress fibre formation in endothelial cells. *EMBO J* **27**, 618-628, doi:emboj20087 [pii]

10.1038/emboj.2008.7 [doi] (2008).

243 Young, K. G. & Copeland, J. W. Formins in cell signaling. *Biochim Biophys Acta* **1803**, 183-190, doi:S0167-4889(08)00342-X [pii]

10.1016/j.bbamcr.2008.09.017 [doi] (2010).

244 Zhang, Q., Calafat, J., Janssen, H. & Greenberg, S. ARF6 is required for growth factor- and rac-mediated membrane ruffling in macrophages at a stage distal to rac membrane targeting. *Mol Cell Biol* **19**, 8158-8168 (1999).

245 Koo, T. H., Eipper, B. A. & Donaldson, J. G. Arf6 recruits the Rac GEF Kalirin to the plasma membrane facilitating Rac activation. *BMC Cell Biol* **8**, 29, doi:1471-2121-8-29 [pii]

10.1186/1471-2121-8-29 [doi] (2007).

246 Albertinazzi, C., Za, L., Paris, S. & de Curtis, I. ADP-ribosylation factor 6 and a functional PIX/p95-APP1 complex are required for Rac1B-mediated neurite outgrowth. *Mol Biol Cell* **14**, 1295-1307, doi:10.1091/mbc.E02-07-0406 [doi] (2003).

247 Palacios, F. & D'Souza-Schorey, C. Modulation of Rac1 and ARF6 activation during epithelial cell scattering. *J Biol Chem* **278**, 17395-17400, doi:10.1074/jbc.M300998200 [doi]

M300998200 [pii] (2003).

248 Palacios, F., Schweitzer, J. K., Boshans, R. L. & D'Souza-Schorey, C. ARF6-GTP recruits Nm23-H1 to facilitate dynamin-mediated endocytosis during adherens junctions disassembly. *Nat Cell Biol* **4**, 929-936, doi:10.1038/ncb881 [doi]

ncb881 [pii] (2002).

249 Balasubramanian, N., Scott, D. W., Castle, J. D., Casanova, J. E. & Schwartz, M. A. Arf6 and microtubules in adhesion-dependent trafficking of lipid rafts. *Nat Cell Biol* **9**, 1381-1391, doi:ncb1657 [pii]

10.1038/ncb1657 [doi] (2007).

250 Hiramoto, K., Negishi, M. & Katoh, H. Dock4 is regulated by RhoG and promotes Rac-dependent cell migration. *Exp Cell Res* **312**, 4205-4216, doi:S0014-4827(06)00384-3 [pii]

10.1016/j.yexcr.2006.09.006 [doi] (2006).

251 Katoh, H., Hiramoto, K. & Negishi, M. Activation of Rac1 by RhoG regulates cell migration. *J Cell Sci* **119**, 56-65, doi:jcs.02720 [pii]

10.1242/jcs.02720 [doi] (2006).

252 Gumienny, T. L. *et al.* CED-12/ELMO, a novel member of the CrkII/Dock180/Rac pathway, is required for phagocytosis and cell migration. *Cell* **107**, 27-41, doi:S0092-8674(01)00520-7 [pii] (2001).

253 Zhou, Z., Caron, E., Hartwieg, E., Hall, A. & Horvitz, H. R. The C. elegans PH domain protein CED-12 regulates cytoskeletal reorganization via a Rho/Rac GTPase signaling pathway. *Dev Cell* **1**, 477-489, doi:S1534-5807(01)00058-2 [pii] (2001).

254 Wu, Y. C., Tsai, M. C., Cheng, L. C., Chou, C. J. & Weng, N. Y. C. elegans CED-12 acts in the conserved crkII/DOCK180/Rac pathway to control cell migration and cell corpse engulfment. *Dev Cell* **1**, 491-502, doi:S1534-5807(01)00056-9 [pii] (2001).

255 deBakker, C. D. *et al.* Phagocytosis of apoptotic cells is regulated by a UNC-73/TRIO-MIG-2/RhoG signaling module and armadillo repeats of CED-12/ELMO. *Curr Biol* **14**, 2208-2216, doi:S0960982204009893 [pii]

10.1016/j.cub.2004.12.029 [doi] (2004).

256 Hu, B. *et al.* ADP-ribosylation factor 6 regulates glioma cell invasion through the IQ-domain GTPase-activating protein 1-Rac1-mediated pathway. *Cancer Res* **69**, 794-801, doi:0008-5472.CAN-08-2110 [pii]

10.1158/0008-5472.CAN-08-2110 [doi] (2009).

257 Palamidessi, A. *et al.* Endocytic trafficking of Rac is required for the spatial restriction of signaling in cell migration. *Cell* **134**, 135-147, doi:S0092-8674(08)00696-X [pii]

10.1016/j.cell.2008.05.034 [doi] (2008).

258 Hasegawa, H. *et al.* DOCK180, a major CRK-binding protein, alters cell morphology upon translocation to the cell membrane. *Mol Cell Biol* **16**, 1770-1776 (1996).

259 Kiyokawa, E. *et al.* Activation of Rac1 by a Crk SH3-binding protein, DOCK180. *Genes Dev* **12**, 3331-3336 (1998).

260 Erickson, M. R., Galletta, B. J. & Abmayr, S. M. Drosophila myoblast city encodes a conserved protein that is essential for myoblast fusion, dorsal closure, and cytoskeletal organization. *J Cell Biol* **138**, 589-603 (1997).

261 Wu, Y. C. & Horvitz, H. R. C. elegans phagocytosis and cell-migration protein CED-5 is similar to human DOCK180. *Nature* **392**, 501-504, doi:10.1038/33163 [doi] (1998).

262 Reddien, P. W. & Horvitz, H. R. CED-2/CrkII and CED-10/Rac control phagocytosis and cell migration in Caenorhabditis elegans. *Nat Cell Biol* **2**, 131-136, doi:10.1038/35004000 [doi] (2000).

263 Albert, M. L., Kim, J. I. & Birge, R. B. alphavbeta5 integrin recruits the CrkII-Dock180-rac1 complex for phagocytosis of apoptotic cells. *Nat Cell Biol* **2**, 899-905, doi:10.1038/35046549 [doi] (2000).

264 Harden, N., Loh, H. Y., Chia, W. & Lim, L. A dominant inhibitory version of the small GTP-binding protein Rac disrupts cytoskeletal structures and inhibits developmental cell shape changes in Drosophila. *Development* **121**, 903-914 (1995).

265 Cote, J. F. & Vuori, K. Identification of an evolutionarily conserved superfamily of DOCK180-related proteins with guanine nucleotide exchange activity. *J Cell Sci* **115**, 4901-4913 (2002).

266 Meller, N., Merlot, S. & Guda, C. CZH proteins: a new family of Rho-GEFs. *J Cell Sci* **118**, 4937-4946, doi:118/21/4937 [pii]

10.1242/jcs.02671 [doi] (2005).

267 Brugnera, E. *et al.* Unconventional Rac-GEF activity is mediated through the Dock180-ELMO complex. *Nat Cell Biol* **4**, 574-582, doi:10.1038/ncb824

ncb824 [pii] (2002).

268 Cote, J. F. & Vuori, K. In vitro guanine nucleotide exchange activity of DHR-2/DOCKER/CZH2 domains. *Methods Enzymol* **406**, 41-57, doi:S0076-6879(06)06004-6 [pii]

10.1016/S0076-6879(06)06004-6 [doi] (2006).

269 Namekata, K., Enokido, Y., Iwasawa, K. & Kimura, H. MOCA induces membrane spreading by activating Rac1. *J Biol Chem* **279**, 14331-14337, doi:10.1074/jbc.M311275200 [doi]

M311275200 [pii] (2004).

270 Miyamoto, Y., Yamauchi, J., Sanbe, A. & Tanoue, A. Dock6, a Dock-C subfamily guanine nucleotide exchanger, has the dual specificity for Rac1 and Cdc42 and regulates neurite outgrowth. *Exp Cell Res* **313**, 791-804, doi:S0014-4827(06)00487-3 [pii]

10.1016/j.yexcr.2006.11.017 [doi] (2007).

271 Watabe-Uchida, M., John, K. A., Janas, J. A., Newey, S. E. & Van Aelst, L. The Rac activator DOCK7 regulates neuronal polarity through local phosphorylation of stathmin/Op18. *Neuron* **51**, 727-739, doi:S0896-6273(06)00585-X [pii]

10.1016/j.neuron.2006.07.020 [doi] (2006).

272 Meller, N., Irani-Tehrani, M., Kiosses, W. B., Del Pozo, M. A. & Schwartz, M. A. Zizimin1, a novel Cdc42 activator, reveals a new GEF domain for Rho proteins. *Nat Cell Biol* **4**, 639-647, doi:10.1038/ncb835 [doi]

ncb835 [pii] (2002).

273 Gadea, G., Sanz-Moreno, V., Self, A., Godi, A. & Marshall, C. J. DOCK10-mediated Cdc42 activation is necessary for amoeboid invasion of melanoma cells. *Curr Biol* **18**, 1456-1465, doi:S0960-9822(08)01131-7 [pii]

10.1016/j.cub.2008.08.053 [doi] (2008).

274 Cote, J. F., Motoyama, A. B., Bush, J. A. & Vuori, K. A novel and evolutionarily conserved PtdIns(3,4,5)P3-binding domain is necessary for DOCK180 signalling. *Nat Cell Biol* **7**, 797-807, doi:ncb1280 [pii]

10.1038/ncb1280 [doi] (2005).

275 Kanai, A. *et al.* Identification of DOCK4 and its splicing variant as PIP3 binding proteins. *IUBMB Life* **60**, 467-472, doi:10.1002/iub.67 [doi] (2008).

276 Nishikimi, A. *et al.* Sequential regulation of DOCK2 dynamics by two phospholipids during neutrophil chemotaxis. *Science* **324**, 384-387, doi:1170179 [pii]

10.1126/science.1170179 [doi] (2009).

277 Meller, N., Westbrook, M. J., Shannon, J. D., Guda, C. & Schwartz, M. A. Function of the N-terminus of zizimin1: autoinhibition and membrane targeting. *The Biochemical journal* **409**, 525-533 (2008).

278 Premkumar, L. *et al.* Structural basis of membrane targeting by the Dock180 family of Rho family guanine exchange factors (Rho-GEFs). *J Biol Chem* **285**, 13211-13222, doi:M110.102517 [pii]

10.1074/jbc.M110.102517 [doi] (2010).

279 Mayer, B. J., Hamaguchi, M. & Hanafusa, H. A novel viral oncogene with structural similarity to phospholipase C. *Nature* **332**, 272-275, doi:10.1038/332272a0 [doi] (1988).

280 ten Hoeve, J., Morris, C., Heisterkamp, N. & Groffen, J. Isolation and chromosomal localization of CRKL, a human crk-like gene. *Oncogene* **8**, 2469-2474 (1993).

281 Prosser, S., Sorokina, E., Pratt, P. & Sorokin, A. CrkIII: a novel and biologically distinct member of the Crk family of adaptor proteins. *Oncogene* **22**, 4799-4806, doi:10.1038/sj.onc.1206714 [doi]

1206714 [pii] (2003).

282 Feller, S. M. Crk family adaptors-signalling complex formation and biological roles. *Oncogene* **20**, 6348-6371, doi:10.1038/sj.onc.1204779 [doi] (2001).

283 Matsuda, M. *et al.* Two species of human CRK cDNA encode proteins with distinct biological activities. *Mol Cell Biol* **12**, 3482-3489 (1992).

284 Birge, R. B., Fajardo, J. E., Mayer, B. J. & Hanafusa, H. Tyrosine-phosphorylated epidermal growth factor receptor and cellular p130 provide high affinity binding substrates to analyze Crk-phosphotyrosine-dependent interactions in vitro. *J Biol Chem* **267**, 10588-10595 (1992).

285 Birge, R. B. *et al.* Identification and characterization of a high-affinity interaction between v-Crk and tyrosine-phosphorylated paxillin in CT10-transformed fibroblasts. *Mol Cell Biol* **13**, 4648-4656 (1993).

286 Garcia-Guzman, M., Dolfi, F., Zeh, K. & Vuori, K. Met-induced JNK activation is mediated by the adapter protein Crk and correlates with the Gab1 - Crk signaling complex formation. *Oncogene* **18**, 7775-7786, doi:10.1038/sj.onc.1203198 [doi] (1999).

287 Kiyokawa, E., Hashimoto, Y., Kurata, T., Sugimura, H. & Matsuda, M. Evidence that DOCK180 up-regulates signals from the CrkII-p130(Cas) complex. *J Biol Chem* **273**, 24479-24484 (1998).

288 Knudsen, B. S., Feller, S. M. & Hanafusa, H. Four proline-rich sequences of the guanine-nucleotide exchange factor C3G bind with unique specificity to the first Src homology 3 domain of Crk. *J Biol Chem* **269**, 32781-32787 (1994).

289 Akakura, S. *et al.* C-terminal SH3 domain of CrkII regulates the assembly and function of the DOCK180/ELMO Rac-GEF. *J Cell Physiol* **204**, 344-351, doi:10.1002/jcp.20288 [doi] (2005).

290 Imaizumi, T. *et al.* Mutant mice lacking Crk-II caused by the gene trap insertional mutagenesis: Crk-II is not essential for embryonic development. *Biochem Biophys Res Commun* **266**, 569-574, doi:10.1006/bbrc.1999.1869 [doi]

S0006291X99918697 [pii] (1999).

291 Guris, D. L., Fantes, J., Tara, D., Druker, B. J. & Imamoto, A. Mice lacking the homologue of the human 22q11.2 gene CRKL phenocopy neurocristopathies of DiGeorge syndrome. *Nat Genet* **27**, 293-298, doi:10.1038/85855 [doi] (2001).

292 Park, T. J., Boyd, K. & Curran, T. Cardiovascular and craniofacial defects in Crk-null mice. *Mol Cell Biol* **26**, 6272-6282, doi:26/16/6272 [pii]

10.1128/MCB.00472-06 [doi] (2006).

293 Park, D. *et al.* BAI1 is an engulfment receptor for apoptotic cells upstream of the ELMO/Dock180/Rac module. *Nature* **450**, 430-434, doi:nature06329 [pii]

10.1038/nature06329 [doi] (2007).

294 Lu, M. *et al.* PH domain of ELMO functions in trans to regulate Rac activation via Dock180. *Nat Struct Mol Biol* **11**, 756-762, doi:10.1038/nsmb800 [doi]

nsmb800 [pii] (2004).

295 Lu, M. *et al.* A Steric-inhibition model for regulation of nucleotide exchange via the Dock180 family of GEFs. *Curr Biol* **15**, 371-377, doi:S0960982205001120 [pii]

10.1016/j.cub.2005.01.050 [doi] (2005).

296 Lu, M. & Ravichandran, K. S. Dock180-ELMO cooperation in Rac activation. *Methods Enzymol* **406**, 388-402, doi:S0076-6879(06)06028-9 [pii]

10.1016/S0076-6879(06)06028-9 [doi] (2006).

297 Haslam, R. J., Koide, H. B. & Hemmings, B. A. Pleckstrin domain homology. *Nature* **363**, 309-310, doi:10.1038/363309b0 [doi] (1993).

298 Mayer, B. J., Ren, R., Clark, K. L. & Baltimore, D. A putative modular domain present in diverse signaling proteins. *Cell* **73**, 629-630, doi:0092-8674(93)90244-K [pii] (1993).

299 Timm, D. *et al.* Crystal structure of the pleckstrin homology domain from dynamin. *Nat Struct Biol* **1**, 782-788 (1994).

300 Ferguson, K. M., Lemmon, M. A., Schlessinger, J. & Sigler, P. B. Crystal structure at 2.2 A resolution of the pleckstrin homology domain from human dynamin. *Cell* **79**, 199-209, doi:0092-8674(94)90190-2 [pii] (1994).

301 Ferguson, K. M., Lemmon, M. A., Schlessinger, J. & Sigler, P. B. Structure of the high affinity complex of inositol trisphosphate with a phospholipase C pleckstrin homology domain. *Cell* **83**, 1037-1046 (1995).

302 Harlan, J. E., Hajduk, P. J., Yoon, H. S. & Fesik, S. W. Pleckstrin homology domains bind to phosphatidylinositol-4,5-bisphosphate. *Nature* **371**, 168-170, doi:10.1038/371168a0 [doi] (1994).

303 Miroshnychenko, D., Dubrovska, A., Maliuta, S., Telegeev, G. & Aspenstrom, P. Novel role of pleckstrin homology domain of the Bcr-Abl protein: analysis of protein-protein and protein-lipid interactions. *Exp Cell Res* **316**, 530-542, doi:S0014-4827(09)00513-8 [pii]

10.1016/j.yexcr.2009.11.014 [doi] (2010).

304 Grimsley, C. M. *et al.* Dock180 and ELMO1 proteins cooperate to promote evolutionarily conserved Rac-dependent cell migration. *J Biol Chem* **279**, 6087-6097, doi:10.1074/jbc.M307087200 [doi]

M307087200 [pii] (2004).

305 Yamauchi, J., Miyamoto, Y., Chan, J. R. & Tanoue, A. ErbB2 directly activates the exchange factor Dock7 to promote Schwann cell migration. *J Cell Biol* **181**, 351-365, doi:jcb.200709033 [pii]

10.1083/jcb.200709033 [doi] (2008).

306 Yokoyama, N. *et al.* Identification of tyrosine residues on ELMO1 that are phosphorylated by the Src-family kinase Hck. *Biochemistry* **44**, 8841-8849, doi:10.1021/bi0500832 [doi] (2005).

307 Makino, Y. *et al.* Elmo1 inhibits ubiquitylation of Dock180. *J Cell Sci* **119**, 923-932, doi:119/5/923 [pii]

10.1242/jcs.02797 [doi] (2006).

308 Rossman, K. L. *et al.* A crystallographic view of interactions between Dbs and Cdc42: PH domain-assisted guanine nucleotide exchange. *EMBO J* **21**, 1315-1326, doi:10.1093/emboj/21.6.1315 [doi] (2002).

309 Zhu, K., Debreceni, B., Bi, F. & Zheng, Y. Oligomerization of DH domain is essential for Dbl-induced transformation. *Mol Cell Biol* **21**, 425-437, doi:10.1128/MCB.21.2.425-437.2001 [doi] (2001).

310 Worthylake, D. K., Rossman, K. L. & Sondek, J. Crystal structure of Rac1 in complex with the guanine nucleotide exchange region of Tiam1. *Nature* **408**, 682-688, doi:10.1038/35047014 [doi] (2000).

311 Anborgh, P. H. *et al.* Ras-specific exchange factor GRF: oligomerization through its Dbl homology domain and calcium-dependent activation of Raf. *Mol Cell Biol* **19**, 4611-4622 (1999).

312 Meller, N., Irani-Tehrani, M., Ratnikov, B. I., Paschal, B. M. & Schwartz, M. A. The novel Cdc42 guanine nucleotide exchange factor, zizimin1, dimerizes via the Cdc42-binding CZH2 domain. *J Biol Chem* **279**, 37470-37476, doi:10.1074/jbc.M404535200 [doi]

M404535200 [pii] (2004).

313 Kinchen, J. M. & Ravichandran, K. S. Journey to the grave: signaling events regulating removal of apoptotic cells. *J Cell Sci* **120**, 2143-2149, doi:120/13/2143 [pii]

10.1242/jcs.03463 [doi] (2007).

314 Ravichandran, K. S. Find-me and eat-me signals in apoptotic cell clearance: progress and conundrums. *J Exp Med* **207**, 1807-1817, doi:jem.20101157 [pii]

10.1084/jem.20101157 [doi] (2010).

315 Ravichandran, K. S. & Lorenz, U. Engulfment of apoptotic cells: signals for a good meal. *Nat Rev Immunol* **7**, 964-974, doi:nri2214 [pii]

10.1038/nri2214 [doi] (2007).

316 Fadok, V. A. *et al.* Exposure of phosphatidylserine on the surface of apoptotic lymphocytes triggers specific recognition and removal by macrophages. *J Immunol* **148**, 2207-2216 (1992).

317 Henson, P. M., Bratton, D. L. & Fadok, V. A. Apoptotic cell removal. *Curr Biol* **11**, R795-805, doi:S0960-9822(01)00474-2 [pii] (2001).

318 Wang, X. *et al.* Cell corpse engulfment mediated by C. elegans phosphatidylserine receptor through CED-5 and CED-12. *Science* **302**, 1563-1566, doi:10.1126/science.1087641 [doi]

302/5650/1563 [pii] (2003).

319 Savill, J. Recognition and phagocytosis of cells undergoing apoptosis. *Br Med Bull* **53**, 491-508 (1997).

320 Couto, J. R., Taylor, M. R., Godwin, S. G., Ceriani, R. L. & Peterson, J. A. Cloning and sequence analysis of human breast epithelial antigen BA46 reveals an RGD cell adhesion sequence presented on an epidermal growth factor-like domain. *DNA Cell Biol* **15**, 281-286 (1996).

321 Andersen, M. H., Graversen, H., Fedosov, S. N., Petersen, T. E. & Rasmussen, J. T. Functional analyses of two cellular binding domains of bovine lactadherin. *Biochemistry* **39**, 6200-6206, doi:bi992221r [pii] (2000).

322 Akakura, S. *et al.* The opsonin MFG-E8 is a ligand for the alphavbeta5 integrin and triggers DOCK180-dependent Rac1 activation for the phagocytosis of apoptotic cells. *Exp Cell Res* **292**, 403-416, doi:S0014482703004877 [pii] (2004).

323 Ishimoto, Y., Ohashi, K., Mizuno, K. & Nakano, T. Promotion of the uptake of PS liposomes and apoptotic cells by a product of growth arrest-specific gene, gas6. *J Biochem* **127**, 411-417 (2000).

324 Wu, Y., Singh, S., Georgescu, M. M. & Birge, R. B. A role for Mer tyrosine kinase in alphavbeta5 integrin-mediated phagocytosis of apoptotic cells. *J Cell Sci* **118**, 539-553, doi:118/3/539 [pii]

10.1242/jcs.01632 [doi] (2005).

325 Elliott, M. R. *et al.* Unexpected requirement for ELMO1 in clearance of apoptotic germ cells in vivo. *Nature* **467**, 333-337, doi:nature09356 [pii]

10.1038/nature09356 [doi] (2010).

326 Kimble, J. & Hirsh, D. The postembryonic cell lineages of the hermaphrodite and male gonads in Caenorhabditis elegans. *Dev Biol* **70**, 396-417, doi:0012-1606(79)90035-6 [pii] (1979).

327 Duchek, P., Somogyi, K., Jekely, G., Beccari, S. & Rorth, P. Guidance of cell migration by the Drosophila PDGF/VEGF receptor. *Cell* **107**, 17-26, doi:S0092-8674(01)00502-5 [pii] (2001).

328 Bianco, A. *et al.* Two distinct modes of guidance signalling during collective migration of border cells. *Nature* **448**, 362-365, doi:nature05965 [pii]

10.1038/nature05965 [doi] (2007).

329 Kim, S. *et al.* A critical function for the actin cytoskeleton in targeted exocytosis of prefusion vesicles during myoblast fusion. *Dev Cell* **12**, 571-586, doi:S1534-5807(07)00098-6 [pii]

10.1016/j.devcel.2007.02.019 [doi] (2007).

330 Rau, A. *et al.* rolling pebbles (rols) is required in Drosophila muscle precursors for recruitment of myoblasts for fusion. *Development* **128**, 5061-5073 (2001).

331 Balagopalan, L., Chen, M. H., Geisbrecht, E. R. & Abmayr, S. M. The CDM superfamily protein MBC directs myoblast fusion through a mechanism that requires phosphatidylinositol 3,4,5-triphosphate binding but is independent of direct interaction with DCrk. *Mol Cell Biol* **26**, 9442-9455, doi:MCB.00016-06 [pii]

10.1128/MCB.00016-06 [doi] (2006).

332 Nolan, K. M. *et al.* Myoblast city, the Drosophila homolog of DOCK180/CED-5, is required in a Rac signaling pathway utilized for multiple developmental processes. *Genes Dev* **12**, 3337-3342 (1998).

333 Geisbrecht, E. R. *et al.* Drosophila ELMO/CED-12 interacts with Myoblast city to direct myoblast fusion and ommatidial organization. *Dev Biol* **314**, 137-149, doi:S0012-1606(07)01553-9 [pii]

10.1016/j.ydbio.2007.11.022 [doi] (2008).

334 Moore, C. A., Parkin, C. A., Bidet, Y. & Ingham, P. W. A role for the Myoblast city homologues Dock1 and Dock5 and the adaptor proteins Crk and Crk-like in zebrafish myoblast fusion. *Development* **134**, 3145-3153, doi:dev.001214 [pii]

10.1242/dev.001214 [doi] (2007).

335 Horsley, V. & Pavlath, G. K. Forming a multinucleated cell: molecules that regulate myoblast fusion. *Cells Tissues Organs* **176**, 67-78, doi:10.1159/000075028 [doi]

CTO20041761_3067 [pii] (2004).

336 Laurin, M. *et al.* The atypical Rac activator Dock180 (Dock1) regulates myoblast fusion in vivo. *Proc Natl Acad Sci U S A* **105**, 15446-15451, doi:0805546105 [pii]

10.1073/pnas.0805546105 (2008).

337 Fukui, Y. *et al.* Haematopoietic cell-specific CDM family protein DOCK2 is essential for lymphocyte migration. *Nature* **412**, 826-831, doi:10.1038/35090591 [doi]

35090591 [pii] (2001).

338 Nishihara, H. *et al.* Non-adherent cell-specific expression of DOCK2, a member of the human CDM-family proteins. *Biochim Biophys Acta* **1452**, 179-187, doi:S0167-4889(99)00133-0 [pii] (1999).

339 Sanui, T. *et al.* DOCK2 regulates Rac activation and cytoskeletal reorganization through interaction with ELMO1. *Blood* **102**, 2948-2950, doi:10.1182/blood-2003-01-0173 [doi]

2003-01-0173 [pii] (2003).

340 Maher, E. A. *et al.* Malignant glioma: genetics and biology of a grave matter. *Genes Dev* **15**, 1311-1333, doi:10.1101/gad.891601 [doi] (2001).

341 Jarzynka, M. J. *et al.* ELMO1 and Dock180, a bipartite Rac1 guanine nucleotide exchange factor, promote human glioma cell invasion. *Cancer Res* **67**, 7203-7211, doi:67/15/7203 [pii]

10.1158/0008-5472.CAN-07-0473 [doi] (2007).

342 Memarzadeh, S. *et al.* Urokinase plasminogen activator receptor: Prognostic biomarker for endometrial cancer. *Proc Natl Acad Sci U S A* **99**, 10647-10652, doi:10.1073/pnas.152127499 [doi]

152127499 [pii] (2002).

343 Kaneko, T., Konno, H., Baba, M., Tanaka, T. & Nakamura, S. Urokinase-type plasminogen activator expression correlates with tumor angiogenesis and poor outcome in gastric cancer. *Cancer Sci* **94**, 43-49 (2003).

344 El-Kott, A. F., Khalil, A. M. & El-Kenawy Ael, M. Immunohistochemical expressions of uPA and its receptor uPAR and their prognostic significant in urinary bladder carcinoma. *Int Urol Nephrol* **36**, 417-423 (2004).

345 Meng, S. *et al.* uPAR and HER-2 gene status in individual breast cancer cells from blood and tissues. *Proc Natl Acad Sci U S A* **103**, 17361-17365, doi:0608113103 [pii]

10.1073/pnas.0608113103 [doi] (2006).

346 Salajegheh, M., Rudnicki, A. & Smith, T. W. Expression of urokinase-type plasminogen activator receptor (uPAR) in primary central nervous system neoplasms. *Appl Immunohistochem Mol Morphol* **13**, 184-189, doi:00129039-200506000-00013 [pii] (2005).

347 Smith, H. W., Marra, P. & Marshall, C. J. uPAR promotes formation of the p130Cas-Crk complex to activate Rac through DOCK180. *J Cell Biol* **182**, 777-790, doi:jcb.200712050 [pii]

10.1083/jcb.200712050 [doi] (2008).

348 Schvartz, I., Seger, D. & Shaltiel, S. Vitronectin. *Int J Biochem Cell Biol* **31**, 539-544, doi:S1357272599000059 [pii] (1999).

349 Namekata, K. *et al.* Dock3 induces axonal outgrowth by stimulating membrane recruitment of the WAVE complex. *Proc Natl Acad Sci U S A* **107**, 7586-7591, doi:0914514107 [pii]

10.1073/pnas.0914514107 [doi] (2010).

350 Sanz-Moreno, V. *et al.* Rac activation and inactivation control plasticity of tumor cell movement. *Cell* **135**, 510-523, doi:S0092-8674(08)01236-1 [pii]

10.1016/j.cell.2008.09.043 [doi] (2008).

351 Yajnik, V. *et al.* DOCK4, a GTPase activator, is disrupted during tumorigenesis. *Cell* **112**, 673-684, doi:S0092867403001557 [pii] (2003).

352 Rushton, E., Drysdale, R., Abmayr, S. M., Michelson, A. M. & Bate, M. Mutations in a novel gene, myoblast city, provide evidence in support of the founder cell hypothesis for Drosophila muscle development. *Development* **121**, 1979-1988 (1995).

353 Wu, Y. C., Cheng, T. W., Lee, M. C. & Weng, N. Y. Distinct rac activation pathways control Caenorhabditis elegans cell migration and axon outgrowth. *Dev.Biol.* **250**, 145-155 (2002).

354 Li, X. *et al.* Netrin signal transduction and the guanine nucleotide exchange factor DOCK180 in attractive signaling. *Nat Neurosci* **11**, 28-35, doi:nn2022 [pii]

10.1038/nn2022 [doi] (2008).

355 Chung, S., Gumienny, T. L., Hengartner, M. O. & Driscoll, M. A common set of engulfment genes mediates removal of both apoptotic and necrotic cell corpses in C. elegans. *Nature cell biology* **2**, 931-937 (2000).

356 Gumienny, T. L. *et al.* CED-12/ELMO, a novel member of the CrkII/Dock180/Rac pathway, is required for phagocytosis and cell migration. *Cell* **107**, 27-41 (2001).

357 Wu, Y. C., Tsai, M. C., Cheng, L. C., Chou, C. J. & Weng, N. Y. C. elegans CED-12 acts in the conserved crkII/DOCK180/Rac pathway to control cell migration and cell corpse engulfment. *Dev.Cell* **1**, 491-502 (2001).

358 Zhou, Z., Caron, E., Hartwieg, E., Hall, A. & Horvitz, H. R. The C. elegans PH domain protein CED-12 regulates cytoskeletal reorganization via a Rho/Rac GTPase signaling pathway. *Dev.Cell* **1**, 477-489 (2001).

359 Meller, N., Merlot, S. & Guda, C. CZH proteins: a new family of Rho-GEFs. *J.Cell Sci.* **118**, 4937-4946 (2005).

360 Grimsley, C. M. *et al.* Dock180 and ELMO1 proteins cooperate to promote evolutionarily conserved Rac-dependent cell migration. *J.Biol.Chem.* **279**, 6087-6097 (2004).

361 Hiramoto, K., Negishi, M. & Katoh, H. Dock4 is regulated by RhoG and promotes Rac-dependent cell migration. *Exp.Cell Res.* **312**, 4205-4216 (2006).

362 Brugnera, E. *et al.* Unconventional Rac-GEF activity is mediated through the Dock180-ELMO complex. *Nat.Cell Biol.* **4**, 574-582 (2002).

363 Cote, J. F. & Vuori, K. Identification of an evolutionarily conserved superfamily of DOCK180-related proteins with guanine nucleotide exchange activity. *J.Cell Sci.* **115**, 4901-4913 (2002).

364 Cote, J. F., Motoyama, A. B., Bush, J. A. & Vuori, K. A novel and evolutionarily conserved PtdIns(3,4,5)P3-binding domain is necessary for DOCK180 signalling. *Nat.Cell Biol.* **7**, 797-807 (2005).

365 Katoh, H. & Negishi, M. RhoG activates Rac1 by direct interaction with the Dock180-binding protein Elmo. *Nature* **424**, 461-464 (2003).

366 Kiyokawa, E. *et al.* Activation of Rac1 by a Crk SH3-binding protein, DOCK180. *Genes Dev.* **12**, 3331-3336 (1998).

367 Lu, M. *et al.* A Steric-inhibition model for regulation of nucleotide exchange via the Dock180 family of GEFs. *Curr.Biol.* **15**, 371-377 (2005).

368 Lu, M. *et al.* PH domain of ELMO functions in trans to regulate Rac activation via Dock180. *Nat.Struct.Mol.Biol.* **11**, 756-762 (2004).

369 Bailey, S. The Ccp4 suite - Program for Protein Crystallography. *Acta Crystallographica Section D-Biological Crystallography* **750**, 760-763 (1994).

370 Pape, T. & Schneider, T. Hkl2map: a graphical user interface for macromolecular phasing with shelx programs. *J Appl Cryst* **37**, 843-844 (2004).

371 Bricogne, G., Vonrhein, C., Flensburg, C., Schiltz, M. & Paciorek, W. Generation, representation and flow of phase information in structure determination: recent developments in and around SHARP 2.0. *Acta crystallographica* **59**, 2023-2030 (2003).

372 Morris, R. J., Perrakis, A. & Lamzin, V. S. ARP/wARP and automatic interpretation of protein electron density maps. *Methods in enzymology* **374**, 229-244 (2003).

373 Emsley, P. & Cowtan, K. Coot: model-building tools for molecular graphics. *Acta crystallographica* **60**, 2126-2132 (2004).

374 Brunger, A. T. *et al.* Crystallography & NMR system: A new software suite for macromolecular structure determination. *Acta crystallographica* **54**, 905-921 (1998).

375 Vagin, A. A. *et al.* REFMAC5 dictionary: organization of prior chemical knowledge and guidelines for its use. *Acta crystallographica* **60**, 2184-2195 (2004).

376 Grimsley, C. M., Lu, M., Haney, L. B., Kinchen, J. M. & Ravichandran, K. S. Characterization of a novel interaction between ELMO1 and ERM proteins. *J.Biol.Chem.* **281**, 5928-5937 (2006).

377 Handa, Y. *et al.* Shigella IpgB1 promotes bacterial entry through the ELMO-Dock180 machinery. *Nat.Cell Biol.* **9**, 121-128 (2007).

378 Tanaka, M., Gupta, R. & Mayer, B. J. Differential inhibition of signaling pathways by dominant-negative SH2/SH3 adapter proteins. *Molecular and cellular biology* **15**, 6829-6837 (1995).

379 Hulo, N. *et al.* The 20 years of PROSITE. *Nucleic acids research* **36**, D245-249 (2008).

380 Komander, D. *et al.* Structural insights into the regulation of PDK1 by phosphoinositides and inositol phosphates. *The EMBO journal* **23**, 3918-3928 (2004).

381 Holm, L. & Sander, C. Protein structure comparison by alignment of distance matrices. *Journal of molecular biology* **233**, 123-138 (1993).

382 Ferguson, K. M. *et al.* Structural basis for discrimination of 3-phosphoinositides by pleckstrin homology domains. *Molecular cell* **6**, 373-384 (2000).

383 Pearson, M. A., Reczek, D., Bretscher, A. & Karplus, P. A. Structure of the ERM protein moesin reveals the FERM domain fold masked by an extended actin binding tail domain. *Cell* **101**, 259-270 (2000).

384 Teo, H. *et al.* ESCRT-I core and ESCRT-II GLUE domain structures reveal role for GLUE in linking to ESCRT-I and membranes. *Cell* **125**, 99-111 (2006).

385 Ceccarelli, D. F. *et al.* Non-canonical interaction of phosphoinositides with pleckstrin homology domains of Tiam1 and ArhGAP9. *The Journal of biological chemistry* **282**, 13864-13874 (2007).

386 Meller, N., Irani-Tehrani, M., Kiosses, W. B., del Pozo, M. A. & Schwartz, M. A. Zizimin1, a novel Cdc42 activator, reveals a new GEF domain for Rho proteins. *Nat.Cell Biol.* **4**, 639-647 (2002).

387 Moore, C. A., Parkin, C. A., Bidet, Y. & Ingham, P. W. A role for the Myoblast city homologues Dock1 and Dock5 and the adaptor proteins Crk and Crk-like in zebrafish myoblast fusion. *Development* (2007).

388 Komander, D. *et al.* An alpha-helical extension of the ELMO1 pleckstrin homology domain mediates direct interaction to DOCK180 and is critical in Rac signaling. *Mol Biol Cell* **19**, 4837-4851, doi:E08-04-0345 [pii]

10.1091/mbc.E08-04-0345 (2008).

389 Erickson, M. R., Galletta, B. J. & Abmayr, S. M. Drosophila myoblast city encodes a conserved protein that is essential for myoblast fusion, dorsal closure, and cytoskeletal organization. *J.Cell Biol.* **138**, 589-603 (1997).

390 Wang, X. *et al.* Cell corpse engulfment mediated by C. elegans phosphatidylserine receptor through CED-5 and CED-12. *Science* **302**, 1563-1566 (2003).

391 Schulte, A. *et al.* The human formin FHOD1 contains a bipartite structure of FH3 and GTPase-binding domains required for activation. *Structure* **16**, 1313-1323, doi:S0969-2126(08)00257-8 [pii]

10.1016/j.str.2008.06.008 (2008).

392 Chesarone, M. A., DuPage, A. G. & Goode, B. L. Unleashing formins to remodel the actin and microtubule cytoskeletons. *Nat Rev Mol Cell Biol* **11**, 62-74, doi:nrm2816 [pii]

10.1038/nrm2816 (2010).

393 Baarlink, C. & Grosse, R. A GBD uncovered: the FHOD1 N terminus is formin'. *Structure* **16**, 1287-1288, doi:S0969-2126(08)00295-5 [pii]

10.1016/j.str.2008.08.002 (2008).

394 Nassar, N. *et al.* Ras/Rap effector specificity determined by charge reversal. *Nat Struct Biol* **3**, 723-729 (1996).

395 Vigorito, E. *et al.* Immunological function in mice lacking the Rac-related GTPase RhoG. *Mol.Cell Biol.* **24**, 719-729 (2004).

396 Kelley, L. A. & Sternberg, M. J. Protein structure prediction on the Web: a case study using the Phyre server. *Nat Protoc* **4**, 363-371, doi:nprot.2009.2 [pii]

10.1038/nprot.2009.2 (2009).

397 Ginalski, K., Elofsson, A., Fischer, D. & Rychlewski, L. 3D-Jury: a simple approach to improve protein structure predictions. *Bioinformatics* **19**, 1015-1018 (2003).

398 Hamdan, F. F., Percherancier, Y., Breton, B. & Bouvier, M. Monitoring protein-protein interactions in living cells by bioluminescence resonance energy transfer (BRET). *Curr Protoc Neurosci* **Chapter 5**, Unit 5 23, doi:10.1002/0471142301.ns0523s34 (2006).

399 Pajcini, K. V., Pomerantz, J. H., Alkan, O., Doyonnas, R. & Blau, H. M. Myoblasts and macrophages share molecular components that contribute to cell-cell fusion. *J Cell Biol* **180**, 1005-1019, doi:jcb.200707191 [pii]

10.1083/jcb.200707191 [doi] (2008).

400 Patel, M. M., Y., Fradet, N., Yang, Q., Wilkes, B., Bouvier, M., Hofmann, K. and Côté, JF. An evolutionarily conserved auto-inhibitory molecular switch in ELMO proteins regulates Rac signaling. *Curr Biol* **20**, 1-7, doi:10.1016/j.cub.2010.10.028 (2010).

401 Chesarone, M. A. & Goode, B. L. Actin nucleation and elongation factors: mechanisms and interplay. *Curr Opin Cell Biol* **21**, 28-37, doi:S0955-0674(08)00198-1 [pii]

10.1016/j.ceb.2008.12.001 [doi] (2009).

402 Handa, Y. *et al.* Shigella IpgB1 promotes bacterial entry through the ELMO-Dock180 machinery. *Nat Cell Biol* **9**, 121-128, doi:ncb1526 [pii]

10.1038/ncb1526 [doi] (2007).

403 Grimsley, C. M., Lu, M., Haney, L. B., Kinchen, J. M. & Ravichandran, K. S. Characterization of a novel interaction between ELMO1 and ERM proteins. *J Biol Chem* **281**, 5928-5937, doi:M510647200 [pii]

10.1074/jbc.M510647200 [doi] (2006).

404 Katoh, H. *et al.* Small GTPase RhoG is a key regulator for neurite outgrowth in PC12 cells. *Mol Cell Biol* **20**, 7378-7387 (2000).

405 Heo, W. D. *et al.* PI(3,4,5)P3 and PI(4,5)P2 lipids target proteins with polybasic clusters to the plasma membrane. *Science* **314**, 1458-1461, doi:1134389 [pii]

10.1126/science.1134389 [doi] (2006).

406 Hannemann, S. *et al.* The Diaphanous-related Formin FHOD1 associates with ROCK1 and promotes Src-dependent plasma membrane blebbing. *J Biol Chem* **283**, 27891-27903, doi:M801800200 [pii]

10.1074/jbc.M801800200 [doi] (2008).

407 Zeke, A., Lukacs, M., Lim, W. A. & Remenyi, A. Scaffolds: interaction platforms for cellular signalling circuits. *Trends Cell Biol* **19**, 364-374, doi:S0962-8924(09)00133-0 [pii]

10.1016/j.tcb.2009.05.007 [doi] (2009).

408 Takeuchi, H. *et al.* Distinct specificity in the binding of inositol phosphates by pleckstrin homology domains of pleckstrin, RAC-protein kinase, diacylglycerol kinase and a new 130 kDa protein. *Biochim Biophys Acta* **1359**, 275-285, doi:S0167-4889(97)00109-2 [pii] (1997).

409 Rameh, L. E. *et al.* A comparative analysis of the phosphoinositide binding specificity of pleckstrin homology domains. *J Biol Chem* **272**, 22059-22066 (1997).

410 Kavran, J. M. *et al.* Specificity and promiscuity in phosphoinositide binding by pleckstrin homology domains. *J Biol Chem* **273**, 30497-30508 (1998).

411 Wohlgemuth, S. *et al.* Recognizing and defining true Ras binding domains I: biochemical analysis. *J Mol Biol* **348**, 741-758, doi:S0022-2836(05)00223-8 [pii]

10.1016/j.jmb.2005.02.048 [doi] (2005).

412 Arthur, W. T., Quilliam, L. A. & Cooper, J. A. Rap1 promotes cell spreading by localizing Rac guanine nucleotide exchange factors. *J Cell Biol* **167**, 111-122, doi:jcb.200404068 [pii]

10.1083/jcb.200404068 [doi] (2004).

413 Brzostowski, J. A., Fey, P., Yan, J., Isik, N. & Jin, T. The Elmo family forms an ancient group of actin-regulating proteins. *Commun Integr Biol* **2**, 337-340 (2009).

414 Isik, N., Brzostowski, J. A. & Jin, T. An Elmo-like protein associated with myosin II restricts spurious F-actin events to coordinate phagocytosis and chemotaxis. *Dev Cell* **15**, 590-602, doi:S1534-5807(08)00330-4 [pii]

10.1016/j.devcel.2008.08.006 [doi] (2008).

415 Song, C. *et al.* Regulation of a novel human phospholipase C, PLCepsilon, through membrane targeting by Ras. *J Biol Chem* **276**, 2752-2757, doi:10.1074/jbc.M008324200 [doi]

M008324200 [pii] (2001).

416 Walker, E. H., Perisic, O., Ried, C., Stephens, L. & Williams, R. L. Structural insights into phosphoinositide 3-kinase catalysis and signalling. *Nature* **402**, 313-320, doi:10.1038/46319 [doi] (1999).

And with that, I have to go split my cells…